

**Natural Products with anticancer activity from Moroccan plant  
*Thymelaea lythroides* and its endophyte *Chaetomium aureum***

Dissertation

zur Erlangung des akademischen Grades

Doktor der Naturwissenschaften (Dr. rer. nat.)

und

Doktor der Biowissenschaften und der Medizin (Dr.)

vorgelegt der

Bergischen Universität Wuppertal

Fachbereich C – Mathematik und Naturwissenschaften

und

Mohammed V-Souissi Universität Rabat

Fakultät – Medizin und Pharmazie

von

Fatima Zahra Kabbaj

Wuppertal 2013

Aus der Arbeitsgruppe der Organischen Chemie  
der Bergischen Universität Wuppertal

Diese Dissertation kann wie folgt zitiert werden:

urn:nbn:de:hbz:468-20140404-113126-9

[<http://nbn-resolving.de/urn/resolver.pl?urn=urn:nbn:de:hbz:468-20140404-113126-9>]

Gedruckt mit der Genehmigung der  
Mathematisch-Naturwissenschaftlichen Fachbereich C der  
Bergischen Universität Wuppertal

und

Medizinisch-Pharmazeutischen Fakultät der  
Mohammed V-Souissi Universität Rabat

Referent: Prof. Dr. Hans-Josef Altenbach

Koreferent: Prof. Dr. Moulay El Abbes Faouzi

Tag der mündlichen Prüfung: 25.11.2013

## Erklärung

Hiermit erkläre ich ehrenwörtlich, dass ich die vorliegende Dissertation mit dem Titel „**Natural Products with anticancer activity from Moroccan plant *Thymelaea lythroides* and its endophyte *Chaetomium aureum***“ selbst angefertigt habe. Außer den angegebenen Quellen und Hilfsmitteln wurden keine weiteren verwendet. Diese Dissertation wurde weder in gleicher noch in abgewandelter Form in einem anderen Prüfungsverfahren vorgelegt. Weiterhin erkläre ich, dass ich früher weder akademische Grade erworben habe, noch dies versucht habe.

Wuppertal, den 21.10.2013  
Fatima Zahra Kabbaj

*I dedicated this work to my husband and my parents*



## **Acknowledgement**

First and foremost thanks to the Almighty God “ALLAH” who has granted me all these graces to fulfill this work and blessed me by His power, mercy and patience during my life. To Him I extent my heartfelt thanks.

It is a pleasure to find the chance to thank all the people that were directly or indirectly involved in the success of the completion of this doctoral thesis.

First of all, I would like to acknowledge Prof. Dr. rer. nat. Hans-Josef Altenbach and Prof. Dr. Moulay El Abbes Faouzi for the excellent working environment, for their patience and encouragement during my first steps in the field of natural product research, and for taking over the supervision of my work with their steady support until the completion of this thesis.

I would like to express my cordial thanks and gratitude to Prof. Dr. rer. nat. Peter Proksch for giving me the opportunity to pursue my doctoral research at his institute, as well as for his valuable recommendations, his fruitful discussions, his unlimited support and for the excellent working facilities at the Institute of Pharmacological Biology and Biotechnology, Heinrich-Heine-Universität, Düsseldorf.

My gratitude and all my regards to Dr. Abdessamad Debbab for his instructive supervision, his kind help, his continuous support and encouragement throughout the completion of this work. Without his guidance this thesis would not be what it is today.

My special thanks to Dr. Aly Hassan Amal and Dr. Lai Daowan for their constructive advises, sharing their expertise in NMR data interpretation as well as for their help and support in good and bad times.

I would like to deeply thank Prof. Yahia Cherrah (Chief of the Division of the National Laboratory of Control of Drugs in Morocco) for his guidance, his continuous encouragement, and his kind advices.

I am deeply grateful to all members of the jury for agreeing to read the manuscript and to participate in the defense of this thesis.

I would like to express my profound gratitude to my professors and colleagues from the Department of Pharmacology, University Mohammed V, Rabat, Morocco, especially Prof. Abdelaziz Bouklouze for defending me during the selection of the candidates of CeDoc at the Faculty of Medicine and Pharmacology of Rabat in Morocco.

My gratitude and all my regards to Prof. Jamal Taoufik (Director of the Doctoral School “Sciences de la Vie et de la Santé” and Vice Doyen of Pharmacy at the Faculty of Medicine and Pharmacy) for giving me the opportunity to access the Doctoral School “Sciences de la Vie et de la Santé” and for carrying out the success of this first education in Morocco.

My sincere gratitude and thankfulness to the professors of ongoing seminars at the Doctoral School “Sciences de la Vie et de la Santé”; for their coaching, assiduity and their sense of responsibility.

I would like to thank Prof. Maati Nejmi (Director of the NIO) who allowed me to carry out the ethnopharmacological survey at the National Institute of Oncology in Rabat. My special thanks also for Dr Abdelouahad Erraki (Head register of the NIO) for his valuable help to get the information concerning the questioned patients. I would like also to thank the clinicians and staff of chemotherapy and radiotherapy for their collaboration. Not to forget to extend my thanks to the patients of NIO for their cooperation.

My special thanks to Prof. Abdelaziz Benjouad (Vice President of Research and Development at the International University of Rabat), who guided me patiently in my first year and help me to select the natural source of this study.

Many thanks for the friendly cooperation to Prof. Dr. Ahmed Chadli, at the Molecular Chaperone/Radiobiology & Cancer Virology in Georgia Regents University, for carrying out the cytotoxic inhibitors of Hsp90 tests, and for his fruitful discussions by interpreting the results.

I would like to specially thank the people who are involved with my success as following;

---

Dr. Victor Wray (Gesellschaft für Biotechnologische Forschung, Braunschweig) for aiding the chemical structure elucidation.

Prof. Dr. Wen Han Lin (Natural Research Laboratory of Natural and Biomimetic drug, Baijing Medical University, Beijing, Republic of China) for the suggestion of structure elucidation of compounds isolated from fungus.

I would like to thank Prof. Dr. rer. nat. Werner E. G. Müller and Mrs. Renate Steffen, Institute of Physiological Chemistry and Pathobiochemistry, University of Mainz, for carrying out the cytotoxicity assays, Prof. Dr. rer. nat. M. U. Kassack and Dr. Alexandra Hamacher, Institut für Pharmazeutische und Medizinische Chemie, Düsseldorf for carrying out the cytotoxicity assays, Dr. Michael Kubbutat, ProQinase GmbH, Freiburg, Germany for conducting the protein kinase inhibition assays and Prof. Ute Hentschel Humeida, Julius-von-Sachs-Institut für Biowissenschaften, University of Würzburg, for carrying out the antibacterial and antifungal assays.

I am grateful to Dr. Tibor Kurtán (Department of Organic Chemistry, University of Debrecen, Hungary) and his coworkers for their splendid CD calculation.

My special thank to Mrs. Andrea Bieck for carrying out of my inscription at the University of Wuppertal, her continuous encouragement and her kind recommendation.

Many thanks to technical assistants of :

- the Institute of Pharmacological Biology and Biotechnology, Heinrich-Heine-Universität, Düsseldorf (Mrs. Miljanovic Simone, Mrs. Katja Friedrich, Mrs. Waltraud Schlag, Mr. Klaus Dieter Jansen, Mrs. Eva Müller, Mrs Goldbach-Gecke Heike) who never gave up providing assistance and continuously supplied me with the laboratory equipment and solvents during my laboratory work.

- the Institute of Organic Chemistry, Bergische Universität, Wuppertal (Mrs. Simone Bettinger, Mr. Jürgen Dönecke, Mrs. Ilka Polanz, Mr. Andreas Siebert) for carrying out the 600 MHz NMR measurements, HR-MS experiments, and for their kind and generous help.

- the Laboratory of Pharmacokinetic, University Mohammed V, Rabat (Mrs. Hayat Houari and Mr. Ahmed Lafrouhi) for their sense of responsibility and their ongoing assistance.

Many thanks to Mr. Andreas Marmann and Ms. Lena Hammerschmidt, who helped me much during my first adaptation months in the institute, introduced me to the variety of isolation techniques, and explained to me regularly the basic NMR spectra interpretation and structure elucidation, respectively.

I would like to extend my thanks to my past and present colleagues and lab-mates Prof. Ag. Bouchra Meddah, Mrs. Mouna Elnekity, Ms. Nisrin Benayad, Ms. Mariam Mousa, Ms. Mounia Rochdi, Mr. Bouchra Faridi, Mr. Nabil Khouya, Ms. Violeta El Alami, Mr. Moustapha El Amrani, Mr. Weaam N. E. Ebrahim, Mr. Ilias Marmouzi, Mrs. Muharini Rini, Mr. Harvé Sergi Akoné and all the others for the nice multicultural time I spent with them, for their help and assistance whenever I needed it.

My special thanks to my friends all over the world Mrs. Zineb Essakali, Mrs. Ruwayda Al Sardi, Mrs. Houda Damour, Mrs. Raha S. Orfali, Mrs. Meryem Carreau and Mrs. Jihane Laafi who encouraged me to stand and never surrender during my difficulties and always listen to me when I needed any moral support.

Last but not least, my gratitude, thankfulness, and my great indebtedness to my Husband Yassir Benmessaoud, my father Taibi Kabbaj, my mother Dikra Yamani, my sister and brother Khadija and Ismail Kabbaj, my stepfather Mohammed Benmessaoud, stepmother Hayat El Jirari, stepsisters Fatima Ezzahra Bemessaoud and Safiya Khalidi, stepbrothers Yassir Nadeif, Mehdi Benmessaoud and Rachid Maakoul and both the Kabbaj and Benmessaoud Families specially my aunt Atika Kabbaj, for their unfailing love, spiritual support and everlasting prayers.

## Zusammenfassung

Heilpflanzen und endophytische Pilze produzieren Naturstoffe mit einer großen Vielfalt von chemischen Strukturen, die für bestimmte medizinische Anwendungen geeignet sein könnten. Die meisten dieser Sekundärmetaboliten zeigen biologische Aktivitäten in pharmazeutisch relevanten Bioassay-Systemen und stellen daher potentielle Leitstrukturen dar, die optimiert werden könnten, um wirksame therapeutische und bioaktive Wirkstoffe zu ergeben.

Das Hitze-Schock-Protein 90 spielt eine entscheidende Rolle bei der Aufrechterhaltung der Homöostase onkogener Proteine. Hsp90 Inhibitoren bietet großes Versprechen in der Behandlung einer Vielzahl von soliden und hämatologischen Malignomen. Zahlreiche natürliche Hsp90-Inhibitoren wurden in den letzten Jahren entwickelt, von denen einige ausgezeichnete Antitumor-Aktivitäten zeigen und in klinische Studien eingetreten sind.

Ziel dieser Arbeit war die Isolierung von Sekundärstoffen aus der ausgewählten Pflanze *Thymelaea lythroides* und deren endophytischen Pilz *Chaetomium aureum*, gefolgt von Strukturaufklärung und Untersuchung der Antitumor-Aktivitäten isolierter Substanzen durch das Screening ihrer inhibierenden Aktivität gegen der Hsp90 Maschinerie.

Die medizinische Pflanze *Thymelaea lythroides* wurde aus 55 Heilpflanzen, die als traditionelle Medizin von den Patienten des „National Institute of Oncology“ in Marokko verwendet werden, ausgewählt. Fünf endophytische Pilzstämme (*Alternaria sp.*, *Chaetomium sp.*, *Cladosporium sp.* und *Pleospora sp.*) wurden aus *Thymelaea lythroides* isoliert. Der Pilz *Chaetomium aureum* wurde zur weiteren Untersuchung ausgewählt und in Wickerham-Flüssigmedium sowie auf 11 festen Medien für einen Zeitraum von drei bis vier Wochen angezogen. Die Extrakte wurden anschließend verschiedenen chromatographischen Trennverfahren unterzogen, um die Sekundärmetaboliten zu isolieren. Zur Strukturaufklärung der isolierten Substanzen wurden moderne Verfahren, einschließlich der Massenspektrometrie (MS) und der Kernresonanzspektroskopie (NMR) eingesetzt. Zusätzlich wurden chirale Derivatisierungsreaktionen bei optisch aktiven Verbindungen angewendet, um deren absolute Konfiguration zu ermitteln.

Schließlich wurden die erhaltenen Verbindungen verschiedenen Biotests unterzogen, um ihre Antitumor-Aktivität zu untersuchen, wobei ihre Fähigkeit die Chaperon Hsp90 Maschinerie

zu hemmen, geprüft wurde. Außerdem wurden die isolierten Verbindungen auf ihre antimikrobiellen, antifungiziden und zytotoxischen Eigenschaften, sowie die Wirkung als Inhibitoren verschiedener Proteinkinasen, getestet.

#### 1 . Isolierte Verbindungen aus der Pflanze *Thymelaea lythroides*

Acht Sekundärmetabolite wurden aus der Heilpflanze *Thymelaea lythroides* isoliert, darunter ein Depsipeptid (**1**; Bassiatin), zwei Coumarine (**2**; Daphneon und **3**; Daphneolon), ein Dicoumarin (**4**; Daphnoretin), zwei Lignane (**5**; Wikstromol und **6**;  $\delta$ -Sesamin), ein Flavonoidglukosid (**8**; *trans*-Tilirosid) und ein Dicoumaringlukosid (**7**; Rutarensin).

Bassiatin (**1**) ist ein ungewöhnlicher pflanzlicher Sekundärmetabolit, der zuvor ausschließlich aus endophytischen Pilzen isoliert wurde. Folglich ist dies der erste Bericht dieser Verbindung aus *Thymelaea lythroides*.

Daphneon (**2**) zeigte eine starke zytotoxische Aktivität gegen der L5178Y Maus-Lymphom-Zelllinie. Eine Hemmung mehrerer der getesteten Proteinkinasen wurde nur bei *trans*-Tilirosid (**8**) und Rutarensin (**7**) beobachtet. Alle aus *Thymelaea lythroides* isolierten Verbindungen waren inaktiv gegen die Hsp90 Chaperon-Maschinerie.

#### 2 . Isolierte Verbindungen aus dem endophytischen Pilz *Chaetomium aureum*

Sechs neue Verbindungen wurden aus diesem Pilzstamm erhalten, einschließlich des neuen Alkylresorcinolderivats (**18**; Chaetoresorcinol), vier neue Xanthoradonderivate (**14**; Xanthoradon D<sub>1</sub>, **15**; Xanthoradon D<sub>2</sub>, **16**; Xanthoradon E<sub>1</sub> und **17**; Xanthoradon E<sub>2</sub>), und ein Pyrochromonderivat (**13**; SB 236050), zusammen mit vier bekannten Azaphilonderivaten (**9**; Sclerotiorin, **10**; Isochromophilon VII, **11**; Sclerotioramin und **12**; Isochromophilon VI).

(+)-Sclerotiorin (**9**), (+)-Isochromophilon VII (**10**), (+)-Sclerotioramin (**11**) und Isochromophilon VI (**12**) waren nicht aktiv im Zytotoxizitätstest gegen der L5178Y Maus-Lymphom-Zelllinie. Allerdings war (+)-Sclerotiorin (**9**) gegen alle getesteten Proteinkinasen außer MEK1wt aktiv, während seine Derivate, Isochromophilone VI (**12**) und Sclerotioramin (**11**), nur wenige der getesteten Enzyme hemmen konnten. Darüber hinaus wurden alle Verbindungen im Hsp 90 Chaperon-Maschinerie Hemmungs-Assay getestet. Nur (+)-Sclerotiorin (**9**) zeigte herausragende Aktivität mit einer dem bekannten Hsp-90-Inhibitor 17-AAG (Geldanamycinderivat) ähnlichen Wirksamkeit.

Chaetoresorcinol (**18**) zeigte eine mittelmäßige fungizide Wirkung gegen *Aspergillus fumigatus*, während die anderen isolierten Verbindungen in den antibakteriellen und fungiziden Tests nicht aktiv waren.

---

---

## Table of Contents

<b>1. General introduction</b>	<b>1</b>
1.1. Aim and scopes of the study	2
<b>2. Literature review</b>	<b>4</b>
2.1. Secondary metabolites as natural products	4
2.2. Medicinal application of natural products	4
2.3. The use of traditional medicine or phytotherapy	6
2.4. Plants as sources of bioactive products	7
2.5. Endophytic fungi as sources of bioactive products	7
2.6. The relationship between the endophyte and the host plant	8
2.7. Pathways to new drug discovery	13
2.7.1. Ethnopharmacological study	13
2.7.2. Screening of the promising natural sources for drug discovery	16
2.8. Anticancer drug discovery	19
2.8.1. Cancer statistics	19
2.8.2. Secondary metabolites as anticancer agents	21
2.9. Natural products as inhibitors of Hsp 90 chaperon machinery	22
2.9.1. Hsp 90 chaperone machinery	22
2.9.2. Hsp 90 inhibitors	23
2.9.3. Example of the inhibition of Hsp 90 in small-cell lung cancer	25
<b>3. Materials and Methods</b>	<b>27</b>
3.1. Biological material	27
3.1.1. Plant material	27
3.1.1.1. Ethnopharmacological study	27
3.1.1.2. Plants worked on during the study	28
3.1.1.3. Field trip and sample collection	29
3.1.1.4. Taxonomy of collected plant samples	29
3.1.2. Fungal Material	29
3.1.2.1. Pure fungal strain isolated from the selected plant	29



---

3.1.2.2. Taxonomy of isolated fungi	30
3.1.2.3. Endophytic fungi worked on during the study	31
3.2. Isolation and cultivation of endophytic fungi	31
3.2.1. Composition of media	31
3.2.2. Short term storage of pure strains	33
3.2.3. Long term storage of pure fungal strains	33
3.2.4. Cultivation for screening and isolation	33
3.3. Identification of plant samples and pure fungal strains	33
3.3.1. Plant identification	33
3.3.2. Fungal identification	33
3.3.2.1. DNA extraction	33
3.3.2.2. DNA amplification	35
3.3.2.3. Purification of PCR products	35
3.3.2.4. Fungi Identification:	37
3.4. Extraction of plant and fungal cultures	37
3.4.1. Extraction and fractionation of <i>Thymelaea lythroides</i> plant material	37
3.4.2. Extraction and fractionation of fungi grown on solid rice medium	37
3.5. Isolation of secondary natural products	38
3.5.1. Thin layer chromatography (TLC)	38
3.5.2. Vacuum liquid chromatography (VLC)	39
3.5.3. Flash chromatography	40
3.5.4. Low pressure liquid chromatography (LC)	40
3.5.5. High pressure liquid chromatography (HPLC)	41
3.5.5.1. Analytical HPLC	42
3.5.5.2. Semi preparative HPLC	42
3.5.6. Isolation and purification of secondary metabolites	43
3.5.6.1. Isolation and purification of plant extract <i>Thymelaea lythroides</i>	43
3.5.6.2. Isolation and purification of endophyte extract <i>Chaetomium aureum</i>	44
3.5.6.2.1. Isolated secondary metabolites from fermentation of <i>Chaetomium aureum</i> on solid rice	44
3.5.6.2.2. Isolated secondary metabolites from <i>Chaetomium aureum</i> on solid beans	45
3.6. Structure elucidation of the isolated metabolites	45
3.6.1. Mass spectrometry (MS)	46

---

---

3.6.1.1. Electron Impact Mass Spectrometry (EI-MS)	46
3.6.1.2. Electron spray ionization mass spectrometry (ESIMS)	46
3.6.1.3. Fast atom bombardment mass spectrometry (FAB-MS)	47
3.6.1.4. High-resolution mass spectrometry (HR-MS)	47
3.6.2. Nuclear magnetic resonance spectroscopy (NMR)	47
3.6.3. Optical activity	48
3.6.4. Circular dichroism (CD) spectroscopy	49
3.7. Testing of the biological activity	50
3.7.2. Cytotoxicity tests	51
3.7.2.1. Microculture tetrazolium (MTT) assay	52
3.7.2.2. MTT cell viability assays	53
3.7.2.3. Protein kinase assay	53
3.8. Inhibiting the hsp90 chaperone pathway	57
3.8.1. Heat shock protein Hsp 90	57
3.8.2. Progesterone receptor PR reconstitution assay	58
3.8.3. Cytotoxicity of Sclerotiorin to breast cancer Hs578T cells	58
3.8.4. Comparison of deacetylsclerotiorin and sclerotiorin by inhibiting the Hsp90 chaperoning of progesterone receptor (PR) in vitro	59
3.9. General laboratory equipments	59
3.10. Solvents	60
3.10.1. General solvents	60
3.10.2. Solvents for HPLC	60
3.10.3. Solvents for optical rotation	60
3.10.4. Solvents for NMR	60
<b>4. Results</b>	<b>61</b>
4.1. Ethnopharmacological study	61
4.1.1. Frequency of cancer according to gender	61
4.1.2. Frequency of cancer according to the localization	61
4.1.3. Frequency of cancer according to the age	63
4.1.4. Frequency of using traditional medicine by NIO patients	63
4.1.5. Use of Traditional Medicine according to the gender	63

---

---

---

4.1.6. Use of Traditional Medicine according to the origin	64
4.1.7. Certainty and error biases	65
4.1.8. Medicinal plants used in traditional medicine by the patients of the National Institute of Oncology in Rabat	65
4.1.9. The toxicity and side effects of medicinal plants	65
4.2. Compounds isolated from the plant <i>Thymelaea lythroides</i>	69
4.3. Bioactivity test results for compounds isolated from the plant <i>Thymelaea lythroides</i>	99
4.4. Compounds isolated from the endophytic fungus <i>Chaetomium aureum</i>	101
4.5. Bioactivity test results for compounds isolated from the endophytic fungus <i>Chaetomium aureum</i>	135
<b>5. Discussion</b>	<b>140</b>
5.1. The use of medicinal plants in Morocco	140
5.2. Selection of interesting medicinal plants based on an ethnopharmacology survey	140
5.3. Chemical diversities of the genus <i>Thymelaea</i> secondary metabolites	141
5.4. Methodologies for profiling of the metabolites	143
5.4.1. HPLC/UV	143
5.4.2. HPLC/ESI-MS	143
5.5. Secondary metabolites isolated from the plant <i>Thymelaea lythroides</i>	144
5.5.1. Depsipeptides	144
5.5.2. Coumarins	144
5.5.3. Flavonoids	145
5.5.4. Lignans	145
5.6. Biosynthesis of the secondary metabolites	145
5.6.1. Biosynthesis pathway of the isolated compounds from <i>Thymelaea lythroides</i>	148
5.7. Bioactivity of the isolated compounds from <i>Thymelaea lythroides</i>	150
5.7.1 Bioactivity of coumarins and dicoumarins isolated from <i>T. lythroides</i>	150
5.7.2. Bioactivity of lignans isolated from <i>T. lythroides</i>	150
5.7.3. Bioactivity of flavonoid glycosides isolated from <i>T. lythroides</i>	150
5.7.3. Bioactivity of depsipetides isolated from <i>T. lythroides</i>	150

---

---

---

5.8. Selection of the interesting endophytic fungus strains isolated from <i>Thymelaea lythroides</i>	151
5.9. Choice of culture media	151
5.10. Chemical diversities of the genus <i>Chaetomium</i> secondary metabolites	152
5.11. Secondary metabolites isolated from the endophytic fungi <i>Chaetomium aureum</i>	153
5.11.1. Azaphilone	153
5.11.2. Pyranochromones	153
5.11.3. Xanthones	154
5.11.4. Alkylresorcinols	154
5.12. Biosynthesis of isolated secondary metabolites from the endophytic fungi <i>Chaetomium aureum</i>	154
5.13. Bioactivity of isolated secondary metabolites from the endophytic fungi <i>Chaetomium aureum</i>	155
5.13.1. Bioactivity of azaphilone derivatives isolated from <i>Chaetomium aureum</i>	155
5.13.2. Bioactivity of xanthone derivatives isolated from <i>Chaetomium aureum</i>	157
5.13.3. Bioactivity of alkylresorcinol derivative isolated from <i>Chaetomium aureum</i>	158
<b>6. Conclusion</b>	<b>159</b>
6.1. Compounds isolated from the plant <i>Thymelaea lythroides</i>	160
6.2. Compounds isolated from the endophytic fungi <i>Chaetomium aureum</i>	160
<b>7. References</b>	<b>165</b>
<b>8. List of Abbreviations</b>	<b>180</b>
<b>9. List of Figures</b>	<b>183</b>
<b>10. List of Tables</b>	<b>185</b>
<b>11. Attachments</b>	<b>187</b>
<b>Curriculum Vitae</b>	<b>196</b>

---

## 1. General introduction

Drug discovery and development has a long history and dates back to the early days of human civilization. In those ancient times, drugs were not just used for physical remedies but were also associated with religious and spiritual healing.

Even today, after more than 100 years of research in pharmaceutical industries, there is still a great need for innovative drugs. Only one third of all diseases can be treated efficiently (Müller *et al.*, 2000). The role of natural products in drug discovery is demonstrated by an analysis of the number and sources of anticancer and antiinfective agents, reported mainly in the Annual Reports of Medicinal Chemistry from 1984 to 1995 (Cragg, 1997). It was observed that over 60% of the approved drugs and pre-NDA (New Drug Applications) candidates (for the period 1989-1995), excluding biologics (vaccines, monoclonals, etc. derived from mammalian sources), developed in these disease areas are of natural origin.

The nature itself, has constantly supplied mankind with a broad and structurally diverse array of pharmacologically active compounds that continue to be utilised as highly effective drugs to combat a multitude of deadly diseases or as lead structures for the development of novel synthetically derived drugs that mirror their models from nature (Proksch *et al.*, 2002).

The ancient medical literature reports that surgery was performed but that physicians also recommended the use of some natural, and especially plant products, which represent an interesting point of comparison with current knowledge. Natural products play a relevant role in cancer therapy today with substantial numbers of anticancer agents used in the clinic being either natural or derived from natural products from various sources such as plants, animals and microorganisms. Large-scale anticancer drug discovery and screening programs such as those promoted by the National Cancer Institute (NCI) have played an important role in the development of anticancer natural compounds (Stefania *et al.*, 2009).

The molecular chaperone Hsp90 has been a promising target for cancer therapy. Cancer is a disease marked by genetic instability. Thus specific inhibition of individual proteins or signaling pathways holds a great potential for subversion of this genetic plasticity of cancers.

### 1.1. Aim and scopes of the study

The aim of this study is to look for natural lead molecules with anticancer activity specially the inhibitors of Hsp90 machine. For this, the drug discovery process was divided into 4 steps namely (Figure 1.1):

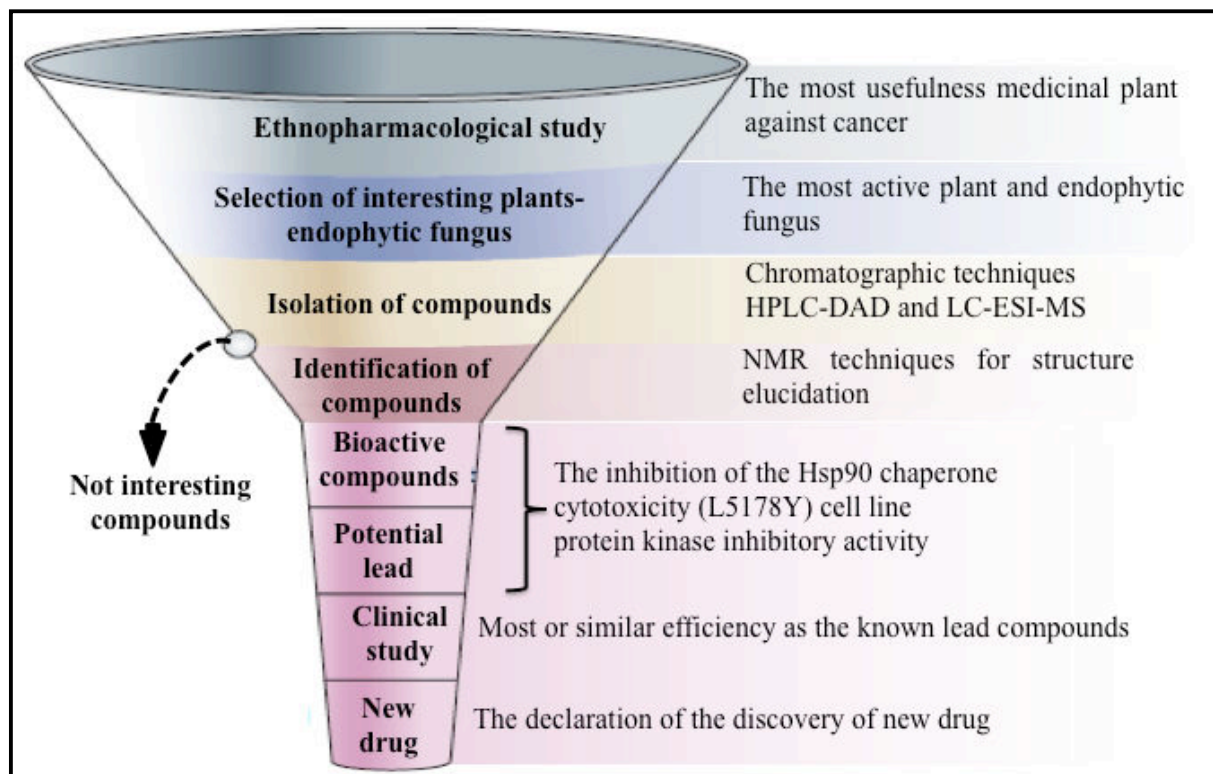


**Figure 1.1.** Steps of drug discovery process

1- *The selection of the interesting natural sources* from an ethnopharmacological study about the most usefulness medicinal plant against cancer, then from the selected plant, a screening of the most active endophytic fungus; this step is basically of two types of natural sources. Firstly, the macro-organism source which are plants, and secondly, the micro-organism source which are endophytic fungi. The plant *Thymelaea lythroides* and the endophytic fungi *Chaetomium aureum* were suspected for this study.

2- *The isolation, characterization and structure elucidation of the secondary metabolites.* The raw extracts of the selected natural sources have to be fractionated and separated using various chromatographic techniques and their fractions have to be analyzed by HPLC-DAD for their purity and ESI-LC/MS for their molecular weight and fragmentation patterns. The pure compounds should then submitted to state-of-the-art one- and two-dimensional NMR techniques for structure elucidation.

3- *The selection of the potential lead compounds.* The pure compounds were subjected to selected bioassays to determine their pharmaceutical potential. Thus, the application of secondary metabolites for the inhibition of the Hsp90 chaperone pathway will be carried out by Prof. A. Chadli at the Cancer Research Center, Molecular Chaperones Biology, Georgia Regents University in USA. The cytotoxicity will be studied *in vitro* using mouse lymphoma (L5178Y) cell line. Moreover, the pure compounds will also be tested for their protein kinase inhibitory activity, whereas, antimicrobial activity will be studied using the agar diffusion assay. The latter three assays will be conducted in cooperation with Prof. W. E. G. Müller, Mainz, ProQinase, Freiburg and Prof. U. Hentschel, Würzburg, respectively.

4- *The clinical study.* Sclerotiorin showed similar efficiency to that of 17-AAG, the classical inhibitor of Hsp90, which make it the first suspect for the clinical essays.

## 2. Literature review

### 2.1. Secondary metabolites as natural products

The compounds known as secondary metabolites were defined in 1891 as materials that were relatively unimportant in the overall physiology of plants and not absolutely essential to the life and growth of the producing organism (Bentley, 1999). From 1900 to 1950 the term secondary metabolites received little use and was restricted to plants. It was not until 1961 that secondary metabolite was applied to microbial products; soon thereafter a new terminology “natural product” was used by organic chemists to refer to materials derived from terrestrial plants, bacteria, filamentous fungi, marine creatures, etc. In the strict sense of the term, natural products encompass also the primary metabolites. As stated by Davies (1992), “a secondary metabolite is a natural product, but a natural product isn’t necessarily a secondary metabolite” (Bentley R., 1999). Secondary metabolites are classified depending on their structural scaffold. These classes include among others polyketides (PKs), non ribosomal peptides (NRPs), terpenoids, alkaloids and hybrid metabolites of the different classes. The function of secondary metabolites in their hosts has not yet been exploited to its fullest; however, they seem to have several functions including defense, communication, and signaling (Calvo *et al.*, 2002; Fox *et al.*, 2008; Kempken and Rohlfs, 2010; Rohlfs and Churchill, 2010).

Although there are notable exceptions (e.g., palytoxin, maitotoxin), most secondary metabolites have relative molecular masses less than 1500 Da. The range of chemical structures is breathtaking from simple aliphatic acids (e.g., itaconic acid, C<sub>5</sub>H<sub>6</sub>O<sub>4</sub>) to complex structures such as alkaloids and toxins (e.g., palytoxin, C<sub>129</sub>H<sub>223</sub>N<sub>3</sub>O<sub>54</sub>). This wide range of chemical types has made secondary metabolites a major topic for study by organic chemists (Bentley, 1999).

### 2.2. Medicinal application of natural products

Medicinal application of natural products has a long history and dates back to the early days of human civilization. In traditional medicine, natural products, mainly botanical drugs, were and are used on the basis of empirical experiences rather than pharmacological knowledge. The World Health Organization has estimated that almost 80% of the world’s inhabitants depend mainly on traditional medicines for their primary health care (Arvigo and Balich, 1993; Farnsworth *et al.*, 1985; Newman, 2008), which Morocco is one of them. Moroccan traditional pharmacopoeia is one of the richest and varied in the world (Bellakhdar *et al.*,

---



1978; Bellakhdar *et al.*, 1982; Bellakhdar *et al.*, 1991; Benjelloun, 1997; Bounejmate, 1995). Clinical, pharmacological, and chemical studies of these traditional medicines, which were derived predominantly from plants, were the basis of most early medicines such as the antipyretic and antimalarial active alkaloid quinine (2) (from *Cinchona pubescens*) or the cardiac glycoside digitoxin (3) (from *Digitalis purpurea*). Even more drugs are derived from natural products, like the world-famous aspirin (4) aspirin (acetylsalicylic acid), which is derived from the glycoside salicin (5) and is found in many species of the plant genera *Salix* and *Populus*. Aspirin is only one, albeit the best known example for the prosperous interaction of synthetic and natural products chemistry.

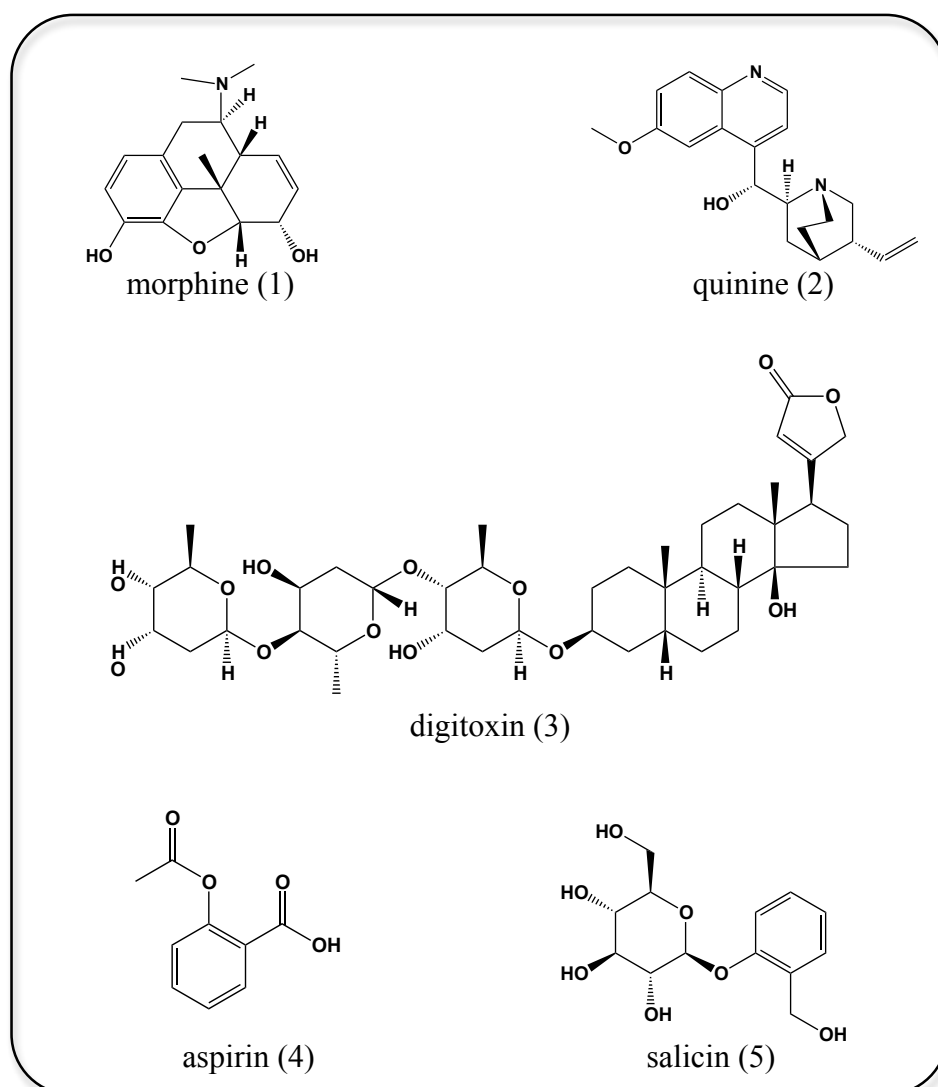


**Figure 2.1.** Natural products of medicinal importance

With the increase of this knowledge and the better understanding of the mode of action of different remedies, more and more distinct drugs were used and chemically modified. Additionally, scores of novel active compounds were introduced to medicines that are produced by means of traditional or combinatorial synthetic chemistry. In fact, around 60% of the new drugs registered during the period 1981-2002 by the FDA as anticancer and anti-hypertensive agents were either natural products or based on them (Newman *et al.*, 2003). Likewise, more recent studies demonstrate that natural products constantly play an important role in drug development (Butler, 2008; Newman and Cragg, 2007; Sneader, 1996).

Hence, a large number of examples from medicine reveal the innovative potential of natural compounds and their impact on progress in drug discovery and development (Tejesvi *et al.*, 2007).

### **2.3. The use of traditional medicine or phytotherapy**

In recent years, there has been growing interest in alternative therapies and the therapeutic use of natural products, especially those derived from plants (Goldfrank *et al.*, 1982; Vulto and Smet, 1988; Mentz and Schenkel, 1989). This interest in drugs of plant origin is due to several reasons, namely, conventional medicine can be inefficient (e.g. side effects and ineffective therapy), abusive and/or incorrect use of synthetic drugs results in side effects and other problems, a large percentage of the world's population does not have access to conventional pharmacological treatment, and folk medicine and ecological awareness suggest that "natural" products are harmless. However, the use of these substances is not always authorised by legal authorities dealing with efficacy and safety procedures, and many published papers point to the lack of quality in the production, trade and prescription of phytomedicinal products. Nevertheless, the phytomedicines are freely marketed and, in underdeveloped or developing countries, the use of medicinal plants is widely accepted. This can result in toxic accidents resulting from the use of plants as food or for therapy or from accidental ingestion by children or animals. Toxicity can result from highly concentrated doses or from the state of conservation of plants and the form of use.

The WHO considers phytotherapy in its health programs and suggests basic procedures for the validation of drugs from plant origin in developing countries (Rates, 2001).

#### **2.4. Plants as sources of bioactive products**

The analysis of data of prescriptions dispensed from community pharmacies in the United States from 1959 to 1980 revealed that approximately 25% contained plant extracts or active principle from higher plants (Newman *et al.*, 2000). About 25% of the drugs prescribed worldwide come from plants, 121 such active compounds being in current use. Of the 252 drugs considered as basic and essential by the World Health Organisation (WHO), 11% are exclusively of plant origin and a significant number are synthetic drugs obtained from natural precursors (Rates, 2001). The vast majority of the drugs isolated from plants cannot yet be synthesised economically and are still obtained from wild or cultivated plants.

In addition, compounds such as muscarine, physostigmine, cannabinoids, yohimbine, forskolin, colchicine and phorbol esters, all obtained from plants, are important tools used in pharmacological, physiological and biochemical studies (Williamson *et al.*, 1996).

However, the potential use of higher plants as a source of new drugs is still poorly explored. Of the estimated 250,000–500,000 plant species, only a small percentage has been investigated phytochemically and even a smaller percentage has been properly studied in terms of their pharmacological properties; in most cases, only pharmacological screening or preliminary studies have been carried out. It is estimated that 5000 species have been studied for medical use (Payne *et al.*, 1991). Between the years 1957 and 1981, the NCI screened around 20,000 plant species from Latin America and Asia for anti-tumour activity, but even these were not screened for other pharmacological activities (Hamburger and Hostettman, 1991).

#### **2.5. Endophytic fungi as sources of bioactive products**

The word endophyte means “in the plant” (from gr. Endo = within, phyton = plant). “Endophytism” is, thus, a unique cost-benefit plant-microbe association defined by “location” (not “function”) that is transiently symptomless, unobtrusive, and established entirely inside the living host plant tissues (Kusari *et al.*, 2012). During this association, none of the interacting partners is discernibly harmed, and the individual benefits depend on both the interacting partners.

The existence of fungi inside the organs of asymptomatic plants has been known since the end of the 19th century (Guerin, 1898) and the term “endophyte” was first proposed in 1866 (de Bary, 1866).

Since endophytes were first described in the Darnel (*Lolium temulentum*) (Kusari, 2012), they have been isolated from various organs of different plant species.

The significance of fungi as unconventional sources of bioactive compounds was first realized by the discovery of penicillin from *Penicillium notatum*, by Alexander Fleming in 1928. Since then, natural product discovery from fungi has gained considerable attention and momentum, especially after the large-scale production of penicillin during World War II.

For the past 50 years, fungal secondary metabolites have revolutionized medicine yielding blockbuster drugs and drug leads of enormous therapeutic and agricultural potential (Amal *et al.*, 2011).

Recent development of screening technologies revealed the great potential of endophytes as a major source of biologically active compounds with promising medicinal or agricultural applications (Zhang *et al.* 2012; Aly *et al.*, 2010).

In addition, natural products from endophytic fungi represent a huge and largely untapped resource of unique chemical structures that have been optimized by (co-)evolution and probably play an important role for communication or adaptation as a response to habitat and environmental changes (Gunatilaka, 2006). It has been estimated that approximately 1.5 million fungal species are present on earth of which only about 7% have been described so far (Aly *et al.*, 2010). Whereas between 1987 and 2000 approximately 140 new natural products were isolated from endophytic fungi, a similar number was subsequently characterised in half of this time span, i.e. between 2000 and 2006 (Zhang *et al.*, 2006). Since then, especially fungi isolated from soil samples have been identified as a rich source of biologically active secondary metabolites. Beside other well known antimicrobial agents like fusidic acid (6) (Aly *et al.*, 2010) and griseofulvin (7) (Kjier, 2009), novel semisynthetic antifungal drugs like anidulafungin (8) (Eraxis) and caspafungin (Cancidas) are likewise derived from fungal metabolites (Kjier, 2009). With the discovery of cyclosporine (9) isolated from

*Tolypocladium inflatum* in 1971, an important step in immunopharmacology was made because this substance prevents rejection after organ or tissue transplantations.

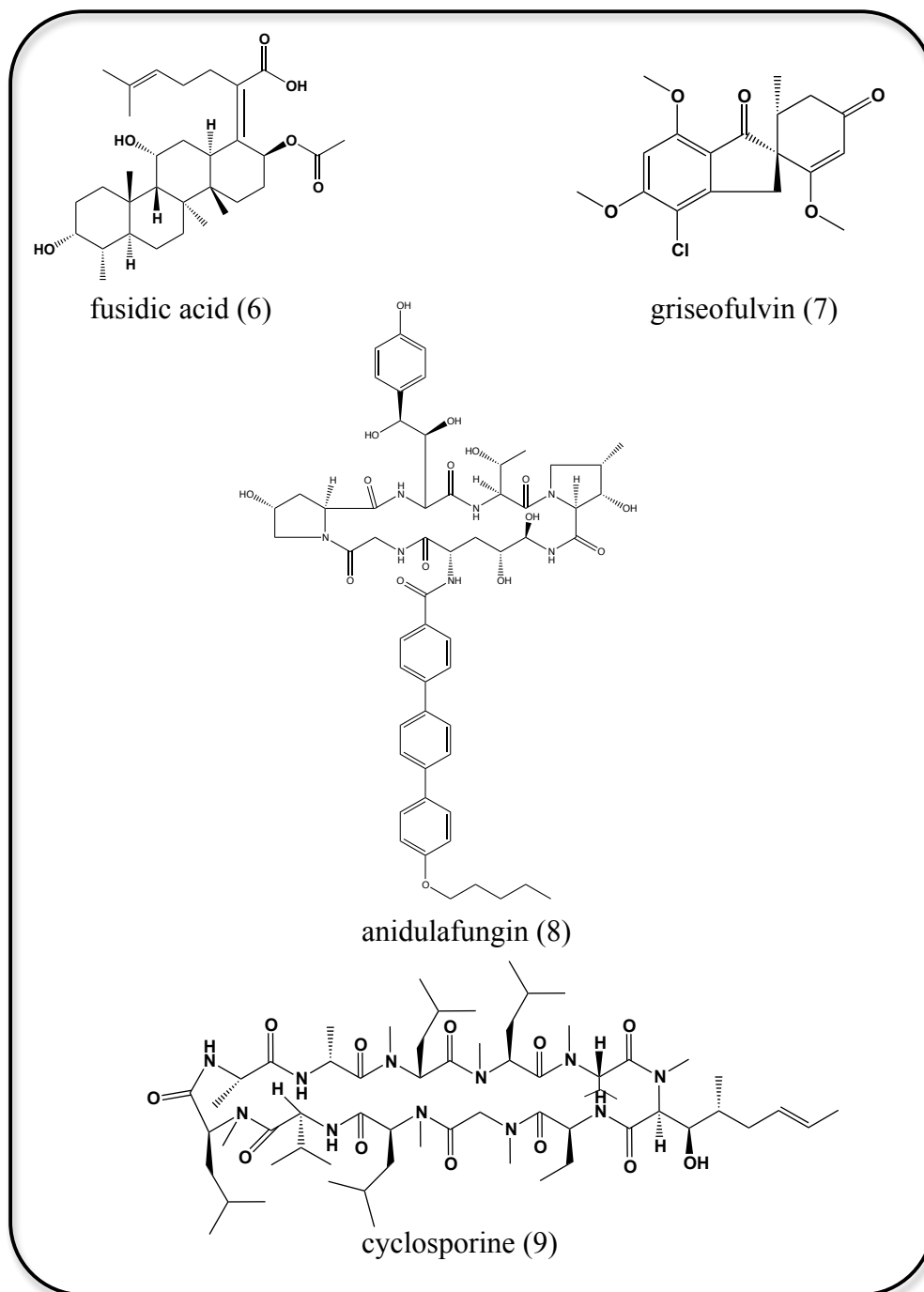


**Figure 2.2.** Bioactive fungal metabolites used in medicine

Probably the most economical important fungal metabolites represent antilipidemic drugs collectively known as “statins”, with their parent compounds mevastatin and lovastatin (10) isolated from *Penicillium citrinum* and *Aspergillus terreus*, respectively. Statins reduce blood cholesterol levels by inhibiting the rate limiting enzyme HMG-CoA reductase in the

mevalonate pathway of cholesterol synthesis, and are used for the treatment of cardiovascular diseases (Dewick, 2006).

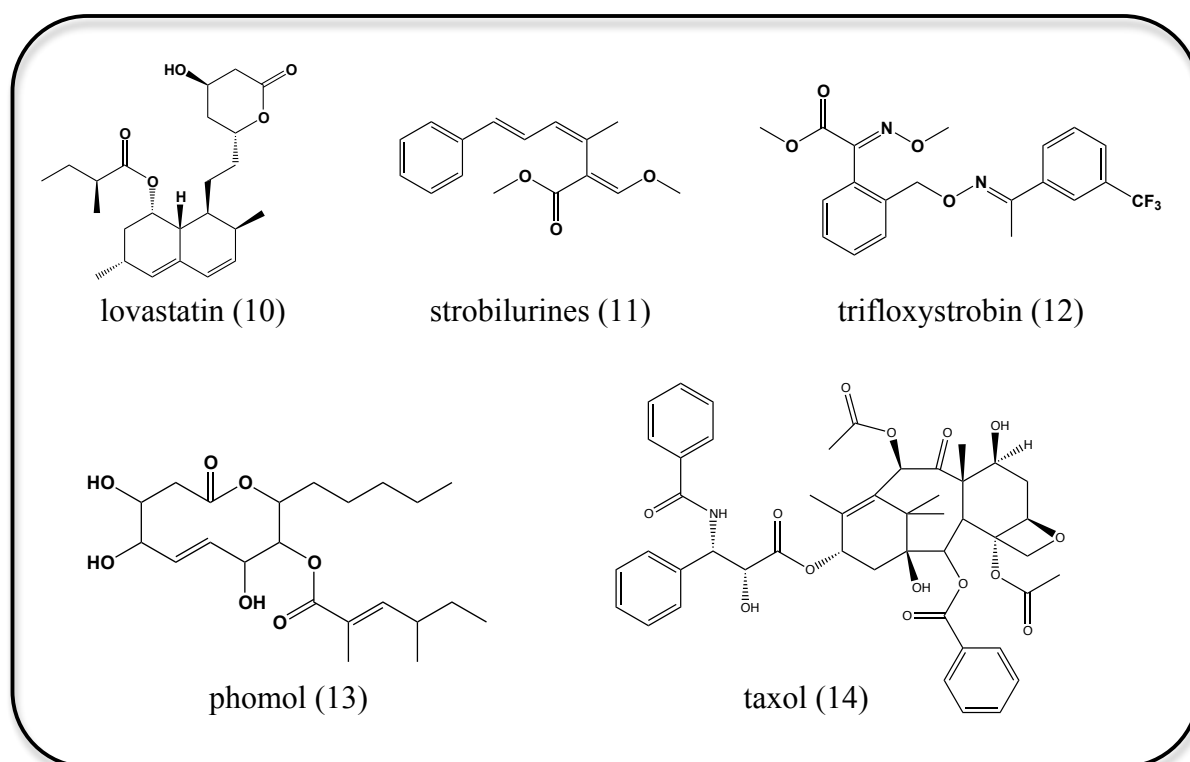


**Figure 2.2.** Bioactive fungal metabolites used in medicine

Fungal metabolites are, however, not only indispensable for medicine but are also important for plant protection as demonstrated by the discovery of the strobilurines (11), that were first isolated from *Strobilurus sp.* and served as lead compounds for synthetic fungicides such as trifloxystrobin (12) (Flint<sup>®</sup>) (Kjier, 2009).

From the medicinal plant *Erythrina crista-galli* the endophyte *Phomopsis sp.* was isolated, which produced the anti-inflammatory as well as antifungal and antibacterial active polyketide lactone, phomol (13) (Weber et al. 2004).

But it is not only new compounds being isolated from endophytes that are promising. The well known plant metabolite taxol (14), the “world’s first billion-dollar anticancer compound” (Strobel, 2004), was originally isolated from the bark of the endemic Pacific yew tree, *Taxus brevifolia*. It interferes with the normal function of microtubule breakdown. Specifically, taxol binds to the  $\beta$ -subunit of tubulin and thereby interrupts the dynamic rearrangement of this important component of the cytoskeleton. This adversely affects cell function due to the

shortening and lengthening of microtubules is necessary for their function as a mechanism to transport other cellular components, e.g. during mitosis. Thus taxol affects dividing cells, especially fast dividing ones like cancer cells. For the treatment of one patient suffering from cancer, 2 g taxol are required, which represents an amount equivalent to twelve trees and thereby posing a challenge to the limited natural resources, since the isolation from the inner bark implies the destruction of trees. Thus, the demand for taxol greatly exceeds the supply that can be sustained by isolation from its natural source and alternative sources of the drug have been sought for a long time. Although the highly functionalized, polycyclic diterpene has been prepared by total synthesis, the process is too complex and not economically feasible. Currently, the supply of the compound is achieved by a successfully implied partial synthetic route based on baccatin III or its 10-deacetyl congener, which are isolated from the needles of other *Taxus* species and thus from a renewable resource. However, the extraction process of these precursors is tedious and costly. In the ongoing search for alternative sources of taxol, the group of Gary Strobel discovered taxol production in a hitherto undescribed endophytic fungus associated with *Taxus brevifolia*, identified as *Taxomyces andreanae* (Stierle et al., 1993). Although initially controversial, these findings prompted further studies, and it is nowadays an emerging picture that the ability to produce taxol upon fermentation seems to be a rather widespread feature among endophytic fungi. So far, more than 10 different fungal strains from at least 6 different host plants, most of them only distantly (if at all) related to *Taxus*, have been identified. However, it is worth mentioning that in all cases the resulting yields are minuscule, so far preventing any commercial exploitation (Strobel et al., 2004).

## **2.6. The relationship between the endophyte and the host plant**

Any plant-fungal interaction is preceded by a physical encounter between a plant and a fungus, followed by several physical and chemical barriers that must be overcome to successfully establish an association. The “balanced antagonism” hypothesis (Schulz et al., 1999; Schulz and Boyle, 2005) was initially proposed to address how an endophyte avoids activating the host defenses, ensures self-resistance before being incapacitated by the toxic metabolites of the host, and manages to grow within its host without causing visible manifestations of infection or disease (Arnold, 2005, 2007, 2008; Schulz and Boyle, 2006) (Figure 2.3.A). This hypothesis led to the proposal that the interactions between host plants and endophytes in natural populations and communities are described as a balanced symbiotic continuum ranging from mutualism through commensalism to parasitism (Tan and Zou, 2001;

---

Kogel *et al.*, 2006). Endophytes and pathogens both possess many virulence factors that are countered by plant defense mechanisms. If fungal virulence and plant defense are balanced, the association remains apparently asymptomatic and a virulent. Although the genetic basis of symbiotic communication is not yet known, studies examining the relation between host genotype and symbiotic lifestyle expression revealed that individual isolates of some fungal species can express either parasitic or mutualistic lifestyles depending on the host genotype colonized (Redman *et al.*, 2001; Unterseher and Schnittler, 2010). Some endophytes are generally viewed as mutualists; by receiving nutrition and protection from their host plants, the endophytes enhance resistance of the host plant against insect herbivores or pathogens (Clay, 1990). Studies showed that vertically transmitted (systemic) endophytes, growing within seeds, are more likely to be mutualistic, while horizontally transmitted (non-systemic) endophytes, via spores, tend to be more antagonistic to the host (Schardl *et al.*, 1991; Saikkonen *et al.*, 1998). Furthermore, upon leaf aging or senescence, endophytic fungi can shift to the pathogenic side of the continuum, thus becoming more widespread and causing external infections (Saikkonen *et al.*, 1998).

The environmental factors play a major role to destabilize the delicate balance of antagonisms. If the plant defense mechanisms completely counteract the fungal virulence factors, the fungus will perish. Conversely, if the plant succumbs to the virulence of the fungus, a plant-pathogen relationship would lead to plant disease (Figure 2.3.B). Because many endophytes could possibly be latent pathogens, they might be influenced by certain intrinsic or environmental factors to express factors that lead to pathogenicity (Arnold, 2008) (Figure 2.3.C).

Recently, it was revealed that the plant-endophyte interaction might not be just equilibrium between virulence and defense, but a much more complex and precisely controlled interaction (Figure 2.3.D). According to the plant-endophyte coevolution hypothesis (Ji *et al.*, 2009), it might be possible for endophytes to assist the plant in chemical defense by producing bioactive secondary metabolites. Two parallel intriguing propositions have been made. Conferring to the “mosaic effect” theory, endophytes might protect host plants by creating a heterogeneous chemical composition within and among plant organs that are otherwise genetically uniform (Carroll, 1991). Consequently, these organs would vary arbitrarily in lusciousness or worth for herbivores, and in terms of infectivity for pathogens. The other



theory holds that endophytes might assist their corresponding host plants as “acquired immune systems” (Arnold *et al.*, 2003).

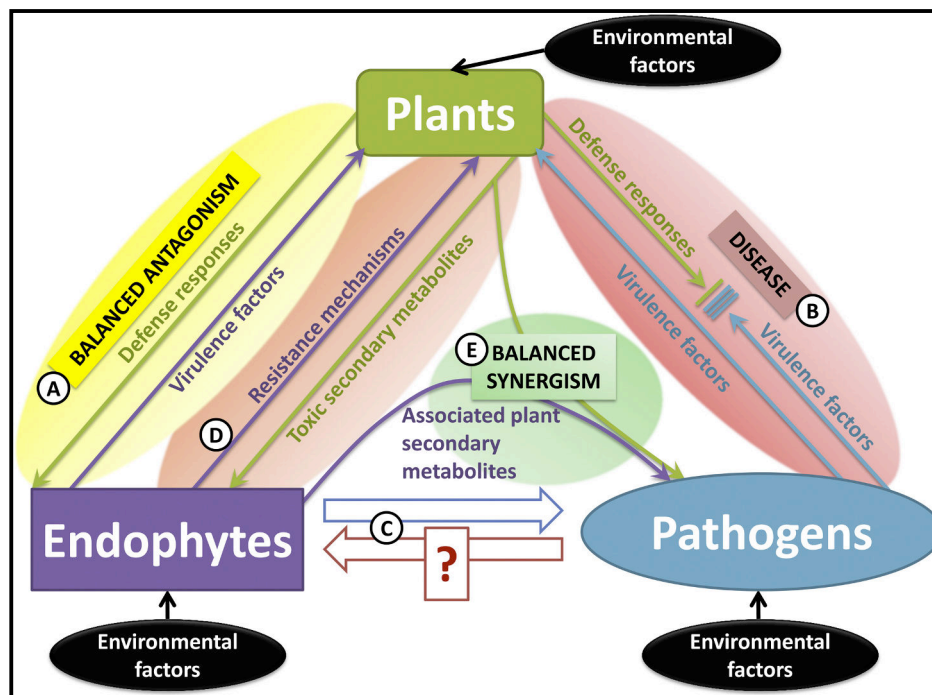


**Figure 2.3.** Chemical-Ecological Schematic Interpretation of Plant-Fungus Cost-Benefit Interactions with Emphasis on Endophytic Fungi (Kusari *et al.*, 2012)

- (A) Balanced antagonism hypothesis is shown.
- (B) Plant disease caused by pathogenic fungi is presented.
- (C) Endophyte-pathogen reciprocity is demonstrated. The question mark (?) indicates that this phenomenon might not be universal, and further research is necessary for verification.
- (D) Endophyte survival strategy is illustrated.
- (E) Balanced synergism is shown.

## 2.7. Pathway to new drug discovery

New medical discoveries and advancement of associated technology is further widening the gap between traditional concepts of diseases, their treatment by healers and the present day physicians. A physician interested in ethnopharmacology could fill this gap and offer modern explanation of old concepts of healing. However, all this requires a modest and collaborative attitude of physicians with healers, botanists and anthropologists which is the key to successful acquisition of the information (Lozoya, 1994).

### 2.7.1. Ethnopharmacological study

Ethnopharmacology and natural product drug discovery remains a significant hope in the current target-rich, lead-poor scenario. Many modern drugs have origin in traditional medicine and ethnopharmacology.

Enormous ethnopharmacological research was carried out by physicians with expertise or interest in chemistry, pharmacology, botany or anthropology during the early period of medicinal plant research 250 years ago. The classic example is of Dr. William Withering, who in 1775 discovered the use of foxglove in the treatment of ‘dropsy’ (i.e. edema) due to cardiac ailment (now known as congestive heart failure). The plant was used for the cure of ‘dropsy’ in the form of aqueous tea of 20 or more herbs by an old woman in Shropshire. Withering combined his medical expertise and knowledge of botany and discovered that foxglove was the active ingredient, and that only dropsy related to heart ailment was curable (Raza, 2006).

**Table 2.1.** Selected physicians and their contributions in ethnopharmacological investigations (Raza, 2006)

Willem William Withering (1741–1799)	Medicinal uses of <i>Pilocarpus jaborandi</i>
Pies (1611–1678)	Use of Foxglove in “Dropsy” (congestive heart failure)
Robert Christison (1797–1882)	Toxicology of <i>Physostigma venenosum</i>
John Hutton Balfour (1808–1884)	Description of <i>Physostigma venenosum</i>
Claude Bernard (1813–1878)	Pharmacological investigation of curare
Paolo Mantegazza (1831–1910)	Medicinal uses of coca
John Kirk (1832–1922)	Effect of African arrow poison ( <i>Strophanthus</i> sp.) on CVS
Symphronio Olympio Cezar Coutinho (1832–1887)	Investigation of medicinal uses and introduction of <i>Pilocarpus jaborandi</i> in medical practice
Douglas Argyll Robertson (1837–1909)	Introduction of <i>Physostigma venenosum</i> in ophthalmic medicine
Thomas Richard Fraser (1841–1920)	Pharmacology of <i>Physostigma venenosum</i>
Nagai Nagayoshi (1844–1929)	Chemistry and pharmacology of ephedrine
John Raleigh Briggs (1851–1907)	Investigation of peyote
Arthur Heffter (1860–1925)	Chemistry and pharmacology of peyote alkaloids
Thomas Moreno Y Maiz (1868) <sup>a</sup>	Pharmacological investigation of cocaine

<sup>a</sup> Year of completion of thesis.

Several investigators (Table 2.1) who played leading roles in the discovery and/or use of physostigmine, cocaine, ephedrine, emetine, pilocarpine, strychnine, etc. from traditional sources were physicians (Raza, 2006).

Moreover, to determine whether the chemical efforts were stimulated by ethnomedical claims and to correlate current uses for the compounds with such ethnomedical claims, in 2001 Fabricant et al., conducted a study on a total of 122 compounds; 80% of these compounds were used for the same (or related) ethnomedical purposes (Table 2.2). Further, it was discovered that these compounds were derived from only 94 species of plants.

**Table 2.2.** Drugs derived from plants, with their ethnomedical correlations and sources.  
(Fabricant, 2001).

<b>Drug</b>	<b>Action or clinical use</b>	<b>Plant source Acetyldigoxin</b>
<b>Acetyldigoxin</b>	Cardiotonic	<i>Digitalis lanata</i> Ehrh.
<b>Adoniside</b>	Cardiotonic	<i>Adonis vernalis</i> L.
<b>Aescin</b>	Anti-inflammatory	<i>Aesculus hippocastanum</i> L.
<b>Aesculetin</b>	Antidysentery	<i>Fraxinus rhynchophylla</i> Hance
<b>Agrimophol</b>	Anthelmintic	<i>Agrimonia eupatoria</i> L.
<b>Ajmalicine</b>	Circulatory disorders	<i>Rauwolfia serpentina</i> (L.) Benth ex. Kurz
<b>Allyl isothiocyanate</b>	Rubefacient	<i>Brassica nigra</i> (L.) Koch
<b>Andrographolide</b>	Bacillary dysentery	<i>Andrographis paniculata</i> Nees
<b>Anisodamine</b>	Anticholinergic	<i>Anisodus tanguticus</i> (Maxim.) Pascher
<b>Anisodine</b>	Anticholinergic	<i>Anisodus tanguticus</i> (Maxim.) Pascher
<b>Arecoline</b>	Anthelmintic	<i>Areca catechu</i> L.
<b>Asiaticoside</b>	Vulnerary	<i>Centella asiatica</i> (L.) Urban
<b>Atropine</b>	Anticholinergic	<i>Atropa belladonna</i> L.
<b>Berberine</b>	Bacillary dysentery	<i>Berberis vulgaris</i> L.
<b>Bergenin</b>	Antitussive	<i>Ardisia japonica</i> Bl.
<b>Bromelain</b>	Anti-inflammatory; proteolytic agent	<i>Ananas comosus</i> (L.) Merrill
<b>Caffeine</b>	CNS stimulant	<i>Camellia sinensis</i> (L.) Kuntze
<b>(+)-Catechin</b>	Haemostatic	<i>Potentilla fragaroides</i> L.
<b>Chymopapain</b>	Proteolytic; mucolytic	<i>Carica papaya</i> L.
<b>Cocaine</b>	Local anaesthetic	<i>Erythroxylum coca</i> Lamk
<b>Codeine</b>	Analgesic; antitussive	<i>Papaver somniferum</i> L.
<b>Colchicine</b>	Antitumor agent; antigout	<i>Colchicum autumnale</i> L.
<b>Convallotoxin</b>	Cardiotonic	<i>Convallaria majalis</i> L.
<b>Curcumin</b>	Choleretic	<i>Curcuma longa</i> L.
<b>Cynarin</b>	Choleretic	<i>Cynara scolymus</i> L.
<b>Danthron</b>	Laxative	<i>Cassia</i> spp.
<b>Deserpidine</b>	Antihypertensive; tranquilizer	<i>Rauwolfia canescens</i> L.
<b>Deslanoside</b>	Cardiotonic	<i>Digitalis lanata</i> Ehrh.
<b>Digitalin</b>	Cardiotonic	<i>Digitalis purpurea</i> L.
<b>Digitoxin</b>	Cardiotonic	<i>Digitalis purpurea</i> L.
<b>Digoxin</b>	Cardiotonic	<i>Digitalis lanata</i> Ehrh
<b>Emetine</b>	Amoebicide; emetic	<i>Cephaelis ipecacuanha</i> (Brotero) A. Richard
<b>Ephedrine</b>	Sympathomimetic	<i>Ephedra sinica</i> Stapf.
<b>Etoposide</b>	Antitumor agent	<i>Podophyllum peltatum</i> L.
<b>Gitalin</b>	Cardiotonic	<i>Digitalis purpurea</i> L.
<b>Glaucaroubin</b>	Amoebicide	<i>Simarouba glauca</i> DC.
<b>Glycyrrhizin</b>	Sweetener	<i>Glycyrrhiza glabra</i> L.
<b>Gossypol</b>	Male contraceptive	<i>Gossypium</i> spp.
<b>Hemsleyadin</b>	Bacillary dysentery	<i>Helmsleya amabilis</i> Diels
<b>Hydrastine</b>	Hemostatic; astringent	<i>Hydrastis canadensis</i> L.
<b>Hyoscamine</b>	Anticholinergic	<i>Hyoscamus niger</i> L.
<b>Kainic Acid</b>	Ascaricide	<i>Digenea simplex</i> (Wulf.) Agardh
<b>Kawain</b>	Tranquilizer	<i>Piper methysicum</i> Forst. f.
<b>Khellin</b>	Bronchodilator	<i>Ammi visnaga</i> (L.) Lamk.
<b>Lanatosides A, B, C</b>	Cardiotonic	<i>Digitalis lanata</i> Ehrh.
<b>Lobeline</b>	Smoking deterrent; respiratory stimulant	<i>Lobelia inflata</i> L.
<b>Monocrotaline</b>	Antitumor agent	<i>Crotalaria sessiliflora</i> L.
<b>Morphine</b>	Analgesic	<i>Papaver somniferum</i> L.
<b>Neoandrographolide</b>	Bacillary dysentery	<i>Andrographis paniculata</i> Nees
<b>Noscapine</b>	Antitussive	<i>Papaver somniferum</i> L.
<b>Ouabain</b>	Cardiotonic	<i>Strophanthus gratus</i> Baill.
<b>Papain</b>	Proteolytic; mucolytic	<i>Carica papaya</i> L.
<b>Phyllodulcin</b>	Sweetener	<i>Hydrangea macrophylla</i> (Thunb.) DC
<b>Physostigmine</b>	Cholinesterase inhibitor	<i>Physostigma venenosum</i> Balf.

<b>Picrotoxin</b>	Analeptic	Anamirta cocculus (L.) W.&A.
<b>Pilocarpine</b>	Parasympathomimetic	Pilocarpus jaborandi Holmes
<b>Podophyllotoxin</b>	Condylomata acuminata	Podophyllum peltatum L.
<b>Protoveratrine A &amp; B</b>	Antihypertensive	Veratrum album L.
<b>Pseudoephedrine</b>	Sympathomimetic	Ephedra sinica Stapf.
<b>Pseudoephedrine, nor-</b>	Sympathomimetic	Ephedra sinica Stapf.
<b>Quinine</b>	Antimalarial	Cinchona ledgeriana Moens ex. Trimen
<b>Quisqualic</b>	Acid Anthelmintic	Quisqualis indica L.
<b>Rescinnamine</b>	Antihypertensive; tranquilizer	Rauvolfia serpentina (L.) Benth ex. Kurz
<b>Reserpine</b>	Antihypertensive; tranquilizer	Rauvolfia serpentina (L.) Benth ex. Kurz
<b>Rhomitoxin</b>	Antihypertensive	Rhododendron molle G. Don
<b>Rorifone</b>	Antitussive	Rorippa indica (L.) Hochr.
<b>Rotenone</b>	Piscicide	Lonchocarpus nicou (Aubl.) DC.
<b>Rotundine</b>	Analgesic; sedative	Stephania sinica Diels
<b>Salicin</b>	Analgesic	Salix alba L.
<b>Santonin</b>	Ascaricide	Artemisia maritima L.
<b>Scillarin A</b>	Cardiotonic	Urginea maritima (L.) Baker
<b>Scopolamine</b>	Sedative	Datura metel L.
<b>Sennosides A &amp; B</b>	Laxative	Cassia spp.
<b>Silymarin</b>	Antihepatotoxic	Silybum marianum (L.) Gaertn.
<b>Stevioside</b>	Sweetener	Stevia rebaudiana Bertoni
<b>Strychnine</b>	CNS stimulant	Strychnos nux-vomica L.
<b>Teniposide</b>	Antitumor agent	Podophyllum peltatum L.
<b>Tetrahydropalmatine</b>	Analgesic; sedative	Corydalis ambigua (Pallas) Cham. & Schltal
<b>Theobromine</b>	Diuretic; bronchodilator	Theobroma cacao L.
<b>Theophylline</b>	Diuretic; bronchodilator	Camellia sinensis (L.) Kuntze
<b>Trichosanthin</b>	Abortifacient	Thymus vulgaris L
<b>Tubocurarine</b>	Skeletal muscle relaxant	Chondodendron tomentosum R. & P.
<b>Valepotriates</b>	Sedative	Valeriana officinalis L.
<b>Vincamine</b>	Cerebral stimulant	Vinca minor L.
<b>Xanthotoxin</b>	Leukoderma; vitiligo	Ammi majus L.
<b>Yohimbine</b>	Aphrodisiac	Pausinystalia yohimbe (K.Schum.) Pierre
<b>Yuanhuacine</b>	Abortifacient	Daphne genkwa Seib. & Zucc
<b>Yuanhuadine</b>	Abortifacient	Daphne genkwa Seib. & Zucc.

The ethnopharmacology knowledge can always serve as an innovative and powerful discovery engine for newer, safer and affordable medicines.

### 2.7.2. Screening of the promising natural sources for drug discovery

To the discovery of natural products with biologic activity three areas are involved, the *observation*, *description*, and *experimental investigation* of indigenous drugs and their biologic activities. It is based on botany, chemistry, biochemistry, pharmacology, and many other disciplines (anthropology, archaeology, history, and linguistics). Several approaches to drug discovery for selecting plants as candidates for drug discovery programs have been published (Phillipson, 1989; Kinghorn, 1994; Vlietinck, 1991; Farnsworth, 1966; Farnsworth, 1977; Harvey, 2000; Farnsworth, 1988); some of these approaches are :

- **Random selection followed by chemical screening.** These so-called phytochemical screening approaches [i.e., for the presence of cardenolides/bufadenolides, alkaloids, triterpenes, flavonoids, isothiocyanates, iridoids, etc. (Farnsworth *et al.*, 1966; Fabricant *et al.*, 2001)] have been used in the past and are currently pursued mainly in the developing countries. The tests are simple to perform, but it is usually impossible to relate one class of phytochemicals to specific biologic targets; for example, the alkaloids or flavonoids produce a vast array of biologic effects that are usually not predictable in advance.

- **Random selection followed by one or more biologic assays.** In the past, plant extracts were evaluated mainly in experimental animals, primarily mice and rats. From 1960 to 1981, more than 35,000 species were screened *in vitro* and later *in vivo* at National Cancer Institute (NCI). Taxol and camptothecin were discovered in this program. In 1986 the NCI program continued to collect and screen plants using a battery of 60 human tumor cell lines. Calanolide A, currently in Phase I clinical trials, was developed from this program (Fabricant *et al.*, 2001).

- **Follow-up of biologic activity reports.** These reports showed that the plant extracts had interesting biologic activity, but the extracts were not studied for their active principles. The literature from the 1930s through the 1970s contains these types of reports.

- **Follow-up of ethnomedical (traditional medicine) uses of plants.** Several types of ethnomedical information are available:

- *Plants used in organized traditional medical systems.* The individual arrangements all emphasize education based on an established, frequently revised body of written knowledge and theory. These systems are still in place today because of their organizational strengths, and they focus primarily on multicomponent mixtures (Bannerman *et al.*, 1983; Fabricant *et al.*, 2001).
- *Herbalism, folklore, and shamanism.* An apprenticeship system of information passed to the next generation through a shaman, curandero, traditional healer, or herbalist. The plants that are used are often kept secret by the practitioner, so little information about them is recorded; thus there is less dependence on scientific evidence as in systems of traditional medicine that can be subject to scrutiny. The shaman or

herbalist combines the roles of pharmacist and medical doctor with the cultural/spiritual/religious beliefs of a region or people, which are often regarded as magic or mysticism. This approach is widely practiced in Africa and South America (Rastogi *et al.*, 1982; Fabricant *et al.*, 2001).

- *Use of databases.* The NAPRALERT database (Fabricant *et al.*, 2001) currently contains information on 43,879 species of higher plants covering ethnomedical, chemical, and pharmacologic (including clinical studies) uses. Of these, 13,599 species contain ethnomedical data, distributed among 3,607 genera and 273 plant families. Thus it is possible to correlate ethnomedical use with experimental biochemical or pharmacologic activities (*in vitro*, *in vivo*, or *in humans*) to identify plants having both types of activity for a given effect-e.g., anticancer, antidiabetic, antimalarial.
- *Ethnomedical approach.* In 1985 an approach based on ethnomedical information to experimentally pursue plants as a source of drugs was established. The approach was designed primarily for implementation by developing countries, where lack of hard currency often prevents sophisticated types of research from being conducted. The possibility of drug development in the form of stable, standardized crude extracts and eventual development of the active principles from these plants was envisioned (Fabricant *et al.*, 2001) (Figure 2.4).

Some examples of drugs from plants that served as models for the next generation of drugs are exemplified as follows: Khellin [from *Ammi visnaga (L.) Lamk.*] was used as a bronchodilator in the United States until it was shown to produce nausea and vomiting after prolonged use. In 1955 a group of chemists in England set about to synthesize khellin analogs as potential bronchodilators with fewer side effects. This eventually led to the discovery of chromolyn (used as sodium chromoglycate), which stabilized cell membranes in the lungs to prevent the allergen induced release of the substance ultimately causing bronchoconstriction in allergic asthma patients (Fabricant *et al.*, 2001).

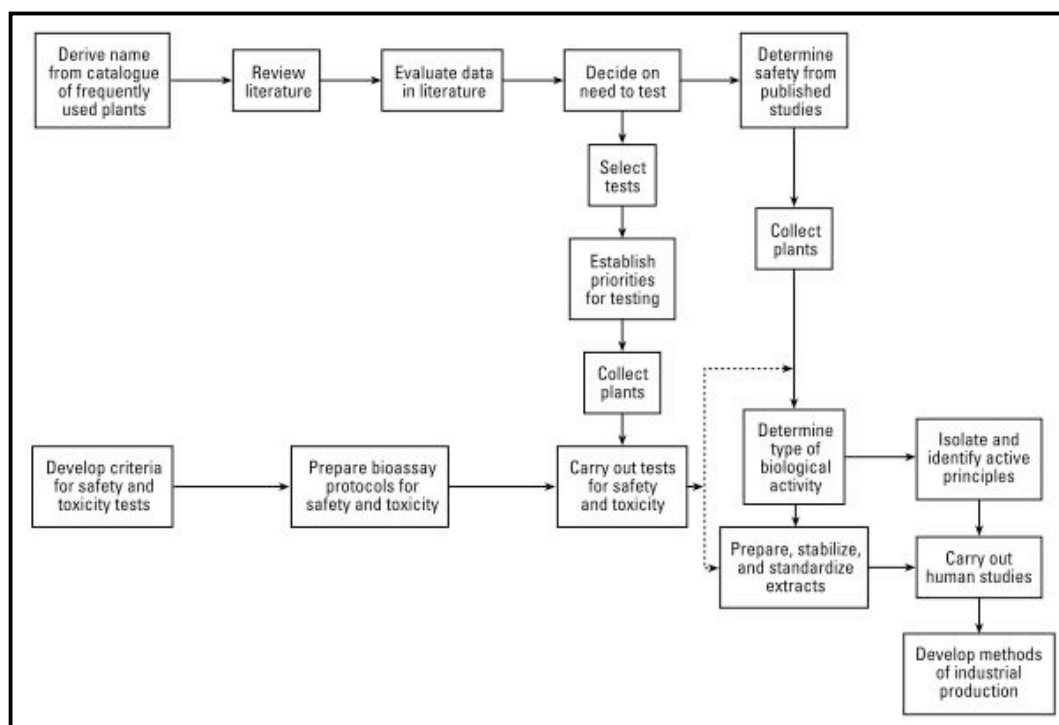


**Figure 2.4.** Flow chart of sequence for the study of plants used in traditional medicine.  
Adapted from Farnsworth et al. (Farnsworth, 1985)

## 2.8. Anticancer drug discovery

### 2.8.1. Cancer statistics

Worldwide, over ten million new cases of cancer (all sites excluding non-melanoma skin), with over six million deaths, were estimated in the year 2000 (Parkin, 2001; Parkin *et al.*, 2001). Since 1990 there has been a 22% increase in cancer incidence and mortality with the four most frequent cancers being lung, breast, colorectal, and stomach and the four most deadly cancers being lung, stomach, liver, and colorectal (Parkin *et al.*, 2001). Cancer is the second leading cause of death in developed countries, surpassed only by cardio-vascular disease (Jemal *et al.*, 2005).

In Morocco, cancer is a major public health problem and is responsible for 56% of morbidity related to chronic diseases (Tazi *et al.*, 2013). A total of 2,473 new cases were registered among residents in Rabat during the period 2006–2008. The overall world age-standardised rate (ASR) for all sites combined was 136.6/100,000 for men and 114.5/100,000 for women (Tazi *et al.*, 2013). About 176,620 new cancer cases are expected to be diagnosed among African Americans in 2013, including 94,540 cases among men and 82,080 cases among women (Figure 2.5). Prostate cancer is expected to be the most commonly diagnosed cancer in men and breast cancer the most common in women. Cancers of the lung and colorectum

will be the second and third most commonly diagnosed cancers in both African American men and women (Desantis *et al.*, 2013).

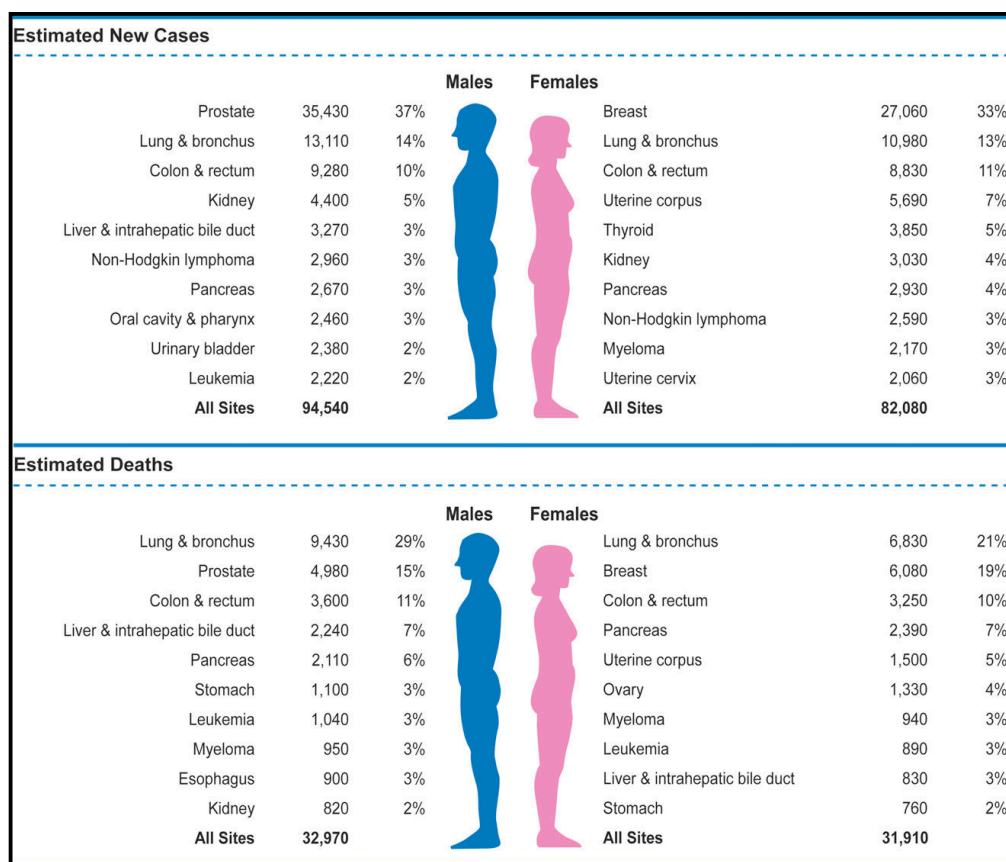


**Figure 2.5.** Leading Sites of New Cancer Cases and Deaths Among African Americans, 2013 Estimates\* (Desantis *et al.*, 2013)

\*Estimates are rounded to the nearest 10 and exclude basal cell and squamous cell skin cancers and in situ carcinoma except urinary bladder.

Although these figures are disquieting, some progress has been made in cancer diagnosis and treatment as evident through the high incidence of lung, breast and prostate, as compared with their relatively lower mortality (Parkin, 2001; Jatoi and Miller, 2003; Jemal *et al.*, 2005). From 2000 to 2009, incidence rates decreased by 1.4% per year among African American men; however, rates have remained unchanged among African American women during this period (Figure 2.6).

Drug discovery from medicinal plants has played an important role in the treatment of cancer and, indeed, most new clinical applications of plant secondary metabolites and their derivatives over the last half century have been applied towards combating cancer (Newman *et al.*, 2000, Newman *et al.*, 2003; Butler, 2004; Balunas *et al.*, 2005).



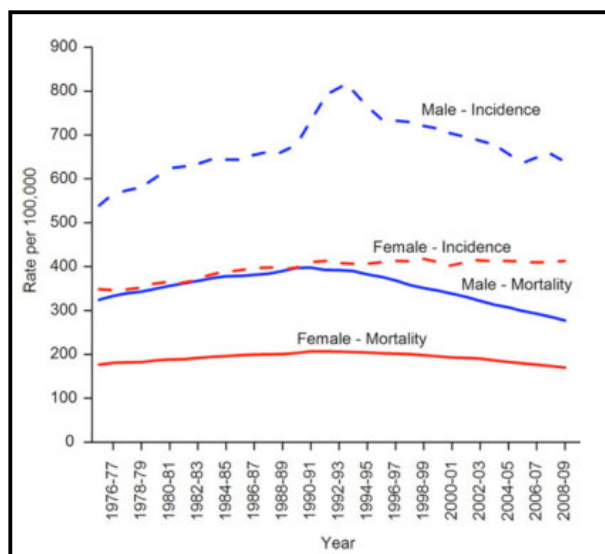


**Figure 2.6.** Age-Adjusted Cancer Incidence and Mortality Rates Among African Americans by Sex, 1975 to 2009 (Desantis *et al.*, 2013)

### 1.8.2. Secondary metabolites as anticancer agents

Large-scale anticancer drug discovery and screening programs such as those promoted by the National Cancer Institute (NCI) have played an important role in the development of anticancer natural compounds. Of all available anticancer drugs between 1940 and 2002, 40% were natural products per se or natural product-derived with another and 8% was considered natural product mimics (Newman *et al.*, 2003). The most famous anticancer natural product is Taxol, which was originally isolated from *Taxus brevifolia* Nutt. (*Taxaceae*) and later was demonstrated that it was produced by endophytic fungus *Taxomyces andreanae* from *Taxus brevifolia* (Strobel *et al.*, 1993; Aly, 2007). Paclitaxel (taxol®) was clinically introduced to the U.S. market in the early 1990s (Wall and Wani, 1996; Oberlies and Kroll, 2004). The taxanes, including paclitaxel and derivatives, act by binding tubulin without allowing depolymerization or interfering with tubulin assembly (Balunas, 2005). Taxol is the world's first billion dollar anticancer drug and is used to treat a number of other human tissue proliferating diseases as well (Strobel, 2002).

Moreover, the cytotoxic plant alkaloid, camptothecin, originally described from *Camptotheca acuminata* and *Nothapodytes foetida*, showed unacceptable myelosuppression (Wall and Wani, 1996; Balunas, 2005). Interest in camptothecin was revived when it was found to act by selective inhibition of topoisomerase I, involved in cleavage and reassembly of DNA (Cragg and Newman, 2004). Clinical trials of camptothecin, which was identified in cultures of

*Entrophospora infrequens* endophytic in *Nothapodytes foetida*, are undergoing since 1992 as anticancer drug (Amna *et al.*, 2006).

Together, the taxanes and the camptothecins accounted for approximately one-third of the global anticancer market in 2002, over 2.75 billion dollars (Oberlies and Kroll, 2004).

Another anticancer drug, which has been given in chemotherapy treatment for some types of cancer including leukemia, lymphoma, breast and lung cancer for many years, is the indole derivative vincristine. This drug, available under the trade names Oncovin®, Vincasar®, and Vincrex®, was originally obtained from *Catharanthus roseus*. Very recently, a Chinese group reported preliminary evidence that vincristine might be produced by *Fusarium oxysporum* endophytic in the same plant (Zhang *et al.*, 2006). Since then fungal microorganisms became a hunting ground for novel drug leads (Strobel and Daisy, 2003; Larsen *et al.*, 2005). This stimulated pharmaceutical companies to sample and screen large collections of fungal strains (Butler, 2004). Consequently, promising novel natural product leads were isolated. Many of these compounds can be produced in large quantities and at a reasonable cost by fermentation employing wild type or genetically altered fungi. The search for new drug candidates is still pressing to find the adequate cures for not only cancer but also newly emerging diseases, such as drug-resistant pathogenic microbes, or parasitic protozoans, are urgently needed. As microorganisms occupy almost every niche on earth (Strobel, 2002), scientists speculate that many undescribed species exist in unexplored habitats, where the incidence of finding microorganisms that produce novel bioactive constituents is high (Hawksworth and Rossman, 1997).

## **2.9. Natural products as inhibitors of Hsp 90 chaperon machinery**

### **2.9.1. Hsp 90 chaperone machinery**

The 90-kDa heat shock protein Hsp90 has an important role in the maintenance of malignant transformation and is required to keep the folded and functionally active conformation of several aberrantly functioning onco-proteins. In this respect, Hsp90 regulates (in a transformation-specific manner) signaling pathways necessary for the growth, survival and limitless replicative potential of most tumors. Whereas in normal cells Hsp90 interacts in a low-affinity 1-2%, dynamic fashion with a plethora of proteins to help them fold and mature, in malignant cells tight association of Hsp90 with onco-client proteins maintains their ability to function in the dysregulated state and seems to be essential for their transforming, aberrant

---

activity which increases its affinity to 4-6%. This is most likely because cancer cells must cope with numerous external and internal stressors that are not experienced by normal cells, such as elevated temperature and oxygen or nutrient deprivation or mutation of important regulatory proteins (Figure 2.7) (Rodina *et al.*, 2007; Chadli *et al.*, 2008).

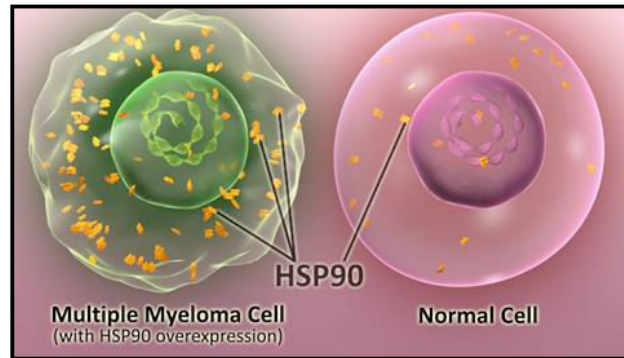


**Figure 2.7.** The expression of Hsp90 in normal and multiple myeloma cell  
(@cancer.gov.com)

Hsp90 was originally identified by chance in the early 1960s as one of a group of so-called ‘heat shock proteins’ (Hsps) that were induced at elevated temperatures in the salivary gland of the fruit fly *Drosophila melanogaster*, providing protection against hyperthermia (thermotolerance) and other cellular stresses (Workman *et al.*, 2007). Hsp90 works in concert with a number of chaperones and co-chaperones to modulate the conformation of Hsp90 and its client proteins. Over 20 co-chaperone proteins, such as p23, Cdc37, HIP, HOP, PP5, UNC45A, and immunophilins (FKBP51, FKBP52, and Cyp40), have been shown to regulate the function of the Hsp90 protein-folding machine (Chadli *et al.*, 2008).

Hsp90’s clientele is dominated by kinases, hormone receptors and transcription factors, many of which are oncogenic and have a key role in the hallmark traits of cancer. In addition to cancer, the Hsp90 machine has also been implicated as a target to treat neurodegenerative and cardiovascular diseases.

### 2.9.2. Hsp 90 inhibitors

Heat shock protein 90 “Hsp90” is a promising therapeutic target. The inactivation of Hsp90 delivers a combinatorial attack on multiple signaling pathways leading to a more efficient killing of cancer cells and reducing resistance to chemotherapy (Workman, 2004). Extensive

research efforts in the last two decades have resulted in over 40 clinical trials in phases I-III with 13 small molecule inhibitors of Hsp90 ongoing worldwide. Hsp90 inhibitors can be classified as those that target the N-terminal domain, the C-terminal domain, Hsp90 co-chaperones or client-protein/Hsp90 interactions (Neckers *et al.*, 2012).

Hsp90 inhibitors, initially natural products and later synthetic small molecules, have proved invaluable as chemical tools to investigate Hsp90 biology; the initial chemical probes have now morphed into drugs showing therapeutic activity in cancer patients.

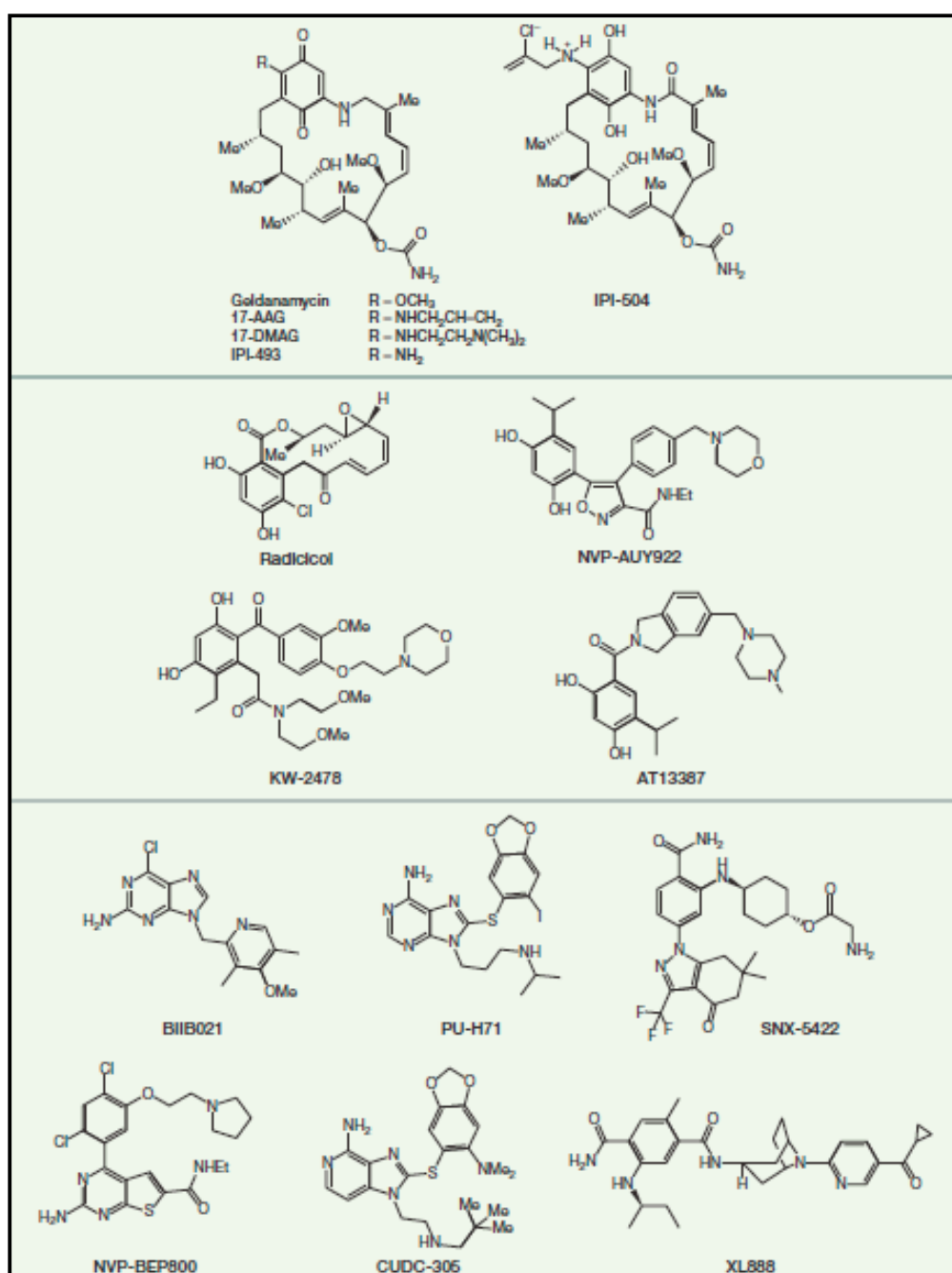


**Figure 2.8.** Chemical structures of selected Hsp90 inhibitors (Neckers, 2012)

The natural products geldanamycin and radicicol as well as semisynthetic derivatives 17-N-allylamino-17-demethoxygeldanamycin (17AAG) (Figure 2.8) target the ATP-binding site of the N-terminal domain to destabilize Hsp90 client complexes, leading to their cellular degradation through the proteasome pathway.

Recently, a Chadli team reported that the natural product gedunin inactivates Hsp90 chaperoning machinery by targeting the co-chaperone p23 *in vivo* and *in vitro*. Gedunin is a tetranortriterpenoid natural product that is isolated from the *Meliaceae* family of medicinal plants and has been used for the treatment of malaria and other infectious diseases in traditional Indian medicine (Chadli, 2008).

### **2.9.3. Example of the inhibition of Hsp 90 in small-cell lung cancer**

Hsp90 operates with a number of co-chaperones, including Hsp70 and Hop (Hsp90 organizing protein, also known as p60), to orchestrate the ATP-dependent maturation of many oncogenic client proteins (CP). Inhibition of Hsp90 function leads to ubiquitin proteasome-dependent client protein degradation and inhibition of multiple aspects of the malignant phenotype, including evasion of apoptosis in SCLC. During apoptosis, cytochrome c (cyt c) is released from the mitochondria to associate with Apaf-1. This triggers the activation of proteolytic caspases, which induce apoptosis. Mitochondrial permeabilization is controlled by a balance of antiapoptotic (for example, BCL2) and proapoptotic (for example, BAX and BAD) members of the BCL2 family.

Activation of the kinase AKT (an Hsp90 client protein) shifts the balance in favor of cell survival by phosphorylating BAD, inducing its inactivation by association with 14-3-3 protein. Hsp90 and Hsp70 are both antiapoptotic, acting at several points in the apoptotic cascade. Rodina group have shown Hsp90 to be a critical dual regulator of apoptosis in SCLC by supporting AKT activation, which in turn prevents cyt c release, and also by negatively regulating the association of Apaf-1 with caspase 9 (Rodina *et al.*, 2007).

Hsp90 inhibition reverses these effects, leading to extensive apoptosis. Several compounds that modulate the activity of Hsp90 (17-AAG, radicicol, PU24FCI) and Hsp70 (MAL3-101) have been described, along with compounds that can alter the expression of Hsp70 and other heat shock proteins in response to stress (for example, KNK437) (Paul Workman *et al.*, 2007).

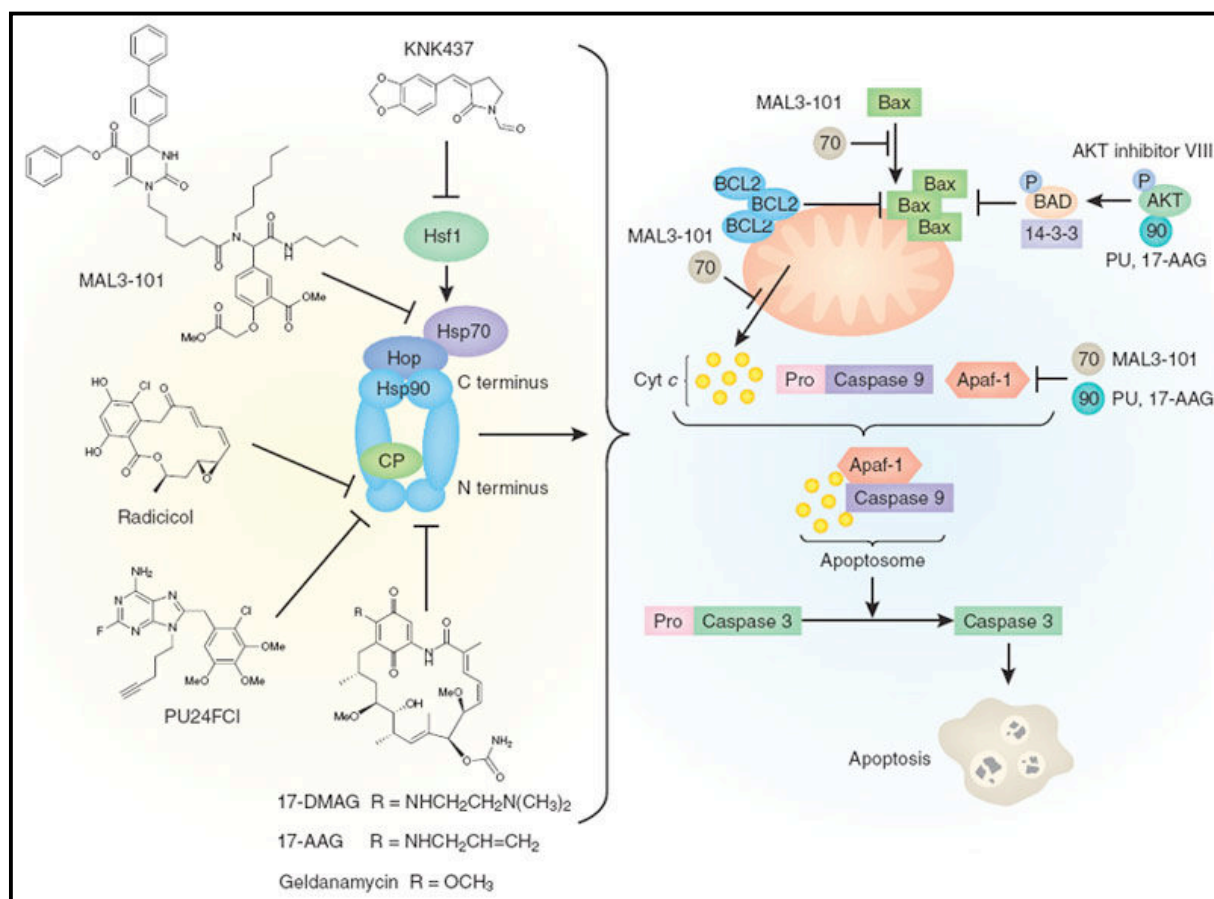


**Figure 2.9.** Inhibition of Hsp90 leads to apoptosis in small-cell lung cancer (SCLC).

(Paul Workman *et al.*, 2007)

Since then, natural drug discovery has focused on the inhibitors of chaperone Hsp90 (heat shock protein 90) because it plays a key role in assisting mutated proteins, making it an attractive cancer drug target.

### **3. Materials and Methods**

#### **3.1. Biological material**

##### **3.1.1. Plant material**

###### **3.1.1.1. Ethnopharmacological study**

###### *Study design*

The work consists of an ethnopharmacological, prospective and randomized investigation. It was carried out on a period of seven months (from September 2009 to March 2010) in two departments at the National Institute of Oncology in Rabat (Department of Chemotherapy and Department of Radiotherapy). The National Institute of Oncology (NIO) is a center where patients come from all over Morocco. The patients are taken randomly, to have a heterogeneous point of view: origin, sex, age, socio-professional class, type and stage of cancer. This study has been carried out with the permission of NIO director. All patients have been informed of the study objective and gave their consent.

###### *Selection of parameters*

An exhaustive questionnaire was established including:

- Information related to the identification of the patient [registration number, sex, age, origin, province region (rural or urban), and socio-professional class];
- Information on pathology [nature, localization, stage and degree of tumor extension as well as protocol and treatment follow-up];
- Information on the use of traditional medicine [use or non use of TM, its use along with modern medicine];
- Information on the anti-cancer plants used [vernacular name and the part of the plant used, the method of preparation, dosage, treatment duration and observance during phytotherapy];

After collecting all the information, a table was prepared to gather different information on the plants used with their vernacular name and their scientific name.

###### *Statistical analysis*

Statistical analysis of data was carried out by Graphpad program (for Windows version 5.01. Graphpad, San Diego, CA, USA) and statistical methodology was based on two axes, which includes descriptive statistics and statistical analysis. Descriptive statistics reveal the



frequencies and characteristics of each parameter (average/mean, minimum, maximum). Results are expressed in raw values for qualitative parameters and in mean  $\pm$  standard deviation for quantitative parameters. The number of valid data (n active) of each variable has been mentioned in results section. Statistical analysis was based on associated tests such as the Khi 2 test which measures the gap between the observed frequencies and theoretical frequencies. We have used this test to compare the two sexes. We have also used one factor variance analysis (ANOVA), which estimates intergroup variation (report F). The results are considered significant where p is below 0.05, very significant when  $p < 0.01$  and highly significant when  $p < 0.001$ .

On the other hand, calculation of relative risk (RR) for each age interval as well as sex variable concerning the use of TM has allowed us to estimate the degree of association between two given parameters. If value 1 is included in the confidence interval (CI) of RR, we deduce that there is no association between these two parameters. However, if value 1 is excluded of the CI of RR, we deduce the existence of association between them.

### 3.1.1.2. Plant worked on during the study

*Thymelaea lythroides* was selected according to an ethnopharmacological study of traditional plants used in Morocco by cancer patients as herbal therapeutics (Kabbaj *et al.*, 2012). *Thymelaea lythroides*, an ibero-endemic plant in Morocco, is popularly used as medicinal plant to treat otitis, diabetes, rheumatism, inflammation of the prostate and uterus cancer (Gmira *et al.*, 2007).

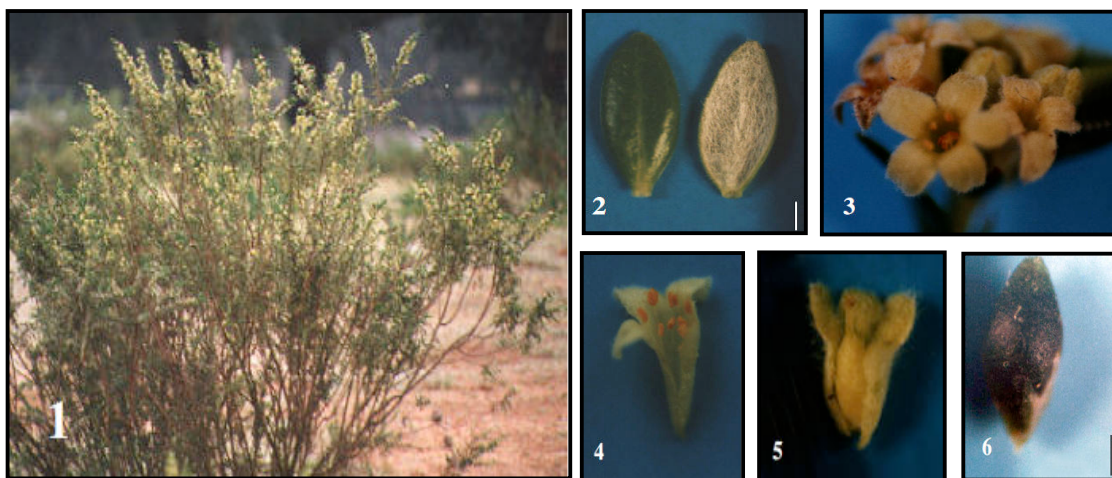


**Figure 3.1.** *Thymelaea lythroides*. (1: Aerial part of *T. lythroides*. 2: Leaf. 3: Flower. 4: Flower male. 5: Flower female. 6: Seed) (Dohou, 2003)



### 3.1.1.3. Field trip and sample collection

Fresh, healthy areal parts of *Thymelaea lythroides* have been collected from the Maâmora forest (NI29-08) in Rabat, Morocco. Small stem, leaf and flower pieces were directly placed in paper bags and stored dark and at 4°C until the isolation procedure of the fungi was performed two days later.

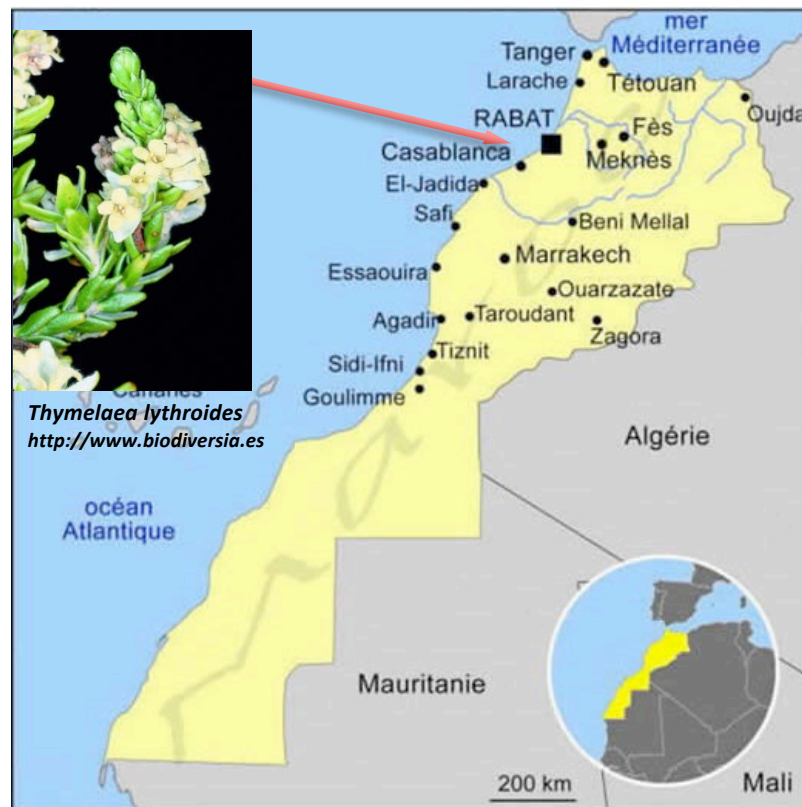


Figure 3.2 Collection area of *Thymelaea lythroides*.

### 3.1.1.4. Taxonomy of collected plant sample

Phylum: *Plantae*

Class: *Magnoliopsida*

Order: *Myrtales*

Family: *Thymelaeaceae*

Genus: *Mentha*

Specie: *Thymelaea lythroides*

## 3.1.2. Fungal Material

### 3.1.2.1. Pure fungal strain isolated from the selected plant

Fresh, healthy parts of *Thymelaea lythroides* (leaf, stem and flower) were rinsed twice with sterilized distilled water. Surface sterilization was achieved by immersing the parts of the

plant in 70% ethanol for 2 min (twice) followed by rinsing in sterilized distilled water. Then, they were cleaved aseptically into small segments (approx.1 cm in length). The material was placed onto a Petri dish with malt agar medium containing chloramphenicol and streptomycin to suppress bacterial growth. After one-week incubation at room temperature, when fungal mycelium tips were observable, each hyphal tip was transferred onto a fresh malt agar dish. For purification of the fungal strains this step was repeated several times until the colony was deemed uniform.

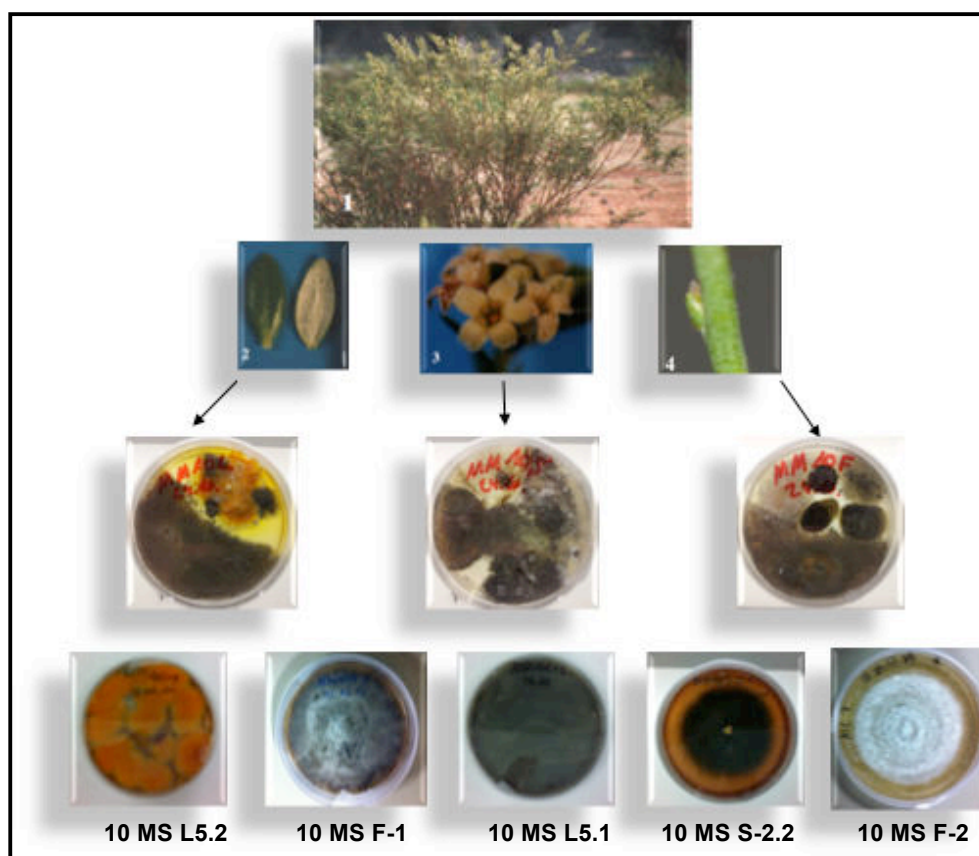


Figure 3.3. Pure fungal strain from *Thymelaea lythroides*.

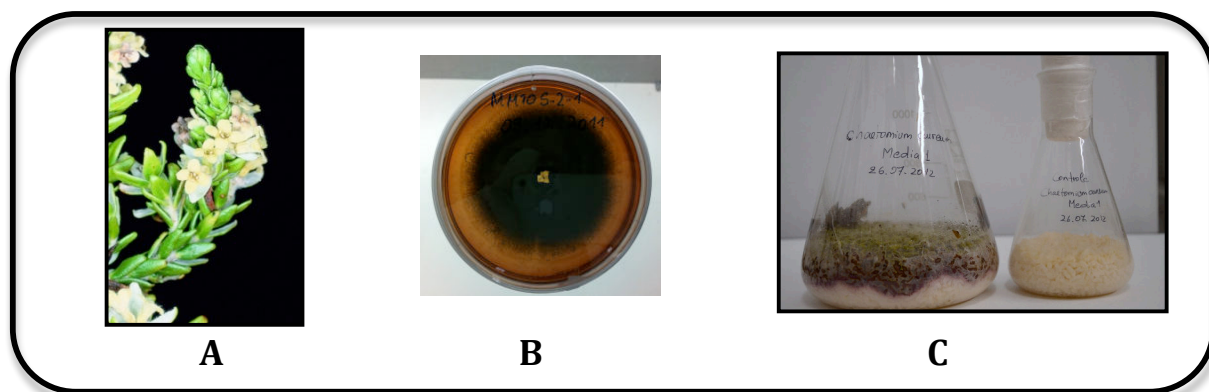
### 3.1.2.2. Taxonomy of isolated fungi

Table 3.1. Taxonomy of isolated fungi.

Fungal code	Plant part	Fungal species	Family
10 MS L-5.2	Leaf	<i>Epicoccum nigrum</i>	Incertae sedis
10 MS F-1	Flower	<i>Altenaria sp.</i>	Pleosporaceae
10 MS L.5.1	Leaf	<i>Cladosporium sp.</i>	Davidiellaceae
10 MS S-2.2	Stem	<i>Chaetomium aureum</i>	Chaetomiaceae
10 MS F-2	Flower	<i>Pleospora sp.</i>	Pleosporaceae

### 3.1.2.3. Endophytic fungi worked on during the study

After conducting biological activity screening test toward the five fungal strains, derived from the plant *Thymelaea lythroides*, originated from Morocco, one fungal strain was eventually selected for further scrutinizing of their secondary metabolite contents, which is *Chaetomium aureum* (Figure 3.4).



**Figure 3.4.** *Chaetomium aureum* (A: *Thymelaea lythroides*; B: pure strain in plate agar; C: Culture on solide rice medium)

## 3.2. Isolation and cultivation of endophytic fungi

### 3.2.1. Composition of media

Medium for isolation of fungal strains from the plant or purification and short term storage of the pure fungal strain

Bacto agar (Galke)	15.0 g
Malt extract (Merck)	15.0 g
Artificial sea salt (Sera)	10.0 g
pH	7.4-7.8 (adjusted with NaOH/HCl)
Dem. Water	ad 1000 mL

For the isolation of endophytic fungi from plant tissues chloramphenicol or streptomycin (0.2 or 0.1 g, respectively) were added to the medium to suppress bacterial growth.

MexA medium for long term storage

Malt extract (Merck)	20.0 g
Yeast extract (Sigma)	0.1 g
Glycerin (Roth)	50.0 g
Artificial sea salt (Sera)	10.0 g
Bacto Agar (BD)	13.0 g
Dem. water	ad 1000 mL

Wickerham medium for liquid cultures

Yeast extract	3.0 g
Malt extract	3.0 g
Peptone	5.0 g
Glucose	10.0 g
Distilled water	to 1000 mL
pH	7.2 - 7.4 (adjusted with NaOH/HCl)

Solid rice medium

Rice	100 g
Dem. Water	110 mL

Solid red bean medium

Bean	100 g
Dem. Water	110 mL

Solid chickpeas medium

Bean	100 g
Dem. Water	110 mL

Solid corn medium

Bean	100 g
Dem. Water	110 mL

Solid peas medium

Bean	100 g
Dem. Water	110 mL

Solid Beans M medium

Bean	100 g
Dem. Water	110 mL

Solid black bean medium

Bean	100 g
Dem. Water	110 mL

Solid lentils medium

Bean	100 g
Dem. Water	110 mL

Solid carrots medium

Bean	100 g
Dem. Water	110 mL

Solid potaetos medium

Bean	100 g
Dem. Water	110 mL

### **3.2.2. Short term storage of pure strains**

For short storage, pure fungal strains in malt agar plate were stored at 4°C for a maximum period of 6 months, and then re-inoculated onto fresh malt agar plate.

### **3.2.3. Long term storage of pure fungal strains**

For long term storage, pieces of pure fungal strains were transferred to 10 mL BD Falcon® tubes containing approx. 5 mL MexA medium. After approx. from three to seven days, the growths strain was placed in a deep freezer at -80°C.

### **3.2.4. Cultivation for screening and isolation**

Pure fungal strain was inoculated in a 1000 mL Erlenmeyer flask containing 100 g of solid rice medium and 110 ml of distilled water, which were autoclaved. Small pieces were cut from a Petri dish containing the purified fungus, and then transferred under sterile conditions to the sterilised rice medium. Cultivation was performed at room temperature under static conditions for 4-6 weeks.

Small scale fermentation was carried out in one Erlenmeyer flask to gain enough extract for first bioactivity screening. For mass growth to gain enough fungal extract for isolation of secondary metabolites, 20 flasks of rice medium were inoculated.

## **3.3. Identification of plant sample and pure fungal strain**

### **3.3.1. Plant identification**

A voucher specimen of the plant was identified by Prof. FZ. ALAOUI, Department of Botany, Faculty of Sciences, Mohamed V University and Prof. Dr. M. IBN TATOU, Scientific Institute of Rabat, Morocco. Reference samples are deposited as a herbarium at the Scientific Institute of Rabat, in which a collection number (RAB 77777) has been assigned.

### **3.3.2. Fungal identification**

Fungal strains were identified based on the analysis of the DNA sequences of the internal transcribed spacer regions (ITS) of its ribosomal RNA gene. The identification was performed according to a molecular biologic protocol previously described (Kjer *et al.*, 2010).

#### **3.3.2.1. DNA extraction**

The extraction of fungus DNA was carried out with ZR Fungal/Bacterial DNA Kit™ (ZYMO RESEARCH, D6005), following the manufacturer protocol:

**Step 1-** Add 50-200 mg of fungal cells to a ZR BashingBead™ Lysis Tube. Add 750 µl Lysis Solution to the tube.

**Step 2-** Vortex for 5 minutes. Processing times may be as little as 40 seconds when using high-speed cell disrupters.

**Step 3-** Centrifuge the ZR BashingBead™ Lysis Tube in a microcentrifuge at 10,000 x g for 1 minute.

**Step 4-** Transfer up to 400 µl supernatant to a Zymo-Spin™ IV Spin Filter (orange top) in a Collection Tube and centrifuge at 7,000 rpm (~7,000 x g) for 1 minute. (Snap off the base of the Zymo-Spin IV™ Spin Filter prior to use).

**Step 5-** Add 1,200 µl of Fungal/Bacterial DNA Binding Buffer to the filtrate in the Collection Tube from Step 4.

**Step 6-** Transfer 800 µl of the mixture from Step 5 to a Zymo-Spin™ IIC Column in a Collection Tube and centrifuge at 10,000 x g for 1 minute.

**Step 7-** Discard the flow through from the Collection Tube and repeat Step 6.

**Step 8-** Add 200 µl DNA Pre-Wash Buffer to the Zymo-Spin™ IIC Column in a new collection Tube and centrifuge at 10,000 x g for 1 minute.

**Step 9-** Add 500 µl Fungal/Bacterial DNA Wash Buffer to the Zymo-Spin™ IIC Column and centrifuge at 10,000 x g for 1 minute.

**Step 10-** Transfer the Zymo-Spin™ IIC Column to a clean 1.5 ml micro-centrifuge tube and add 100 µl (25 µl minimum) DNA Elution Buffer directly to the column matrix or sterile water.

**Step 11-** Centrifuge at 10,000 x g for 30 seconds to elute the DNA.

After isolation of the genomic DNA, quantification was done after agarose Gel Electrophoresis for DNA with the Software GelQuant.NET, where the fluorescent of the samples, were compared to that of a known amount of the latter.

### 3.3.2.2. DNA amplification

DNA amplification by PCR was performed using Hot StarTaq Master Mix Taq polymerase (Qiagen) and the primers (Invitrogen):

ITS1	5'-TCCGTAGGTGAACCTGCGG-3'	White <i>et al.</i> 1990
ITS4	5'-TCCTCCGCTTATTGATATGC-3'	White <i>et al.</i> 1990
NS1	5'-GTAGTCATATGCTTGTCTC-3'	White <i>et al.</i> 1990
Fung	5'-ATTCCCCGTTACCCGTTG-3'	May <i>et al.</i> 2001

PCR program:

ITS1\ITS4:

Initial denaturation	95,0 °C	15:00	min.	35 times
Denaturation	95,0 °C	1:00	min.	
Annealing	56,0 °C	0:30	sec.	
Extension	72,0 °C	1:00	min.	
Final extension	72,0 °C	10:00	min.	

### 3.3.2.3. Purification of PCR products

DNA purification from Agarose Gel was carried out with QiaQuick Gel Extraction Kit (Quiagen) following the manufacturer instructions:

**Step 1-** Excise the DNA fragment from the agarose gel with a clean, sharp scalpel. Minimize the size of the gel slice by removing extra agarose.

**Step 2-** Weigh the gel slice in a colorless tube. Add 3 volumes of Buffer QG to 1 volume of gel (100 mg ~ 100 µl).

**Step 3-** Add 300 µl of Buffer QG to each 100 mg of gel. For >2% agarose gels, add 6 volumes of Buffer QG. The maximum amount of gel slice per QIAquick column is 400 mg; for gel slices >400 mg use more than one QIAquick column.

**Step 4-** Incubate at 50°C for 10 min (or until the gel slice has completely dissolved). To help dissolve gel, mix by vortexing the tube every 2–3 min during the incubation.

IMPORTANT: Solubilize agarose completely. For >2% gels, increase incubation time.

**Step 5-** After the gel slice has dissolved completely, check that the color of the mixture is yellow (similar to Buffer QG without dissolved agarose). If the color of the mixture is orange or violet, add 10 µl of 3 M sodium acetate, pH 5.0, and mix. The color of the mixture will turn to yellow. The adsorption of DNA to the QIAquick membrane is efficient only at pH ≤7.5. Buffer QG contains a pH indicator which is yellow at pH ≤7.5 and orange or violet at higher pH, allowing easy determination of the optimal pH for DNA binding.

**Step 6-** Add 1 gel volume of isopropanol to the sample and mix. For example, if the agarose gel slice is 100 mg, add 100 µl isopropanol. This step increases the yield of DNA fragments <500 bp and >4 kb. For DNA fragments between 500 bp and 4 kb, addition of isopropanol has no effect on yield. Do not centrifuge the sample at this stage.

**Step 7-** Place a QIAquick spin column in a provided 2 ml collection tube.

**Step 8-** To bind DNA, apply the sample to the QIAquick column, and centrifuge for 1 min. The maximum volume of the column reservoir is 800 µl. For sample volumes of more than 800 µl, simply load and spin again.

**Step 9-** Discard flow-through and place QIAquick column back in the same collection tube. Collection tubes are re-used to reduce plastic waste.

**Step 10-** Add 0.5 ml of Buffer QG to QIAquick column and centrifuge for 1 min. This step will remove all traces of agarose. It is only required when the DNA will subsequently be used for direct sequencing, in vitro transcription or microinjection.

**Step 11-** To wash, add 0.75 ml of Buffer PE to QIAquick column and centrifuge for 1 min.  
Note: If the DNA will be used for salt sensitive applications, such as blunt-end ligation and direct sequencing, let the column stand 2–5 min after addition of Buffer PE, before centrifuging.



**Step 12-** Discard the flow-through and centrifuge the QIAquick column for an additional 1 min at  $\geq 10,000 \times g$  ( $\sim 13,000$  rpm).

IMPORTANT: Residual ethanol from Buffer PE will not be completely removed unless the flow-through is discarded before this additional centrifugation.

**Step 13-** Place QIAquick column into a clean 1.5 ml micro-centrifuge tube.

**Step 14-** To elute DNA, add 50  $\mu$ l of Buffer EB (10 mM Tris•Cl, pH 8.5) or H<sub>2</sub>O to the center of the QIAquick membrane and centrifuge the column for 1 min at maximum speed. Alternatively, for increased DNA concentration, add 30  $\mu$ l elution buffer to the center of the QIAquick membrane, let the column stand for 1 min, and then centrifuge for 1 min. The purified PCR products can be stored at -20 °C before sequencing.

#### **3.3.2.4. Fungi Identification**

DNA sequencing was performed using primers ITS1 or NS1 and performed by BMBF, Heinrich Heine Universität Düsseldorf or GATC Biotech AG. Nucleotide sequences of ITS rDNA of each taxon were compared using a Blast search in the nucleotide database in GenBank.

### **3.4. Extraction of plant and fungal cultures**

#### **3.4.1 Extraction and fractionation of *Thymelaea lythroides* plant material**

The dried aerial part of *Thymelaea lythroides* was extracted extensively with EtOAc. The EtOAc extract was washed with water, taken to dryness, and partitioned between *n*-hexane and 90% MeOH. The 90% MeOH soluble fraction was fractionated over Silica using *n*-Hexane:EtOAc and DCM:MeOH gradient elution and the obtained fractions were analysed by HPLC and LC/MS.

#### **3.4.2. Extraction and fractionation of fungi grown on solid rice medium**

To each 1L Erlenmeyer about 250 mL EtOAc were added and culture media were then cut into small pieces to allow exhaustive extraction with EtOAc. The extraction left 24h under agitation. The contents were filtered under vacuum using a Buchner funnel. The extraction repeated three times with EtOAc until exhaustion. The combined EtOAc phases were washed with 300 mL demineralised water to eliminate remaining sugar and starch.

All obtained extracts were taken to dryness under reduced pressure at 40°C and partitioned between 90% MeOH and *n*-hexane to remove the fatty acids. After evaporating the solvent, these crude extracts were submitted to TLC, analytical HPLC, LC-MS and also to bioactivity screening including cytotoxicity and antimicrobial assays. The extraction scheme is described in Figure 3.4.

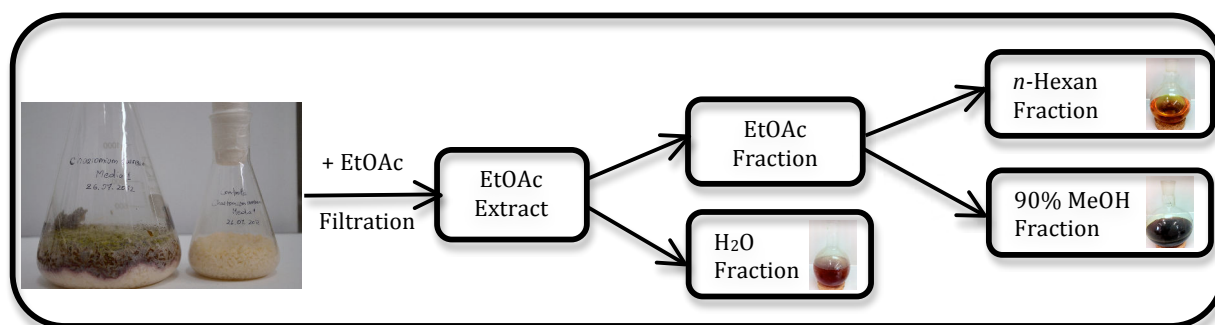


**Figure 3.5.** Extraction and fractionation of solid rice culture

### 3.5. Isolation of secondary natural products

For the isolation of natural products different chromatographic methods depending on the nature of the product have been used. A chromatographic system comprises two phases, a stationary phase absorbing the compounds according to their physical properties, e. g. polarity (silica gel, normal or reversed phase), size (Sephadex LH-20) or charge (Diaion), whereas the mobile phase moves through the stationary phase and gradually elutes the compounds according to their affinity from it.

#### 3.5.1. Thin layer chromatography (TLC)

Thin-layer chromatography is, in essence, liquid chromatography performed on a stationary phase present as a sheet or layer of solid particles immobilized on a planar support, or a layer of polymerized substance (Yrjönen, 2004). TLC is a mature and very established technique, frequently used in many fields of applications ranging from natural product analysis to chemistry or pharmaceutical applications.

For rapid characterization and testing of extracts, fractions and isolated compounds the thin layer chromatography was used. After development of the TLC plate in a saturated fluid chamber, the band separation was observed under a UV lamp at 254 or 366 nm, followed by spraying TLC plates with anisaldehyde-sulphuric acid or ninhydrin spraying reagent and

heating plates at 110°C for 10 min in an oven heated.

During this work, TLC was performed on pre-coated TLC plates using the following systems:

TLC on silica gel 60 F254, layer thickness 0.2 mm (Merck):

- *n*-hexane:EtOAc [90:10, 80:20 and 70:30 (V/V)] and *n*-hexane:MeOH [95:5 and 90:10 (V/V)] for non-polar compounds
- DCM:MeOH [95:5, 90:10, 85:15, 80:20 and 70:30 (V/V)] for semi-polar compounds
- EtOAc:MeOH:H<sub>2</sub>O [30:5:4, 30:65 and 30:7:6 (V/V)] for polar compounds TLC on Diol F254S, layer thickness 0.25 mm (Merck):
- *n*-hexane:EtOAc [90:10, 80:20 and 70:30 (v/v)] EtOAc:acetone [95:5 and 90:10 (V/V)]

TLC on reversed phase RP-18, F254 S, layer thickness 0.25 mm (Merck):

- MeOH:H<sub>2</sub>O (90:10, 80:20, 70:30 and 60:40 (V/V)).

The different compounds could be compared and identified due to their specific retention factors in defined chromatographic systems. These so-called R<sub>f</sub>-values can be calculated as migration distance of compound migration distance of solvent front.

With ninhydrin spray reagent (0.2 % in MeOH, m/V) amino acids, amines and amino sugars can be detected, and the anisaldehyde/sulphuric acid spray reagent was used for the detection of phenols, steroids, sugars and terpenes.

The composition of anisaldehyde/sulphuric acid spray reagent was:

- Methanol                    85 mL
- Glacial acetic acid    10 mL
- Conc. sulphuric aci    5 mL
- Anisaldehyde            0.5 mL

### 3.5.2. Vacuum liquid chromatography (VLC)

Vacuum liquid chromatography (VLC) is a useful method for the initial isolation procedure for large amounts of a sample. The apparatus consists of a 500 mL sintered glass Büchner filter funnel with an inner diameter of 12 cm. Fractions were collected in Erlenmeyer flasks. Silica gel 60 was packed to a hard cake at a height of 5 cm under applied vacuum. The sample

used was covered onto a small amount of silica gel using volatile solvents. The resulting sample mixture was then packed onto the top of the column. Step gradient elution with a non-polar solvent (Hexane) and increasing the gradient of a polar solvents (EtOAc, MeOH) gave successive fractions. The flow was produced by vacuum and the column was allowed to run dry after each fraction collected.

### **3.5.3. Flash chromatography**

Flash chromatography is a preparative column chromatography based on optimized prepacked columns and an air pressure driven eluent at a high flow rate. It is a simple and quick technique widely used to separate a variety of organic compounds. Normally, the columns are dry Silica Gel 60 GF254 pre-packed, of 18 cm height, vertically clamped and assembled in the system. The column is filled and saturated with the desired mobile phase just prior to sample loading. Samples are dissolved in a small volume of the initial solvent used and the resulting mixture was then packed onto the top of the column using special syringe. The mobile phase (isocratic or gradient elution) is then pumped through the column with the help of air pressure resulting in sample separation. This technique is considered as a low to medium pressure technique and is applied to samples from few milligrams to some gram of sample.

### **3.5.4. Low pressure liquid chromatography (LC)**

Open column chromatography plays a vital role in the separation of compounds from natural product extracts. The separation takes place through selective distribution of the components between a mobile phase and a stationary phase. Different choice of packing material and mobile phase can be applied depending on the class of compounds or fractions. Fractions derived from VLC were subjected to repeated separation through column chromatography using appropriate stationary and mobile phase solvent systems previously determined by TLC.

The following types of separation systems were used in this study:

- **Normal phase chromatography** using a polar stationary phase, typically silica gel (Silica Gel 60, 0.04 – 0.063 mm mesh size, Merck) or Diol (LiChroprep® Diol (40 – 63 µm) for liquid chromatography, Merck), in conjunction with a non- polar mobile phase (e.g. n-hexane,

DCM) or with a gradually increasing amount of a polar solvent (e.g. EtOAc or MeOH). Hydrophobic compounds elute quicker than hydrophilic compounds.

- **Reversed phase (RP) chromatography** using a non-polar stationary phase and a polar mobile phase (e.g. H<sub>2</sub>O or MeOH). The stationary phase consists of reversed phase silica material. For instance, RP-18 stands for an octadecyl ligand in the matrix of the RP-18, 0.04 – 0.063 mm mesh size (Merck) material that was used. The more hydrophobic the matrix, the greater the tendency of the column to retain hydrophobic compounds.

Thus, hydrophilic compounds elute more quickly than do hydrophobic compounds. Elution was performed using H<sub>2</sub>O with gradually increasing amounts of MeOH or acetonitrile.

- **Size exclusion chromatography** involves separations based on molecular sizes of analyzed compounds. The stationary phase consists of porous beads (Sephadex LH-20, 0.25 – 0.1 mm mesh size, GE Healthcare). Compounds having larger molecular diameter are excluded from the interior of the bead and thus elute firstly, while compounds with smaller molecular diameters enter the beads and elute according to their ability to exit from the small sized pores where they are trapped. Elution was performed using MeOH or MeOH:DCM [1:1 (V/V)] as mobile phases.

- **Ion exclusion chromatography** uses ion exchange resin beds (Diaion HP-20, Supelco) that act as a charged solid separation medium. The components of the processed sample have different electrical affinities to this medium and consequently are differently retained by the resin according to their different affinities.

The eluted fractions were collected by an automate fraction collector and combined according to TLC results.

### **3.5.5. High pressure liquid chromatography (HPLC)**

High pressure liquid chromatography (HPLC) is a high resolution chromatographic technique, where the mobile phase is forced through the column containing the stationary phase by a pump, resulting in a fast separation. The high resolution is achieved by the use of small particle size of the absorbent material, which mostly is RP silica material. Adjacent to the HPLC a UV detector is connected for monitoring the separation of the eluted compounds

shown in a chromatogram. The method can be used for analytical purposes or semi preparative.

### 3.5.5.1. Analytical HPLC

Analytical HPLC was used to identify interesting peaks from extracts and fractions as well as to evaluate the purity of isolated compounds. The gradient used started with 10:90 [MeOH: nanopure H<sub>2</sub>O (0.1% *o*-phosphoric acid)] to 100% MeOH in 35 minutes; then 10 minutes with 100% MeOH to wash the column and finally 15 min with 10:90 [MeOH: nanopure H<sub>2</sub>O (0.1% *o*-phosphoric acid)] to stabilize the column for the next injection. Peaks are detected by UV-VIS diode array detector.

#### Parameters:

Pump	Dionex P580A LPG
Detector	Dionex Photodiode Array Detector UVD 340S
Column	Knauer (125 × 4 mm, ID), pre-packed with Eurosphere 100-5 C18, with integrated pre-column. (Knauer, Berlin, Germany).
Column thermostat	STH 585
Autosampler	ASI-100T
HPLC Program	Chromeleon (V. 6.3)
Run time	60 min
Injection volume	20 µL
Flow rate	1,0 mL/min
Detection	235 nm; 254 nm; 280 nm and 340 nm

In case of insufficient separation the gradient was adjusted adequate to the substances to be separated.

### 3.5.5.2. Semi preparative HPLC

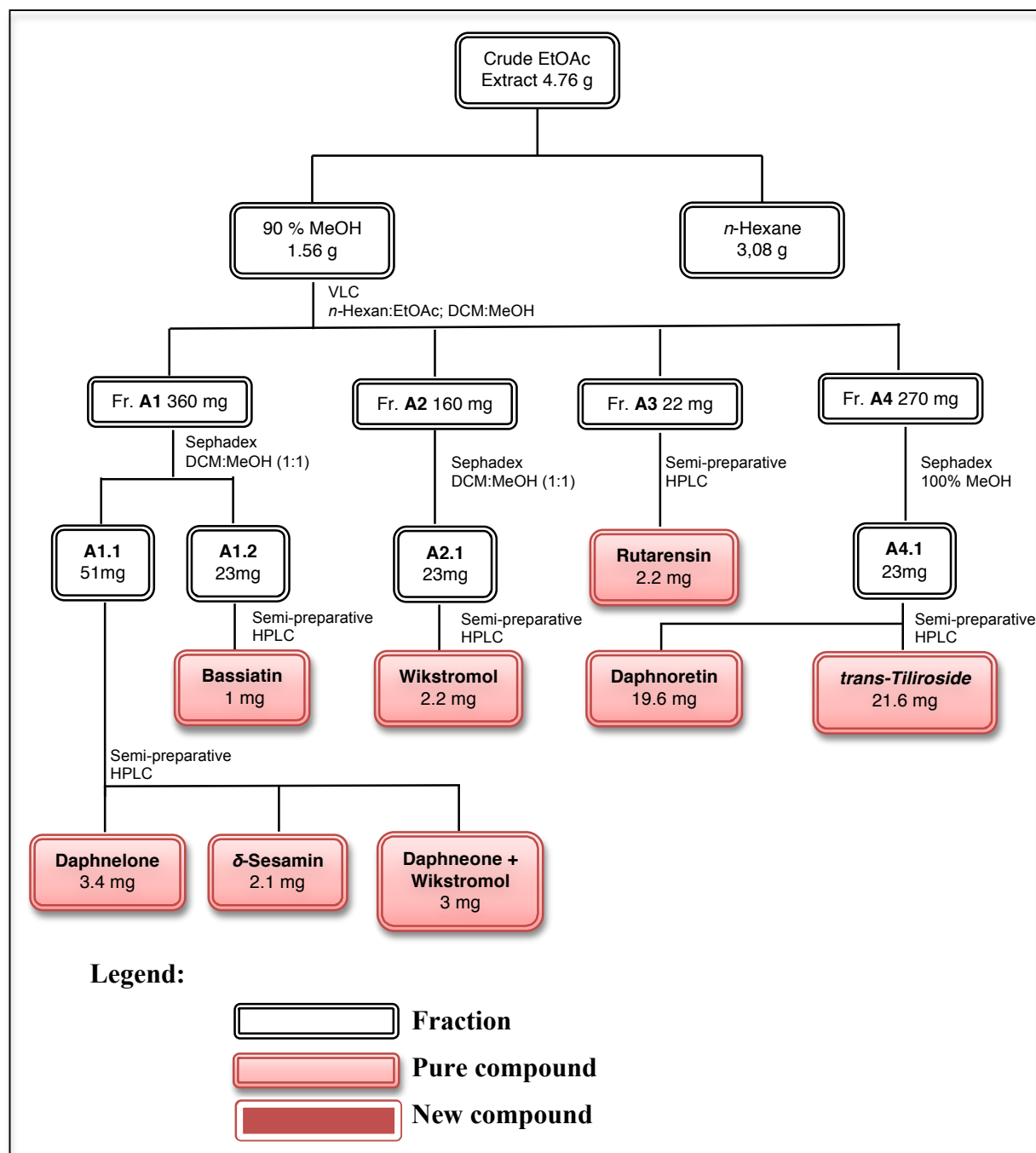
The semipreparative HPLC was used for the isolation of pure compounds from fractions previously separated using column chromatography. Each injection consists of 1-3 mg of the fraction dissolved in 1 mL of the solvent system. The most appropriate solvent system was determined before running the HPLC separation. The solvent system, which is composed of MeOH and Nanopure water with or without 0.1% TFA, was pumped through the column at a rate of 5 mL/min. The eluted peaks, which were detected by the online UV detector, were collected separately in glass tubes.

### Semi-preparative HPLC system specifications are described as follows:

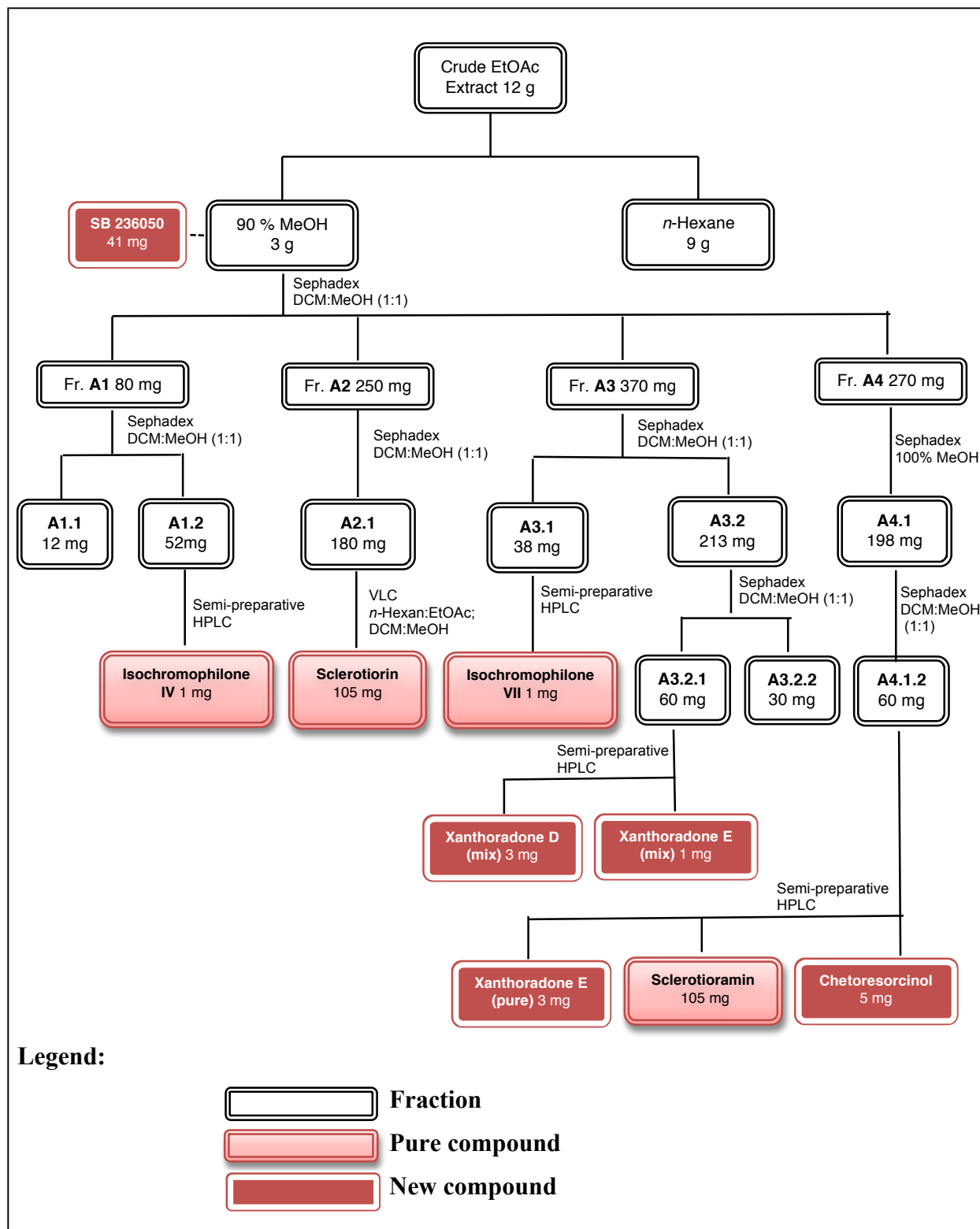
Pump	Merck Hitachi L-7100
Detector	Merck Hitachi UV detector L-7400
Column	Knauer (300 × 8 mm, ID), prepacked with Eurosphere 100-10 C18, with integrated pre-column.

### 3.5.6. Isolation and purification of secondary metabolites

#### 3.5.6.1. Isolation and purification of plant extract *Thymelaea lythroides*



**Scheme 3.1.** Isolation and purification of plant extract *Thymelaea lythroides*

3.5.5.2 Isolation and purification of endophyte extract *Chaetomium aureum*3.5.5.2.1 Isolated secondary metabolites from fermentation of *Chaetomium aureum* on solid riceScheme 3.2. Isolation and purification of plant extract *Chaetomium aureum*



### **3.6. Structure elucidation of the isolated metabolites**

The structure elucidation of the isolated compounds followed a standard scheme. Firstly, the data obtained from analytical HPLC were compared with the in-house substance library regarding their retention times at the standard gradient program and their UV spectra. Comparable hits indicated the class to which the compound belongs. From LCMS measurement the mass of the compound and from <sup>1</sup>H-NMR measurement substructures could be compiled. With this information, together with the identity of the fungus, a literature search using the latest versions of Dictionary of Natural Products (DNP, Chapman and Hall, 2005-2009), Antibase (2002-2007), Antimarin 0512, 2012 and SciFinder was performed. In some cases these data were insufficient and additional measurements, especially one and two-dimensional NMR experiments were necessary to finally identify the secondary metabolite.

#### **3.6.1. Mass spectrometry (MS)**

Mass spectroscopy (MS) is an analytical technique used to determine the molecular weight, the elemental composition of a molecule and for the chemical structures elucidation of the molecules. It is a very sensitive technique and even from micro gram amounts good spectra can be obtained. Technically, mass spectrometers consist of three parts: ionization source, analyzer, and detector, which should be maintained under high vacuum conditions so as to maintain the ions flight through the instrument without any hindrance from air molecules. The sample is ionized in the ionization source and the rising ions are sorted and separated according to their mass (m) charge (z) ratio (m/z) in the mass analyzer. Both negative and positive charged ions can be observed. Once the separated ions reach the detector, the signals are transmitted to the data system where the mass spectrum is recorded. The molecular ion (parent ion) has to be identified giving the molecular weight of the compound. Therefore, mass spectrometry is used to determine the molecular weights of pure compounds or compounds in a mixture. From the fragmentation patterns of the compound information about substructures can be attained.

Many different method of ionization are used in mass spectrometry and the selection of the method depends on the type of samples to be analyzed. Some known ionization methods include:

- Electron Impact (EI)
- Electro-Spray Ionization (ESI)
- Fast Atom Bombardment (FAB)

- Chemical Ionization (CI)
- Atmospheric Pressure Chemical Ionization (APCI)
- Matrix Assisted Laser Desorption Ionization (MALDI)
- Field Desorption / Field Ionization (FD/FI)
- Thermo-Spray Ionization (TSI)

Low resolution mass spectra were measured by ESI-, EI-, CI- and FAB-MS on a Bruker micrOTOF with Liquid chromatography Agilent 1100 Serie mass spectrometer.

### **3.6.1.1. Electron Impact Mass Spectrometry (EI-MS)**

Analysis involves vaporizing a compound in an evacuated chamber and then bombarding it with electrons having 25.80 eV (2.4-7.6 MJ/mol) of energy. The high-energy electron stream not only ionizes an organic molecule (requiring about 7-10 eV) but also causes extensive fragmentation (the strongest single bonds in organic molecules have strengths of about 4 eV). The advantage is that fragmentation is extensive, giving rise to a pattern of fragment ions, which can help to characterize the compound. The disadvantage is the frequent absence of a molecular ion.

### **3.6.1.2. Electron spray ionization mass spectrometry (ESIMS)**

ESI-MS is a gentle ionization method where the sample is passed through a high voltage metal capillary. At the end of this capillary it is sprayed by a flow of nitrogen gas at atmospheric pressure to form an aerosol. Together with heating, the nitrogen evaporates the emerging droplets forcing the ions in each droplet together until repulsion causes them to eject from the surface. The ions are extracted into the vacuum of the mass analyzer where they are detected. Additionally to the molecular ion peaks  $[M+H]^+$  or  $[M-H]^-$  fragments of these can be detected.

#### **⇒ Liquid chromatography mass spectrometry (LC/MS)**

High pressure liquid chromatography is a powerful method for the separation of complex mixtures, especially when many of the components may have similar polarities. If a mass spectrum of each component can be recorded as it elutes from the LC column, quick characterization of the components is greatly facilitated. Usually, ESI-MS is interfaced with LC to make an effective on-line LC/MS. HPLC/ESI-MS was carried out using a Finnigan LCQ-DECA mass spectrometer connected to a UV detector. The samples were dissolved in

water/MeOH mixtures and injected to HPLC/ESI-MS set-up. For standard MS/MS measurements, a solvent gradient that started with acetonitrile:nanopure H<sub>2</sub>O (10:90), adjusted with 0.1 % HCOOH, and reached to 100 % acetonitrile in 35 minutes was used.

LC/UV/MS system specifications are described as follows:

HPLC system	Agilent 1100 series (pump, detector and autosampler) Finnigan LC Q-DECA
MS spectrometer	Knauer, (250 × 2 mm, ID), prepacked with Eurosphere 100-5
Column	C18, with integrated pre-column

### 3.6.1.3. Fast atom bombardment mass spectrometry (FAB-MS)

This was the first widely accepted method that employs energy sudden ionization. FAB is useful for compounds, especially polar molecules, unresponsive to either EI or CI mass spectrometry. It enables both non-volatile and high molecular weight compounds to be analyzed. In this technique, a sample is dissolved or dispersed in a polar and relatively non-volatile liquid matrix, introduced into the source on a copper probe tip. Then, this matrix is bombarded with a beam of atoms of about 8 Kev. It uses a beam of neutral gas (Ar or Xe atoms) and both positive and negative ion FAB spectra can be obtained.

### 3.6.1.4. High-resolution mass spectrometry (HR-MS)

High resolution is achieved by passing the ion beam through an electrostatic analyzer before it enters the magnetic sector. In such a double focusing mass spectrometer, ion masses can be measured with an accuracy of about 1 ppm. With measurement of this accuracy, the atomic composition of the molecular ions can be determined.

After the determination of molecular weight, pure compounds are then submitted to the measurement of nuclear magnetic resonance (NMR) spectra.

### 3.6.2. Nuclear magnetic resonance spectroscopy (NMR)

First observed in 1946, nuclear magnetic resonance leads to the development of a technic, called NMR spectroscopy, which is now almost indispensable for structure elucidation. NMR spectroscopy allows determining chemical and physical proprieties of those nuclei of atoms having magnetic properties. Some nuclei experience this phenomenon, and others do not, depending upon whether they possess a property called spin. NMR spectroscopy is nowadays

routinely used to study chemical structure by giving not only the constituent of a molecule but also its relative stereochemistry.

This technique utilizes the atomic nuclei spinning behavior of atoms with an odd number of nucleons, e. g.  $^1\text{H}$  and  $^{13}\text{C}$ . A NMR spectrum is acquired by varying the magnetic field that is applied to the sample dissolved in a deuterated solvent over a small range while observing the resonance signal from the sample. Depending on the electron density around each proton they obtain different shielding and deshielding effects appearing in different parts of the resulting NMR spectrum and thus provide information about the environment of each proton. The resulting frequency where the nuclei resonate, the so-called chemical shift, is given in ppm and the coupling constants between adjacent nuclei in Hertz (Hz). NMR experiments can be conducted in a one (1D) or two (2D) dimensional manner. 2D NMR spectra can be either measured between two equal (H, H-COSY, correlated spectroscopy) or two different (H, C-COSY) frequency axes. For the H-H 2D experiments the connection between two adjacent protons (COSY), between two protons through space (NOESY, nuclear Overhauser enhancement spectroscopy; ROESY, rotating-frame enhancement spectroscopy) or between all protons in one spin system (TOCSY, total correlation spectroscopy) are given. H-C 2D experiments measure the direct correlation between a proton and a carbon (HMQC, heteronuclear multiple quantum correlation) or the connection of protons over two, three and even four bonds to carbon atoms, so-called long range coupling (HMBC, heteronuclear multiple bond correlation). Correlations are shown as cross peaks in the plane between two axes containing the 1D NMR shifts.

Most NMR spectra were measured at the University Wuppertal with BRUKER AVANCE III 600 (1H - Messfrequenz 600.13 MHz) by Andreas Siebert and Ilka Polanz.

### **3.6.3. Optical activity**

Optical rotation or optical activity is a phenomenon observed in the 1811 in quartz by the French physicist Dominique F.J. Arago. Polarized light changes its polarization after passing through a chiral molecule; this can be measured with a polarimeter. This equipment consists of a light source, two polarizing filters and a cell that contains a solution of the analyzed compound.

Optical activity is a macroscopic property of a molecule and differs between enantiomers. Samples containing two enantiomers in the same ratio are optically inactive. In a solution the measured optical rotation depends on concentration (c) and light path length (l) of the sample. The specific rotation,  $[\alpha]$ , expresses the optical rotation degree after correction of concentration and path length. Thus the specific rotation is a specific quantity for a chiral molecule at certain temperature (T) and at certain wavelength ( $\lambda$ ).

$$[\alpha]_{\lambda}^T = 100 \alpha / c.l$$

where:

$[\alpha]_{\lambda}^T$  is specific rotation at certain temperature T and wavelength  $\lambda$

a = the angle of rotation ( $^{\circ}$ ),

l = optical path length in (dm)

$\lambda$  = wavelength

T = temperature

c = concentration (g/100 mL)

The measurement of optical rotation presented in this study, was recorded on Perkin-Elmer 241 MC polarimeter and using a 0.5 mL cuvette with 1 dm length.

$[\alpha]_D^{20}$  is the specific optical rotation of Sodium-D-line at the wavelength, 589 nm and at a temperature of 20  $^{\circ}$ C.

Pure substances were dissolved in appropriate spectroscopic grade solvent. The optical rotation of known compounds was compared to literature data.

#### 3.6.4. Circular dichroism (CD) spectroscopy

Circular dichroism is based on the difference between the absorption of left-handed circularly polarized light (L-CPL) and right-handed circularly polarized light (R-CPL). It occurs when a molecule contains one or more chiral chromophores (light-absorbing groups).

$$\text{Circular dichroism} = \Delta A(\lambda) = A(\lambda)_{\text{LCPL}} - A(\lambda)_{\text{RCPL}}$$

where  $\lambda$  is the wavelength.

Circular dichroism (CD) spectroscopy is a spectroscopic method. The CD of molecules is recorded over a range of wavelengths. CD spectroscopy is widely used to study chirality of molecules.

Measurements are carried out in the visible and ultra-violet region of the electro-magnetic spectrum to monitor electronic transitions. If the molecule under investigation contains chiral chromophores, one CPL state will be absorbed to a greater extent than the other and the CD signal over the corresponding wavelengths will be non-zero. A circular dichroism signal can be positive or negative, depending on whether L-CPL is absorbed to a greater extent than R-CPL (CD signal positive) or to a lesser extent (CD signal negative).

Circular dichroism spectra are measured using a circular dichroism spectrometer, which is a highly specialized descendant of an ordinary absorption spectrometer. CD spectrometers alternately measure the absorption of L- and R-CPL, usually at a frequency of 50 KHz, and then calculate the circular dichroism signal.

In this study, the CD spectra were recorded on a J-810 CD spectropolarimeter. Conformational searches were carried out by means of the MacroModel 9.7.211 (MacroModel *et al.*, 2009) software using Merck Molecular Force Field (MMFF) with implicit solvent model for chloroform. Geometry reoptimizations at B3LYP/6-31G(d) level of theory followed by TDDFT calculations using various functionals (B3LYP, BH&HLYP, PBE0) and TZVP basis set were performed by the Gaussian 03 (Frisch *et al.*, 2004) package. Boltzman distributions were estimated from the ZPVE corrected B3LYP/6-31G(d) energies. CD spectra were generated as the sum of Gaussians (Stephens and Harada, 2010) with 3000 cm<sup>-1</sup> half-height width (corresponding to ca. 16 nm at 230 nm), using dipole-velocity computed rotational strengths for conformers above 5%. The MOLEKEL (Varetto, 2009) software package was used for visualization of the results.

### 3.7. Testing the biological activity

A bioassay-guided separation can lead to the discovery of compounds with interesting activity. Samples from crude extracts and from different fractions, resulting of different separation were submitted to biological activity tests.

### 3.7.1. Antimicrobial assay

#### *Agar diffusion assay*

This method was used to detect the capability of a substance to inhibit the growth of microorganisms by measuring the diameter of inhibition zone around a tested compound on an agar plate. The agar diffusion assay was performed according to the Bauer-Kirby-Test (Bauer et al., 1966).

#### *Culture preparation*

The agar diffusion assay was performed according to the Bauer-Kirby-Test (DIN 58940, Bauer et al, 1966). Prior to testing, a few colonies (3 to 10) of the organism to be tested, were subcultured in 4 ml of tryptose-soy broth (Sigma, FRG) and incubated for 2 to 5 h to produce a bacterial suspension of moderate cloudiness. The suspension was diluted with sterile saline solution to a density visually equivalent to that of a BaSO<sub>4</sub> standards. The standards were prepared by adding 0.5 ml of 1 % BaCl<sub>2</sub> to 99.5 ml of 1% H<sub>2</sub>SO<sub>4</sub> (0.36 N). The prepared bacterial broth is inoculated onto Müller-Hinton-Agar plates (Difco, USA) and dispersed by means of sterile beads.

#### *Microorganisms*

Crude extracts and isolated pure compounds were tested for activity against the following standard strains:

- Gram-positive bacteria *Bacillus subtilis*
- Gram-negative bacteria *Escherichia coli*
- Yeast *Saccharomyces cerevisiae*
- Fungi *Cladosporium cucumerinum*
- Fungi *Cladosporium herbarum*.

### 3.7.2. Cytotoxicity tests

#### 3.7.2.1. Microculture tetrazolium (MTT) assay

Cytotoxicity tests were carried out by Prof. Dr. W. E. G. Müller, Institut für Physiologische Chemie und Pathobiochemie, University of Mainz, Mainz. The cytotoxicity was tested against L5178Y mouse lymphoma cells using the microculture tetrazolium (MTT) assay, and compared to that of untreated controls (Carmichael, 1987).

### **Cell cultures**

L5178Y mouse lymphoma cells were grown in Eagle's minimal essential medium supplement with 10% horse serum in roller tube culture. The medium contained 100 units/mL penicillin and 100 µg/mL streptomycin. The cells were maintained in a humidified atmosphere at 37° C with 5% CO<sub>2</sub>.

### **MTT colorimetric assay**

Of the test samples, stock solutions in ethanol 96% (v/v) were prepared. Exponentially growing cells were harvested, counted and diluted appropriately. Of the cell suspension, 50 µL containing 3750 cells were pipetted into 96-well microliter plates. Subsequently, 50 µL of a solution of the test samples containing the appropriate concentration was added to each well. The concentration range was 3 and 10 µg/mL. The small amount of ethanol present in the wells did not affect the experiments. The test plates were incubated at 37° C with 5% CO<sub>2</sub> for 72 h. A solution of 3-(4,5-dimethylthiazol-2-yl)-2,5-diphenyltetrazolium bromide (MTT) was prepared at 5 mg/mL in phosphate buffered saline (PBS; 1.5 mM KH<sub>2</sub>PO<sub>4</sub>, 6.5 mM Na<sub>2</sub>HPO<sub>4</sub>, 137 mM NaCl, 2.7 mM KCl; pH 7.4) and from this solution, 20 µL was pipetted into each well.

The yellow MTT penetrates the healthy living cells and in the presence of mitochondrial dehydrogenases, MTT is transformed to its blue formazan complex. After an incubation period of 3h 45 min at 37° C in a humidified incubator with 5% CO<sub>2</sub>, the medium was centrifuged (15 min, 20 °C, 210 x g) with 200 µL DMSO, the cells were lysed to liberate the formed formazan product. After thorough mixing, the absorbance was measured at 520 nm using a scanning microliter-well spectrophotometer. The color intensity is correlated with the number of healthy living cells. Cell survival was calculated using the formula:

$$\text{Survival \%} = 100 \frac{\text{Absorbance of treated cells} - \text{absorbance of culture}}{\text{Absorbance of untreated cells} - \text{absorbance of culture}}$$

All experiments were carried out in triplicates and repeated three times. As controls, media with 0.1% EGMME/DMSO were included in the experiments.



### 3.7.2.2. MTT cell viability assays

Cytotoxicity tests were carried out by Prof. Dr. M. U. Kassack, Institut für Pharmazeutische und Medizinische Chemie, Heinrich-Heine University, Düsseldorf.

#### *Materials, cell lines and cell culture*

The human ovarian carcinoma cell line A2780 (A2780 sens) was obtained from European Collection of Cell Cultures (ECACC, Salisbury, UK). A2780 cells were exposed to weekly cycles of 2  $\mu\text{mol/L}$  cisplatin over a period of 24 weeks.

Cisplatin-resistant cells were denoted A2780 *CisR*. The human chronic myelogenous leukemia cell line K562 was obtained from the German Collection of Microorganisms and Cell Cultures (DSMZ, Germany). All other reagents were supplied by Sigma Chemicals unless otherwise stated. All cell lines were grown at 37 °C under humidified air supplemented with 5% CO<sub>2</sub> in RPMI 1640 (PAN Biotech, Germany) containing 10% fetal calf serum (PAN Biotech, Germany), 100 IU/mL penicillin and 100  $\mu\text{g/mL}$  streptomycin. The cells were grown to 80% confluency before using them for the MTT cell viability assay.

#### *MTT cell viability assays*

The rate of cell-survival under the action of test substances was evaluated by an improved MTT assay (Müller *et al.*, 2004). The assay is based on the ability of viable cells to metabolize yellow 3-(4,5-dimethylthiazol-2-yl)-2,5-diphenyl tetrazolium bromide (MTT, Applichem, Germany) to violet formazane crystals that can be detected spectrophotometrically. In brief, A2780 cells were seeded at a density of 8,000 cells/well and K562 at a density of 30,000 cells/well in 96 well plates (Corning, Germany). After 24 h, cells were exposed to the test compounds at concentrations of 10<sup>-5</sup> M and 10<sup>-4</sup> M. Incubation was stopped after 72 h and cell survival was determined by addition of MTT solution (5 mg/mL in phosphate buffered saline). The formazan precipitate was dissolved in DMSO. Absorbance was measured at 544 nm and 620 nm in a FLUO starmicroplate-reader (BMG LabTech, Offenburg, Germany). The absorbance of untreated control cells was taken as 100% viability. All tests were performed in triplicate.

### 3.7.2.3. Protein kinase assay

Protein kinase assays were carried out by Dr. Michael Kubbutat (ProQinase GmbH, Freiburg, Germany).

Protein kinase enzymes are integral components of numerous signal transduction pathways involved in the regulation of cell growth, differentiation, and response to changes in the extracellular environment. Consequently, kinases are major targets for potentially developing novel drugs to treat diseases such as cancer and various inflammatory disorders.

The inhibitory potency of the samples was determined using 24 protein kinases (see Table 3.2). The IC<sub>50</sub> profile of compounds/fractions showing an inhibitory potency of  $\geq 40\%$  with at least one of the 24 kinases at an assay concentration of  $1 \times 10^{-06}$  g/mL was determined. IC<sub>50</sub> values were measured by testing 10 concentrations of each sample in singlicate (n=1).

### ***Sample preparation***

The compounds/fractions were provided as  $1 \times 10^{-03}$  g/mL stock solutions in 100% DMSO (1000 or 500  $\mu$ L) in micronic boxes. The boxes were stored at -20° C. Prior to the assays, 100  $\mu$ L of the stock solutions were transferred into separate microtiter plates. Subsequently, they were subjected to serial, semi-logarithmic dilution using 100% DMSO as a solvent resulting in 10 different concentrations. 100% DMSO was used as control. Subsequently,  $7 \times 5$   $\mu$ L of each concentration were aliquoted and diluted with 45  $\mu$ L H<sub>2</sub>O only a few minutes before the transfer into the assay plate to minimize precipitation. The plates were shaken thoroughly and then used for the transfer of 5  $\mu$ L compound solution into the assay plates.

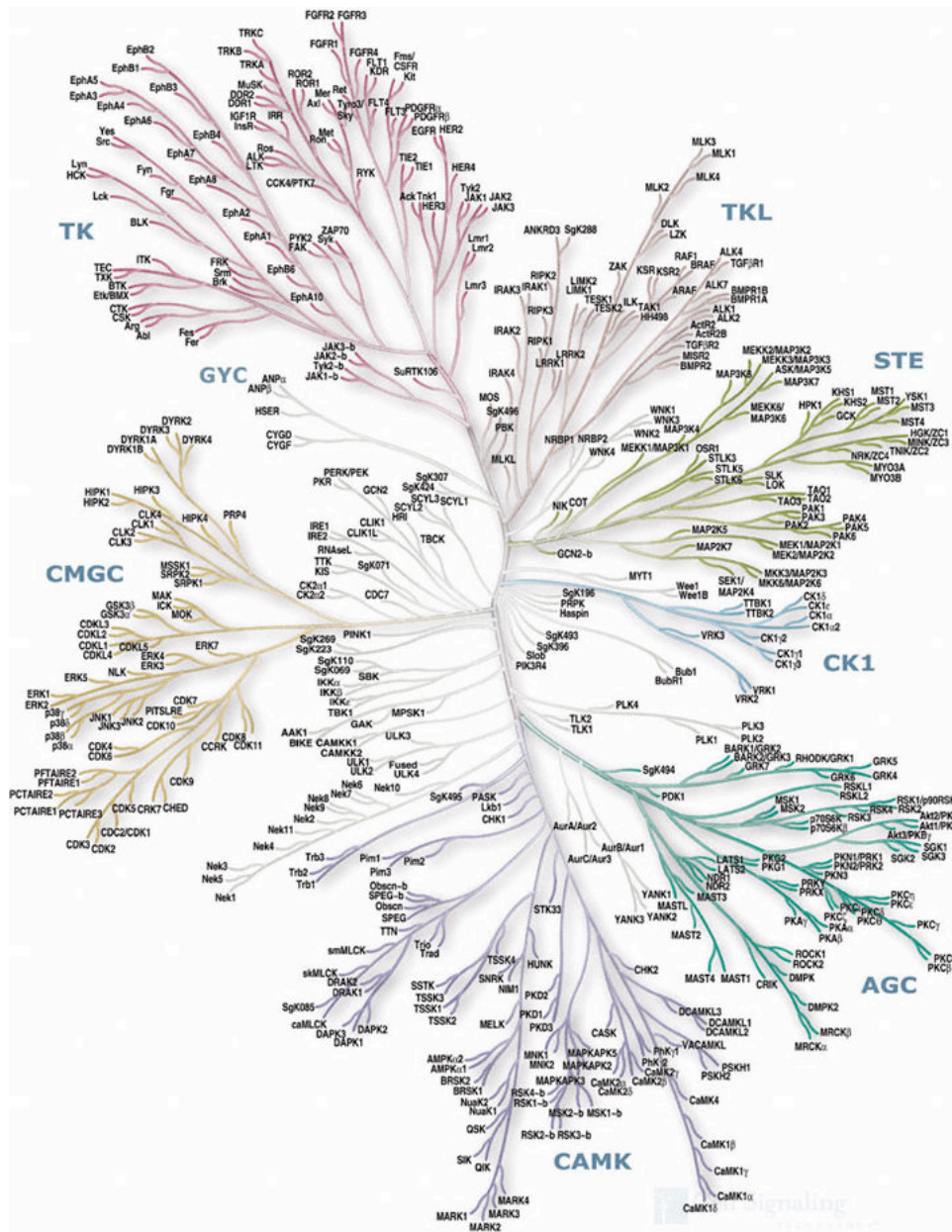
### ***Recombinant protein kinases***

All protein kinases were expressed in Sf9 insect cells as human recombinant GST-fusion proteins or His-tagged proteins by means of the baculovirus expression system. Kinases were purified by affinity chromatography using either GSH-agarose (Sigma) or NiNTH-agarose (Qiagen). Purity was checked by SDS-PAGE/silver staining and the identity of each kinase was verified by western blot analysis with kinase specific antibodies or by mass spectrometry.

### ***Protein kinase assay***

A proprietary protein kinase assay (33PanQinase<sup>®</sup> Activity Assay) was used for measuring the kinase activity of the protein kinases. All kinase assays were performed in 96-well Flash Plates<sup>™</sup> from Perkin Elmer/NEN (Boston, MA, USA) in a 50  $\mu$ L reaction volume. The reaction mixture was pipetted in the following order: 20  $\mu$ L assay buffer, 5  $\mu$ L ATP solution in H<sub>2</sub>O, 5  $\mu$ L test compound in 10% DMSO and 10  $\mu$ L substrate/10  $\mu$ L enzyme solution

(premixed). The assay for all enzymes contained 60 mM HEPES-NaOH (pH 7.5), 3 mM  $MgCl_2$ , 3mM  $MnCl_2$ , 3 pM Na-orthovanadate, 1.2 mM DTT, 50  $\mu g/mL$  PEG20000, 1 pM [ $\gamma$ - $^{33}P$ ]-ATP. The reaction mixtures were incubated at 30°C for 80 minutes and stopped with 50  $\mu L$  2% (v/v)  $H_3PO_4$ . The plates were aspirated and washed two times with 200  $\mu L$  of 0.9% (w/v) NaCl or 200  $\mu L$   $H_2O$ . Incorporation of  $^{33}P$  was determined with a microplate scintillation counter (Microbeta Trilux, Wallac). All assays were performed with a Beckman Coulter/Sagian robotic system.



**Group Names** AGC Containing PKA, PKG, PKC families; CAMK Calcium/calmodulin-dependent protein kinase; CK1 Casein kinase 1; CMGC Containing CDK, MAPK, GSK3, CLK families; STE Homologs of yeast Sterile 7, Sterile 11, Sterile 20 kinases; TK Tyrosine kinase; TKL Tyrosine kinase-like (@ cellsignal.com).

**Table 3.2:** List of Protein kinases and their substrates

Family	Kinase	Substrate	Oncologically relevant mechanism	Disease
Serine/threonine kinases	AKT1/PKB Alpha	GSC3 (14-27)	Apoptosis	Gastric cancer (Staal, 1987)
	ARK5	Autophos.	Apoptosis	Colorectal cancer (Kusakai <i>et al.</i> , 2004)
	Aurora B	Tetra(LRRWSLG)	Proliferation	Breast cancer (Keen and Tylor 2004)
	PLK-1	Casein	Proliferation	Prostate cancer (Weichert <i>et al.</i> , 2004)
	MEK1 wt	ERK2-KR	Apoptosis	Multiple cancers (Ryan <i>et al.</i> , 2000)
	NEK2	RB-CTF	Apoptosis	Ewing's tumors & B cell lymphoma (Schultz <i>et al.</i> , 1994)
	NEK6	GSK3(14-27)	Apoptosis	Multiple cancers (Li <i>et al.</i> , 2003)
	PIM1	GSK3(14-27)	Apoptosis	prostate cancer (Dhanasekaran <i>et al.</i> , 2001)
	PRK1	RBER-CHKtide	Proliferation	Prostate cancer (Manser <i>et al.</i> , 1994)
Receptor tyrosine kinase	IGF1-R	Poly(glu,Tyr) <sub>4:1</sub>	Apoptosis	Braest cancer (Zhang and Yee 2000)
	MET wt	Poly(Ala,glu,Lys,Tyr) <sub>6:2:4:1</sub>	Metastasis	Lung cancer (Qiao <i>et al.</i> , 2002)
	VEGF-R2	Poly(glu,Tyr) <sub>4:1</sub>	Angiogenesis	Pancreatic cancer (Li <i>et al.</i> , 2003)
	ALK	poly(Glu,Tyr) <sub>4:1</sub>	Apoptosis	anaplastic large-cell lymphoma (Morris <i>et al.</i> , 1994)
	AXL	poly(Glu,Tyr) <sub>4:1</sub>	Proliferation	Ovarian, gastric and breast cancer (Liu <i>et al.</i> , 1988)
Soluble tyrosine kinase	FAK	Poly(glu,Tyr) <sub>4:1</sub>	Metastasis	Breast cancer (Schmitz <i>et al.</i> , 2005)
	SRC	Poly(glu,Tyr) <sub>4:1</sub>	Metastasis	Colon cancer (Dehm <i>et al.</i> , 2001)

### **3.8. Inhibiting the hsp90 chaperone pathway**

#### **3.8.1. Heat shock protein Hsp 90**

Heat shock proteins (HSPs) are chaperone proteins that become up-regulated in response to cellular environmental stresses, such as elevated temperature and oxygen or nutrient deprivation. Hsps are chaperones that facilitate the proper folding and repair of other cellular proteins, referred to as “client proteins”, and also aid the refolding of misfolded proteins. Of the several families of Hsps, the Hsp90 family is one of the most abundant, representing approximately 1-2% of the total protein content in non-stressed cells and 4-6% of the protein content of cells that are stressed.

The N-terminal domain of Hsp90 comprises an ATP-binding site that is central to the chaperone function. The C-terminal domain of Hsp90 mediates constitutive Hsp90 dimerization. Conformational changes of Hsp90 are orchestrated with the hydrolysis of ATP. Hsp90 is highly conserved and facilitates the folding and maturation of over 200 client proteins, which are involved in a broad range of critical cellular pathways and processes. In non-stressed cells Hsp90 participates in low affinity interactions to facilitate protein folding and maturation. In stressed cells Hsp90 can assist the folding of dysregulated proteins, and is known to be involved in the development and maintenance of multiple diseases.

Hsp90 maintains the conformation and stability of many oncogenic proteins, transcription factors, steroid receptors, metalloproteases and nitric oxide synthases that are essential for survival and proliferation of cancer cells (Whitesell *et al.*, 2005). Thus, Hsp90 client proteins have been associated with the development and progression of cancer. Furthermore, Hsp90 is thought to contribute to maintenance of multiple neurodegenerative diseases that are associated with protein degradation and misfolding (proteinopathy), such as Alzheimer’s disease, Huntingdon’s disease and Parkinson’s disease, through the mis-folding or stabilization of aberrant (neurotoxic) client- proteins.

Inhibition of Hsp90 function results in the misfolding of client proteins, which are subsequently ubiquitinated and degraded through proteasome-dependent pathways. Hence, inactivation of the Hsp90 pathway represents a combinatorial attack on multiple signaling pathways and Hsp90 inhibitors have been developed as therapeutics with efficacy in a broad variety of human diseases.

### 3.8.2. Progesterone receptor PR reconstitution assay

An in vitro progesterone receptor PR reconstitution assay as a model system was used to identify novel compounds that may inhibit the Hsp90 chaperoning machine. This assay uses RRL as a source of molecular chaperones and it has been fundamental in further understanding of how geldanamycin and related compounds such as 17-AAG inhibit Hsp90-dependent chaperoning (Pratt *et al.*, 2003). The assay directly measures the ability of molecular chaperones to refold the heat denatured PR to its hormone binding state. Hormone binding activity of the PR therefore reflects the functional integrity of molecular chaperones. Whether compounds isolated from endophyte affected the recovery of hormone binding activity of PR after mild heat denaturation was tested. Compounds with diverse chemical structures from Moroccan medicinal plants and microorganisms living in these plants were screened.

For the progesterone receptor (PR) reconstitution assay, purified PR was adsorbed onto PR22 antibody-protein A-sepharose resin beads and was assembled into complexes as described previously (Kosano *et al.*, 1998). Briefly, about 0.05  $\mu$ M PR was incubated with RRL diluted twice in reaction buffer (20 mM Tris/HCl, pH 7.5, 10 mM MgCl<sub>2</sub>, 4 mM DTT, 0.02% NP-40, 100 mM KCl and 10 mM ATP). After incubation for 30 min at 30°C, 0.1  $\mu$ M [3H]-progesterone (American Radiolabeled Chemicals, Inc #ART 0063) was added. Samples were incubated on ice for 3 h at 4°C. Complexes were then washed three times with 1ml of reaction buffer and assessed for bound progesterone by liquid scintillation using PerkinElmer Microbeta plate reader.

### 3.8.3. Cytotoxicity of Sclerotiorin to breast cancer Hs578T cells

#### *Cell Culture*

Cell lines were purchased from American type culture collection (ATCC). Cell culture medium (MEM) and fetal bovine serum (FBS) were obtained from Gibco. Penicillin/streptomycin, and tissue culture grade trypsin were bought from Sigma Chemical Co. 3.103.

#### *Cytotoxicity Assay*

Cells of breast cancer triple negative cell lines Hs578T and MDA-MB-231 and prostate cancer cell line LNCaP were seeded in 6-well plates (Corning #3516). The next day, cells were treated with various concentrations of sclerotiorin and deacetyl-sclerotiorin for 48h.

Every 24h, the old media was substituted with new media containing new drug at the same concentration. Cells were harvested at 48 h and cell lysate were made.

### 3.8.4. Comparison of deacetylsclerotiorin and sclerotiorin by inhibiting the Hsp90 chaperoning of progesterone receptor (PR) *in vitro*

#### *Production of deacetylsclerotiorin*

Sclerotiorin was chemically modified by deacetylation. Deacetylsclerotiorin was obtained by deacetylation of sclerotiorin, according to the procedure described previously by Isaka *et al.*, 2001.

Isaka describes a method for deacetylation, including adding concentrated H<sub>2</sub>SO<sub>4</sub> (0.2 mL) to a compound (9.0 mg) suspended in dry MeOH (2.0 mL) and stirring the mixture for 45 h. The resulting homogeneous solution is partially concentrated under reduced pressure, and the residue is diluted with EtOAc (30 mL). The EtOAc solution was washed with H<sub>2</sub>O (3 x 10 mL) and concentrated in vacuo to yield the deacetylated compound as a powder that is subsequently purified by preparative HPLC (MeCN/H<sub>2</sub>O)

### 3.9. General laboratory equipments

Autoclave	Varioklav, H&P
Balances	Mettler 200, Mettler AT 250, Mettler PE 1600, Sartorius MC1 AC210S
Centrifuge	Biofuge pico, Heraeus
Cleanbench	HERAsafe, Heraeus
Digital pH meter	420Aplus, Orion
Drying Ovens	Kelvitron t, Heraeus
Fraction collector	Cygnnet, ISCO
Freeze dryer	Lyovac GT2, Steris
- 80 °C Freezer	Forma Scientific, 86-Freezer
Hot plate	Camag
Magnetic stirrer	Combi Mag, IKA
Rotary evaporator	Vacuubrand, IKA
Sonicator	Sonorex RK 102, Bandelin
Syringes	Hamilton
Ultra Turrax	T18 basic, IKA

UV Lamp	Camag (254 and 366)
Vacuum centrifuge	SpeedVac SPD 111V, Savant

### 3.10. Solvents

#### 3.10.1. General solvents

Acetone, acetonitrile, dichloromethane, ethanol, ethyl acetate, n-hexane and methanol were used. They were distilled before using and special grades were used for spectroscopic measurements.

#### 3.10.2. Solvents for HPLC

Acetonitrile	LiChroSolv HPLC grade (Merck)
Methanol	LiChroSolv HPLC grade (Merck)
Nanopure water	distilled and heavy metals free water obtained by passing distilled water through nano- and ionexchange filter cells (Barnstead, France)

#### 3.10.3. Solvents for optical rotation

Chloroform	Spectral grade (Sigma)
Methanol	Spectral grade (Sigma)
Water	Spectral grade (Fluka)

#### 3.10.4. Solvents for NMR

Acetone-d <sub>6</sub>	Uvasol, Merck
Chloroform-d	Uvasol, Merck
DMF-d <sub>7</sub>	Uvasol, Merck
DMSO-d <sub>6</sub>	Uvasol, Merck
Methanol-d <sub>4</sub>	Uvasol, Merck
Pyridine-d <sub>5</sub>	Uvasol, Merck



---

---

### 3. Results

#### 4.1. Ethnopharmacological study

##### 4.1.1. Frequency of Cancer according to gender

During our investigation, we found that the incidence of cancer in the patients attending the National Institute of Oncology in Rabat is higher among women than men. Of 691 patients, 422 were women (61.1 %), and 301 were men (43.5%). This data coincides with that of NIO register during the period of our investigation. Out of a total of 2693 patients hospitalized or treated, 1677 were women (62.2%) and 1016 were men (37.7%).

This may be explained by the high frequencies of gyneco-mammary cancers that present 57% of all cancers affecting women in Morocco (RCRC, 2007). According to cancers register of Casablanca of 2004, the incidence of global standardized cancers in Morocco is of 10.171 new cases per 100.000 inhabitants per year. Cancer affects more frequently women (raw incidence = 100.1) than man (raw incidence = 84.3), while in other developed countries, cancer is more frequent in man than women (RCRC, 2007).

##### 4.1.2. Frequency of cancer according to the localization

Breast cancer in women is the most frequent cause of mortality and represents 16% of death in adult women (The World Health Statistics, 2008). In our study it was found that the incidence of breast cancer comes in the first place with a percentage of 34%, and according to the register of Rabat region in 2005, one cancer out of three is breast cancer with a risk cumulated 0-74 years of 3.8%. The number of new cases expected yearly would be 4660. However, the incidence of breast cancer in Morocco (396 for 100000) remains clearly inferior to incidences found in western countries (more than 80 for 100000) (RCR, 2009). In men broncho-pulmonary cancer comes in first place with percentage of 11%.

RECRAB (2005) estimates that the number of new cases expected yearly in Morocco is 3000 with a risk cumulated 0-74 years, that is 3.0% (RCR, 2009). In developed countries, smoking causes over 80% of such cancers and generally, heavy smoking increases the risk by around 30-fold making lung cancer a major problem in developing countries where the consumption of tobacco is flourishing (Boutayeb A and Boutayeb S, 2005) Non Hodgkin Lymphoma is ranked third, 7%, and it is the most frequent of malignant homeopathies. The incidence of cancers of the lung, colon and rectum, breast and prostate generally increases in parallel with economic development, while the incidence of stomach cancer usually declines with

development (The World Health Statistics, 2008). In developing countries, around 60% of such cancers are thought to be a result of micronutrient deficiencies related to a restricted diet that is low in fruit and vegetables and animal products. There is also consistent evidence that consuming drinks and foods at a very high temperature increases the risk for these cancers (The World Health Statistics, 2008) (Table 4.1).

**Table 4.1.** The incidence of cancer according to its localization (RECRAB, 2009)

Localization	Number of patients		Frequency (%)		Frequencies of 2005 in Rabat (%)	
	W	M	W	M	W	M
Tonsil	3	2	0,43	0,28	0,26	0,26
Oral cavity	5	1	0,72	0,14	0	0,26
Pharynx	11	26	1,60	3,76	0	0
Colon	11	14	1,60	2,02	1,58	2,60
Cervical	7	-	1,01	0	13,46	-
Stomach	17	17	2,46	2,46	3,17	4,69
Liver	2	2	0,28	0,28	1,06	2,34
Intestine	9	4	1,30	0,57	0,26	0
Tongue	0	1	0	0,14	1,32	0,26
Larynx	0	3	0	0,43	0	3,65
Naso-pharynx	1	2	0,14	0,28	1,58	2,60
Oro-pharynx	0	1	0	0,14	0	0
Lips	0	2	0	0,28	0	0
Mediastinal	0	1	0	0,14	0,26	0,52
Esophagus	1	3	0,14	0,43	0,53	0,78
Bone	6	12	0,86	1,73	1,06	0,78
Orbit	0	2	0	0,28	0	0
Pancreas	0	4	0	0,57	1,85	2,86
Ovaries	27	-	4,00	0	4,49	-
Skin	3	7	0,43	1,01	0,26	0,26
Peritoneum	4	0	0,57	0	0,26	0
Pleura	1	0	0,14	0	0,26	0,52
Lung	8	64	1,15	9,26	2,9	19,89
Prostate	-	3	0	0,43	-	16,67
Rectum	12	13	1,73	1,88	2,64	3,13
Breast	229	2	33,14	0,28	33,51	0,78
Central nervous system	2	3	0,28	0,43	2,37	2,60
Testicle	-	8	0	1,15	-	0,52
Gallbladder	3	1	0,43	0,14	1,58	1,04
Uterus	5	-	0,72	0	3,43	-
Bladder	1	5	0,14	0,72	0,79	8,07
Vulva	1	0	0,14	0	0,53	-
Hodgkin lymphoma	22	21	3,18	3,03	1,06	1,04
Non Hodgkin Lymphoma	28	27	4,05	3,90	2,64	5,73
Leukemia	0	2	0	0,28	0,26	1,04

Globally, many of the risk factors are due to lifestyle and can be prevented. Physical inactivity, western diet and smoking are prominent causes (Alberti, 2001). It should be

remembered that the patients surveyed were under treatment with either chemotherapy or radiotherapy.

#### 4.1.3. Frequency of cancer according to the age

According to cancer register of NIO, the age interval mostly affected by cancer in the course of our investigation is that between 41 and 60 years. This data is similar to that found during our study (Table 4.2)

**Table 4.2.** The incidence of cancer according to age

Ages	Frequency data of study	Overall frequency between September 2009 and March 2010
Between 1 and 20 years	25 patients (3,6%)	116 patients (4,3%)
Between 21 and 40 years	180 patients (26%)	499 patients (18,5%)
Between 41 and 60 years	363 patients (52,5%)	1342 patients (50%)
More than 61 years old	117 patients (17%)	742 patients (27,5%)

This shows that the incidence of cancer increases with age, while its decrease from 61 years on may be explained only by the high rate of deaths.

#### 4.1.4. Frequency of using traditional medicine by NIO patients

Among the total 691 questioned patients, 272 patients (39%) were identified to regularly use medicinal plants along with medical treatment, while 159 patients have used traditional medicine before using medical treatment. This data show that phytotherapy is still being practiced in Morocco.

#### 4.1.5. Use of Traditional Medicine according to the gender

We have found that women (22.5%) use medicinal plants more frequently than men (16,4%); which confirms results from previous studies (Hamdani S.E, 1984; El Beghdadi M, 1991; Jaouad L, 1992; Nabih M, 1992; Ziyat A and al., 1997). This may be explained by the high rate of illiteracy among women in relation to men, as well as the transmission of information from mothers to daughters. When we compare the intragroup variation, the use of medicinal plant was markedly increased  $60.60 \pm 7.98$  and  $45.20 \pm 5.58$  respectively, when comparing women to men. The difference was significant ( $p < 0.05$ ). The age interval between 41 years and 60 years use more frequently TM compared to other age intervals.

In some ethnopharmacological studies (El Beghdadi M, 1991; Nabih M, 1992) the same results have been found.

#### 4.1.6. Use of Traditional Medicine according to the origin

The origin and the educational level were also a variable, because in traditional medicine the statements of an illiterate or of an expert are not the same.

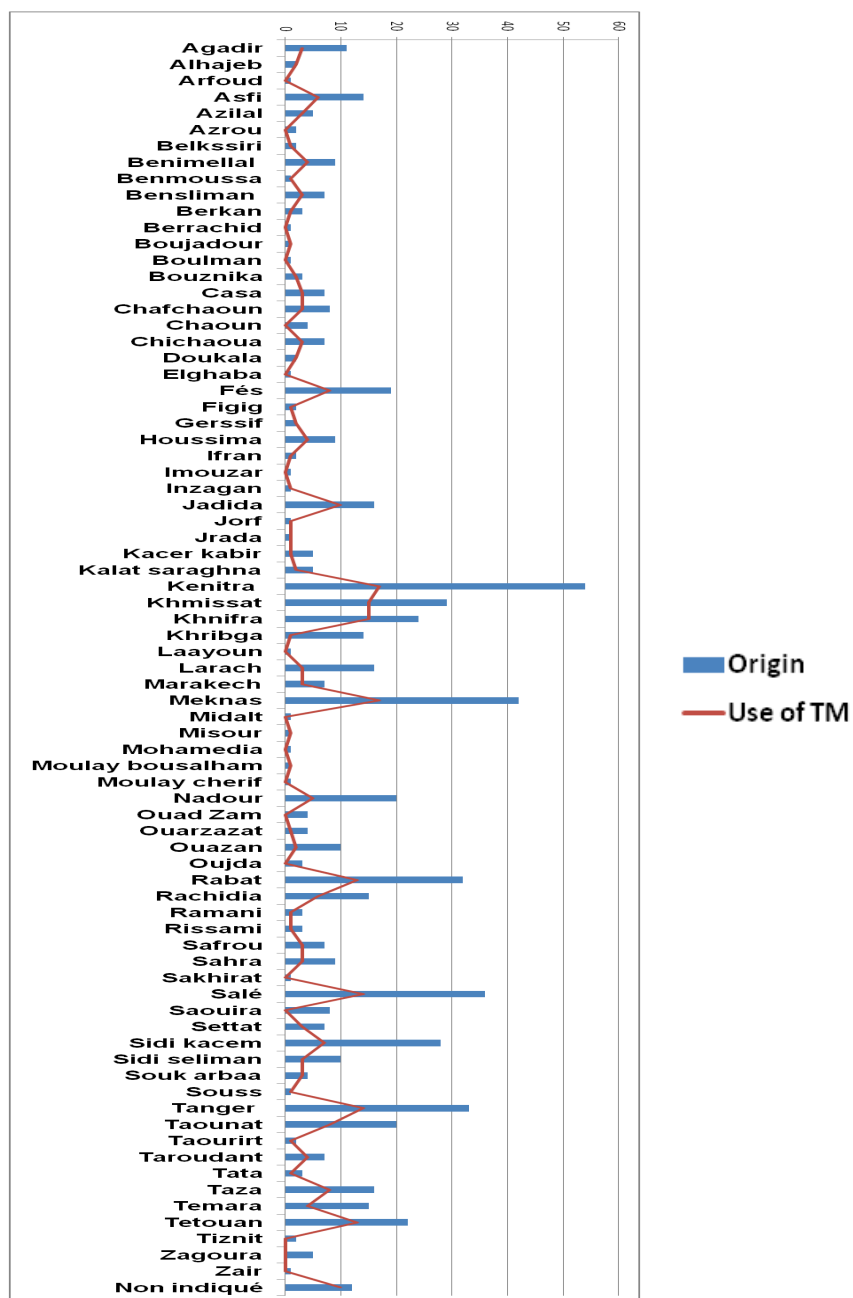


Figure 4.1. Use of Traditional Medicine according to the origin

---

---

#### 4.1.7. Certainty and error biases

Data collection relative to origin, place of residence, age as well as type, stage and localization of tumor have been established with the help of the person responsible of hospital register of NIO, and with the study of medical files of each questioned patient. The accuracy of information on the use of traditional medicine as well as the socio-professional class remains underestimated since it depends on the degree of the goodwill of participation.

During the investigation, there was some reluctance from some patients about clearly and honestly answering questions concerning their use of medicinal plants, either out of fear of their clinician, or fear of the consequences of our investigation. The variable of sex has never been missing in our data.

#### 4.1.8. Medicinal plants used in traditional medicine by the patients of the National Institute of Oncology in Rabat

Fiftyfive plants have been cited during this investigation of which *Aristolochia longa*, *Trigonella foenum-graecum*, *Cassia absus* and *Nigella sativa* are the most used (Table 3.3). Among these plants, 28 are proven to have anticancer activity (Table 3.4).

#### 4.1.9. The toxicity and side effects of medicinal plants

The effect of the action of a drug results in the risk benefit ratio. It depends on the drug itself, dose, disease, other drugs consumed in parallel and the patient him self. Only the clinician can find the balance between the toxic doses and the therapeutic doses expected. However, the role of the clinician is lacking in Traditional Medicine, which explains the high rate of poisoning caused by this treatment.

Moreover, there are plants that are proven to be toxic such as *Pinus halepensis*, *Peganum harmala*, *Aristolochia longa* and *Euphorbia resinifera*, regardless of their toxicity these plants are used by patients in the INO, but have a degree of toxicity or side effects. Nevertheless, despite the existence of the modern medicine for cancer treatment, traditional medicine continues to be a viable health alternative for the large underprivileged section of the Moroccan population.

**Table 4.3.** Medicinal plants used in traditional medicine by the patients of the National Institute of Oncology in Rabat

Scientific name	Vernacular name	Ecological distribution	Part used	Preparation	Administration	Types of Cancer	Number of citation	
<b>Anacardiaceae</b>								
<i>Pistacia lentiscus</i> L.	Drou	ضرو	Mediterranean region	Leaf	Brut, Decoction	Oral	Digestive	5
<b>Apiaceae</b>								
<i>Apium graveolens</i> L.	Krafess	لكرافس	Littoral, Mediterranean et Asia	Leaf	Decoction	Oral	Digestive, Kidney	1
<i>Ammodaucus leucotrichus</i>	Kamoun sooufi	كامون الصوفي		Seed	Grind with honey	Oral	Lung	4
<i>Carum carvi</i> L.	Karwiya	كروية	Europe, Asia occidental-Orient	Seed	Grind with honey	Oral	Lung	2
<i>Coriandrum sativum</i> L.	Qezbour	قزبور	Africa	Aerial parts	Grind with honey	Oral	Digestive, Kidney	3
<i>Cuminum cyminum</i> L.	Kamoun	كامون		Seed	Grind with honey	Oral	Lung	1
<i>Daucus carota</i> L.	Khizzou	خيزو	Asia	Root	Decoction	Oral	Digestive, Kidney	5
<i>Foeniculum vulgare</i> Mill.	Nafaâ	نافع	Mediterranean Basin	Seed	Decoction	Oral	Digestive	6
<i>Petroselinum crispum</i> Mill.	Maâdanous	معدنوس	Europe central, Macedonia.	Aerial parts	Decoction	Oral	Kidney	3
<i>Pimpinella anisum</i> L.	Habbat hlawa	حبة حلاوة	Chine et East	Seed	Decoction	Oral	Digestive, Kidney	1
<b>Apocynaceae</b>								
<i>Nerium oleander</i> L.	Defla	دفلة	Africa du Nord, Asia (South West)	Leaf	Decoction	Mouthwash	Gingival	1
<b>Araliacées</b>								
<i>Panax ginseng</i> C.A. Meyes.	Jinsin	جنسن	Nord-East of china and of Korea	Leaf	Grind with honey	Oral	Lung	1
<b>Arécacées</b>								
<i>Phoenix dactylifera</i>	Tamer	التمر	Saudi and Gulf Country Nord Africa,	Fruit	Brut	Oral	Lymphoma	2
<b>Aristolochiaceae</b>								
<i>Aristolochia longa</i> L.	Berraztam	برزطم		Root	Grind with honey	Oral	General	98
<b>Boraginacées</b>								
<i>Borago officinalis</i>	Hoboub allikaah	حبوب اللقاح		Stamen	Grind with honey	Oral	General	2
<b>Cruciferae</b>								
<i>Lepidium sativum</i> L.	Hebb rchad	حب الرشاد		Seed	Grind with honey	Oral	Lung,, Digestive	9
<b>Capparaceae</b>								
<i>Capparis spinosa</i> L.	Kebbar	الكبار		Fruit	Grind with honey	Oral	Lymphoma	2
<b>Caryophyllaceae</b>								
<i>Corrigiola telephiifolia</i>	Sarghina	صرغينة		Root	Decoction	Oral	Digestive, Liver	1
<i>Herniaria glabra</i> L.	Hrasset lehjer	هراست الحجر		Aerial parts			Digestive, Renal	1

<b>Chenopodiaceae</b>								
<i>Chenopodium ambrosioides</i>	Mkhinza	مخينزة	Mexico	Leaf	Decoction	Oral	Amygdale	1
<i>Haloxylon scoparium</i> Pomel	Eremt	الرمث		Leaf, Fruit	Decoction	Oral	Liver	1
<b>Compositae</b>								
<i>Artemisia absinthium</i> L.	Chiba	الشيبا		Leaf	Infusion	Oral	Digestive	1
<i>Artemisia vulgaris</i>	Chih	الشيح	Orient, Occident	Aerial parts	Infusion	Oral	Digestive	2
<i>Artemisia herba-alba</i>	Chih	الشيح الخرساني		Aerial parts	Infusion	Oral	Digestive	1
<i>Inula viscosa</i> (L.) Ait.	elkhorrassani Bagraman	بكرمان	Tlemcen	Leaf, Flower	Grind with honey	Oral	Breast	22
<b>Euphorbiaceae</b>								
<i>Euphorbia resinifera</i>	Daghmous	الدغموس	Morocco	Aerial parts	Grind with honey	Oral	General	8
<b>Fabaceae</b>								
<i>Cassia absus</i>	Habat albaraka	الحبة البركة	Saudi	Seed	Grind with honey	Oral	General	58
<i>Cicer arietinum</i>	Homos	الحمص	India and Mediterranean Basin	Seed	Grind with honey	Oral	Lung	1
<i>Vicia faba</i>	Foul	الفاول	Asia	Seed	Grind with honey	Oral	Lung	1
<b>Iridacées</b>								
<i>Crocus sativus</i>	Zâafran	الزعفران		Stamen	Decoction	Oral	General	3
<b>Lamiaceae</b>								
<i>Ajuga iva</i> L.	Chendgoura	الشندگورة		Rod, Leaf	Grind with honey	Oral	Breast	6
<i>Lavandula officinalis</i> L.	Khzama	خزامة	Mediterranean region	Leaf	Infusion	Oral	The urinary and genital system	9
<i>Marrubium vulgare</i> L.	Marrîwet	مريوت	Europe méridionale	Rod, Leaf	Decoction	Oral	Digestive, Gingival	19
<i>Mentha pulegium</i> L.	Fliyou	فليو	Zarifet, El-Meffrouche, Hafir	Rod, Leaf	Infusion	Oral	Digestive, Gingival	7
<i>Origanum compactum</i> Beneth	Zaâtar	زعتر		Rod, Leaf	Infusion	Oral	Digestive, Gingival	44
<i>Rosmarinus officinalis</i> L.	Azîr	أزير	Mediterranean	Leaf	Decoction	Oral	Digestive	4
<i>Salvia officinalis</i> L.	Salmiya	سلمية		Leaf	Infusion	Oral	Intestine, Lung	2
<i>Thymus</i> ssp.	Zitra	زعترة	Mediterranean	Rod, Leaf	Infusion	Oral	Digestive	1
<b>Leguminosae</b>								
<i>Trigonella foenum-graecum</i>	Halba	حلبة		Seed	Grind with honey	Oral	Digestive	60
<b>Liliaceae</b>								
<i>Allium cepa</i> L.	El Bassla	بصل		Bulb	Brut	Oral	General	1
<i>Allium sativum</i> L.	Touma	الثوم		Bulb	Brut	Oral	General	14
<b>Linaceae</b>								
<i>Linum usitatissimum</i>	Zariat alkhatan	زريعة الكتان	Morocco, Argentina and Egypt	Seed	Grind with honey	Oral	Lymphoma	13
<b>Liliacées</b>								
<i>Aloe ferox</i> Mill.	Siber	الصبر	Oriental Africa et méridionale	Leaf	Extraction	Oral	Digestive	4
<b>Lythraceae</b>								
<i>Lawsonia inermis</i>	Henna	الحناء	La carie région de l'asie mineure	Flower	Grind with water	Cataplasm	Skin	5

<b>Moracées</b>									
<i>Ficus carica</i>	Karmous	كرموس	Mediterranean Region	Fruit	Brut	Oral	Digestive	2	
<b>Myrtaceae</b>									
<i>Myrtus communis</i> L.	Rihan	الريحان	Ouest d'Asie sud, Europe	Leaf	Decoction	Oral	Digestive	3	
<b>Oléacées</b>									
<i>Olea europaea</i>	Zaytoun	الزيتون	Nord de l'Asie.	Fruit	Extraction	Oral	Lung	2	
<b>Pinacées</b>									
<i>Pinus halepensis</i> mill	Katran	قطران	Mediterranean Region	Seed	Extraction	Oral	Esophagi	1	
<b>Punicaceae</b>									
<i>Punica granatum</i> L.	Rouman	رمان	Afrique orientale et méridionale	Rind	Decoction	Oral	Skin	2	
<b>Ranunculaceae</b>									
<i>Nigella sativa</i> L.	Samouj, Haba Saoudaâ	سارانوج الحبة السوداء	Bassin méditerranéen	Seed	Grind with honey	Oral	General	54	
<b>Sapotaceae</b>									
<i>Argania spinosa</i>	Argan	أركان	Endémique marocaine	Seed	Extraction	Oral	Skin	1	
<b>Thymelaeaceae</b>									
<i>Thymelaea lhytroides</i>	Ftiticha , matnan	مثنان فتيتشة	Endémique ibéro-marocaine	Aerial parts	Decoction	Oral	Uterus	2	
<b>Verbenaceae</b>									
<i>Verbena officinalis</i>	Louiza	اللويزة	Espèce cultivée dans les jardins des maisons	Leaf	Infusion	Oral	Gallbladder	1	
<b>Zingiberacées</b>									
<i>Zingiber officinale</i> roscoe	Sknjbir	سكنجبير	Sud de l'Asie ; Pays tropicaux	Root	Grind with honey	Oral	General	1	
<b>Zygophylaceae</b>									
<i>Peganum harmala</i> L.	alharmal	الحارمل		Seed	Grind with honey	Oral	General	1	



**Table 4.4.** List of plants reported to have anticancer activity

Species	Family	Reference
<i>Pistacia lentiscus</i> L.	Anacardiaceae	Balan K.V, 2007
<i>Petroselinum crispum</i> Mill.	Apiaceae	Hui Z and al., 2006
<i>Nerium oleander</i>	Apocynaceae	Luay J.R and al., 2001
<i>Panax ginseng</i> C.A. Meyes	Araliaceae	Shi S and al., 2011
<i>Phoenix dactylifera</i>	Arécaceae	Biglari F and al., 2011
<i>Capparis spinosa</i> L.	Cruciferae	Sze-Kwan L and al., 2009
<i>Chenopodium ambrosioides</i>	Chenopodiaceae	Ruffa M. J and al., 2002
<i>Artemisia vulgaris</i>	Compositae	Nibret E and al., 2010
<i>Artemisia herba-alba</i>	Compositae	Nibret E and al., 2010
<i>Inula viscosa</i> (L.) Ait.	Compositae	Danino O and al., 2009
<i>Euphorbia resinifera</i>	Euphorbiaceae	Lavie D and al., 1963
<i>Cicer arietinum</i>	Fabaceae	Ajjaikebaier A and al., 2011
<i>Crocus sativus</i>	Iridaceae	Akshi H. A and al., 2009
<i>Rosmarinus officinalis</i> L.	Lamiaceae	Shuwen C and al., 2001
<i>Salvia officinalis</i> L.	Lamiaceae	Toshiya M and al., 2002
<i>Trigonella foenum-graecum</i>	Leguminosae	Jayadev R and al., 2004
<i>Allium cepa</i> L.	Liliaceae	Jun Y and al., 2004
<i>Allium sativum</i> L.	Liliaceae	Yoshiyuki M and al., 2010
<i>Linum usitatissimum</i>	Linaceae Moraceae	Abarzua S and al., 2007
<i>Ficus carica</i>	Myrtaceae	Sarfaraz Khan M and al., 2011
<i>Olea europaea</i>	Oléaceae	Mijatovic S.A and al., 1955
<i>Pinus halepensis</i> mill	Pinaceae	Volker M-S and al., 2011
<i>Punica granatum</i> L.	Punicaceae	Oliveira L.P and al., 2010
<i>Nigella sativa</i> L.	Ranunculaceae	Worthen D.R and al., 1998
<i>Argania spinosa</i>	Sapotaceae	El Babili F and al., 2010
<i>Verbena officinalis</i>	Verbenaceae	Ucar Turker A and al., 2010
<i>Zingiber officinale roscoe</i>	Zingiberaceae	Kim E-C and al., 2005
<i>Peganum harmala</i> L.	Zygophyllaceae	Changhong W and al., 2005

#### 4.2. Compounds isolated from the plant *Thymelaea lythroides*

The genus *Thymelaea* Mill. (Thymelaeaceae) comprises 31 species of xerophyllous shrubs and herbs (Galicia-Herbada, 2006). *Thymelaea lythroides*, an ibero-endemic plant in Morocco, is popularly used as medicinal plant to treat otitis, diabetes, rheumatism, inflammation of the prostate and uterus cancer (Gmira *et al.*, 2007). *Thymelaea lythroides* was selected according to an ethnopharmacological study of traditional plants used in Morocco by cancer patients as herbal therapeutics (Kabbaj *et al.*, 2012).

Fresh, healthy parts of *Thymelaea lythroides* have been collected from Maâmora forest in Rabat, Morocco. Voucher specimens were identified by Prof. FZ. ALAOUI, Department of Botany, Faculty of Sciences, Mohamed V University and Prof. Dr. M. IBN TATOU,

Scientific Institute of Rabat, Morocco. Reference samples are deposited as the herbarium of the Scientific Institute of Rabat, and a collection number (RAB 77777) has been assigned.

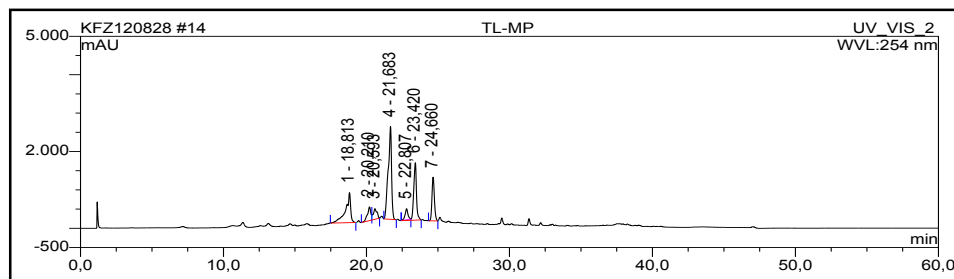


**Figure 4.5.** HPLC chromatogram of methanol fraction of *Thymelaea lythroides*

Comparison of the HPLC chromatograms of the different fractions of *Thymelaea lythroides* and the preliminary biological screening assays, i.e. antibacterial, antifungal, and cytotoxicity showed that the methanol fraction had the best range of secondary metabolites and the most active one (see Table 4.5 and Figure 4.2).

**Table 4.1.** Preliminary biological screening assays of the different fractions of *Thymelaea lythroides*

Fungal strain	L5178Y	MRSA	<i>Strep. pneumonia</i>	<i>Entero. Faecalis</i>
<b>Ethylacetate Fraction</b>	99.7%	>62,5µg/ml	>62.5µg/ml	n.a
<b>Hexane Fraction</b>	125%	n.a	>3.2µg/ml	n.a
<b>Methanol Fraction</b>	99.7%	>31.25µg/ml	>62.2µg/ml	>61.5µg/ml
<b>Water Fraction</b>	99,7%	>31.25µg/ml	> 31.25µg/ml	>61.5µg/ml



**1** was isolated from *Thymelaea lythroides* extracted with EtOAc. The EtOAc extract was portioned between *n*-hexane and 90% MeOH. The 90% MeOH fraction was chromatographed over silica gel F254 using gradient elution (*n*-hexane/EtOAc/CH<sub>2</sub>Cl<sub>2</sub>/MeOH). The fraction was subjected to a sephadex LH-20 column using CH<sub>2</sub>Cl<sub>2</sub>/MeOH (1:1) as eluent system, then purified by semi-preparative HPLC (Merck, Hitachi L-7100) using an Eurosphere 100–10 C18 column (300 x 8mm, L x i.d.) with the following gradient (MeOH/H<sub>2</sub>O): 0 min, 10% MeOH; 5 min, 10% MeOH; 35 min 100% MeOH; 45 min, 100 % MeOH, which afforded white powder (yield, 1 mg). It showed UV absorbance at  $\lambda_{\text{max}}$  (MeOH) 213.2 and 356.2 nm. Positive ESI-MS of **1** exhibited a prominent peak at  $m/z$  261.9 [M+H]<sup>+</sup> (base peak) indicating a molecular weight of 261 g/mol, which established a molecular formula of C<sub>15</sub>H<sub>19</sub>NO<sub>3</sub>. The <sup>1</sup>H NMR spectrum showed the presence of 19 protons signals, two methyl protons at ( $\delta_{\text{H}}$  0.26 ppm) and ( $\delta_{\text{H}}$  0.85 ppm) assigned to H-8 and H-9; one N-methyl protons at ( $\delta_{\text{H}}$  3.14 ppm) assigned to 4-CH<sub>3</sub>; three methine protons at ( $\delta_{\text{H}}$  5.79 ppm) ( $\delta_{\text{H}}$  4.84 ppm) ( $\delta_{\text{H}}$  1.81 ppm) assigned to H-3, H-6 and H-7; one pair of methylene protons ( $\delta_{\text{H}}$  3.03-3.39 ppm) assigned to H-10 and five aromatic protons, four of them are overlapping at ( $\delta_{\text{H}}$  7.24-7.25 ppm) assigned to H-12, H-13, H-15 and H-16, the H-14 appears at ( $\delta_{\text{H}}$  7.18 ppm).

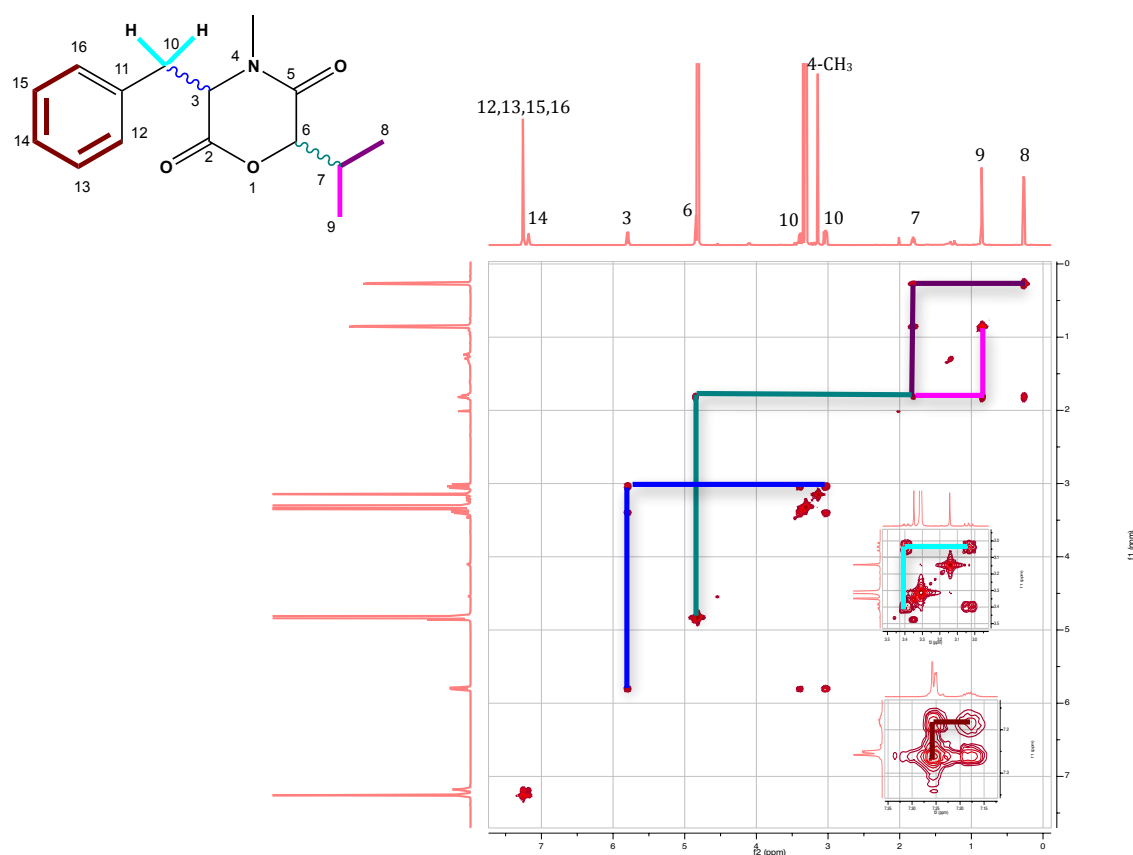


**Figure 4.3.** <sup>1</sup>H-<sup>1</sup>H NMR COSY

The  $^1\text{H}$ - $^1\text{H}$  NMR COSY showed the presence of four spin systems assigned H(3)H(10), H(6)→H(8), from H(7)H(9) and the aromatic ring system H(12)H(13)H(14)H(15)H(16), whereas the connection of these spin systems was established by inspection of  $^2J$  and  $^3J$  HMBC correlations (Figure 4.3 and 4.4).

4-CH<sub>3</sub> showed a correlation to the carbon C-3 ( $\delta_{\text{C}}$  58.0 ppm) and C-5 ( $\delta_{\text{C}}$  170.3 ppm), H-3 showed a correlation to the carbon C-2 and C-5 appearing at ( $\delta_{\text{C}}$  172.3 ppm) and ( $\delta_{\text{C}}$  170.3 ppm), the same H-6 showed a correlation to the two carbonyl carbons C-2 and C-5. On the other hand, H-10 showed correlations to the overlapping aromatic carbons, which were attributed to C-12, C-13, C-15 and C-16 ( $\delta_{\text{C}}$  129.8-130.0 ppm), as well as to an isolated aromatic carbon assigned to C-11 ( $\delta_{\text{C}}$  138.2 ppm), hence establishing the connection between the identified spin systems (Figure 4.3). Thus the structure of **1** was elucidated as 4-methyl-6-(1-methylethyl)-3-phenylmethyl-1,4-perhydrooxazine-2,5-dione, consisting of one mole each of *N*-methylphenylalanine and 2-hydroxy-3-methylbutyric acid.

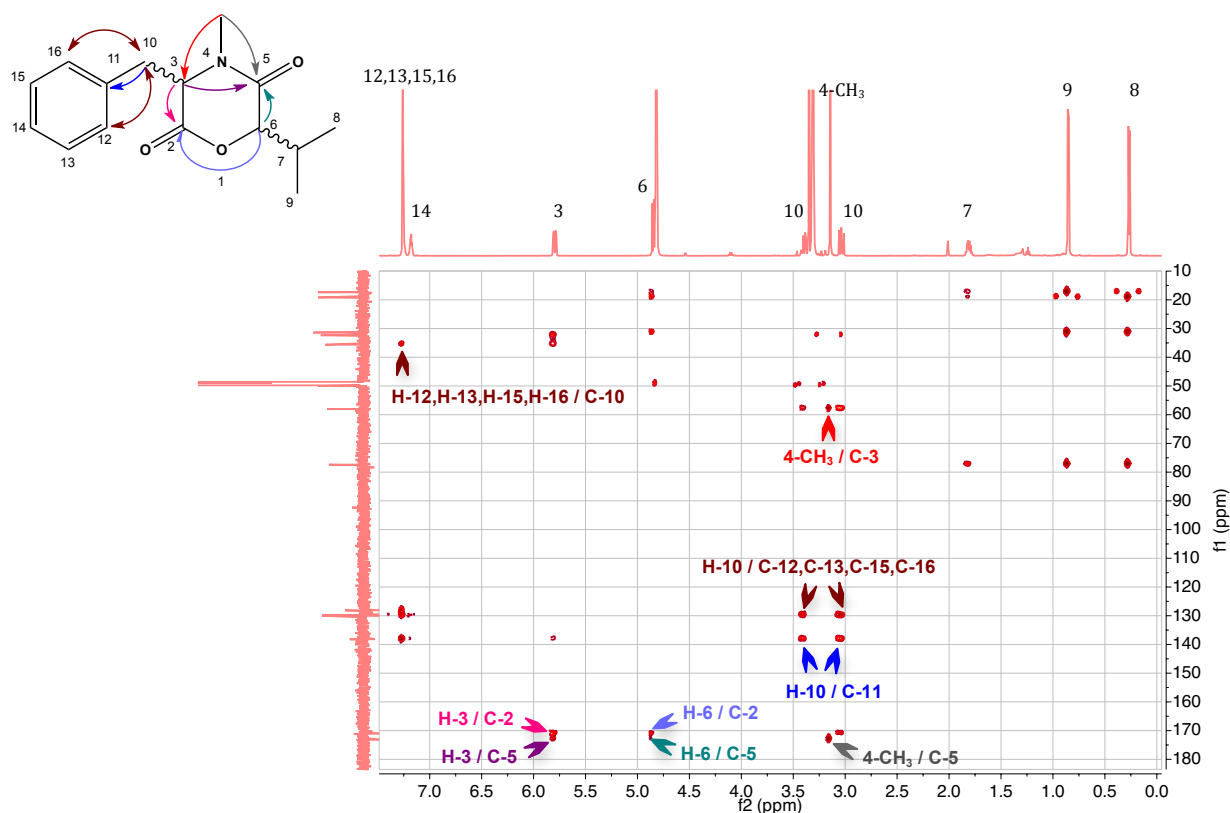


**Figure 4.4.** Selected  $^{13}\text{C}$ - $^1\text{H}$  NMR HMBC correlations

The optical rotations of **4** ( $[\alpha]_{\text{D}} + 176.09^\circ$  (c 0.02, CH<sub>3</sub>Cl)) was compared with that of bassiatin [(3*S*,6*R*)-4-methyl-6-(1-methylethyl)-3-phenylmethyl-1,4-perhydrooxazine-2,5-di-

one] ( $[\alpha]_D + 181.05^\circ$  (c 0.024, CH<sub>3</sub>Cl)) and to the other three isomeric - (3R,6S)-, (3R,6R)-, (3S,6S)- compounds (Kagamizono *et al.*, 1995). The structure of **1** was determined to be (3S,6R)-4-methyl-6-(1-methylethyl)-3-phenylmethyl-1,4-perhydrooxazine-2,5-dione, (3S,6R) Bassiatin.

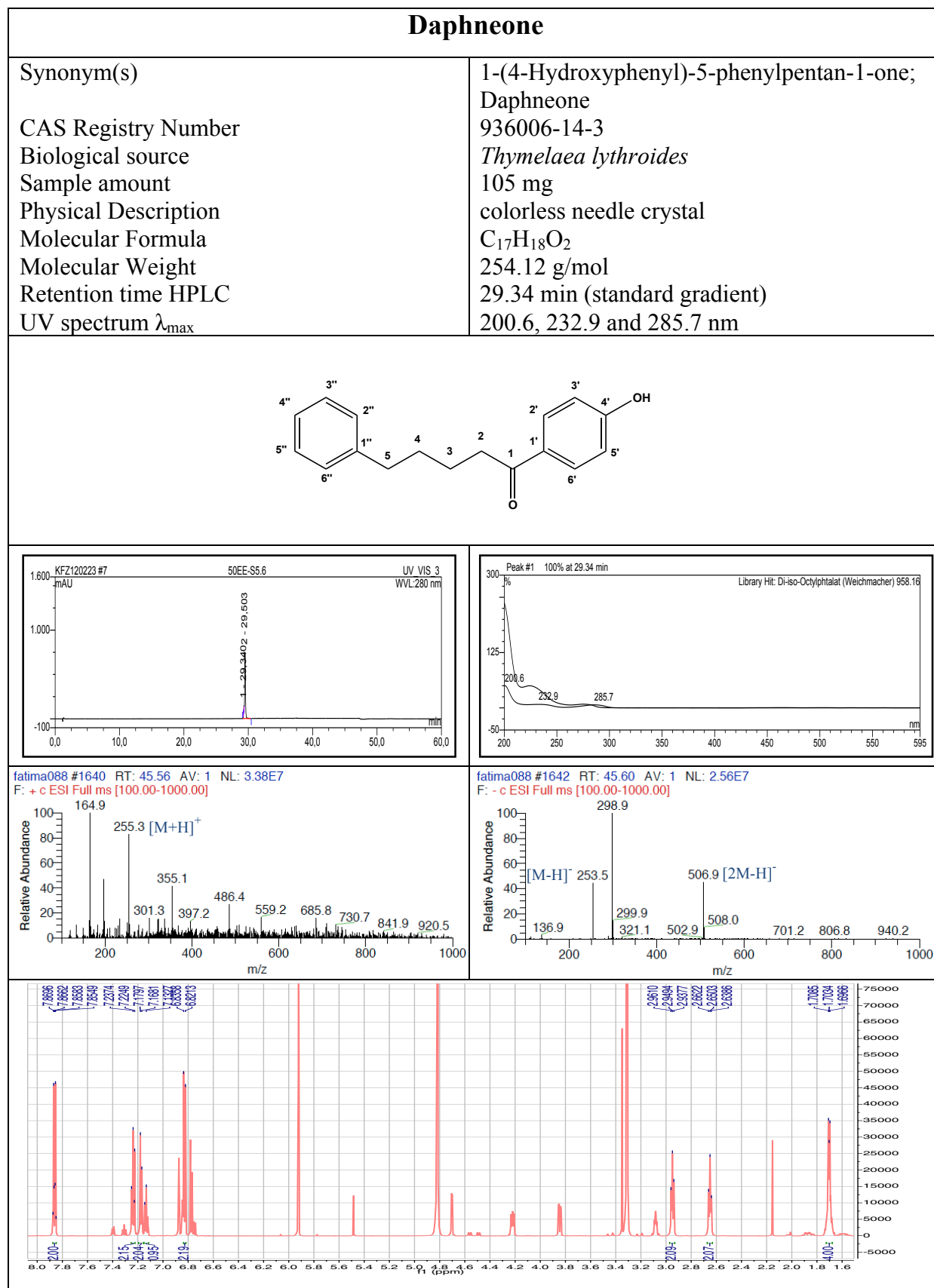
**Table 4.6.** Comparison of <sup>1</sup>H and <sup>13</sup>C NMR chemical shifts of **1** with Bassiatin (Kagamizono *et al.*, 1995)

Position	<b>1</b>		<b>Bassiatin</b>	
	$\delta_H$ (mult., <i>J</i> in Hz)	$\delta_C$	$\delta_H$ (mult., <i>J</i> in Hz)	$\delta_C$
<b>2</b>	-	172.3	-	170.2
<b>3</b>	5.79, 1H (dd, <i>J</i> = 12.6, 4.5 Hz)	58.0	5.47 (br d)	57.6
<b>4-CH<sub>3</sub></b>	3.14, 3H (s)	32.3	3.00 (s)	32.6
<b>5</b>	-	170.3	-	169.5
<b>6</b>	4.84, 1H (d, <i>J</i> = 8.9 Hz)	77.3	4.92 (d, 8.7 Hz)	75.7
<b>7</b>	1.81, 1H (m)	31.3	2.02 (m)	29.9
<b>8</b>	0.26, 3H (d, <i>J</i> = 6.9 Hz)	17.3	0.42 (d, <i>J</i> = 6.9 Hz)	17.8
<b>9</b>	0.85, 3H (d, <i>J</i> = 6.6 Hz)	19.1	0.80 (d, <i>J</i> = 6.9 Hz)	18.5
<b>10</b>	3.39, 1H (dd, <i>J</i> = 14.7, 4.6 Hz)	35.6	3.36 (dd, <i>J</i> = 14.5, 5.1 Hz)	35.0
	3.03, 1H(dd, <i>J</i> = 14.7, 12.7 Hz)		2.98 (dd, <i>J</i> = 14.5, 11.9 Hz)	
<b>11</b>	-	138.2	-	136.9
<b>12, 16</b>	7.25 - 7.24, 2H (m)	130.0	7.23 - 7.23 (m)	129.1
<b>13, 15</b>	7.25 - 7.24, 2H (m)	129.8	7.23 - 7.23 (m)	128.8
<b>14</b>	7.18, 1H (m)	128.1	7.17 (m)	127.0

Bassiatin is an unusual secondary metabolite to be obtained from plants. To the best of our knowledge, bassiatin was only described as natural product from the cultured broth of *Beauveria bassiana* (Kagamaizono *et al.*, 1995), from the insect-body portions of *Cordyceps cicadae* (Kuo *et al.*, 2002) and later isolated from the endophytic fungus *Fusarium oxysporum* J8-1-2 (Meng *et al.*, 2011). This is the first report of this compound from the plant *Thymelaea lythroides*. This can possibly be explained by the presence of an endophyte, which produced bassiatin in large quantity to be detected in the host plant.

Compound isolated from the plant *Thymelaea lythroides*

Daphneone (2, Known)



**2** was isolated from *Thymelaea lythroides* extracted with EtOAc. The EtOAc extract was portioned between *n*-hexane and 90% MeOH. The 90% MeOH fraction was chromatographed over silica gel F254 using gradient elution (*n*-hexane/EtOAc/CH<sub>2</sub>Cl<sub>2</sub>/MeOH). The fraction was subjected to a sephadex LH-20 column using CH<sub>2</sub>Cl<sub>2</sub>/MeOH (1:1) as eluent system, then purified by semi-preparative HPLC (Merck, Hitachi L-7100) using an Eurosphere 100–10 C18 column (300 x 8mm, L x i.d.) with the following gradient (MeOH/H<sub>2</sub>O): 0 min, 10% MeOH; 5 min, 10% MeOH; 35 min 100% MeOH; 45 min, 100 % MeOH. Compound **2** was obtained as a mixture with compound **6** forming colorless needle crystals with colorless oil (yield, 3 mg). It showed UV absorbance at  $\lambda_{\text{max}}$  (MeOH) 200.6, 232.9 and 285.7 nm. Positive and negative ESI-MS of **2** exhibited a prominent peak at  $m/z$  255.3 [M+H]<sup>+</sup> (base peak) and  $m/z$  253.5 [M-H]<sup>-</sup> (base peak) indicating a molecular weight of 254 g/mol. The molecular formula of compound **2** was determined to be C<sub>17</sub>H<sub>18</sub>O<sub>2</sub> based on the analysis of the molecular weight and <sup>13</sup>C NMR data. The <sup>1</sup>H NMR spectrum (MeOD) (Table 4.7) displayed signals of a *p*-substituted aromatic protons at ( $\delta_{\text{H}}$  6.82 and 7.86 ppm; each 2H) assigned to H-3', H-5', H-2' and H-6' respectively and mono-substituted aromatic protons at ( $\delta_{\text{H}}$  7.16 and 7.23 ppm; each 2H) with ( $\delta_{\text{H}}$  7.13 ppm; 1H) assigned to H-2'', H-6'', H-3'', H-5'' and H-4'' respectively, indicated that there are two aromatic rings in the structure. In addition, four methylene protons at ( $\delta_{\text{H}}$  1.70 ppm; 4H), ( $\delta_{\text{H}}$  2.65 ppm; 2H) and ( $\delta_{\text{H}}$  2.95 ppm; 2H) assigned to H-3, H-4, H-5 and H-2 respectively. The <sup>13</sup>C NMR spectrum indicated the presence of 17 carbon signals displayed of four aliphatic methylene carbons, nine aromatic methine carbons and four quaternary carbons, one carbonyl carbon and one oxygenated quaternary carbon. The <sup>1</sup>H-<sup>1</sup>H COSY NMR spectrum (Figure 4.5.A) showed 4 spin systems assigned for H(2')H(3'), H(5')H(6'), from H(2) to H(5) and the aromatic ring from H(2'')to H(6''), whereas the connection of these spin systems was established by inspection of <sup>2</sup>J and <sup>3</sup>J HMBC correlations (Figure 4.5.B).

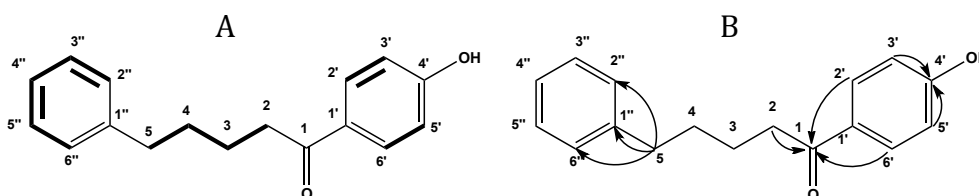


**Figure 4.5** A) <sup>1</sup>H-<sup>1</sup>H COSY correlations B) selected <sup>13</sup>C-<sup>1</sup>H NMR correlations of **2**

H-5 showed a correlations to the overlapping aromatic carbons, which were attributed to C-2'' and C-6'' ( $\delta_{\text{C}}$  129.9 ppm), as well as to an isolated aromatic carbon assigned to C-1'' ( $\delta_{\text{C}}$  144.1



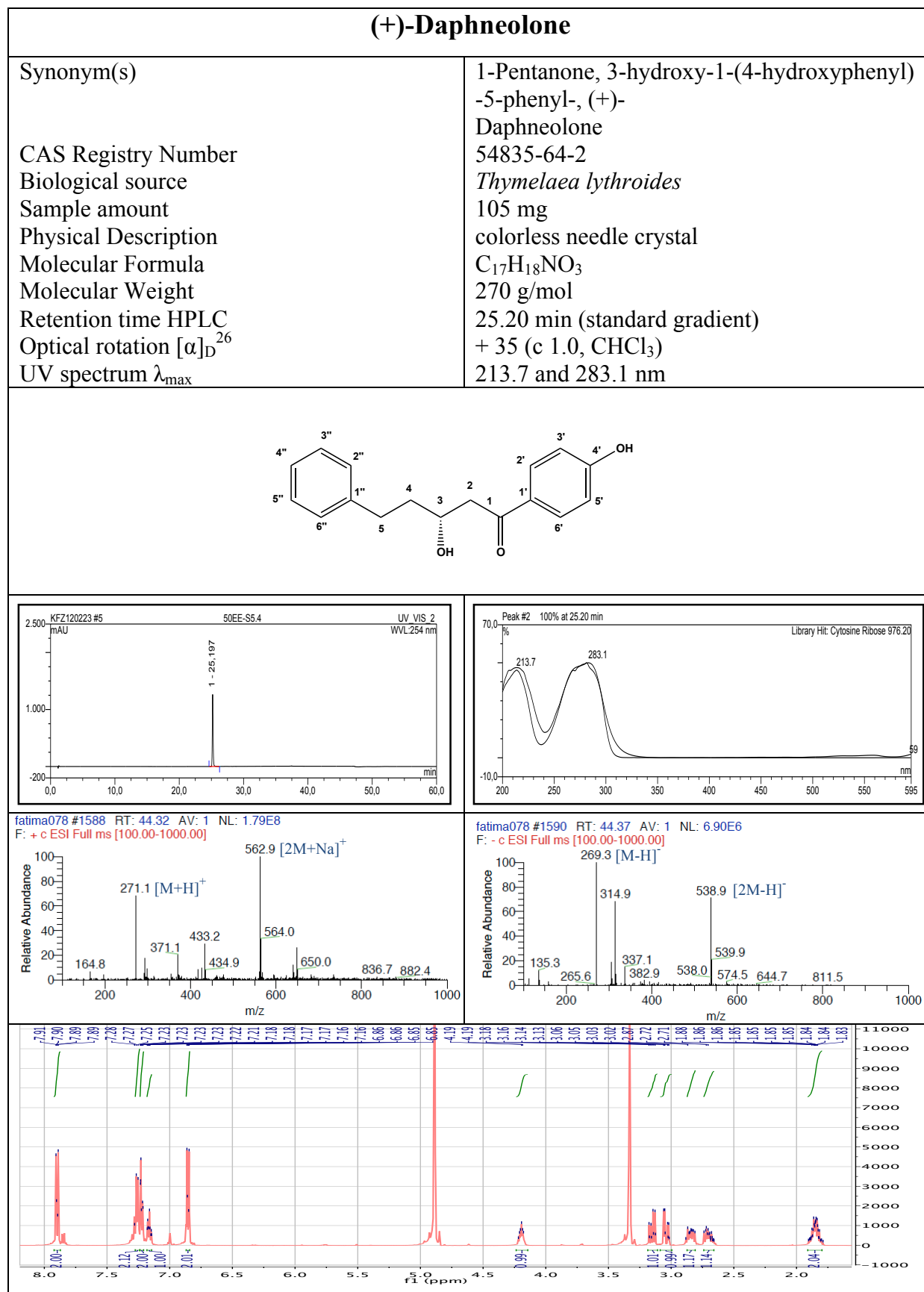
---

---

ppm), these correlations indicated that the mono-substituted aromatic ring is connected to the side chain of four methylene groups at C-1". On the other hand, the second *p*-substituted aromatic ring is connected to a hydroxyl group at C-4' ( $\delta_C$  164.30 ppm) and to carbonyl group at C-1' ( $\delta_C$  130.6 ppm), these connection were confirmed with the correlations between the overlapping aromatic protons H-3' and H-5' to the C-4' and from the overlapping aromatic protons H-2' and H-6' to the carbon C-1 ( $\delta_C$  202.28 ppm). Furthermore, the carbonyl carbon C-1 ( $\delta_C$  202.28 ppm) was connected to side chain of four methylene groups at C-2 ( $\delta_C$  39.43 ppm), which was confirmed with the correlation between H-2 to C-1, thus, establishing the connection between the identified spin systems.

The identification was further corroborated by comparison of UV,  $^1\text{H}$ ,  $^{13}\text{C}$  NMR, mass spectral data as well as  $[\alpha]_D$  value of **2** with those previously published data for Daphenone (Zhang *et al.*, 2006).

Daphenone was previously isolated from some species of Daphne including, *Daphne odora*, which is the first biological source report (Zhang *et al.*, 2006), from *Daphne giraldii* Nitsche (Sun *et al.*, 2006) and from *Daphne acutiloba* (Huang *et al.*, 2012). This the first report of Daphenone from the species *Thymelaea lythroides*.

Compound isolated from the plant *Thymelaea lythroides*(+) -Daphneolone (**3**, Known)

**3** was isolated from *Thymelaea lythroides* extracted with EtOAc. The EtOAc extract was portioned between *n*-hexane and 90% MeOH. The 90% MeOH fraction was chromatographed over silica gel F254 using gradient elution (*n*-hexane/EtOAc/CH<sub>2</sub>Cl<sub>2</sub>/MeOH). The fraction was subjected to a sephadex LH-20 column using CH<sub>2</sub>Cl<sub>2</sub>/MeOH (1:1) as eluent system, then purified by semi-preparative HPLC (Merck, Hitachi L-7100) using an Eurosphere 100–10 C18 column (300 x 8mm, L x i.d.) with the following gradient (MeOH/H<sub>2</sub>O): 0 min, 10% MeOH; 5 min, 10% MeOH; 35 min 100% MeOH; 45 min, 100 % MeOH, which afforded colorless needle crystal (yield, 3 mg). It showed UV absorbance at  $\lambda_{\max}$  (MeOH) 213.7 and 283.1 nm. Positive and negative ESI-MS of **3** exhibited a prominent peak at *m/z* 271.1 [M+H]<sup>+</sup> (base peak) and *m/z* 269.3 [M-H]<sup>-</sup> (base peak) indicating a molecular weight of 270 g/mol with a 16 mass unit decrease compared to **2**. To fulfill the molecular weight, the presence of one hydroxyl group was supposed. The molecular formula of compound **3** was determined to be C<sub>17</sub>H<sub>18</sub>NO<sub>3</sub> based on the analysis of the molecular weight and <sup>13</sup>C NMR data.

The <sup>1</sup>H NMR spectrum (MeOD) (Table 4.3) displayed the same aromatic protons signals as compound **2**, indicating that there are also two aromatic rings in the structure. In addition, two typical AMX system at ( $\delta_{\text{H}}$  3.02 ppm ; 1H, dd, *J*= 17.6, 8.5 Hz, assigned to H-2<sub>A</sub>), ( $\delta_{\text{H}}$  3.13 ppm ; 1H, dd, *J*= 17.6, 2.6 Hz, assigned to H-2<sub>M</sub>) and ( $\delta_{\text{H}}$  4.21 ppm ; 1H, m, assigned to H-3<sub>X</sub>) together with the second AMX<sub>2</sub> system at ( $\delta_{\text{H}}$  2.75 ppm ; 1H, m, H-5<sub>A</sub>), ( $\delta_{\text{H}}$  2.89 ppm ; 1H, m, H-5<sub>M</sub>) and ( $\delta_{\text{H}}$  1.81 ppm ; 2H, m, H-4<sub>X1</sub> and H-4<sub>X2</sub>) indicate that there are three methylene protons and one methine proton with hydroxyl group substitution. The <sup>1</sup>H-<sup>1</sup>H COSY NMR spectrum showed the same spin systems as daphenone (Figure 4.6).

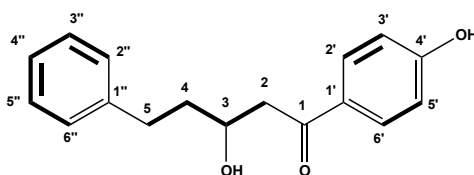


**Figure 4.6.** <sup>1</sup>H-<sup>1</sup>H COSY correlations of **3**

The optical rotation of **3** was close to the rotation reported in the literature for (+)-daphneolone (Zhuang *et al.*, 1982).

The identification was further corroborated by comparison of UV, NMR, MS data as well as  $[\alpha]_D$  value of **3** and those previously published data for daphneolone (Zhuang *et al.*, 1982).

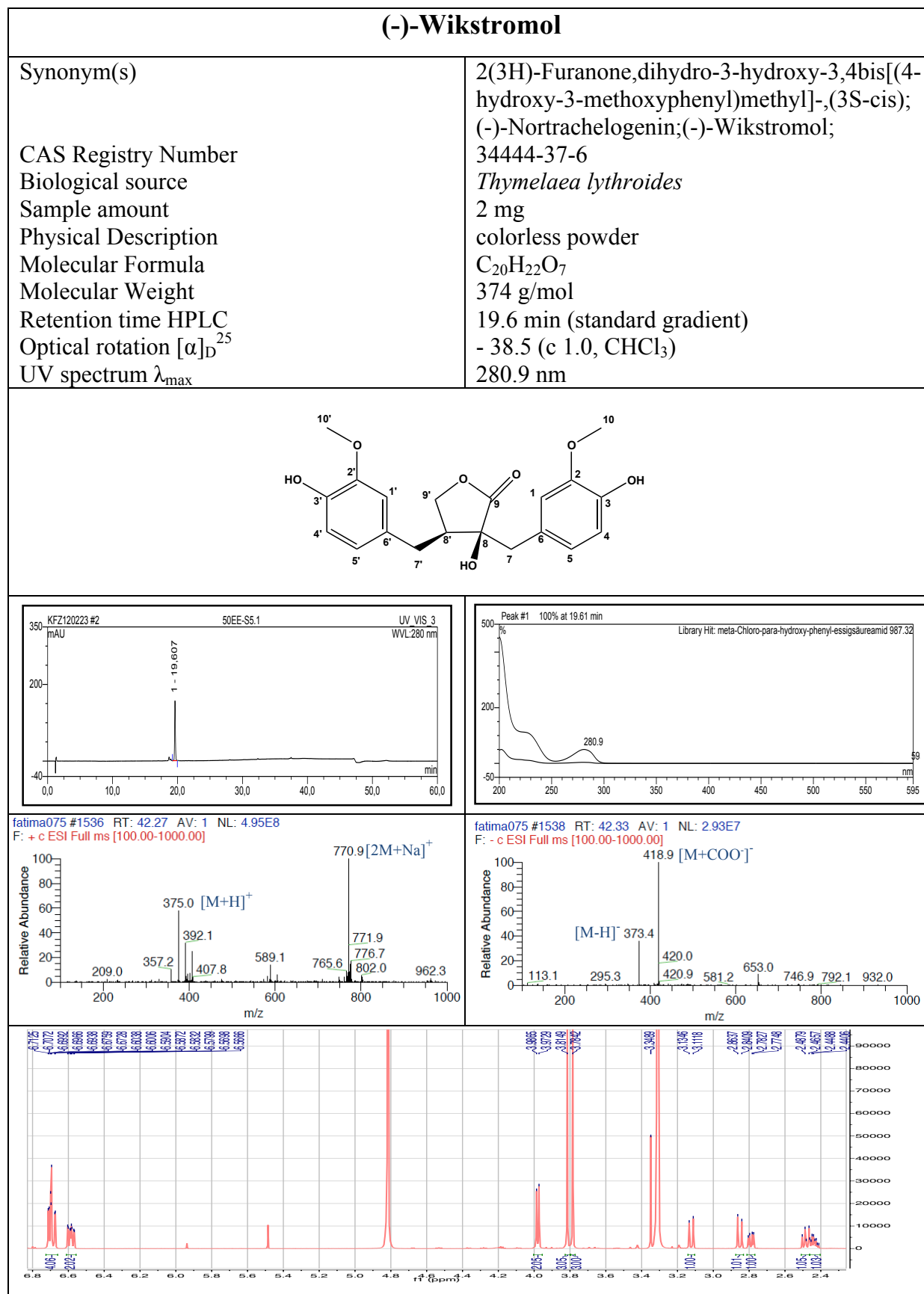
Daphnelone was previously isolated from some species of *Daphne* including, *Daphne odora*, which is the first biological source report (Kogiso *et al.*, 1974), from *Daphne tangutica* (Zhuang *et al.*, 1982), from *Daphne mezereum* (Kreher *et al.*, 1990), from *Daphne pedunculata* (Xu *et al.*, 2008), from *Daphne giraldii* (Wu *et al.*, 2009), from *Daphne bholua* (Chen *et al.*, 2009), from *Daphne retusa* (Hu *et al.*, 2011), from *Daphne papyracea* var. *crassiuscula* (Wei *et al.*, 2012) and from *Daphne genkwa* (Chen *et al.*, 2013). This the first report of Daphnelone from the species *Thymelaea lythroides*.

**Table 4.7.** The  $^1\text{H}$  and  $^{13}\text{C}$  chemical shifts of **2** and **3**

Position	<b>2</b>		<b>3</b>	
	$\delta_{\text{H}}$ (mult., $J$ in Hz)	$\delta_{\text{C}}$	$\delta_{\text{H}}$ (mult., $J$ in Hz)	$\delta_{\text{C}}$
<b>1</b>	-	202.28	-	202.28
<b>2</b>	2.95 (2H, t, $J=6.96$ Hz)	39.43	3.02 (1H, dd, $J=17.6, 8.5$ Hz) 3.13 (1H, dd, $J=17.6, 2.6$ Hz)	44.3
<b>3</b>	1.70 (2H, m)	26.17	4.21 (1H, m)	67.2
<b>4</b>	1.70 (2H, m)	32.85	1.81 (2H, m)	38.1
<b>5</b>	2.65 (2H, t, $J=7.14$ Hz)	37.29	2.75 (1H, m) 2.89 (1H, m)	31.9
<b>1'</b>	-	130.66	-	130.66
<b>2'</b>	7.86 (2H, d, $J=8.82$ Hz)	132.40	7.90 (2H, d, $J=8.82$ Hz)	132.40
<b>3'</b>	7.23 (2H, t, $J=7.56$ Hz)	116.80	6.86 (1H, d, $J=8.82$ Hz)	116.80
<b>4'</b>	-	164.30	-	164.30
<b>5'</b>	7.23 (2H, t, $J=7.56$ Hz)	116.80	6.86 (1H, d, $J=8.82$ Hz)	116.80
<b>6'</b>	7.86 (2H, d, $J=8.82$ Hz)	132.40	7.90 (2H, d, $J=8.82$ Hz)	132.40
<b>1''</b>	-	144.17	-	144.17
<b>2''</b>	7.16 (2H, d, $J=6.96$ Hz)	129.99	7.24 (2H, d, $J=6.96$ Hz)	129.99
<b>3''</b>	6.82 (1H, d, $J=8.82$ Hz)	127.29	7.25 (2H, t, $J=7.56$ Hz)	127.29
<b>4''</b>	7.13 (1H, t, $J=7.32$ Hz)	129.87	7.19 (1H, t, $J=7.32$ Hz)	129.87
<b>5''</b>	6.82 (1H, d, $J=8.82$ Hz)	127.29	7.25 (2H, t, $J=7.56$ Hz)	127.29
<b>6''</b>	7.16 (2H, d, $J=6.96$ Hz)	129.99	7.24 (2H, d, $J=6.96$ Hz)	129.99

Compound isolated from the plant *Thymelaea lythroides*

(-)-Wikstromol (4, Known)



**4** was isolated from *Thymelaea lythroides* extracted with EtOAc. The EtOAc extract was portioned between *n*-hexane and 90% MeOH. The 90% MeOH fraction was chromatographed over silica gel F254 using gradient elution (*n*-hexane/EtOAc/CH<sub>2</sub>Cl<sub>2</sub>/MeOH). The fraction was subjected to a sephadex LH-20 column using CH<sub>2</sub>Cl<sub>2</sub>/MeOH (1:1) as eluent system, then purified by semi-preparative HPLC (Merck, Hitachi L-7100) using an Eurosphere 100–10 C18 column (300 x 8mm, L x i.d.) with the following gradient (MeOH/H<sub>2</sub>O): 0 min, 10% MeOH; 5 min, 10% MeOH; 35 min 100% MeOH; 45 min, 100 % MeOH, which afforded colorless powder (yield, 2 mg). It showed UV absorbance at  $\lambda_{\text{max}}$  (MeOH) 280.9 nm. Positive and negative ESI-MS of **4** exhibited a prominent peak at  $m/z$  375.0 [M+H]<sup>+</sup> (base peak) and  $m/z$  373.3 [M-H]<sup>-</sup> (base peak) indicating a molecular weight of 374 g/mol. The molecular formula of compound **4** was determined to be C<sub>20</sub>H<sub>22</sub>O<sub>7</sub> based on the analysis of the molecular weight and <sup>13</sup>C NMR data.

The <sup>1</sup>H NMR spectrum (MeOD) (Table 4.8) displayed signals of two- tri-substituted aromatic systems at ( $\delta_{\text{H}}$  6.70 ppm ; 4H) assigned to H-1, H-1', H-4 and H-4' with ( $\delta_{\text{H}}$  6.59 ppm ; 2H) assigned to H-5 and H-5', in addition, two methoxy protons at ( $\delta_{\text{H}}$  3.78 ppm and 3.81 ppm) assigned to H-10 and H-10', three methylene protons at ( $\delta_{\text{H}}$  2.48-2.79 ppm), ( $\delta_{\text{H}}$  2.85-3.12 ppm) and ( $\delta_{\text{H}}$  3.98 ppm) assigned to H-7', H-7 and H-9' and one methine proton at ( $\delta_{\text{H}}$  2.44 ppm) assigned to H-8'.

<sup>13</sup>C NMR and DEPT NMR spectrum showed the presence of two oxygenated methyl carbons, two aliphatic methylene carbons, one oxygenated methylene carbon, one aliphatic methine carbon, six aromatic methine carbons, four oxygenated aromatic quaternary carbons, two aromatic quaternary carbons, one oxygenated aliphatic quaternary carbon and one carbonyl carbon.

The <sup>1</sup>H-<sup>1</sup>H COSY showed the presence of four spin systems assigned for H(4-4')H(5-5'), a continuous spin system H(7')→H(9') and a spin system between the protons of the three methylene groups as showed in the Figure 4.7.A.

The HMBC-NMR spectra (Figure 4.7.B) showed the connection between the previously mentioned spin systems. The cross peak of the proton H-7' to the aromatic carbons, which were attributed to C-1', C-5' and C-6', indicated that the aromatic ring is connected to the aliphatic side at the C-6'. In opposite, from the protons H-7 to the aromatic carbons assigned

to C-1, C-5 and C-6, indicating that the aromatic ring is connected to the aliphatic side at the C-6. Furthermore, the cross peak from the proton H-7 to the carbonyl carbons C-9 and C-8 and in the opposite, from the H-7' to the carbons C-9' and C-8' showed that the partial structure 1 and 2 (Figure 4.8) was connected at C-8 and at the carbonyl carbon C-9, these connections were confirmed with the correlations between the proton H-8' and the carbon C-8 and from H-9' to the carbonyl carbon C-9, thus establishing the connection between the identified spin systems.

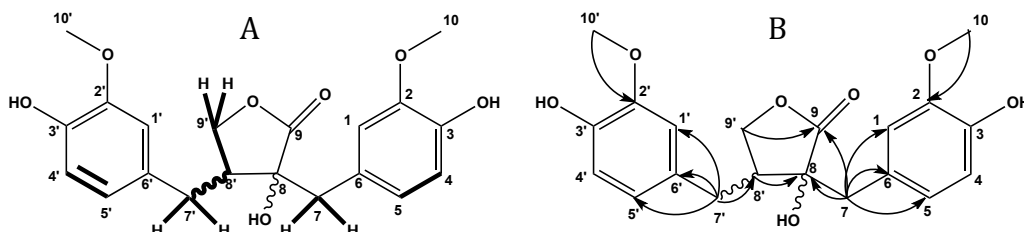


**Figure 4.7.** A)  $^1\text{H}$ - $^1\text{H}$  COSY correlations B) Selected  $^{13}\text{C}$ - $^1\text{H}$  NMR correlations of **4**

**Table 4.8.**  $^1\text{H}$  and  $^{13}\text{C}$  NMR chemical shifts of (-)-wikstromol (**4**)

N <sup>o</sup>	<b>4</b>	
	$\delta_{\text{H}}$	$\delta_{\text{C}}$
<b>1</b>	6.70, 1H (m)	113.9 <sup>a</sup>
<b>2</b>	-	146.3 <sup>c</sup>
<b>3</b>	-	149.1 <sup>f</sup>
<b>4</b>	6.59, 1H (ddd, $J= 1.92, 8.01, 12.39$ Hz)	116.3 <sup>b</sup>
<b>5</b>	6.70, 1H (m)	122.6 <sup>c</sup>
<b>6</b>	-	128.5
<b>7</b>	3.98, 2H (d, $J= 13.8$ Hz)	42.1
<b>8</b>	-	77.7
<b>9</b>	-	77.6
<b>10</b>	3.81, 3H (s) <sup>x</sup>	56.6 <sup>d</sup>
<b>1'</b>	6.70, 1H (m)	115.3 <sup>a</sup>
<b>2'</b>	-	146.3 <sup>e</sup>
<b>3'</b>	-	149.1 <sup>f</sup>
<b>4'</b>	6.59, 1H (ddd, $J= 1.92, 8.01, 12.39$ Hz)	116.4 <sup>b</sup>
<b>5'</b>	6.70, 1H (m)	124.2 <sup>c</sup>
<b>6'</b>	-	122.1
<b>7'</b>	2.48, 1H (dd, $J= 9.37, 13.35$ Hz) 2.79, 1H (dd, $J= 4.77, 13.35$ Hz)	32.3
<b>8'</b>	2.44, 2H (qd, $J= 4.72, 8.13, 8.60, 8.60$ Hz)	44.7
<b>9'</b>	3.98, 2H (d, $J= 8.13$ Hz)	72.1
<b>10'</b>	3.78, 3H (s) <sup>x</sup>	56.7 <sup>d</sup>

a, b, c, d, f, x could be opposite

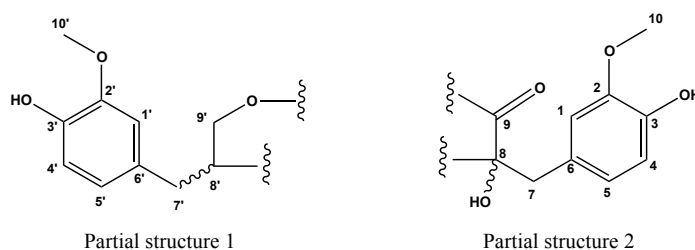


**Figure 4.8.** The partial structure 1 and 2

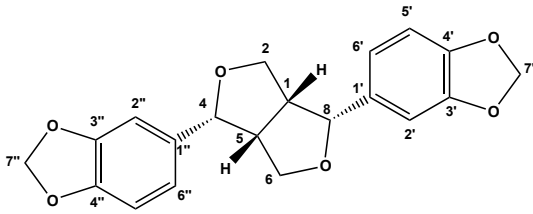
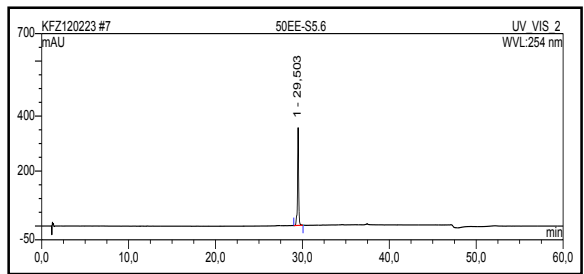
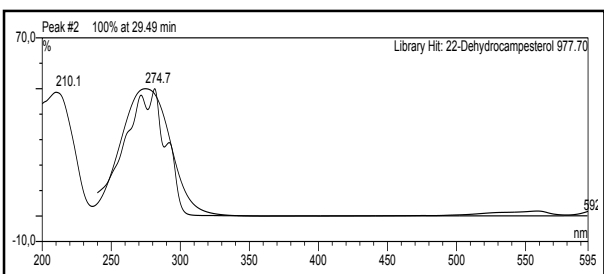
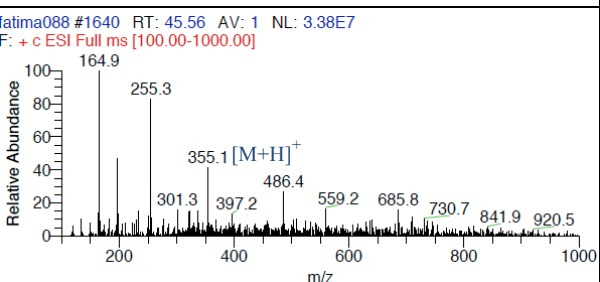
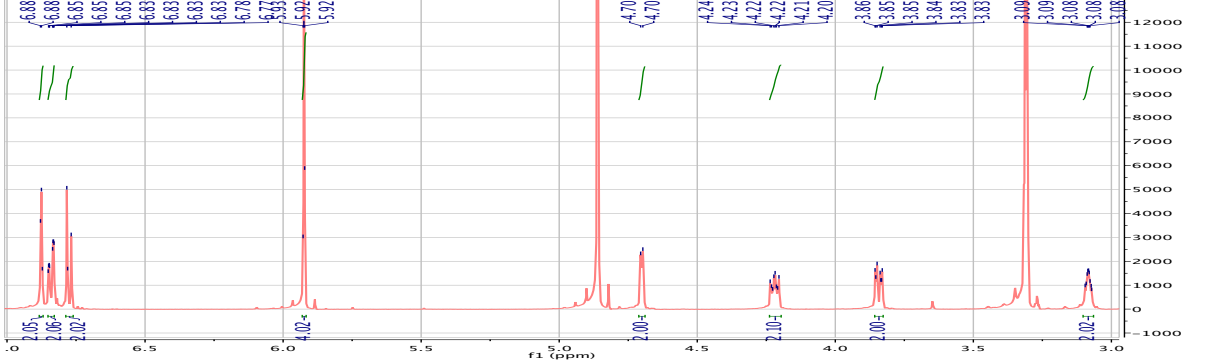
The optical rotation was found to be  $[\alpha]_D^{25} - 38.5$  (c 1.0,  $\text{CHCl}_3$ ).

The identification was further corroborated by comparison of UV,  $^1\text{H}$ ,  $^{13}\text{C}$  NMR, mass spectral data as well as  $[\alpha]_D$  value of **2** and those previously published data for (-)-wikstromol (Sefkow, 2001).

(-)-Wikstromol was reported for the first time from *Wikstroemia viridiflora* (Tandon and Rasiig, 1976). Then from *Cedrus deodara* (*Piniaceae*) (Rao *et al.*, 2002) and from *Didymochlaena truncatula* (*Hypodematiaceae*) (Cao *et al.*, 2006). We report here the presence of wikstromol in *T. lythroides* for the first time.



Compound isolated from the plant *Thymelaea lythroides* $\delta$ -Sesamin (5, Known)

<b><math>\delta</math>-Sesamin</b>	
Synonym(s)  CAS Registry Number Biological source Sample amount Physical Description Molecular Formula Molecular Weight Retention time HPLC Optical rotation $[\alpha]_D^{25}$ UV spectrum $\lambda_{max}$	Tetrahydro-1,4-bis[3,4 (methylenedioxy)phenyl ]-1H,3H-furo[3,4- c]furan; $\delta$ -Sesamin 607-80-7 <i>Thymelaea lythroides</i> 2 mg colorless oil $C_{20}H_{18}O_6$ 382 g/mol 29.50 min (standard gradient) - 60 (c 1.0, $CHCl_3$ ) 210.1 and 274.7 nm
	
	
fatima088 #1640 RT: 45.56 AV: 1 NL: 3.38E7 F: + c ESI Full ms [100.00-1000.00] 	<p>No ionisation in the negative mode</p>
	

**5** was isolated from *Thymelaea lythroides* extracted with EtOAc. The EtOAc extract was portioned between *n*-hexane and 90% MeOH. The 90% MeOH fraction was chromatographed over silica gel F254 using gradient elution (*n*-hexane/EtOAc/CH<sub>2</sub>Cl<sub>2</sub>/MeOH). The fraction was subjected to a sephadex LH-20 column using CH<sub>2</sub>Cl<sub>2</sub>/MeOH (1:1) as eluent system, then purified by semi-preparative HPLC (Merck, Hitachi L-7100) using an Eurosphere 100–10 C18 column (300 x 8mm, L x i.d.) with the following gradient (MeOH/H<sub>2</sub>O): 0 min, 10% MeOH; 5 min, 10% MeOH; 35 min 100% MeOH; 45 min, 100 % MeOH, which afforded colorless powder (yield, 2 mg). It showed UV absorbance at  $\lambda_{\text{max}}$  (MeOH) 280.9 nm. Positive ESI-MS of **5** exhibited a prominent peak at *m/z* 355.1 [M+H]<sup>+</sup> (base peak) and *m/z* 253.5 [M-H]<sup>-</sup> (base peak) indicating a molecular weight of 354 g/mol. The molecular formula of compound **5** was determined to be C<sub>20</sub>H<sub>18</sub>O<sub>6</sub> based on the analysis of the molecular weight and <sup>13</sup>C NMR data.

**Table 4.9.** Comparison of <sup>1</sup>H and <sup>13</sup>C NMR chemical shifts of (+)-sesamin (**5**)

N°	<b>5</b>	
	$\delta_{\text{H}}$	$\delta_{\text{C}}$
1	3.08, 1H (m)	137.0
2	4.70, 1H (d, <i>J</i> = 3.95 Hz)	87.8
3	-	149.9
4 <sub>A</sub>	3.84, 1H (dd; <i>J</i> = 3.77, 9.10 Hz)	73.2
4 <sub>M</sub>	4.22, 1H, dd; <i>J</i> = 6.80, 9.10 Hz	73.2
5	3.08, 1H (m)	109.5
6	4.70, 1H (d, <i>J</i> = 3.95 Hz)	121.1
7	-	-
8 <sub>A</sub>	3.84, 1H (dd; <i>J</i> = 3.77, 9.10 Hz)	73.2
8 <sub>M</sub>	4.22, 1H, dd; <i>J</i> = 6.80, 9.10 Hz	73.2
1'	-	137.0
2'	6.88, 1H (d; <i>J</i> = 1.72 Hz)	108.1
3'	-	149.9
4'	-	149.1
5'	6.78, 1H (d; <i>J</i> = 7.76 Hz)	109.5
6'	6.84, 1H (dd; <i>J</i> = 1.05, 7.92 Hz)	121.1
7'	5.92, 2H (d; <i>J</i> = 1.46 Hz)	-
1''	-	137.0
2''	6.88, 1H (d; <i>J</i> = 1.72 Hz)	108.1
3''	-	149.9
4''	-	149.1
5''	6.78, 1H (dd, <i>J</i> = 7.76 Hz)	109.5
6''	6.84, 1H (dd; <i>J</i> = 1.05, 7.92 Hz)	121.1
7''	5.92, 2H (d; <i>J</i> = 1.46 Hz)	-

The <sup>1</sup>H NMR spectrum (MeOD) (Table 4.9) displayed 18 protons signals: a typical AMX system at ( $\delta_{\text{H}}$  3.84 ppm; 2H, dd; *J*= 3.77, 9.10 Hz, H-4<sub>A</sub> and H-8<sub>A</sub>), ( $\delta_{\text{H}}$  4.22 ppm; 2H, dd; *J*= 6.80, 9.10 Hz, H-4<sub>M</sub> and H-8<sub>M</sub>) and ( $\delta_{\text{H}}$  3.08 ppm; 2H m, H-1<sub>X</sub> and H-5<sub>X</sub>) indicating the presence of two overlapping methylene protons, each one was connected to one methine proton; 2 overlapping -O-CH<sub>2</sub>-O- at ( $\delta_{\text{H}}$  6.78 ppm) assigned to H-7' and H-7''; two overlapped

methine protons at ( $\delta_{\text{H}}$  4.70 ppm) assigned to H-1 and H-5; six aromatic protons of two tri-substituted benzene moieties at ( $\delta_{\text{H}}$  6.78 ppm) assigned to H-2' and H-2'', ( $\delta_{\text{H}}$  6.84 ppm) assigned to H-6' and H-6'' and ( $\delta_{\text{H}}$  6.88 ppm) assigned to H-5' and H-5''.

The  $^1\text{H}$ - $^1\text{H}$  COSY showed the presence of four spin systems assigned for H(5-5')H(6-6'), a continuous spin system H(4) $\rightarrow$ H(6), H(1)H(2)H(8) and spin system between the protons H(1)H(5) as shown in the Figure 4.9.A.

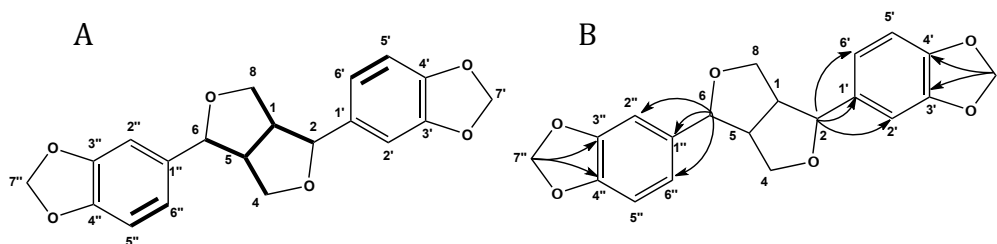


**Figure 4.9.** A)  $^1\text{H}$ - $^1\text{H}$  COSY correlations B) selected  $^{13}\text{C}$ - $^1\text{H}$  NMR correlations of **5**

The  $^1\text{H}$ - $^{13}\text{C}$  MBC NMR spectra showed the connection between the previously mentioned spin systems. H-4 showed correlations to the overlapping aromatic carbons, which were attributed to C-2'' and C-6'' ( $\delta_{\text{C}}$  129.9 ppm), as well as to an isolated aromatic carbon assigned to C-1'' ( $\delta_{\text{C}}$  144.1 ppm), these correlations indicated that the tri-substituted aromatic ring is connected to the 3,7-O-bicyclooctane moieties at C-1''. The same correlations appeared for the other tri-substituted aromatic ring, from H-8 to the overlapping aromatic carbons C-2' and C-6', together with C-1', to confirm that the second tri-substituted aromatic ring was connected to the 3,7-O-bicyclooctane moieties at C-1'. On the other hand, the two overlapping -O-CH<sub>2</sub>-O- showed correlations to the overlapped aromatic carbons C-3'-C-3'' and to C-4'-C-4'', to prove that -O-CH<sub>2</sub>-O- was connected to the tri-substituted aromatic ring at C-3' and C-4' for the first one, and at C-3'' and C-4'' for the second aromatic ring, thus establishing the connection between the identified spin systems.

The identification was further corroborated by comparison of UV,  $^1\text{H}$ ,  $^{13}\text{C}$  NMR, mass spectral data as well as  $[\alpha]_{\text{D}}$  value (Lin et al., 2004) of **5** with those published data for (+)-sesamin.

(+)-Sesamin is a natural product, isolated for the first time from *Piper sylvaticum* (Banerji and Dhara, 1974), then from *Artemisia argentea* (El-Emary and Attia, 1988). Later, **5** was reported from *Thymelaeaceae* family (Takaku *et al.*, 2001), from *Plectranthus mollis* (Kulkarni *et al.*, 2012), and from *Sesamum indicum* (Yoshida *et al.*, 2007). This is the first report of this compound from genus *Thymelaea*.

Compound isolated from the plant *Thymelaea lythroides*

Daphnoretin (6, Known)

**Daphnoretin**

Synonym(s)

Coumarin, 7-hydroxy-6-methoxy-3,7'-oxydi-(7CI,8CI); Daphnoretin; NSC 291852; Thymelol

CAS Registry Number

2034-69-7

Biological source

*Thymelaea lythroides*

Sample amount

19 mg

Physical Description

faint yellow needle crystals

Molecular Formula

C<sub>19</sub>H<sub>12</sub>O<sub>7</sub>

Molecular Weight

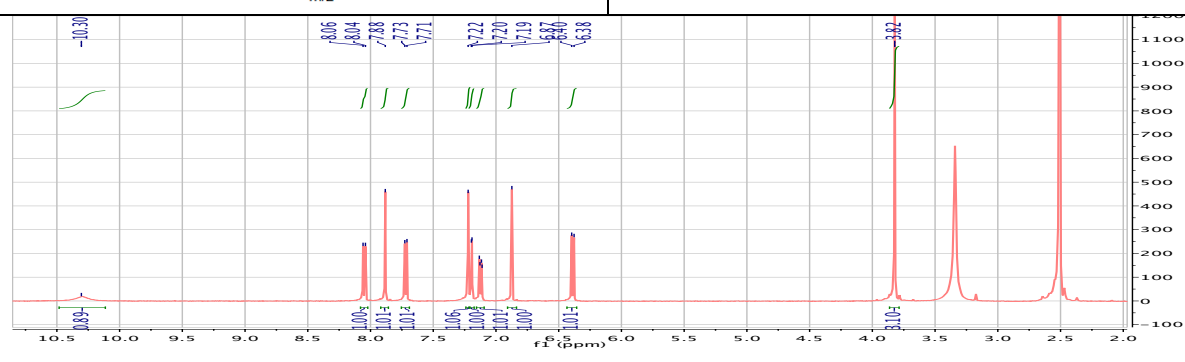
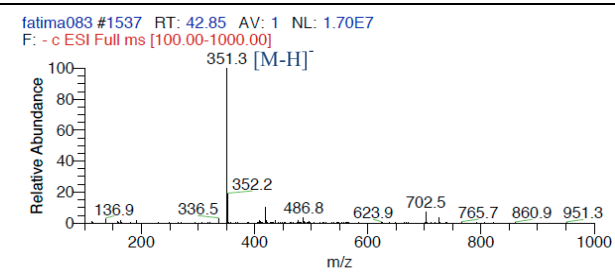
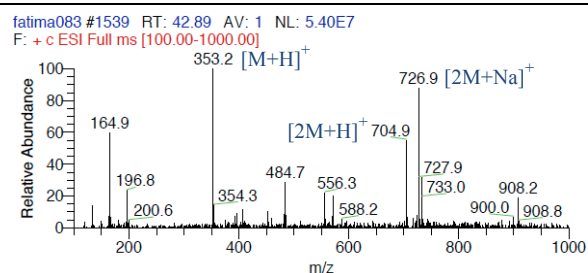
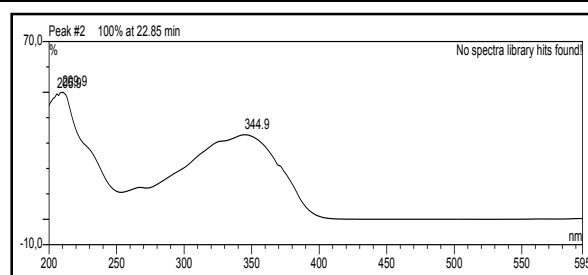
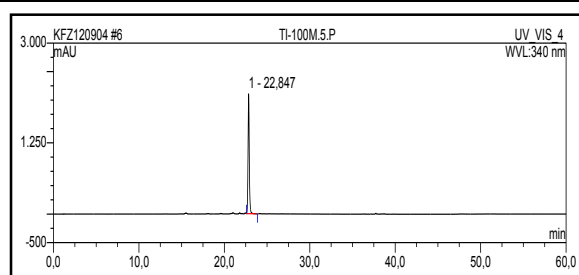
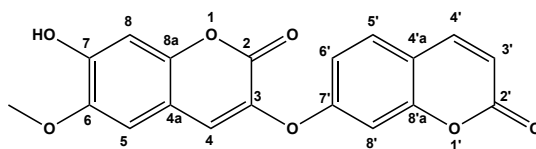
252 g/mol

Retention time HPLC

22.84 min (standard gradient)

UV spectrum  $\lambda_{\max}$ 

200.0, 259.9 and 344.9 nm



**6** was isolated from *Thymelaea lythroides* extracted with EtOAc. The EtOAc extract was portioned between *n*-hexane and 90% MeOH. The 90% MeOH fraction was chromatographed over silica gel F254 using gradient elution (*n*-hexane/EtOAc/CH<sub>2</sub>Cl<sub>2</sub>/MeOH). The fraction was subjected to a sephadex LH-20 column using CH<sub>2</sub>Cl<sub>2</sub>/MeOH (1:1) as eluent system, then purified by semipreparative HPLC (Merck, Hitachi L-7100) using an Eurosphere 100–10 C18 column (300 x 8mm, L x i.d.) with the following gradient (MeOH/H<sub>2</sub>O): 0 min, 10% MeOH; 5 min, 10% MeOH; 35 min 100% MeOH; 45 min, 100 % MeOH, which afforded colorless powder (yield, 19 mg). It showed UV absorbance at  $\lambda_{\max}$  (MeOH) 200.0, 259.9 and 344.9 nm. Positive and negative ESI-MS of **6** exhibited a prominent peak at  $m/z$  353.1 [M+H]<sup>+</sup> (base peak) and  $m/z$  351.3 [M-H]<sup>-</sup> (base peak) indicating a molecular weight of 352 g/mol. The molecular formula of compound **6** was determined to be C<sub>19</sub>H<sub>12</sub>O<sub>7</sub> based on the analysis of the molecular weight and <sup>13</sup>C NMR data.

The <sup>1</sup>H NMR spectrum of **6** (Table 4.10) displayed 12 proton signals, one methoxy group at ( $\delta_{\text{H}}$  3.82 ppm) assigned to 6-CH<sub>3</sub>, one hydroxyl group signal at ( $\delta_{\text{H}}$  10.30 ppm) assigned to 7-OH, five aromatic protons at ( $\delta_{\text{H}}$  6.87 ppm), ( $\delta_{\text{H}}$  7.12 ppm), ( $\delta_{\text{H}}$  7.19 ppm), ( $\delta_{\text{H}}$  7.22 ppm), and ( $\delta_{\text{H}}$  7.72 ppm), which were assigned to H-8, H-6', H-8', H-5 and H-5', three heterocyclic protons at ( $\delta_{\text{H}}$  6.39 ppm), ( $\delta_{\text{H}}$  7.88 ppm) and ( $\delta_{\text{H}}$  8.05 ppm) assigned to H-3', H-4 and H-4'.

The <sup>1</sup>H-<sup>1</sup>H COSY showed the presence of two spin systems assigned for H(5')H(6') and between the protons H(3')H(4') as shown in the Figure 4.10.A

Furthermore, <sup>13</sup>C-<sup>1</sup>H long range couplings of <sup>2</sup>*J* and <sup>3</sup>*J* observed in <sup>13</sup>C-<sup>1</sup>H heteronuclear multiple bond coherence (HMBC) spectrum gave the following linkages (Figure 4.10.B) :

(A) Cross peaks from H-4' to C-2', C-3', C-4a' and C-8a', From H-5' to C-4' and C-4a', from H-8' to C-8a' and C-7'. These correlations indicated that A is 1-benzopyran-2-one, the core of coumarin compounds, which is oxygenated at C-7'. On the other hand, the same correlations could be seen for the selected cross peaks of (B), from H-4 to C-2, C-3, C-4a and C-8a, from H-5 to C-4 and C-4a, from H-8 to C-8a and C-7, in addition, from 6-CH<sub>3</sub> to C-6. These correlations indicated that B is an other benzopyrone, which is tri-substituted with a methoxy group at carbon 6 and a hydroxygroup at C-7 and also an oxygenated carbon at C-3. Thus, the partial structure A and B were connected at the C-7'-O- and C-3-O-positions.

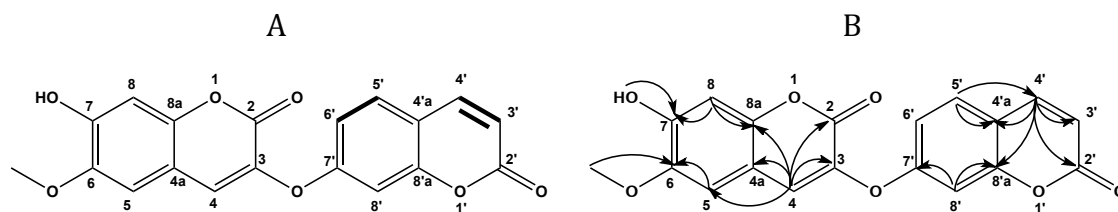


**Figure 4.10.** A)  $^1\text{H}$ - $^1\text{H}$  COSY correlations B) selected  $^{13}\text{C}$ - $^1\text{H}$  NMR correlations of **6**

The identification was further corroborated by comparison of UV,  $^1\text{H}$ ,  $^{13}\text{C}$  NMR, mass spectral data as well as  $[\alpha]_{\text{D}}$  value of **6** with those data published for Daphnoretin. (Ho *et al.*, 2010).

Daphnoretin has been previously isolated for first time from *Ladino clover* (*Fabaceae*) (Livingston *et al.*, 1964), then later in some genus of the *Thymelaeaceae* family *Daphne*, including *Wikstroemia*, *Daphnopsis*, *Edgeworthia*, *Thymelaea*, *Diarthron*, *Dirca*, *Enkleia* and *Peddiea* (Zhang *et al.*, 2008), However, this the first report of Daphnoretin from the species *Thymelaea lythroides*.

**Table 4.10.** Comparison of  $^1\text{H}$  and  $^{13}\text{C}$  NMR chemical shifts of **5** with Daphnoretin (Wing *et al.*, 2010)

N°	<b>5</b>	<b>Daphnoretin</b>
	$\delta_{\text{H}}$	$\delta_{\text{H}}$
<b>1</b>	-	-
<b>2</b>	-	-
<b>3</b>	6.42 (1H, d, $J= 9.6$ Hz)	6.37 (1H, d, $J= 9.6$ Hz)
<b>4</b>	8.11 (1H, d, $J= 9.5$ Hz)	8.03 (1H, d, $J= 9.5$ Hz)
<b>4a</b>	-	-
<b>5</b>	7.78 (1H, d, $J= 8.6$ Hz)	7.71 (1H, d, $J= 8.6$ Hz)
<b>6</b>	7.18 (1H, dd, $J= 8.6, 2.4$ Hz)	7.11 (1H, dd, $J= 8.6; 2.4$ Hz)
<b>6-OCH<sub>3</sub></b>	3.89 (3H, s)	3.77 (3H, s)
<b>7</b>	-	-
<b>7-OH</b>	10.30 (1H, s)	10.23 (1H, s)
<b>8</b>	7.23 (1H, d, $J= 2.4$ Hz)	7.17 (1H, d, $J= 2.4$ Hz)
<b>8a</b>	-	-
<b>1'</b>	-	-
<b>2'</b>	-	-
<b>3'</b>	-	-
<b>4'</b>	7.91 (1H, s)	7.86 (1H, s)
<b>4a'</b>	-	-
<b>5'</b>	7.25 (1H, s)	7.21 (1H, s)
<b>6'</b>	-	-
<b>7'</b>	-	-
<b>8'</b>	6.96 (1H, s)	6.87 (1H, s)
<b>8a'</b>	-	-

Compound isolated from the plant *Thymelaea lythroides*

Rutarensin (7, Known)

## Rutarensin

Synonym(s)

6'-ester with 7-(β-D-glucopyranosyloxy)-6-methoxy-3-[(2-oxo-2H-1-benzopyran-7-yl)oxy]-2H-1-benzopyran-2-one; Rutarensin  
119179-04-3

CAS Registry Number

Biological source

*Thymelaea lythroides*

Sample amount

5.7 mg

Physical Description

yellow needle crystal

Molecular Formula

C<sub>31</sub>H<sub>20</sub>O<sub>16</sub>

Molecular Weight

658 g/mol

Retention time HPLC

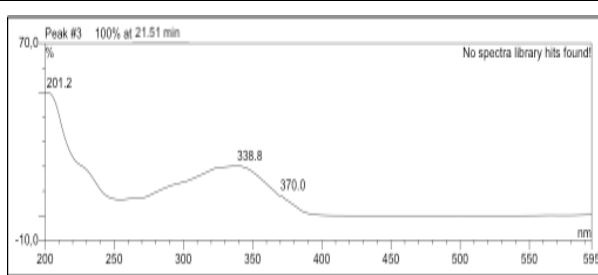
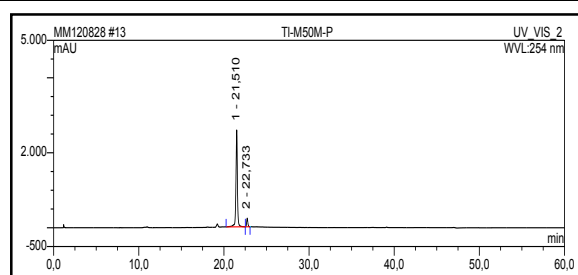
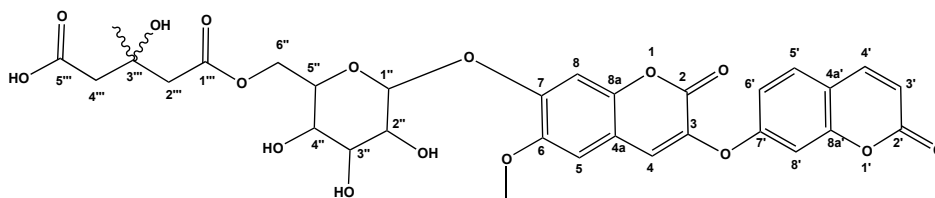
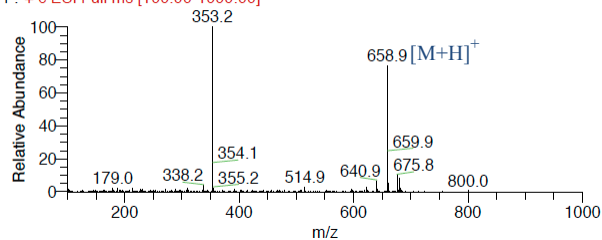
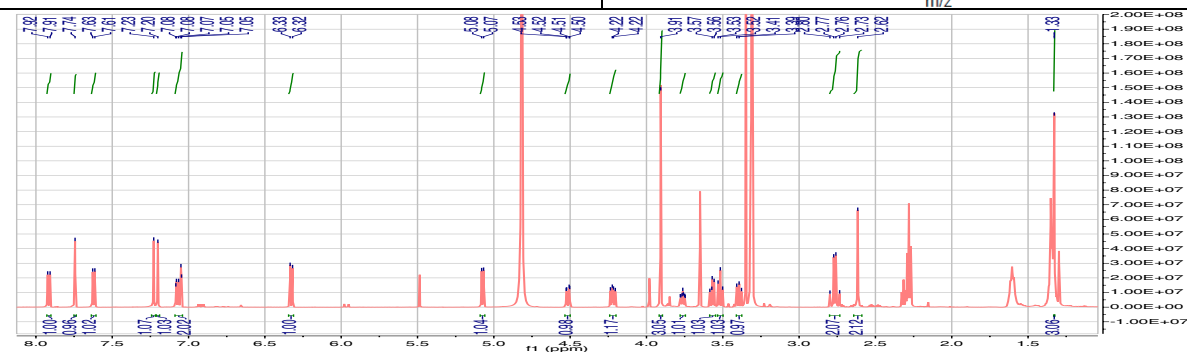
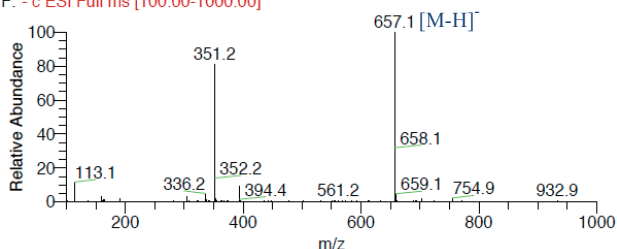
21.51 min (standard gradient)

Optical rotation [α]<sub>D</sub><sup>26</sup>

- 2.0 (c 0.017, DMSO)

UV spectrum λ<sub>max</sub>

201.2, 338.8 and 370 nm

fatima021 #996 RT: 26.17 AV: 1 NL: 1.96E8  
F: + c ESI Full ms [100.00-1000.00]fatima021 #998 RT: 26.21 AV: 1 NL: 2.90E7  
F: - c ESI Full ms [100.00-1000.00]



**7** was isolated from *Thymelaea lythroides* extracted with EtOAc. The EtOAc extract was portioned between *n*-hexane and 90% MeOH. The 90% MeOH fraction was chromatographed over silica gel F254 using gradient elution (*n*-hexane/EtOAc/CH<sub>2</sub>Cl<sub>2</sub>/MeOH). The fraction was subjected to a sephadex LH-20 column using CH<sub>2</sub>Cl<sub>2</sub>/MeOH (1:1) as eluent system, then purified by semi-preparative HPLC (Merck, Hitachi L-7100) using an Eurosphere 100–10 C18 column (300 x 8mm, L x i.d.) with the following gradient (MeOH/H<sub>2</sub>O): 0 min, 10% MeOH; 5 min, 10% MeOH; 35 min 100% MeOH; 45 min, 100 % MeOH, which afforded colorless powder (yield, 19 mg). It showed UV absorbance at  $\lambda_{\max}$  (MeOH) 201.2, 338.8 and 370 nm. Positive and negative ESI-MS of **7** exhibited a prominent peak at  $m/z$  658.9 [M+H]<sup>+</sup> (base peak) and  $m/z$  657.1 [M-H]<sup>-</sup> (base peak) indicating a molecular weight of 658 g/mol. The prominent fragment ion peak of 352 ( $m/z$  353.2 [M+H]<sup>+</sup> and 351.2 [M-H]<sup>-</sup>) in EI-MS suggested the presence of a daphnoretin in the molecule. The molecular formula of compound **7** was determined to be C<sub>31</sub>H<sub>20</sub>O<sub>16</sub> based on the analysis of the molecular weight and <sup>13</sup>C NMR data.

From the <sup>1</sup>H NMR of **7** (Table 4.11) a daphnoretin system and hexopyranose was suggested with the presence of unassigned signals: two methylene ( $\delta_{\text{H}}$  2.62 ppm), ( $\delta_{\text{H}}$  2.72 ppm) and one methyl group ( $\delta_{\text{H}}$  1.33 ppm). Thus, the glucose moiety is bound at CO-1'' ( $\delta_{\text{C}}$  102.0 ppm) to daphnoretin. A daphnoretin-7- $\beta$ -D-glucoside is already known as daphnorin (Tschesche *et al.*, 1963) (Figure 3.11).

The <sup>13</sup>C NMR spectrum of **7** showed all signals of daphnorin, whereas the signal for C-6'' of glucose was found to be at lower field than expected (+ 3 ppm) and the signal for C-5'' of glucose was shifted upfield (- 3 ppm), indicating that an acylation must be present at position C-6'' of glucose. Further possibilities of acylation at C-2'', C-3'', and C-4'' of glucose were excluded by comparison with data given in literature (Kashiwada *et al.*, 1986; Adegawa *et al.*, 1986).

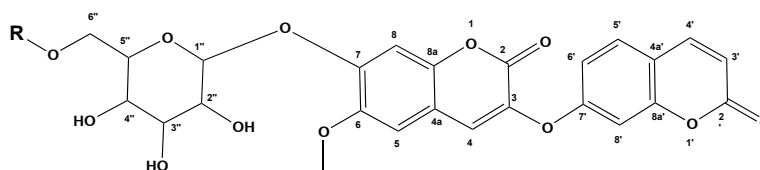


**Figure 4.11.** Structure of Daphnorin (R= H)

**Table 4.11.** Comparison of  $^1\text{H}$  and  $^{13}\text{C}$  NMR chemical shifts of **7** with Rutarensin

N°	<b>7</b>		<b>Rutarensin</b>	
	$\delta_{\text{H}}$	$\delta_{\text{C}}$	$\delta_{\text{H}}$	$\delta_{\text{C}}$
<b>1</b>	-	-	-	-
<b>2</b>	-	161.3	-	159.6
<b>3</b>	-	139.3	-	137.3
<b>4</b>	7.74 (1H, s)	131.3	7.87 (1H, s)	130.1
<b>4a</b>	-	114.5	-	112.4
<b>5</b>	7.22 (1H, s)	110.8	7.28 (1H, s)	109.8
<b>6</b>	-	148.4	-	146.5
<b>6-OCH<sub>3</sub></b>	3.90 (3H, s)	57.2	3.80 (3H, s)	56.1
<b>7</b>	-	150.8	-	149.0
<b>8</b>	7.20 (1H, s)	105.5	7.23 (1H, s)	103.1
<b>8a</b>	-	148.8	-	146.9
<b>1'</b>	-	-	-	-
<b>2'</b>	-	162.8	-	160.1
<b>3'</b>	6.32 (1H, d, $J=9.54$ Hz)	116.4	6.39 (1H, d, $J=9.8$ Hz)	114.1
<b>4'</b>	7.91 (1H, d, $J=9.6$ Hz)	145.4	8.05 (1H, d, $J=9.8$ Hz)	144.2
<b>4a'</b>	-	114.5	-	114.7
<b>5'</b>	7.61 (1H, d, $J=8.52$ Hz)	131.0	7.72 (1H, d, $J=8.7$ Hz)	129.9
<b>6'</b>	7.07 (1H, dd, $J=2.4$ Hz)	115.2	7.15 (1H, dd, $J=8.7; 2.5$ Hz)	113.8
<b>7'</b>	-	159.2	-	156.9
<b>8'</b>	7.04 (1H, d, $J=2.34$ Hz)	105.8	7.26 (1H, d, $J=2.5$ Hz)	104.6
<b>8a'</b>	-	156.8	-	155.2
<b>1''</b>	5.05 (1H, d, $J=7.62$ Hz)	102.0	5.16 (1H, d, $J=6.9$ Hz)	99.6
<b>2''</b>	3.56 (1H, m)	74.8	3.10-3.50 (1H, m)	73.0
<b>3''</b>	3.51 (1H, m)	77.9	3.10-3.50 (1H, m)	76.5
<b>4''</b>	3.51 (1H, m)	71.8	3.10-3.50 (1H, m)	69.6
<b>5''</b>	3.76 (1H, m)	75.8	3.75 (1H, m)	73.9
<b>6''</b>	4.51 (1H, dd, $J=2.1, 11.82$ Hz)	64.7	4.25 (1H, dd, $J=11.5; 2.0$ Hz)	62.8
	4.20 (1H, dd, $J=7.32, 11.94$ Hz)	64.7	4.03 (1H, dd, $J=11.5; 6.5$ Hz)	62.8
<b>1'''</b>	-	172.6	-	170.8
<b>2'''<sub>a</sub></b>	2.61 (2H, s)	45.9	1.93 (1H, AB syst. $J=15.3$ Hz)	47.0
<b>2'''<sub>b</sub></b>	-	45.9	2.20 (1H, AB syst. $J=15.3$ Hz)	47.0
<b>3'''</b>	-	70.9	-	68.8
<b>3'''-CH<sub>3</sub></b>	1.32 (3H, s)	27.9	1.06 (1H, s)	28.3
<b>4'''<sub>a</sub></b>	2.75 (2H, m)	46.4	2.30 (1H, AB syst. $J=13.4$ Hz)	47.0
<b>4'''<sub>b</sub></b>	2.75 (2H, m)	46.4	2.38 (1H, AB syst. $J=13.4$ Hz)	47.0
<b>5'''</b>	-	177.7	-	176.0

Moreover, the  $^{13}\text{C}$  NMR spectrum of **7** showed six further signals, which were characterized by DEPT-experiments as two carbonyl-carbons ( $\delta_{\text{C}}$  172.6 and 177.7 ppm) one quaternary carbon ( $\delta_{\text{C}}$  70.9 ppm), two methylene-carbons ( $\delta_{\text{C}}$  45.9 and 46.4 ppm) and one methyl group ( $\delta_{\text{C}}$  27.9 ppm). These data indicated that the glucose moieties is connected to a partial structure A at CO-6''.

The COSY NMR spectrum showed the same correlations as Daphnoretin and those of glucose.  $^{13}\text{C}$ - $^1\text{H}$  long range couplings of  $^2J$  and  $^3J$  observed in a  $^{13}\text{C}$ - $^1\text{H}$  heteronuclear multiple bond coherence (HMBC) spectrum gave the same linkages as Daphnoretin as well as those of the glucose. Furthermore, the partial structure A showed the selected following linkages (Figure 4.12): From H-2''' to C-1''', C-3''', C-4''' and 3'''-CH<sub>3</sub>; from H-4''' to C-2''', C-3''', 3'''-CH<sub>3</sub> and C-5''' and from the protons of 3'''-CH<sub>3</sub> to C-3''', C-2''' and C-4'''. From these results, it

was concluded that the substituent at C-6'' of the glucose was 3-hydroxy-3-methylglutaric acid.

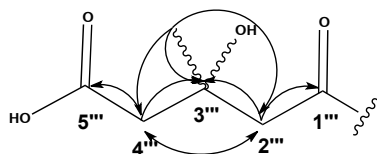


**Figure 4.12.** Selected correlations of partial structure A

The identification was further corroborated by comparison of UV,  $^1\text{H}$ ,  $^{13}\text{C}$  NMR, mass spectral data as well as  $[\alpha]_{\text{D}}$  value of **7** with those published for rutarensin (Fischer *et al.*, 1988).

Rutarensin was described for the first time as a constituent of cell cultures of *Ruta chalepensis* L. (*Rutaceae*), then from of *Edgeworthia chrysantha* (*Thymelaeaceae*). Further acylglycosides esterified at C-6 of glucose with 3-hydroxy-3-methylglutaric acid are palustroside from *Ledurn palustre* L., the tubeimosides from *Bolbostemma puniculatum*, one pyridoxin glucoside from *Pisum satioum* L. and the betacyanin glucosides from *Phyllocactus hybridus*, *Celosia cristata* and *Iresine herbstii* (Centrospermae). (Kreher *et al.*, 1990). This is the first report of Rutarensin from *Thymelaea lythroides*.

Compound isolated from the plant *Thymelaea lythroides**trans*-Tiliroside (**8**, Known)***trans*-Tiliroside**

Synonym(s)

Kaempferol-3-O- $\beta$ -D-(6''-O-(E)-p-coumaroyl)glucopyranoside; *trans*-Tiliroside  
20316-62-5

CAS Registry Number

*Thymelaea lythroides*

Biological source

20 mg

Sample amount

yellowish powder

Physical Description

Molecular Formula

C<sub>30</sub>H<sub>26</sub>O<sub>13</sub>

Molecular Weight

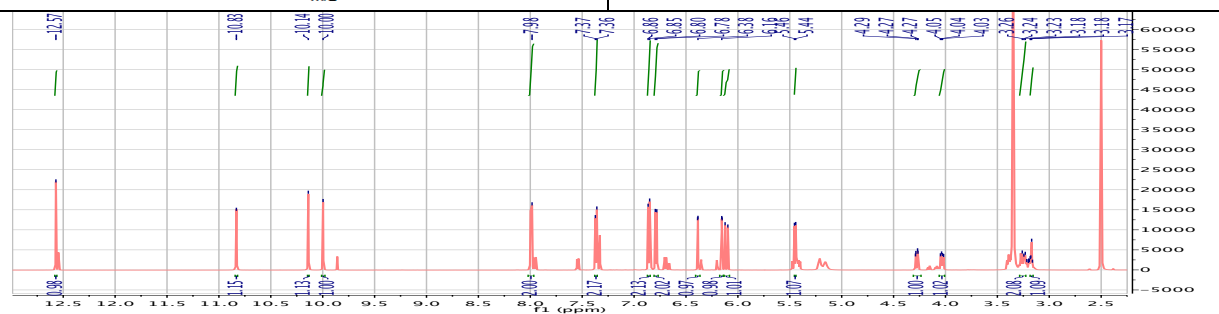
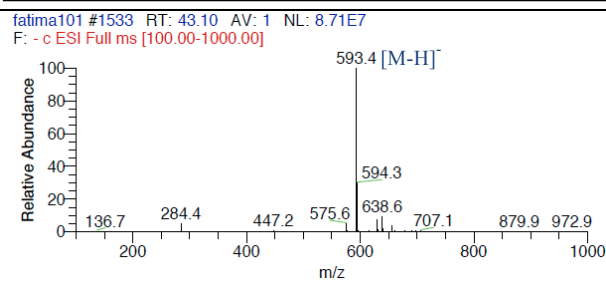
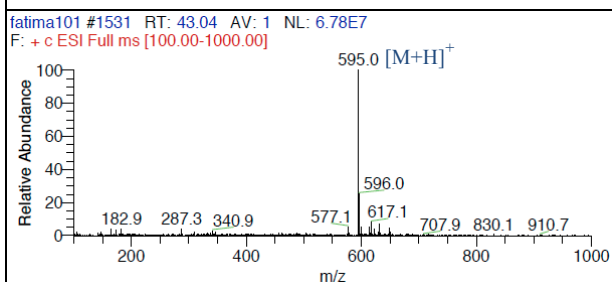
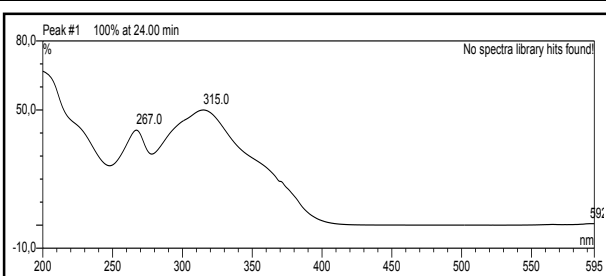
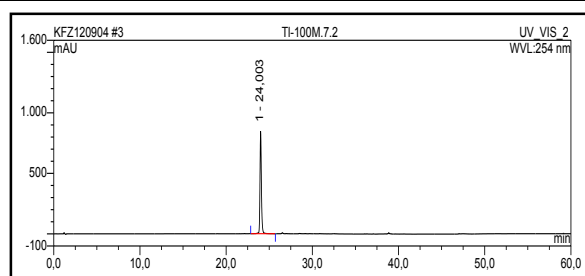
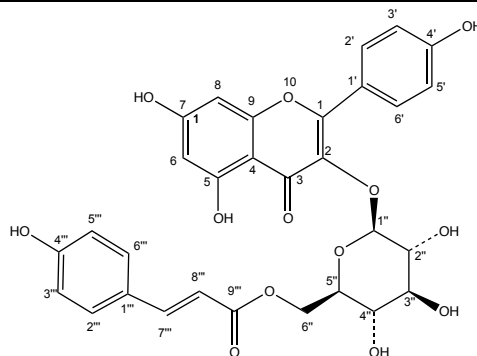
594 g/mol

Retention time HPLC

24.0 min (standard gradient)

Optical rotation  $[\alpha]_D^{26}$ - 65 (C 1.0, CHCl<sub>3</sub>)UV spectrum  $\lambda_{\max}$ 

267.0 and 315.0 nm



**8** was isolated from *Thymelaea lythroides* extracted with EtOAc. The EtOAc extract was portioned between *n*-hexane and 90% MeOH. The 90% MeOH fraction was chromatographed over silica gel F254 using gradient elution (*n*-hexane/EtOAc/CH<sub>2</sub>Cl<sub>2</sub>/MeOH). The fraction was directly purified by semi-preparative HPLC (Merck, Hitachi L-7100) using an Eurosphere 100–10 C18 column (300 x 8mm, L x i.d.) with the following gradient (MeOH/H<sub>2</sub>O): 0 min, 10% MeOH; 5 min, 10% MeOH; 35 min 100% MeOH; 45 min, 100 % MeOH, which afforded colorless powder (yield, 19 mg). It showed UV absorbance at  $\lambda_{\max}$  (MeOH) 267.0 and 315.0 nm. Positive and negative ESI-MS of **8** exhibited a prominent peak at  $m/z$  695.0 [M+H]<sup>+</sup> (base peak) and  $m/z$  695.3 [M-H]<sup>-</sup> (base peak) indicating a molecular weight of 694 g/mol. The molecular formula of compound **8** was determined to be C<sub>30</sub>H<sub>26</sub>O<sub>13</sub> based on the analysis of the molecular weight and <sup>13</sup>C NMR data.

The <sup>1</sup>H NMR of **7** (Table 4.12) displayed 26 proton signals, a kaempferol and hexopyranose was suggested with the presence of coumarin acid. The <sup>13</sup>C NMR of **7** showed the presence of 30 signals carbons (Table 4.12).

The <sup>1</sup>H-<sup>1</sup>H COSY (Figure 4.13.A) spectra showed 6 spin systems, H(2'')H(3''), H(5'')H(6''), H(2''')H(3'''), H(5''')H(6'''), H(7''')H(8''') and a continuous spin system H(1'')→(6'').

The <sup>1</sup>H-<sup>13</sup>C HMBC exhibited the selected following linkage: from H-8 to C-4 and C-9, from H-7-OH to C-7, C-6 and C-8, from H-4'-OH to C-4', C-5' and C-3', from H-2' to C-1' and C-1, from H-6' to C-1' and C-1, from H-4'''-OH to C-4''', C-3''' and C-5'', from H-7''' to C-1''', C-2''' and C-6''', from H-8''' to C-1''' and from H-6'' to C-9''' as shown in Figure 4.13. B.

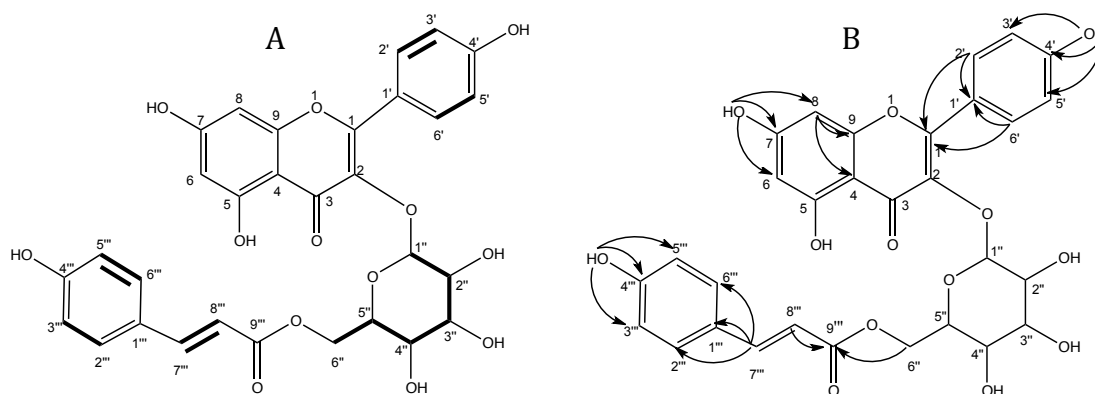


**Figure 4.13.** A) <sup>1</sup>H-<sup>1</sup>H COSY correlations. B) Selected <sup>1</sup>H-<sup>13</sup>C HMBC correlation of **8**

The identification was further corroborated by comparison of UV,  $^1\text{H}$ ,  $^{13}\text{C}$  NMR, mass spectral data as well as  $[\alpha]_{\text{D}}$  value of **7** with those published for *trans*-Tiliroside (Budzianowski *et al.*, 1995).

*trans*-Tiliroside or kaempferol-3-*O*- $\beta$ -D-(6'''-*E*-p-coumaroyl)-glucopyranoside is an acylated glucoside of kaempferol, first isolated from *Rosa canina* and *Tilia argentea* and then from several *Tiliaceae* (Budzianowski *et al.*, 1995), later from *Daphne genkwa* (Song *et al.*, 2009), and from *Edgeworthia gardneri* (Xu *et al.*, 2012) of the *Thymeleaceae* family. This is the first report of *trans*-Tiliroside from *Thymelaea lythroides*.

**Table 4.12.** Comparison of  $^1\text{H}$  and  $^{13}\text{C}$  NMR chemical shifts of **8** with *trans*-Tiliroside

N <sup>o</sup>	<b>8</b>		<i>trans</i> -Tiliroside	
	$\delta_{\text{H}}$	$\delta_{\text{C}}$	$\delta_{\text{H}}$	$\delta_{\text{C}}$
<b>1</b>	-	-	-	-
<b>2</b>	-	156.4	-	156.4
<b>3</b>	-	133.0	-	133.0
<b>4</b>	-	177.3	-	177.3
<b>5</b>	-	161.1	-	161.1
<b>5-OH</b>	12.57 (1H, s)	-	12.60 (1H, s)	-
<b>6</b>	6.15 (1H, d, <i>J</i> = 2.06 Hz)	98.7	6.18 (1H, d, <i>J</i> = 2.1 Hz)	98.7
<b>7</b>	-	164.1	-	164.1
<b>7-OH</b>	10.83 (1H, s)	-	10.87 (1H, s)	-
<b>8</b>	6.39 (1H, d, <i>J</i> = 2.06 Hz)	93.6	6.41 (1H, d, <i>J</i> = 2.1 Hz)	93.6
<b>9</b>	-	156.3	-	156.3
<b>10</b>	-	103.8	-	103.8
<b>1'</b>	-	120.7	-	120.7
<b>2'</b>	7.98 (1H, d, <i>J</i> = 8.8 Hz)	130.1	8.02 (1H, d, <i>J</i> = 8.9 Hz)	130.0
<b>3'</b>	6.86 (1H, d, <i>J</i> = 8.8 Hz)	115.7	6.88 (1H, d, <i>J</i> = 8.9 Hz)	115.7
<b>4'</b>	-	159.9	-	159.9
<b>4'-OH</b>	10.14 (1H, s)	-	10.18 (1H, s)	-
<b>5'</b>	6.86 (1H, d, <i>J</i> = 8.8 Hz)	115.7	6.88 (1H, d, <i>J</i> = 8.9 Hz)	115.7
<b>6'</b>	7.98 (1H, d, <i>J</i> = 8.8 Hz)	130.1	8.02 (1H, d, <i>J</i> = 8.9 Hz)	130.1
<b>1''</b>	5.45 (1H, d, <i>J</i> = 7.5 Hz)	100.9	5.48 (1H, d, <i>J</i> = 7.5 Hz)	100.9
<b>2''</b>	3.25 (1H, m)	74.2	3.20-3.35 (1H, m)	74.2
<b>2''-OH</b>	5.16 (1H, s)	-	5.23 (1H, s)	-
<b>3''</b>	3.25 (1H, m)	76.2	3.20-3.35 (1H, m)	76.2
<b>3''-OH</b>	5.21 (1H, s)	-	5.27 (1H, s)	-
<b>4''</b>	3.25 (1H, m)	69.9	3.20-3.35 (1H, m)	69.9
<b>4''-OH</b>	5.43 (1H, s)	-	5.50 (1H, s)	-
<b>5''</b>	3.25 (1H, m)	74.1	3.20-3.35 (1H, m)	74.0
<b>6''<sub>a</sub></b>	4.31 (1H, dd, <i>J</i> = 2.2, 11.9 Hz)	62.9	4.30 (1H, dd, <i>J</i> = 2, 11.7 Hz)	62.9
<b>6''<sub>b</sub></b>	4.03 (1H, dd, <i>J</i> = 6.4, 11.8 Hz)	-	4.06 (1H, dd, <i>J</i> = 6.3, 11.7 Hz)	-
<b>1'''</b>	-	124.9	-	124.8
<b>2'''</b>	7.37 (1H, d, <i>J</i> = 8.5 Hz)	130.7	7.39 (1H, d, <i>J</i> = 8.8 Hz)	130.7
<b>3'''</b>	6.81 (1H, d, <i>J</i> = 8.6 Hz)	115.0	6.81 (1H, d, <i>J</i> = 8.8 Hz)	115.0
<b>4'''</b>	-	159.7	-	159.7
<b>4'''-OH</b>	10.00 (1H, s)	-	10.06 (1H, s)	-
<b>5'''</b>	6.81 (1H, d, <i>J</i> = 8.6 Hz)	115.0	6.81 (1H, d, <i>J</i> = 8.8 Hz)	115.0
<b>6'''</b>	7.37 (1H, d, <i>J</i> = 8.5 Hz)	130.7	7.39 (1H, d, <i>J</i> = 8.8 Hz)	130.7
<b>7'''</b>	7.33 (1H, d, <i>J</i> = 15 Hz)	144.5	7.37 (1H, d, <i>J</i> = 16 Hz)	144.5
<b>8'''</b>	6.11 (1H, d, <i>J</i> = 15 Hz)	113.6	6.14 (1H, d, <i>J</i> = 16 Hz)	113.6
<b>9'''</b>	-	166.1	-	166.1

#### 4.3. Bioactivity test results for compounds isolated from the plant *Thymelaea lythroides*

The isolated compounds were subjected to cytotoxicity and protein kinase bioassays. Some of the isolated pure compounds were also subjected to Hsp 90 inhibitor assays. The results are shown in Tables 4.13 and Table 4.14.

**Table 4.13.** Cytotoxicity test results for the compounds isolated from *Thymelaea lythroides*

Nr.	Compounds tested	L5178Y growth in %* (Conc. 10 µg/mL)
-	Control	0
3	(+)-Dapheolone	83.3
4	(-)-Wikstromol	7.6
5	δ-Sesamin	26.7
6	Daphnoretin	-10.7
7	Rutarensin	6
8	<i>trans</i> -Tiliroside	28.7

\*Data provided by Prof. W. E. G. Müller, Mainz

The coumarin (+)-Dapheolone showed moderate activity against L5178Y cell line, while no activity was detected for the other compounds.

**Table 4.14.** Protein kinase assay results for the compounds isolated from *Thymelaea lythroides*

Compound tested (Conc. 1µg/mL)	Activity on various protein kinases based on IC50 [g/mL]*															
	AKT1	ALK	ARK 5	Aurora-B	AXL	FAK	IGF 1-R	MEK 1 wt	MET wt	NEK 2	NEK 6	PIM 1	PLK 1	PRK 1	SRC	VEGF-R2
Bassiatin	0	0	0	M	0	M	M	0	0	0	0	0	0	0	0	M
(+)-Dapheolone	0	0	0	M	0	0	0	0	0	0	0	0	0	0	0	0
(-)-Wikstromol	0	0	0	M	0	M	M	0	0	0	0	0	0	0	0	0
δ-Sesamin	0	0	0	M	0	M	M	0	0	0	0	0	0	0	0	0
Daphnoretin	0	0	0	M	0	M	M	0	0	0	0	0	0	0	0	M
Rutarensin	0	0	0	A	M	M	A	0	0	M	M	0	0	0	0	A
<i>trans</i> -Tiliroside	0	A	0	A	M	M	M	0	M	M	0	S	0	0	0	A

\* Data provided by ProQinase, Freiburg.

S: strongly active, A: active, M: moderately active, 0: not active

The isolated compounds of *Thymelaea lythroides* were subjected to biochemical protein kinase activity assays using 16 different human protein kinases. Only compounds Tiliroside and Rutarensin inhibited several of the tested kinases.

The IC<sub>50</sub> values observed for both compounds were in the low micromolar range against some protein kinases which inhibition is known to confer antitumoral effects.

The Hsp 90 chaperone showed no activity for all compounds isolated from *Thymelaea lythroides*.



#### 4.4. Compounds isolated from the endophytic fungus *Chaetomium aureum*

Five endophytic fungi were isolated from the Moroccan medicinal plant *Thymelaea lythroides*, namely *Alternaria sp.*, *Chaetomium aureus*, *Epicoccum nigrum*, *Cladosporium sp.* and *Pleospora sp.* Comparison of the HPLC chromatograms of the EtOAc extracts of all pure strain cultures and the preliminary biological screening assays, i.e. antibacterial, antifungal, and cytotoxicity showed that *Chaetomium aureum* is the most stable and active strain (Table 4.15).

The fungal strain of *Chaetomium aureum* (EMBL accession number HF546136) (Kabbaj *et al.*, 2012) was identified based on analysis of the DNA sequences of internal transcribed spacer regions of its ribosomal RNA gene. A voucher strain (strain designation MM10S2-1) is kept in the Institute of Pharmaceutical Biology and Biotechnology, Düsseldorf, Germany.

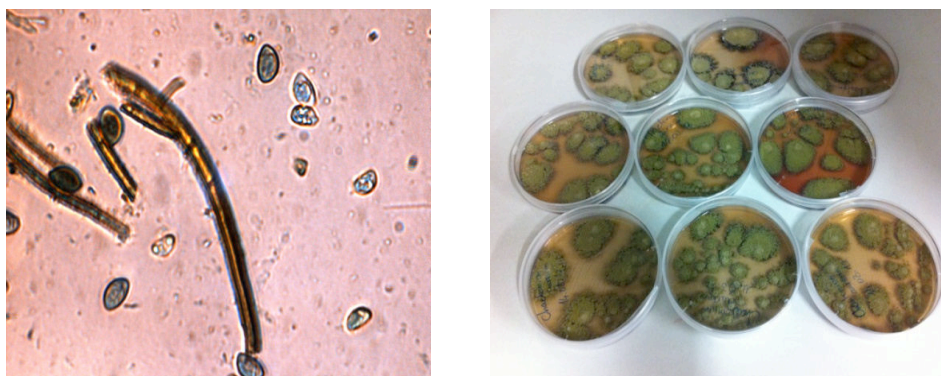


**Figure 4.14.** Photos of *Chaetomium aureum*

The pure fungal strain was cultivated on 11 media medium. Interestingly, chemical screening studies indicated a clear difference between *C. aureum* extracts obtained from liquid Wickerham medium, rice media culture, pulses media cultures and legumes media cultures. Comparison of the HPLC chromatograms of the EtOAc extracts of all cultures showed a different chemical pattern. While the rice culture extract showed (+)-sclerotiorin (9) as major substance, two unstable main components were detected in liquid cultures, with no traces of (+)-sclerotiorin (Figure 4.15). From the 10 others media, pulses media cultures showed the presence of the same two major compounds as in liquid cultures with the presence of (+)-sclerotiorin as minor compound, in legumes media steroids have been detected as major compounds.

In this part the investigation results on the natural products produced by *Chaetomium aureum* when grown on solid rice medium are presented.

**Table 4.15.** Preliminary biological screening assays of the five pure strains

Fungal strain	L5178Y	MRSA	<i>Strep. pneumonia</i>	<i>Entero. Faecalis</i>
<i>Epicocom nigrum</i>	100,3%	>62,5µg/ml	>31,25µg/ml	>62,5µg/ml
<i>Alternaria sp.</i>	95,5%	>31,25µg/ml	>62,5µg/ml	>31,25µg/ml
<i>Cladosporium sp</i>	25,2%	n.a	n.a	n.a
<i>Chaetomium aureum</i>	99,7%	>62,5µg/ml	> 62,5µg/ml	>62,5µg/ml
<i>Pleospora sp.</i>	101,3%	n.a	>125µg/ml	n.a

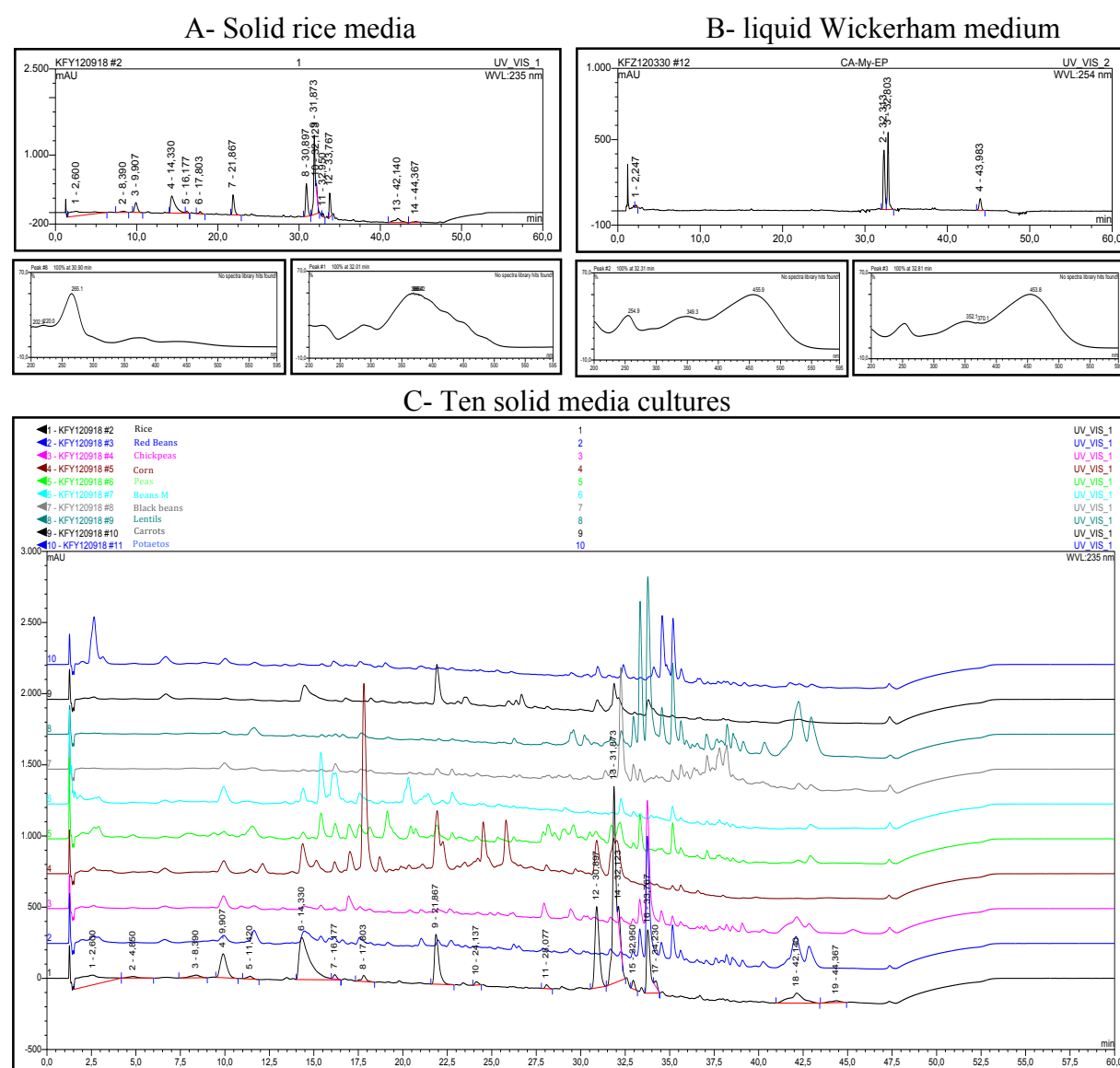


**Figure 4.15.** Comparison of the 11 media cultures of *Chaetomium aureum*. A- Solid rice media. B- liquid Wickerham medium. C- Ten solid media cultures

Compound isolated from the endophytic fungus *Chaetomium aureum*(+) -Sclerotiorin (**9**, Known)**(+) -Sclerotiorin**

Synonym(s)

6H-2-Benzopyran-6,8(7H)-dione, 5-chloro-3-(3,5-dimethyl-1,3-heptadienyl)-7-hydroxy-7-methyl-, acetate (8CI)

CAS Registry Number

549-23-5

Biological source

*Chaetomium aureum*

Sample amount

105 mg

Physical Description

yellow crystals

Molecular Formula

C<sub>21</sub>H<sub>23</sub>ClO<sub>5</sub>

Molecular Weight

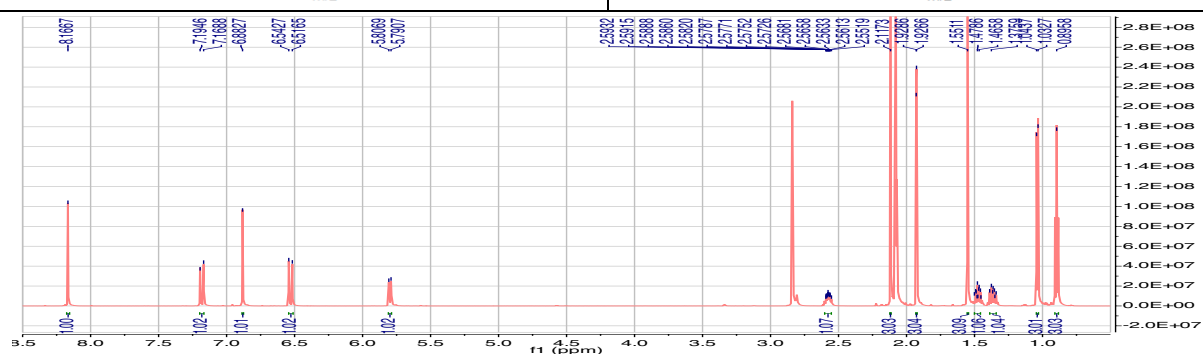
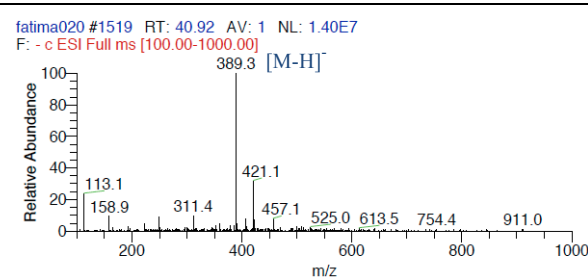
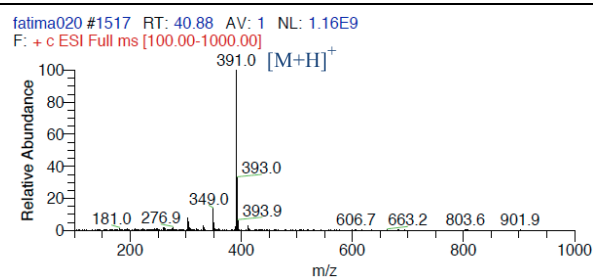
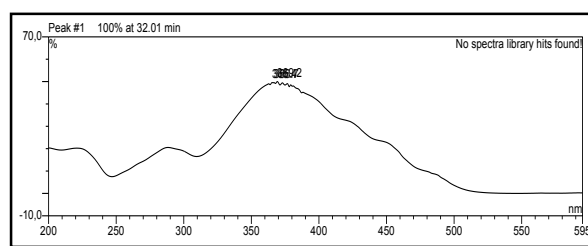
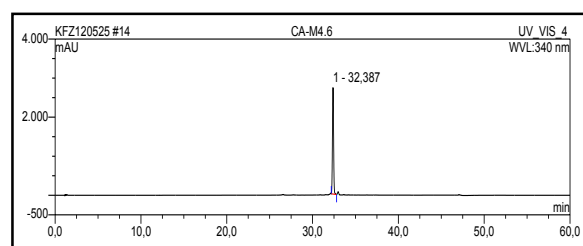
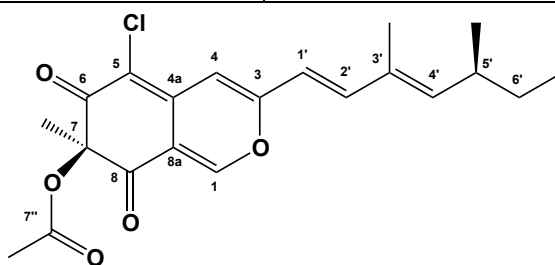
390 g/mol

Retention time HPLC

32,01 min (standard gradient)

Optical rotation  $[\alpha]_D^{26}$ +515 (c 1.0, CHCl<sub>3</sub>)UV spectrum  $\lambda_{max}$ 

220, 288 and 370 nm



**9** was isolated from *Chaetomium aureum* grown at room temperature for 30 days in Fernbach flasks on solid rice medium. The EtOAc extract was portioned between *n*-hexane and 90% MeOH. The MeOH fraction was chromatographed over a successive Sephadex LH-20 column using CH<sub>2</sub>Cl<sub>2</sub>/MeOH (1:1) as eluent (repeated twice) then purified by silica gel F254 (Merck, Darmstadt, Germany) using gradient elution (*n*-hexane/EtOAc/CH<sub>2</sub>Cl<sub>2</sub>/MeOH), which afforded yellow needles (yield, 105 mg). It showed UV absorbance at  $\lambda_{\max}$  (MeOH) 220, 288 and 370 nm. Positive and negative ESI-MS showed molecular ion peaks at *m/z* 391, [M+H]<sup>+</sup> (base peak) and *m/z* 389, [M-H]<sup>-</sup> (base peak), respectively, indicating a molecular weight of 390 g/mol.

The <sup>1</sup>H NMR (Table 4.16) showed five methyl group, which appeared at ( $\delta_{\text{H}}$  0.89, 1.03, 1.55, 1.92 and 2.11 ppm), assigned to 6'-CH<sub>3</sub>, 5'-CH<sub>3</sub>, 7-CH<sub>3</sub>, 3'-CH<sub>3</sub>, and 7''-CH<sub>3</sub> respectively; one methylene group, which appeared as AB spin system at ( $\delta_{\text{H}}$  1.36 and 1.47 ppm), assigned to 6'-CH<sub>2</sub>; and six methine proton at ( $\delta_{\text{H}}$  2.57, 5.80, 6.53, 6.88, 7.18 and 8.16 ppm), assigned to 5'-CH, 4'-CH, 1'-CH, 4-CH, 2'-CH and 1-CH.

The <sup>13</sup>C NMR showed the presence of 21 resolved signals, which were assigned to five methyl carbons, one methylene carbon, six *sp*<sup>2</sup> methine carbons, four *sp*<sup>2</sup> quaternary carbons, three oxygenated *sp*<sup>2</sup> quaternary carbons and three carbonyl carbons.

Analyses of <sup>1</sup>H-<sup>1</sup>H NMR COSY revealed the presence of two spin systems, as showed in Figure 4.16.A.

Furthermore, <sup>13</sup>C-<sup>1</sup>H long range couplings of <sup>2</sup>*J* and <sup>3</sup>*J* observed in the <sup>13</sup>C-<sup>1</sup>H heteronuclear multiple bond coherence (HMBC) spectrum gave the following linkages (Figure 4.16.B): from H-1 ( $\delta_{\text{H}}$  8.14 ppm) to C-3 ( $\delta_{\text{C}}$  159 ppm), C-4a ( $\delta_{\text{C}}$  139.8 ppm), C-8 ( $\delta_{\text{C}}$  192 ppm) and C-8a ( $\delta_{\text{C}}$  115.5 ppm); from H-4 to C-3, C-1' ( $\delta_{\text{H}}$  117 ppm), C-4a, and C-5 ( $\delta_{\text{C}}$  110 ppm); from H<sub>3</sub>-7-CH<sub>3</sub> ( $\delta_{\text{C}}$  1.52 ppm) to C-7 ( $\delta_{\text{C}}$  85.4 ppm), C-6 ( $\delta_{\text{C}}$  186.2 ppm) and C-8; from H<sub>3</sub>-7''-CH<sub>3</sub> to C-7'' ( $\delta_{\text{C}}$  170.1 ppm); from H-1' ( $\delta_{\text{C}}$  6.50 ppm) to C-2' ( $\delta_{\text{C}}$  142.8 ppm), C-3' ( $\delta_{\text{C}}$  133.5 ppm), C-3 and C-4 ( $\delta_{\text{C}}$  106.7 ppm); from H-2' ( $\delta_{\text{H}}$  7.16 ppm) to C-1', C-3', C-4' ( $\delta_{\text{C}}$  148.3 ppm), C-3'-CH<sub>3</sub> ( $\delta_{\text{C}}$  12.1 ppm) and C-3; from H<sub>3</sub>-3'-CH<sub>3</sub> ( $\delta_{\text{H}}$  1.90 ppm) to C-2', C-4' and C-3'; from H-4' ( $\delta_{\text{H}}$  5.77 ppm) to C-2', C-3'-CH<sub>3</sub>, C-5' ( $\delta_{\text{C}}$  35.4 ppm) and C-6' ( $\delta_{\text{C}}$  30.4 ppm); from H<sub>3</sub>-5'-CH<sub>3</sub> ( $\delta_{\text{H}}$  1.01) to C-6', C-5' and C-4'; from H<sub>2</sub>-6' ( $\delta_{\text{H}}$  1.33, 1.44) to C-4', C-5', C-5'-CH<sub>3</sub> ( $\delta_{\text{C}}$

20.1 ppm) and C-6'-CH<sub>3</sub> ( $\delta_C$  11.82 ppm) and from H<sub>3</sub>-6'-CH<sub>3</sub> ( $\delta_H$  0.86 ppm) to C-5', C-5'-CH<sub>3</sub> and C-6'. The connection of the acetyl group was confirmed by the chemical shift of C-7' ( $\delta_C$  170.1 ppm) assigned to an ester bond and the long-rang coupling of  $J^4$  observed from H<sub>3</sub>-7''-CH<sub>3</sub> to C-7 in <sup>13</sup>C-<sup>1</sup>H NMR spectrum (Figure 4.16.B). Furthermore, the chemical shift of C-1 ( $\delta_C$  154.1 ppm) and C-3 ( $\delta_C$  159.6 ppm) indicated the presence of an oxygenated carbon between both carbons and the correlation between the H-1 and the C-3 confirms ring closure. Thus, these data indicated that **9** was found to be 6H-2-Benzopyran-6,8(7H)-dione-5-chloro-3-(3,5-dimethyl-1,3-heptadienyl)-7-hydroxy-7-methyl-, acetate (8Cl). On the basis of the coupling constants of H-1' with H-2' and the chemical shift of the neighbor carbon of C-5', the configurations of these two double bonds were both determined to be E.

The identification was further corroborated by comparison of UV, <sup>1</sup>H, <sup>13</sup>C NMR, mass spectral data as well as  $[\alpha]_D$  value of **9** with those data previously published for (+)-sclerotiorin (Natsume *et al.*, 1988).

The compound was previously reported from *Penicillium sclerotiorum*, *P. multicolor*, *P. implicatum*, *P. hirayamae*, *P. frequentans*, *P. faveolata*, lichen mycobionts of *Pyrenula japonica*, ascommycete *T. luteus* and from unidentified fungus 98F134 (Gregory and Turner, 1963; Takenaka *et al.*, 1963; Takenaka *et al.*, 2000; Periyasamy *et al.*, 2012; Li *et al.*, 2010; Chidananda *et al.*, 2006). This is the first finding of this compound from *Chaetomium aureum*.

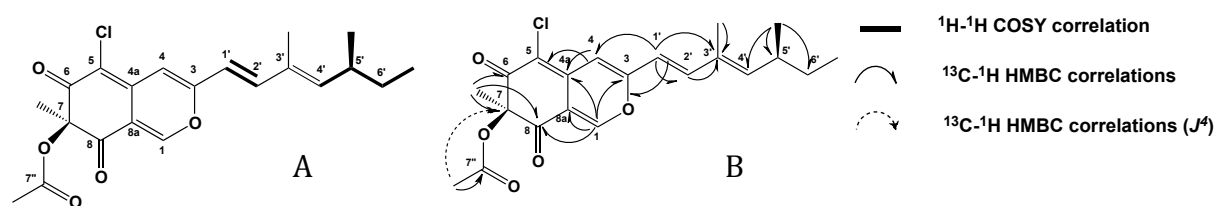
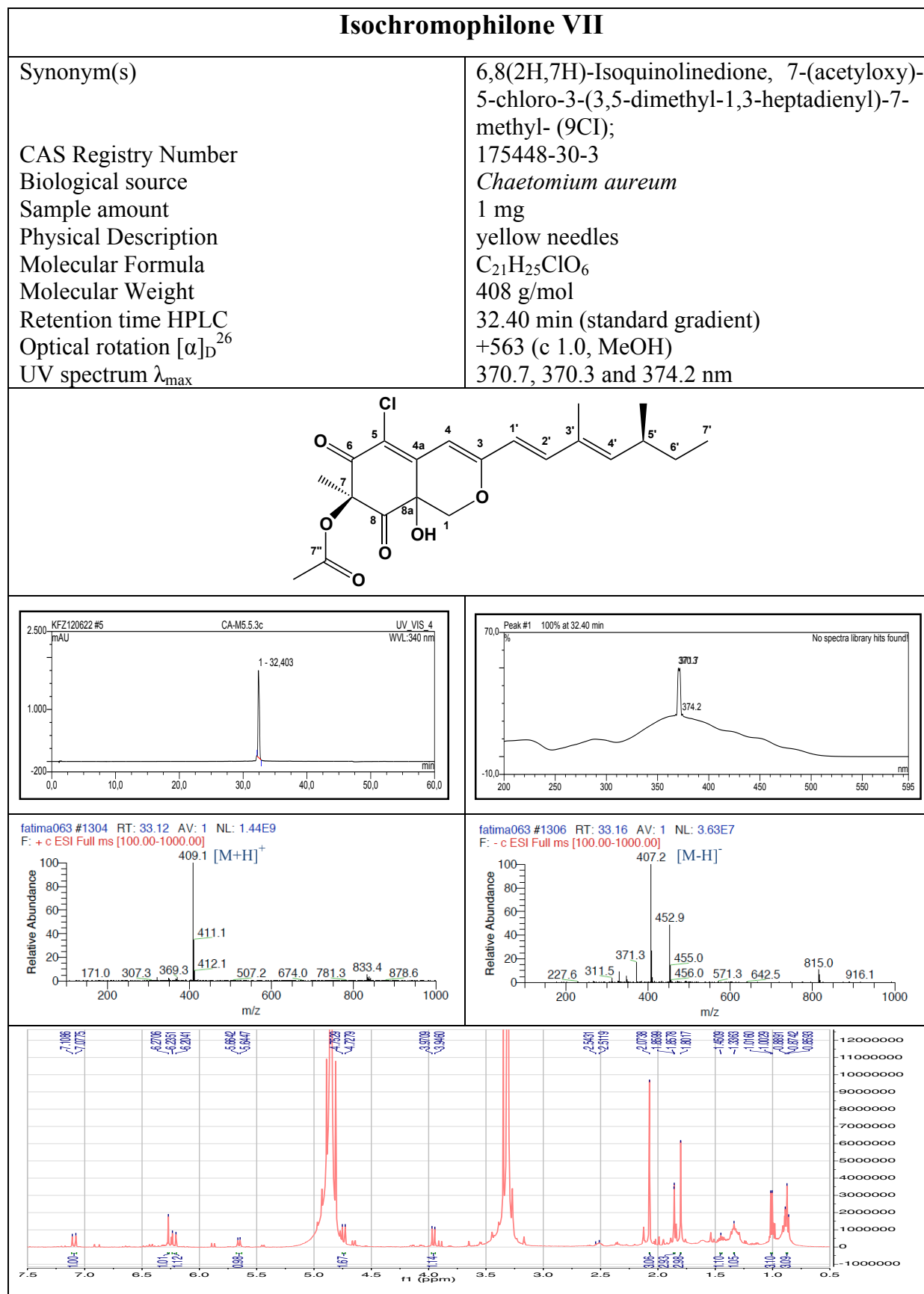


**Figure 4.16.** A) <sup>1</sup>H-<sup>1</sup>H COSY correlations of **1** B) selected <sup>13</sup>C-<sup>1</sup>H HMBC correlations

Compound isolated from the endophytic fungus *Chaetomium aureum*

Isochromophilone VII (10, Known)



**10** was isolated from *Chaetomium aureum* grown at room temperature for 30 days in Fernbach flasks on solid rice medium. The EtOAc extract was portioned between *n*-hexane and 90% MeOH. The MeOH fraction was chromatographed over a successive sephadex LH-20 column using CH<sub>2</sub>Cl<sub>2</sub>/MeOH (1:1) as eluent (repeated twice), then purified by semi-preparative HPLC (Merck, Hitachi L-7100) using a Eurosphere 100–10 C18 column (300 x 8mm, L x i.d.) with the following gradient (MeOH/H<sub>2</sub>O): 0 min, 10% MeOH; 5 min, 10% MeOH; 35 min, 100% MeOH; 45 min, 100 % MeOH, which afforded yellow needles (yield, 1 mg). It showed UV absorbance at  $\lambda_{\max}$  (MeOH) 370.7, 370.3 and 374.2 nm. Positive and negative ESI-MS showed molecular ion peaks at *m/z* 409.1 [M+H]<sup>+</sup> (base peak) and *m/z* 407.2 [M-H]<sup>-</sup> (base peak), respectively, indicating a molecular weight of 408 g/mol. The molecular formula of **10** was determined to be C<sub>21</sub>H<sub>25</sub>O<sub>6</sub>Cl.

The <sup>1</sup>H NMR spectra (MeOD) (Table 4.16) showed 24 proton signals. To fulfill the molecular formula, the presence of one hydroxyl group was suggested.

From the <sup>1</sup>H-<sup>1</sup>H COSY spectrum, three spin system, H-4'→H-6'-CH<sub>3</sub>, between the two protons of H<sub>α</sub>-1-H<sub>β</sub>-1 and between H-1' and H-2' were determined (Figure 4.17).

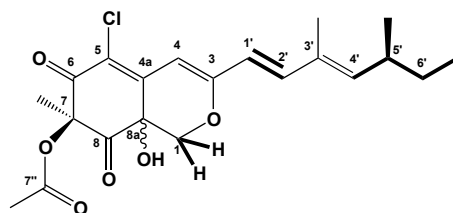


**Figure 4.17.** <sup>1</sup>H-<sup>1</sup>H COSY correlations of **10**

<sup>13</sup>C-<sup>1</sup>H long range couplings of <sup>2</sup>*J* and <sup>3</sup>*J* observed in the HMBC spectrum showed cross peaks from H-3'-CH<sub>3</sub> ( $\delta_{\text{H}}$  1.82 ppm) to C-2' ( $\delta_{\text{C}}$  142.9 ppm), C-3' ( $\delta_{\text{C}}$  132.2 ppm) and C-4' ( $\delta_{\text{C}}$  148.1 ppm), forming the 3,5-dimethyl-1,3-heptadienyl moiety containing the above two proton sequences. The cross peaks from H-2' ( $\delta_{\text{H}}$  7.07 ppm), H-1' ( $\delta_{\text{H}}$  6.04 ppm) and H-4 ( $\delta_{\text{H}}$  6.18 ppm) to C-3 ( $\delta_{\text{C}}$  162.2 ppm), from H-4 to C-1' ( $\delta_{\text{C}}$  118.2 ppm) and from H-1' to C-4 revealed the presence of an extended conjugation system.

Furthermore, the cross peaks from H<sub>2</sub>-1 ( $\delta_{\text{H}}$  4.02, 4.74 ppm) to C-3, C-4a ( $\delta_{\text{C}}$  142.8 ppm) and

---

---

C-8a ( $\delta_C$  67.9 ppm), and from H-4 to C-3 and C-8a, and  $^{13}\text{C}$  shifts of C-1 ( $\delta_C$  70.0 ppm) and C-3 revealed a pyran ring. The HMBC NMR showed correlations from H-7"-CH<sub>3</sub> ( $\delta_C$  2.12 ppm) to C-7" ( $\delta_C$  169.7 ppm). The presence of another 6-membered ring was suggested because of the cross peaks from C-7-CH<sub>3</sub> ( $\delta_C$  1.83 ppm) to C-6 ( $\delta_C$  185.4 ppm), C-7 ( $\delta_C$  83.4 ppm) and C-8. ( $\delta_C$  197.1 ppm), from H-1 to C-8, and from H-4 to C-5 ( $\delta_C$  121.0 ppm) in the HMBC spectrum and the degree of unsaturation. The UV-spectrum also revealed that the structure contained a continuous conjugated ketone. Finally the remaining hydroxyl group, acetyl group and Cl should be attached to C-8a, C-7 and C-5, respectively, due to the  $^{13}\text{C}$  chemical shifts. Taken together, the structure was comparable with previously published data for isochromophilone VII isolated from *Penicillium sp.* FO-4164 (Yang *et al.*, 1995).

Isochromophilone VII was isolated only from *Penicillium sp.* FO-4164 (Yang *et al.*, 1995), this is the first report of Isochromophilone VII from *Chaetomiun aureum*.



Compound isolated from the endophytic fungus *Chaetomium aureum*

Sclerotioramin (11, Known)

## Sclerotioramin

Synonym(s)

1H-2-Benzopyran-6,8(7H,8aH)-dione, 7-(acetyloxy)-5-chloro-3-(3,5-dimethyl-1,3-heptadienyl)-8a-hydroxy-7-methyl- (9CI)  
34695-81-3

CAS Registry Number

Biological source

*Chaetomium aureum*

Sample amount

7 mg

Physical Description

red needles

Molecular Formula

 $C_{21}H_{24}ClNO_4$ 

Molecular Weight

389 g/mol

Retention time HPLC

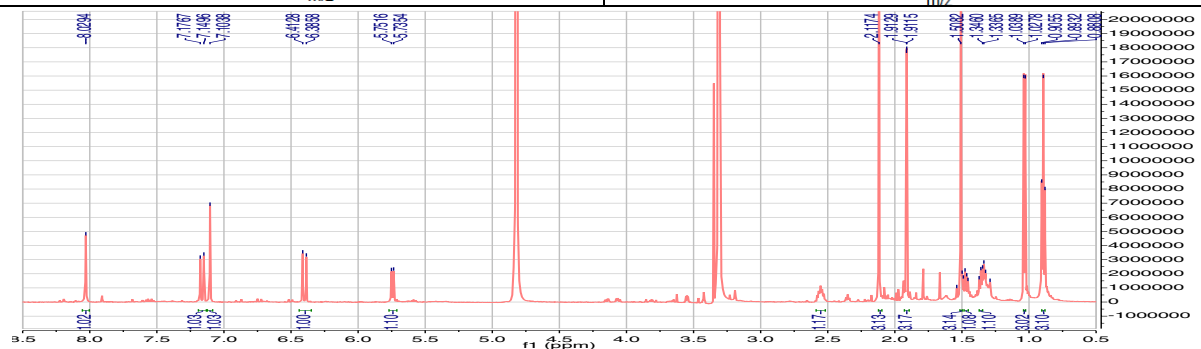
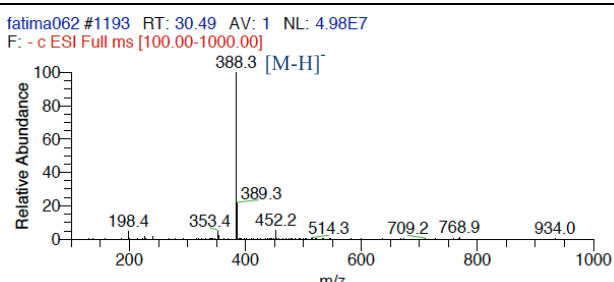
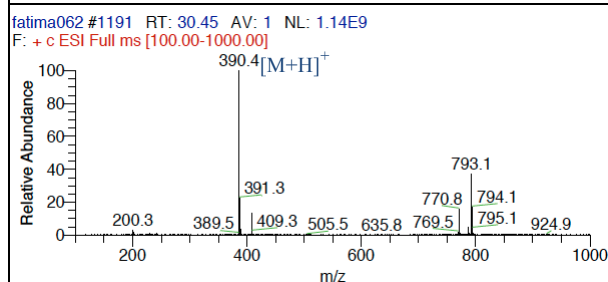
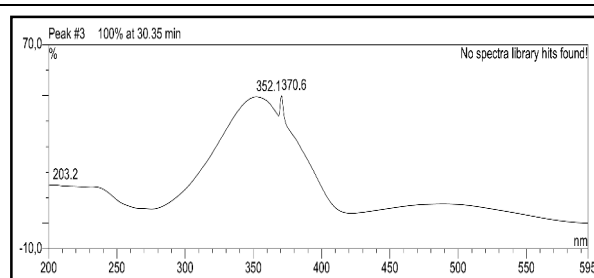
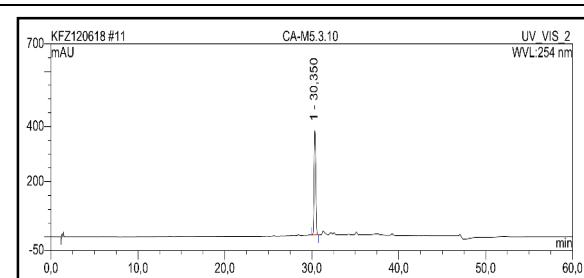
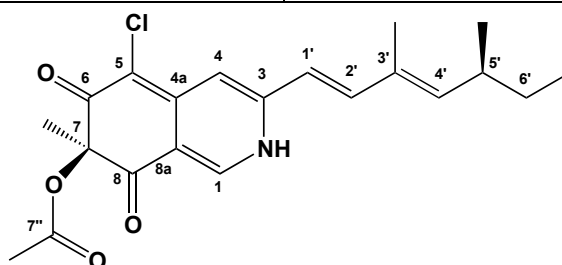
30.35 min (standard gradient)

Optical rotation  $[\alpha]_D^{26}$ 

+505 (c 1.0, MeOH)

UV spectrum  $\lambda_{max}$ 

203.2, 352.1 and 370.6 nm



**11** was isolated from *Chaetomium aureum* grown at room temperature for 30 days in Fernbach flasks on solid rice medium. The EtOAc extract was portioned between *n*-hexane and 90% MeOH. The MeOH fraction was chromatographed over a successive Sephadex LH-20 column using CH<sub>2</sub>Cl<sub>2</sub>/MeOH (1:1) as eluent (repeated three times) then purified by semi-preparative HPLC (Merck, Hitachi L-7100) using a Eurosphere 100–10 C18 column (300 x 8mm, L x i.d.) with the following gradient (MeOH/H<sub>2</sub>O): 0 min, 10% MeOH; 5 min, 10% MeOH; 35 min, 100% MeOH; 45 min, 100 % MeOH, which afforded red needles (yield, 7 mg). It showed UV absorbance at  $\lambda_{\max}$  (MeOH) 203.2, 352.1 and 370.6 nm. Positive and negative ESI-MS showed molecular ion peaks at  $m/z$  390.4 [M+H]<sup>+</sup> (base peak) and  $m/z$  388.3 [M-H]<sup>-</sup> (base peak), respectively, indicating a molecular weight of 389 g/mol. The molecular formula of **11** was assigned as C<sub>21</sub>H<sub>24</sub>ClNO<sub>4</sub>. To achieve the molecular formula, the presence of one secondary amine group was suggested.

The <sup>1</sup>H NMR spectra (MeOD) (Table 4.16) showed 23 protons signals, which were almost identical to sclerotiorin except the chemical shift of 2 signals at ( $\delta_{\text{H}}$  8.03 ppm) and ( $\delta_{\text{H}}$  7.10 ppm), assigned to H-1 and H-4. In the <sup>13</sup>C NMR showed the presence of 21 resolved signals, which were almost the same as sclerotiorin except the chemical shift of 3 signals at ( $\delta_{\text{C}}$  139.6 ppm), ( $\delta_{\text{C}}$  144.9 ppm) and ( $\delta_{\text{C}}$  112.5 ppm), assigned to C-1, C-3 and C-4.

The 2D NMR, <sup>1</sup>H-<sup>1</sup>H NMR COSY and <sup>13</sup>C-<sup>1</sup>H NMR HMBC showed the same correlation as sclerotiorin. The <sup>15</sup>N-<sup>1</sup>H NMR HMBC showed the cross peaks from one nitrogen signal, N ( $\delta_{\text{N}}$  -351.7 ppm) to H-1 ( $\delta_{\text{H}}$  8.03 ppm), H-4 ( $\delta_{\text{H}}$  7.10 ppm) and H-1' ( $\delta_{\text{H}}$  6.40 pmm). Thus, these data indicated the presence of nitrogen in the position **2**.

The identification was further corroborated by comparison of UV, <sup>1</sup>H, <sup>13</sup>C NMR, mass spectral data as well as  $[\alpha]_{\text{D}}$  value of **11** with the data previously published for (+)-sclerotioramin (Wang *et al.*, 2010).

Sclerotioramin is a natural product, which has been isolated, together with sclerotiorin, from the mycelium of *P. multicolour* and *P. sclerotiorum* grown under special conditions (Page *et al.*, 1957). The compound was previously also reported from *P. citreonigrum* (Wang *et al.*, 2010) from *Diaporthe sp* (Zang *et al.*, 2012), from *Penicillium implicatum* (Yuzuru *et al.*, 1959). But this is the first report of this compound from *Chaetomium aureum*.

Compound isolated from the endophytic fungus *Chaetomium aureum*Sclerotioramin (**12**, Known)**Isochromphilone VI**

Synonym(s)

6,8(2H,7H)-Isoquinolinedione, 7-(acetyloxy)-5-chloro-3-[(1E,3E,5S)-3,5-dimethyl-1,3-heptadienyl]-2-(2-hydroxyethyl)-7-methyl-, (7R)- (9CI)

CAS Registry Number

167173-91-3

Biological source

*Chaetomium aureum*

Sample amount

5 mg

Physical Description

red needles

Molecular Formula

 $C_{23}H_{28}ClNO_5$ 

Molecular Weight

433 g/mol

Retention time HPLC

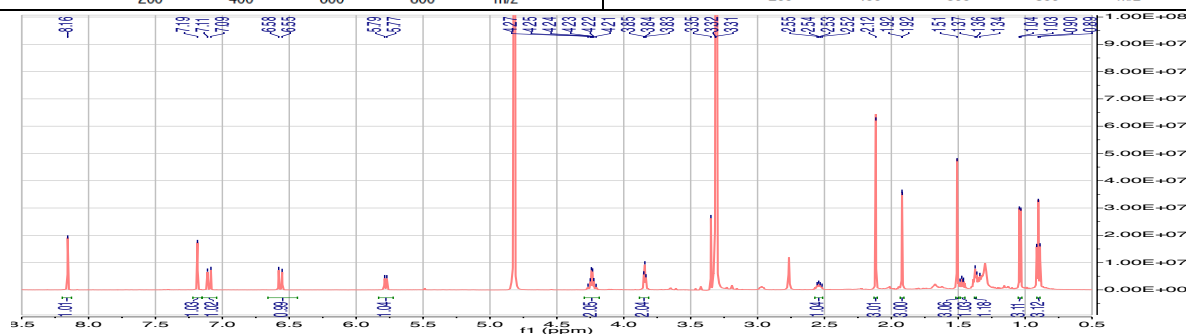
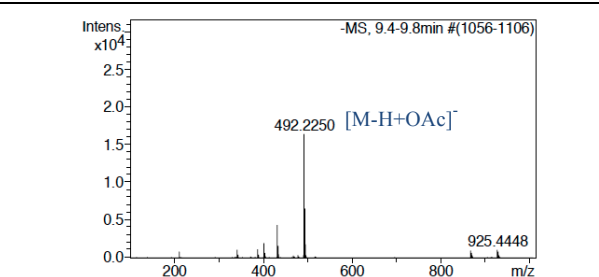
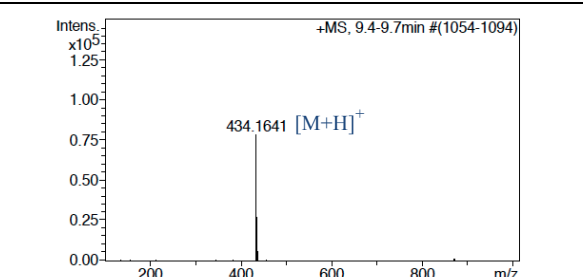
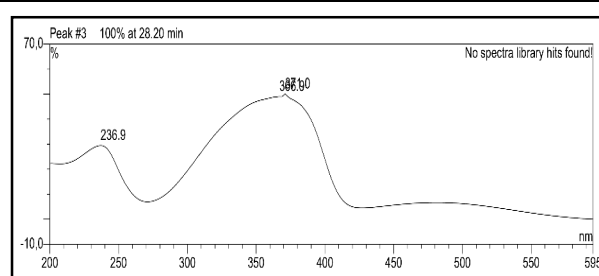
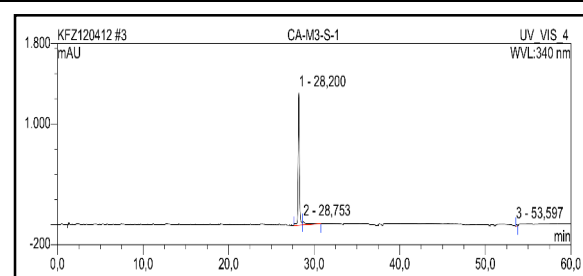
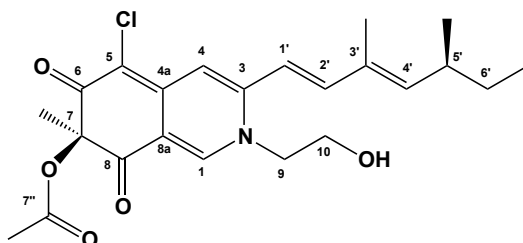
28.2 min (standard gradient)

Optical rotation  $[\alpha]_D^{26}$ 

+489 (c 1.0, MeOH)

UV spectrum  $\lambda_{max}$ 

236.9, 306.9 and 371.0 nm



**12** was isolated from *Chaetomium aureum* grown at room temperature for 30 days in Fernbach flasks on solid rice medium. The EtOAc extract was portioned between *n*-hexane and 90% MeOH. The MeOH fraction was chromatographed over a successive sephadex LH-20 column using CH<sub>2</sub>Cl<sub>2</sub>/MeOH (1:1) as eluent (repeated twice) then purified by semi-preparative HPLC (Merck, Hitachi L-7100) using a Eurosphere 100–10 C18 column (300 x 8mm, L x i.d.) with the following gradient (MeOH/H<sub>2</sub>O): 0 min, 10% MeOH; 5 min, 10% MeOH; 35 min, 100% MeOH; 45 min, 100 % MeOH, which afforded red needles (yield, 5 mg). It showed UV absorbance at  $\lambda_{\max}$  (MeOH) 236.9, 306.9 and 371.0 nm. Positive and negative ESI-MS showed molecular ion peaks at  $m/z$  434.16 [M+H]<sup>+</sup> (base peak) and  $m/z$  492.22 [M-H+OAc]<sup>-</sup> (base peak), respectively, indicating a molecular weight of 433 g/mol, with a 44 mass unit increase compared to sclerotioramin, which established a molecular formula of C<sub>23</sub>H<sub>28</sub>ClNO<sub>5</sub>.

The <sup>1</sup>H NMR spectra (MeOD) (Table 4.16) showed 28 protons signals, which were almost identical to sclerotioramin except the presence of two more signals at ( $\delta_H$  3.84 ppm) and ( $\delta_H$  4.23 ppm), assigned to H-9 and H-10. In the <sup>13</sup>C NMR showed the presence of 23 resolved signals, which were almost the same as sclerotioramin except the presence of two more signals at ( $\delta_C$  61.1 ppm) and ( $\delta_C$  57.4 ppm), assigned to C-9 and C-10.

From the <sup>1</sup>H-<sup>1</sup>H COSY spectrum, three spin system, H-4'→H-6'-CH<sub>3</sub>, between the two protons H-9 and H-10 and between H-1' and H-2' were determined (Figure 3.18.A).

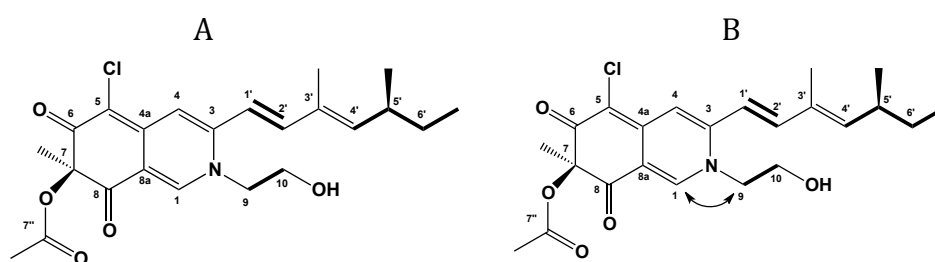


**Figure 4.18.** A) <sup>1</sup>H-<sup>1</sup>H COSY correlations B) selected <sup>13</sup>C-<sup>1</sup>H HMBC correlations of **12**

The more important correlations of <sup>13</sup>C-<sup>1</sup>H long range couplings of <sup>2</sup>J and <sup>3</sup>J observed in the HMBC spectrum are the cross peaks from H-1 ( $\delta_H$  8.16 ppm) to C-9 ( $\delta_C$  57.4 ppm) and from H-9 ( $\delta_H$  3.84 ppm) to C-1 ( $\delta_C$  138.0 ppm), which confirm that the proton of NH in sclerotioramin has been replaced by a side chain of two carbons and a hydroxyl group (CH<sub>2</sub>-CH<sub>2</sub>-OH) (Figure 4.18.B).

The identification was further corroborated by comparison of UV,  $^1\text{H}$ ,  $^{13}\text{C}$  NMR, mass spectral data as well as  $[\alpha]_{\text{D}}$  value of **12** with the previously published data for (+)-isochromophilone VI (Arai *et al.*, 1995).

Isochromophilone VI was previously reported from *Penicillium multicolor* FO-3216 (Arai *et al.*, 1995), from *Diaporthe sp.* (Zang *et al.*, 2012), however, this is the first report of this compound from *Chaetomium aureum*.

**Table 4.16.**  $^1\text{H}$  and  $^{13}\text{C}$  NMR chemical shifts of sclerotiorin and its derivatives

No.	sclerotiorin		Isochromophilone VII	Sclerotioramin		Isochromophilone VI	
	$\delta_{\text{C}}$	$\delta_{\text{H}}$	$\delta_{\text{H}}$	$\delta_{\text{C}}$	$\delta_{\text{H}}$	$\delta_{\text{C}}$	$\delta_{\text{H}}$
<b>1</b>	154.1	8.14 (s)	3.96 (d, $J=12.46$ Hz) 4.74 (d, $J=12.47$ Hz)	139.6	8.03 (s)	138.0	8.16 (s)
<b>2</b>	-	-	-	-	-	-	-
<b>3</b>	159.5	-	-	144.9	-	146.4	-
<b>4</b>	106.7	6.85 (s)	6.27 (s)	112.5	7.10 (s)	112.6	7.19 (s)
<b>4a</b>	139.8	-	-	148.3	-	148.3	-
<b>5</b>	110.2	-	-	101.1	-	101.2	-
<b>6</b>	186.3	-	-	185.9	-	185.5	-
<b>7</b>	85.5	-	-	85.9	-	86.2	-
<b>7-CH<sub>3</sub></b>	22.3	1.52 (s)	1.80 (s)	23.8	1.51 (s)	23.8	1.51 (s)
<b>7''</b>	170.1	-	-	171.5	-	171.5	-
<b>7''-CH<sub>3</sub></b>	19.6	2.09 (s)	2.07 (s)	20.1	2.12 (s)	20.1	2.12 (s)
<b>8</b>	192.7	-	-	195.0	-	195.1	-
<b>8a</b>	115.2	-	-	115.8	-	114.8	-
<b>9</b>	-	-	-	-	-	57.4	4.23 (dd, $J=4.86; 5.46$ Hz)
<b>10</b>	-	-	-	-	-	61.1	3.84 (dd, $J=4.38; 5.16$ Hz)
<b>1'</b>	117.3	6.50 (d, $J=15.7$ Hz)	6.22 (d, $J=15.53$ Hz)	118.3	6.40 (d, $J=16.22$ Hz)	117.2	6.57 (d, $J=15.49$ Hz)
<b>2'</b>	142.8	7.16 (d, $J=15.7$ Hz)	7.02 (d, $J=15.59$ Hz)	143.4	7.16 (d, $J=16.22$ Hz)	144.4	7.10 (d, $J=15.44$ Hz)
<b>3'</b>	133.5	-	-	133.8	-	133.8	-
<b>3'-CH<sub>3</sub></b>	12.1	1.90 (s)	1.84 (d, $J=1.05$ Hz)	12.5	1.91 (s)	12.6	1.92 (s)
<b>4'</b>	148.3	5.77 (d, $J=9.7$ )	5.65 (d, $J=9.72$ Hz)	148.9	5.74 (d, $J=9.74$ Hz)	148.7	5.78 (d, $J=9.75$ Hz)
<b>5'</b>	35.4	2.54 (m)	2.54 (m)	36.2	2.55 (m)	36.2	2.53 (m)
<b>5'-CH<sub>3</sub></b>	20.1	1.01 (d, $J=6.61$ )	1.01 (d, $J=6.55$ Hz)	20.5	1.03 (d, $J=6.68$ Hz)	20.5	1.03 (d, $J=6.66$ Hz)
<b>6'</b>	30.4	1.33-1.44 (m)	1.33-1.44 (m)	31.1	1.34-1.48 (m)	31.1	1.37-1.47 (m)
<b>6'-CH<sub>3</sub></b>	11.8	0.86 (t, $J=7.4, 7.4$ Hz)	0.87 (t, $J=7.45; 7.45$ Hz)	12.3	0.89 (t, $J=7.42; 7.42$ Hz)	12.3	0.90 (t, $J=7.5; 7.3$ Hz)

Compound isolated from the endophytic fungus *Chaetomium aureum*Sclerotioramin (**13**, New)

## SB 236050

Synonym(s)

1H, 3H-Pyrano[4,3-b][1]benzopyran-9-carboxylic acid, 4,10-dihydro-7,8-dihydroxy-1-methoxy-3-methyl-10-oxo-

CAS Registry Number

335377-65-6

Biological source

*Chaetomium aureum*

Sample amount

40 mg

Physical Description

grau powder

Molecular Formula

C<sub>15</sub>H<sub>14</sub>O<sub>8</sub>

Molecular Weight

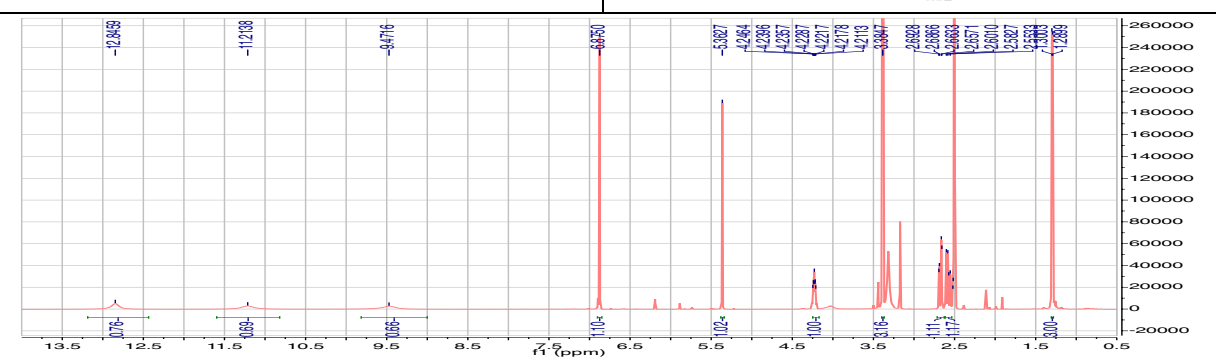
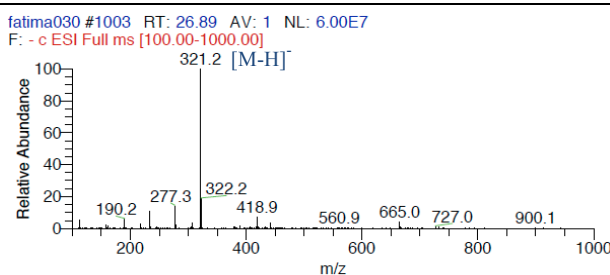
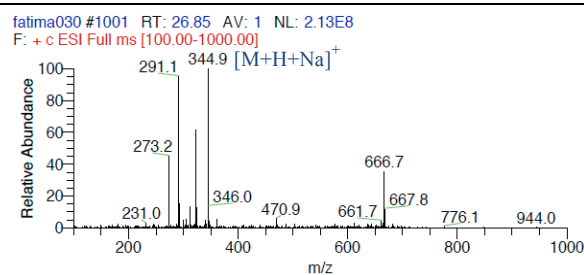
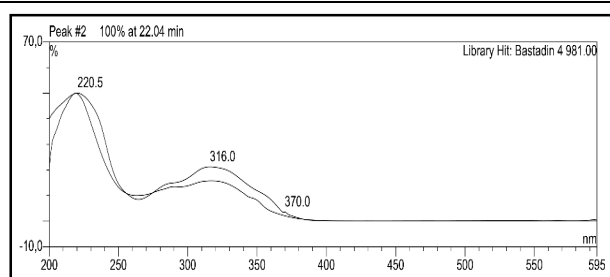
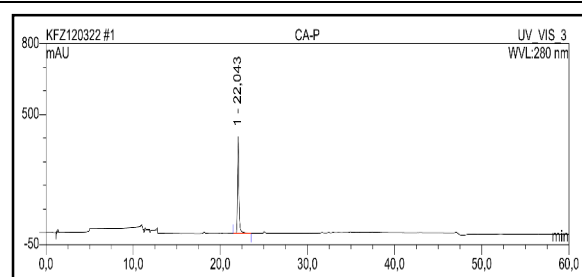
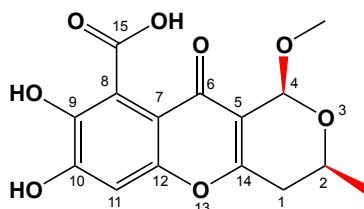
322 g/mol

Retention time HPLC

22.04 min (standard gradient)

Optical rotation [ $\alpha$ ]<sub>D</sub><sup>20</sup>+35.6 (c 1.0, CHCl<sub>3</sub>)UV spectrum  $\lambda_{\max}$ 

220.5, 316.0 and 370.0 nm



**13** was isolated from *Chaetomium aureum* grown at room temperature for 30 days in Fernbach flasks on solid rice medium. The EtOAc extract was portioned between *n*-hexane and 90% MeOH. The MeOH fraction gave a precipitate, which was washed several times with methanol until obtaining grey powder (yield, 40 mg). It showed UV absorbance at  $\lambda_{\max}$  (MeOH) 220.5, 316.0 and 370.0 nm. Positive and negative ESI-MS showed molecular ion peaks at  $m/z$  344.9  $[M+H+Na]^+$  (base peak) and  $m/z$  321.2  $[M-H]^-$  (base peak), respectively, indicating a molecular weight of 322 g/mol. The molecular formula of **13** was assigned as  $C_{21}H_{24}ClNO_4$ .

The  $^1H$  NMR (DMSO- $d_6$ ) (Table 4.17) showed one methyl group at ( $\delta_H$  1.30 ppm) assigned to H-2-CH<sub>3</sub>, one methoxy group at ( $\delta_H$  3.28 ppm) assigned to H-4-OCH<sub>3</sub>, one methylene proton at ( $\delta_H$  2.67 ppm) and ( $\delta_H$  2.58 ppm) assigned to H-1, two aliphatic proton CH at ( $\delta_H$  4.22 ppm) and ( $\delta_H$  5.36 ppm) assigned to H-2 and H-4 respectively, one aromatic proton at ( $\delta_H$  6.87 ppm) assigned to H-11 and three hydroxyl group at ( $\delta_H$  9.47, 11.21 and 12.81 ppm) assigned to H-10-OH, H-9-OH and H-15-OH. The  $^{13}C$  NMR and DEPT NMR showed the presence of 21 resolved signals, which were assigned to one methyl carbon ( $\delta_C$  20.3 ppm) assigned to 2-CH<sub>3</sub>, one methylene carbon ( $\delta_C$  33.1 ppm) assigned to C-1, three methine carbons ( $\delta_C$  61.7, 93.8 and 102.1 ppm) assigned to C-2, C-4 and C-11 respectively, two carbonyl carbons ( $\delta_C$  172.1 and 167.5 ppm) assigned to C-6 and C-15 and seven  $sp^2$  quaternary carbons.

The  $^1H$ - $^1H$  COSY spectra showed the presence of one spin system from H(1)→H(2)→H(2-CH<sub>3</sub>) as shown in the Figure 4.19.A.

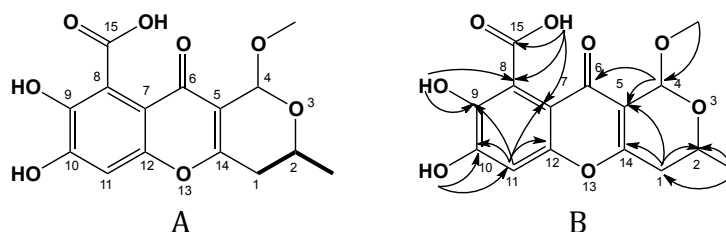


**Figure 4.19.** A)  $^1H$ - $^1H$  COSY correlations B) selected  $^1H$ - $^{13}C$  HMBC correlations of **13**

The  $^1H$ - $^{13}C$  HMBC spectra (Figure 4.19.B) showed the selected following correlations: The cross peak from H-2-CH<sub>3</sub> to C-2 and C-1, from H-1 to C-2, C-14 and C-5, from H-4-OCH<sub>3</sub> to C-4, from H-4 to C-5 and C-6, from H-11 to C-10, C-12, C-7 and C-9, from H-9-OH to C-8

and C-9, from H-10-OH to C-10 and C-11, from H-15-OH to C-7, C-8 and C-15.

The identification was further corroborated by comparison of UV,  $^1\text{H}$ ,  $^{13}\text{C}$  NMR, mass spectral data of **13** and the previously published data for SB 236050 (Payne *et al.*, 2002).

Regarding the structure of SB 236050, which has two chiral carbon centers at C-2 and C-4, the relative stereochemistry was determined by REOSY NMR spectra as shown in Figure 4.20.

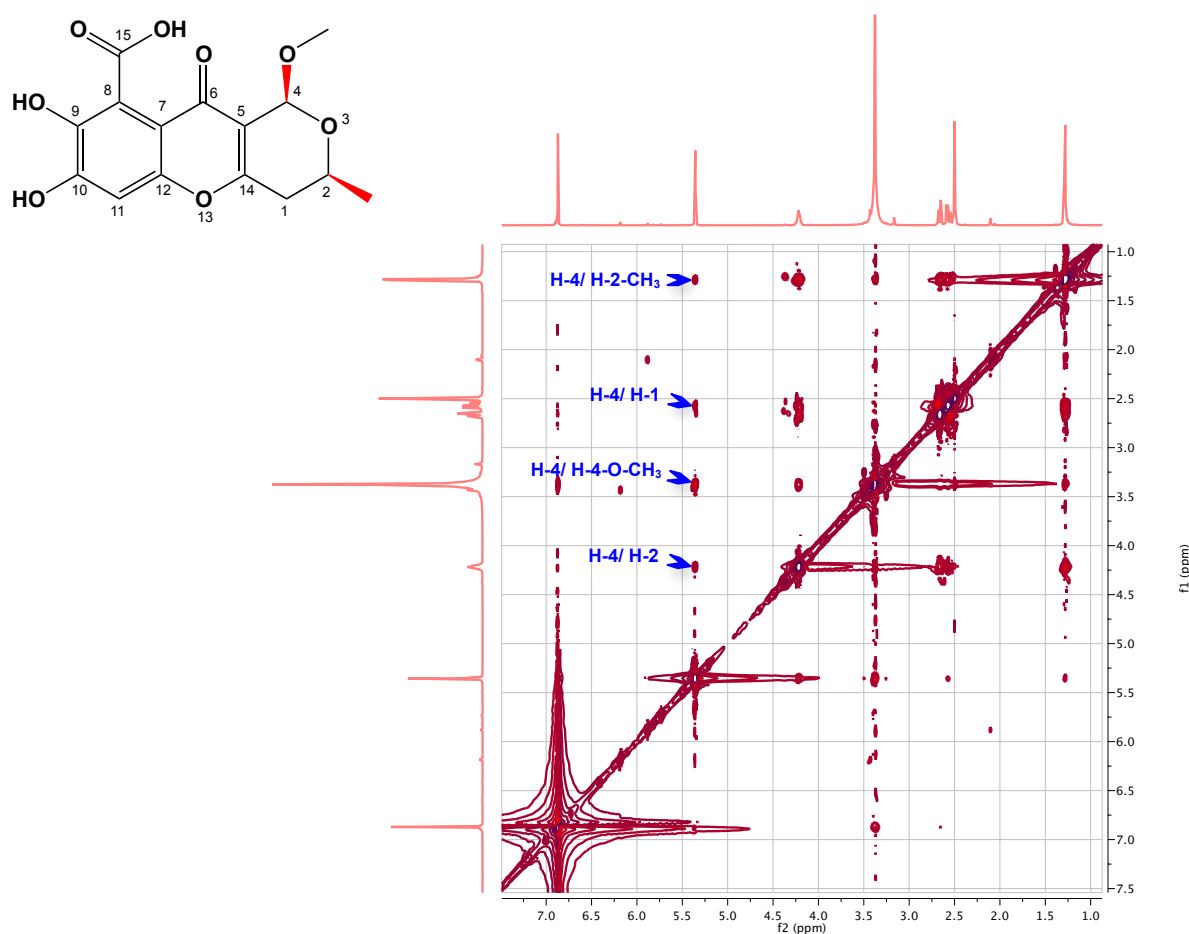


**Figure 4.20.**  $^1\text{H}$ - $^1\text{H}$  ROESY correlations

The H-4 correlated with H-2-CH<sub>3</sub>, H-1, H-4-OCH<sub>3</sub> and H-2 (see Figure 4.17).  $^1\text{H}$ - $^1\text{H}$  ROESY spectra permitted the assignment of the cis-stereochemistry of SB 236050 to be as shown in Figure 4.17, which is reported for the first time. The absolute stereochemistry could not be confirmed yet.

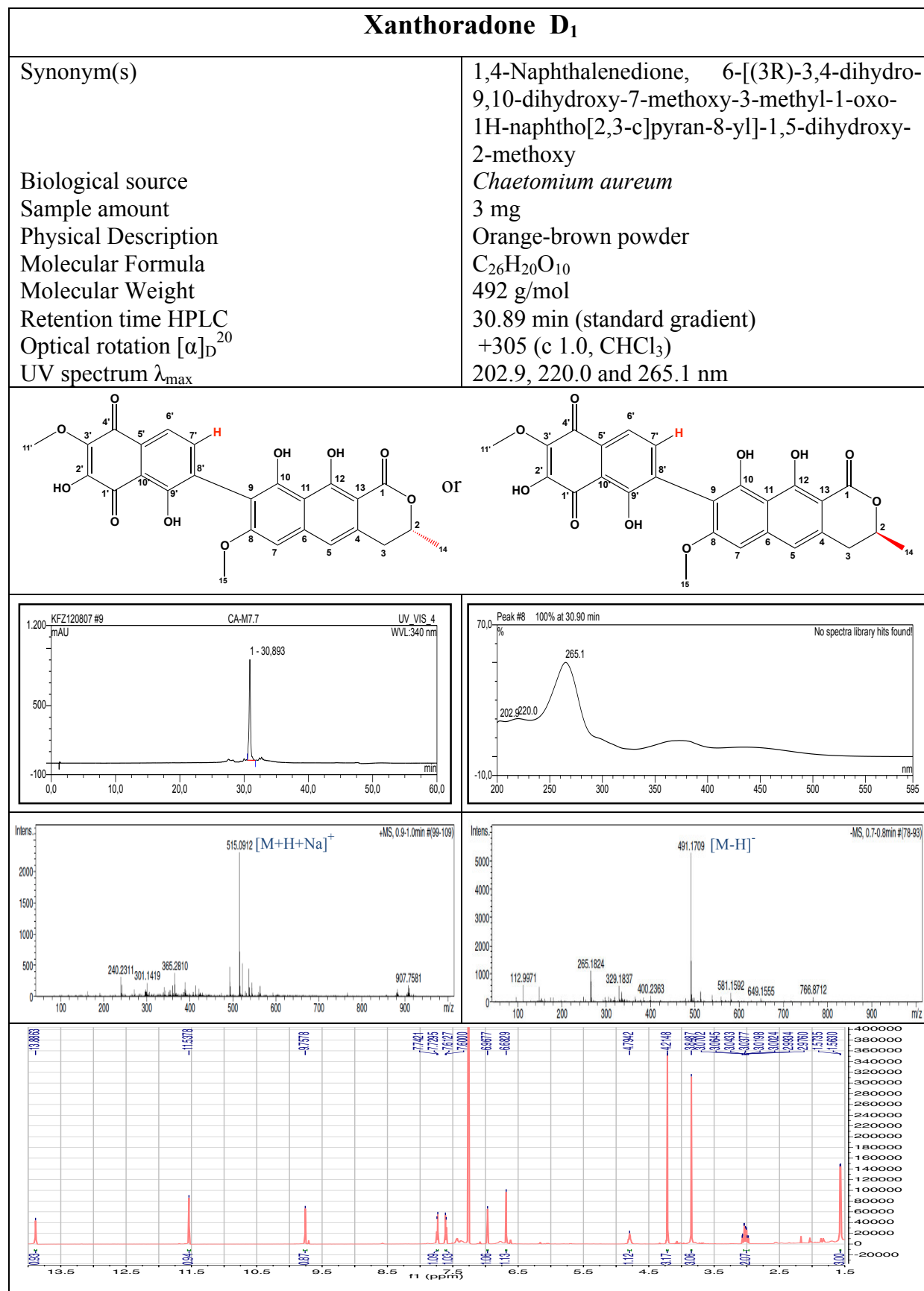


SB 236050 was previously reported from *Chaetomium funicola* (Payne *et al.*, 2002). From the best of our knowledge, the relative stereochemistry of SB 236050 was not previously reported in the literature. This is the first report of the stereochemistry of SB 236050 isolated from *Chaetomium aureum*.

**Table 4.17.** Comparison of  $^1\text{H}$  and  $^{13}\text{C}$  NMR chemical shifts of **13** with SB 236050 (Payne *et al.*, 2002)

N°	13 (DMSO)		SB 236050 (DMSO)	
	$\delta_{\text{H}}$	$\delta_{\text{C}}$	$\delta_{\text{H}}$	$\delta_{\text{C}}$
1	2.58 (1H, dd, $J= 10.92, 17.71$ Hz) 2.67 (1H, dd, $J= 3.76, 17.7$ Hz)	33.1	2.56 (1H, dd, $J= 12, 15$ Hz) 2.67 (1H, dd, $J= 4, 15$ Hz)	33.2
2	4.23 (1H, m)	61.7	4.21 (1H, m)	61.9
2-CH3	1.30 (3H, d, $J= 6.23$ )	20.3	1.28 (1H, d, $J= 6$ Hz)	20.5
3	-	-	-	-
4	5.36 (1H, s)	93.8	5.35 (1H, s)	99.0
4-OCH3	3.40 (3H, s)	54.9	3.37 (1H, s)	55.0
5	-	112.3	-	112.1
6	-	172.1	-	172.2
7	-	114.9	-	115.4
8	6.87 (1H, s)	119.1	6.84 (1H, s)	119.0
9	-	141.3	-	141.8
9-OH	9.47	-	-	-
10	-	151.8	-	152.4
10-OH	11.21	-	-	-
11	-	102.1	-	102.2
12	-	149.9	-	150.2
13	-	-	-	-
14	-	162.3	-	162.3
15	-	167.5	-	167.8
15-OH	12.84	-	-	-

<sup>a, b, c, d, f, x</sup> could be opposite

Compound isolated from the endophytic fungus *Chaetomium aureum*Xanthoradone D<sub>1</sub> (14, New)

**14** was isolated from *Chaetomium aureum* grown at room temperature for 30 days in Fernbach flasks on solid rice medium. The EtOAc extract was portioned between *n*-hexane and 90% MeOH. The MeOH fraction was chromatographed over a successive sephadex LH-20 column using CH<sub>2</sub>Cl<sub>2</sub>/MeOH (1:1) as eluent (repeated three times) then purified by semi-preparative HPLC (Merck, Hitachi L-7100) using a Eurosphere 100–10 C18 column (300 x 8mm, L x i.d.) with the following gradient (MeOH/H<sub>2</sub>O): 0 min, 10% MeOH; 5 min, 10% MeOH; 35 min, 100% MeOH; 45 min, 100 % MeOH, which afforded orange-brown powder (yield, 3 mg). It showed UV absorbance at  $\lambda_{\max}$  (MeOH) 202.9, 220.0 and 265.1 nm. Positive and negative HR-ESI-MS exhibited a prominent peak at *m/z* 515.09 [M+H+Na]<sup>+</sup> (base peak) and *m/z* 491.17 [M-H]<sup>-</sup> (base peak), respectively, indicating a molecular weight of 492 g/mol, which established a molecular formula of C<sub>26</sub>H<sub>20</sub>O<sub>10</sub>.

The <sup>1</sup>H NMR spectrum (Table 4.18) showed the presence of one olefinic methyl group, which appeared as one doublet at ( $\delta_{\text{H}}$  1.57 ppm), assigned to 2-CH<sub>3</sub>; two methoxy group, which appeared at ( $\delta_{\text{H}}$  3.84 and 4.21 ppm), assigned to 8-OCH<sub>3</sub> and 3'-OCH<sub>3</sub> respectively; one olefinic methine group at ( $\delta_{\text{H}}$  4.79 ppm), assigned to 2-CH, one olefinic methylene group, which appeared as two doublet of doublet, assigned to 3-CH<sub>2</sub> and four aromatic methine group, which appeared at ( $\delta_{\text{H}}$  6.68, 6.96, 7.72 and 7.74 ppm), assigned to 7'-CH, 6-CH, 7'-CH and 6'-CH and three hydroxyl group at ( $\delta_{\text{H}}$  9.75, 11.53 and 13.88 ppm), assigned to 10-OH, 9'-OH and 12-OH respectively.

The <sup>13</sup>C NMR spectrum (in CDCl<sub>3</sub>) showed 26 resolved signals, which were assigned to one methyl carbon, one methylene carbon, four sp<sup>2</sup> methine carbons, one oxygenated methine carbon, two oxygenated methyl carbons, eight sp<sup>2</sup> quaternary carbons, six oxygenated sp<sup>2</sup> quaternary carbons and three carbonyl carbons.

Analyses of <sup>1</sup>H-<sup>1</sup>H NMR COSY revealed the presence of two spin systems, as shown in Figure 4.21, the aromatic spin system composed of H-6' and H-7' and the second spin system from 2-CH<sub>3</sub> to 5-CH. Furthermore, <sup>13</sup>C-<sup>1</sup>H long range couplings of <sup>2</sup>*J* and <sup>3</sup>*J* observed in <sup>13</sup>C-<sup>1</sup>H heteronuclear multiple bond coherence (HMBC) spectrum gave the following linkages (Figure 4.22): (A) Cross peaks from H<sub>2</sub>-3 ( $\delta_{\text{H}}$  2.96 ppm) to C-14 ( $\delta_{\text{C}}$  20.4 ppm), C-2 ( $\delta_{\text{C}}$  76.2 ppm), C-13 ( $\delta_{\text{C}}$  99.4 ppm), C-5 ( $\delta_{\text{C}}$  115.7 ppm) and C-4 ( $\delta_{\text{C}}$  133.4); from H-5 ( $\delta_{\text{H}}$  6.95 ppm) to C-3 ( $\delta_{\text{C}}$  34.3 ppm), C-6 ( $\delta_{\text{C}}$  140.1 ppm), C-7 ( $\delta_{\text{C}}$  97.7 ppm), C-11 ( $\delta_{\text{C}}$  107.8 ppm), C-13 and

C-12 ( $\delta_C$  162.7 ppm); from H-7 ( $\delta_H$  6.66 ppm) to C-5, C-8 ( $\delta_C$  159.9 ppm), C-9 ( $\delta_C$  109.6 ppm), C-11; from H<sub>3</sub>-14 ( $\delta_H$  1.56 ppm) to C-2 and C-3; from H<sub>3</sub>-15 ( $\delta_H$  3.86 ppm) to C-8; from OH-10 ( $\delta_H$  9.74 ppm) to C-9, C-11 and C-10 ( $\delta_C$  155.0 ppm) and from OH-12 ( $\delta_H$  13.85 ppm) to C-11, C-12 and C-13. Furthermore, the chemical shift of C-2 ( $\delta_C$  76.2 ppm) indicated the presence of an oxygenated carbon and that the OH-12 ( $\delta_H$  13.85 ppm) is shifted to a lower field explains the presence of an ester bond between C-2 and C-13. This connection was confirmed by the chemical shift of C-1 ( $\delta_C$  171.3 ppm), which is typical for an ester group. Thus, these data indicated that **14** was found to have a dihydronaphthopyranone skeleton.

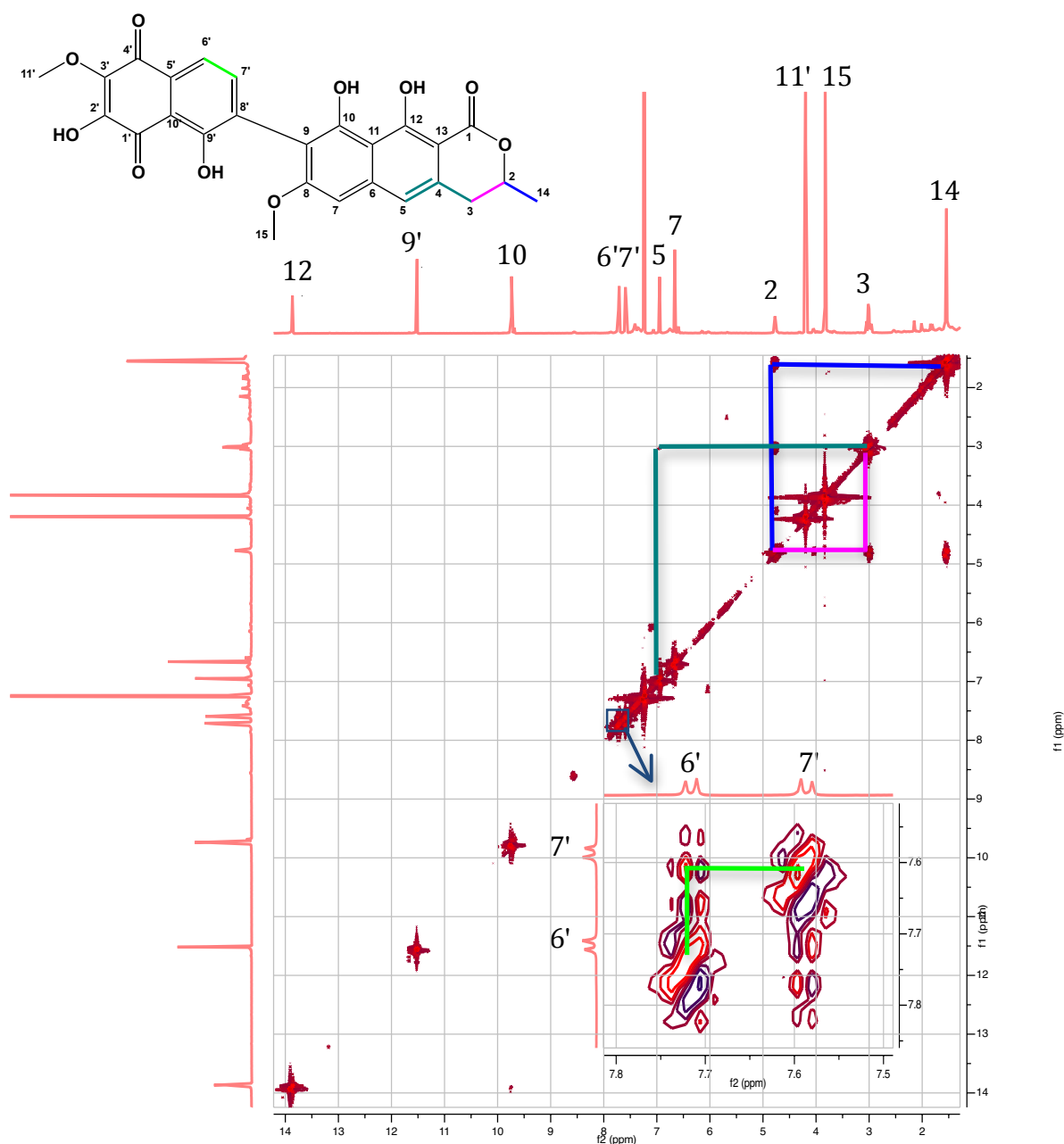
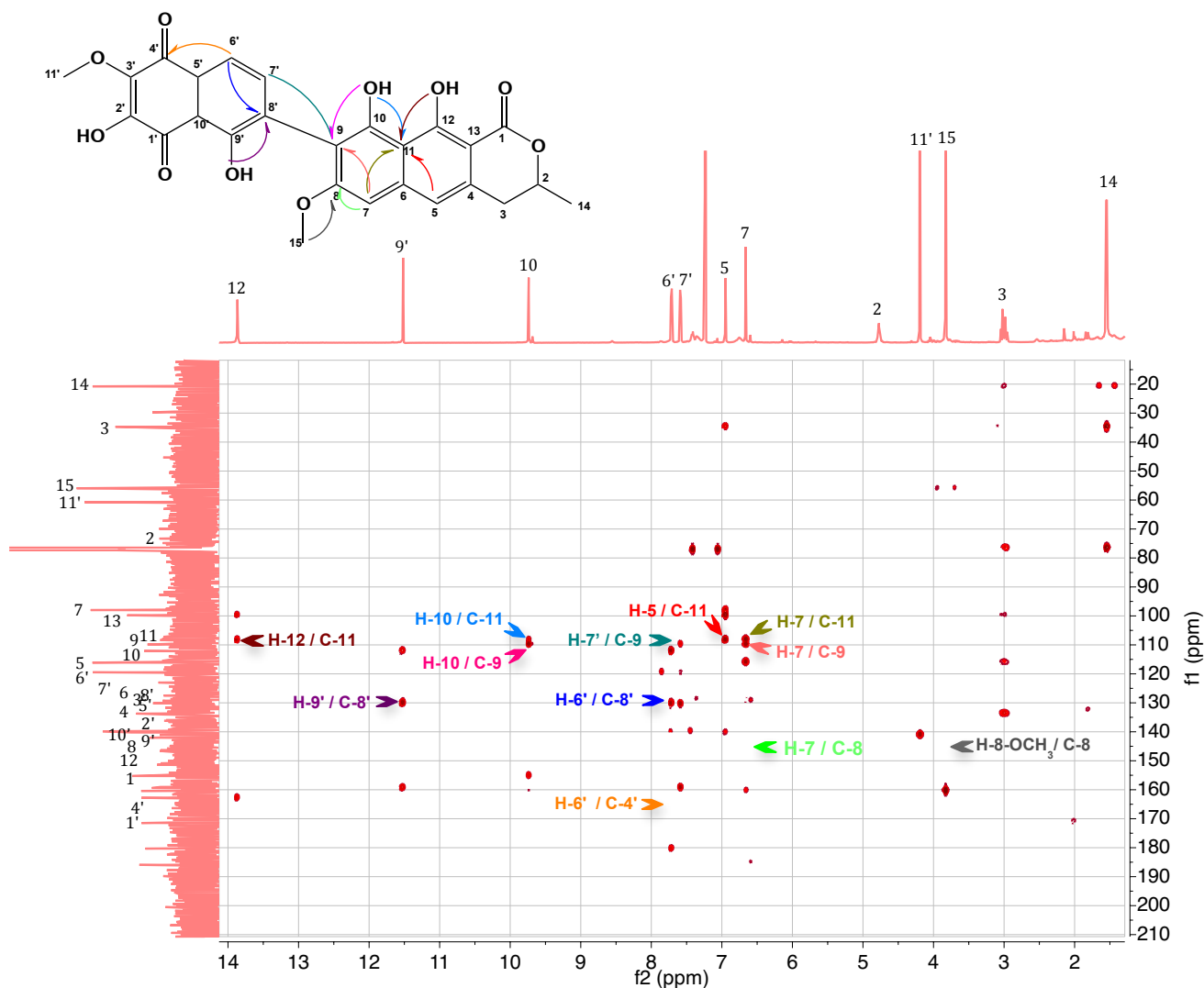


Figure 4.21. <sup>1</sup>H-<sup>1</sup>H NMR COSY



**Figure 4.22.** Selected  $^{13}\text{C}$ - $^1\text{H}$  HMBC correlations

(B) Cross peaks from H-6' ( $\delta_{\text{H}}$  7.71 ppm) to C-4' ( $\delta_{\text{C}}$  180.0 ppm), C-5' ( $\delta_{\text{C}}$  129.9 ppm), C-7' ( $\delta_{\text{C}}$  139.8 ppm) and C-10' ( $\delta_{\text{C}}$  111.8 ppm); from H-7' ( $\delta_{\text{H}}$  7.58 ppm) to C-6' ( $\delta_{\text{C}}$  119.4 ppm), C-8' ( $\delta_{\text{C}}$  130.6 ppm), C-9' ( $\delta_{\text{C}}$  158.9 ppm) and C-9; from OH-9' ( $\delta_{\text{H}}$  11.51 ppm) to C-8', C-9' and C-10'; from H<sub>3</sub>-11' ( $\delta_{\text{H}}$  4.19 ppm) to C-3' ( $\delta_{\text{C}}$  141.0 ppm). Therewith, the chemical shifts of C-1' ( $\delta_{\text{C}}$  185.0 ppm) and C-4' ( $\delta_{\text{C}}$  180.0 ppm) indicated the presence of two carbonyl carbons derived from quinone skeleton and the UV absorption at 165.1 nm confirmed the proposed structure. Thus, these data confirmed that **14** has another dihydronaphthoquinone skeleton.

The connection between the two dihydronaphthopyranone and dihydronaphthoquinone substructures was established by the presence of the correlation between H-7' and C-9,

between OH-10 and C-9 and between H-7' and C-8' confirming that they are connected at C-9-C-8'. The structure of **14** was elucidated as shown in Figure 3.20. The structure satisfied the degree of unsaturation and the molecular formula. Finally, **14** was identified as a new natural product for which the name xanthoradone D<sub>1</sub> was given.

Regarding the stereochemistry of xanthoradone D<sub>1</sub>, which has one chiral carbon center at C-2, the structure was suggested as shown as in Figure 4.23 by TDDFT ECD calculations of their solution conformers.

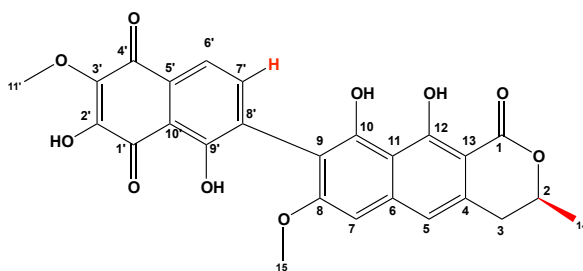


**Figure 4.23.** The structure of xanthoradone D<sub>1</sub>

The comparison of the <sup>1</sup>H NMR spectra of **14** and **xanthoradone A** (Yamazaki *et al.*, 2009) (Table 4.15) showed a close relationship between both compounds except for the presence of an additional methyl group at ( $\delta_{\text{H}}$  2.21 ppm) and the absence of a hydroxyl group in **xanthoradone A**.

Compound isolated from the endophytic fungus *Chaetomium aureum*

Xanthoradone D<sub>2</sub> (**15**, New) (Mixture with its atropisomers xanthoradone D<sub>1</sub>)

<b>Xanthoradone D<sub>2</sub></b>	
Synonym(s)  Biological source Sample amount Physical Description Molecular Formula Molecular Weight Retention time HPLC Optical rotation $[\alpha]_D^{20}$ UV spectrum $\lambda_{\max}$	1,4-Naphthalenedione, 6-[(3R)-3,4-dihydro-9,10-dihydroxy-7-methoxy-3-methyl-1-oxo-1H-naphtho[2,3-c]pyran-8-yl]-1,5-dihydroxy-2-methoxy <i>Chaetomium aureum</i> 5 mg Orange-brown powder C <sub>26</sub> H <sub>20</sub> O <sub>10</sub> 492 g/mol 30.89 min (standard gradient) +3 (c 1.0, CHCl <sub>3</sub> ) 202.9, 220.0 and 265.1 nm
<p>fatima093 #1584 RT: 44.24 AV: 1 NL: 5.39E7 F: + c ESI Full ms [100.00-1000.00]</p>	<p>fatima093 #1586 RT: 44.28 AV: 1 NL: 8.85E6 F: - c ESI Full ms [100.00-1000.00]</p>

**15** was isolated from *Chaetomium aureum* grown at room temperature for 30 days in Fernbach flasks on solid rice medium. The EtOAc extract was portioned between *n*-hexane and 90% MeOH. The MeOH fraction was chromatographed over a successive sephadex LH-20 column using CH<sub>2</sub>Cl<sub>2</sub>/MeOH (1:1) as eluent (repeated three times) then purified by semi-preparative HPLC (Merck, Hitachi L-7100) using a Eurosphere 100–10 C18 column (300 x 8mm, L x i.d.) with the following gradient (MeOH/H<sub>2</sub>O): 0 min, 10% MeOH; 5 min, 10% MeOH; 35 min, 100% MeOH; 45 min, 100 % MeOH, Compound **15** was obtained as a mixture with compound **14** forming an orange-brown powder (yield, 5 mg). It showed UV absorbance at  $\lambda_{\text{max}}$  (MeOH) 202.9, 220.0 and 265.1 nm. Positive and negative LC-ESI-MS of the mixture exhibited a prominent peak at  $m/z$  493.2 [M+H]<sup>+</sup> (base peak) and  $m/z$  491.3 [M-H]<sup>-</sup> (base peak), respectively, indicating a molecular weight of 492 g/mol, which established a molecular formula of C<sub>26</sub>H<sub>20</sub>O<sub>10</sub> identical to that of **14**.

In <sup>1</sup>H NMR spectrum (Table 4.18) showed the same protons signals as xanthoradone D<sub>1</sub>, which are almost overlapped protons with proportion of (1:3). In Figure 4.24, the proton at ( $\delta_{\text{H}}$  7.57 ppm) assigned to H-6' of one of the isomers is very close to the proton at ( $\delta_{\text{H}}$  7.58 ppm) assigned to H-6' of the other one.

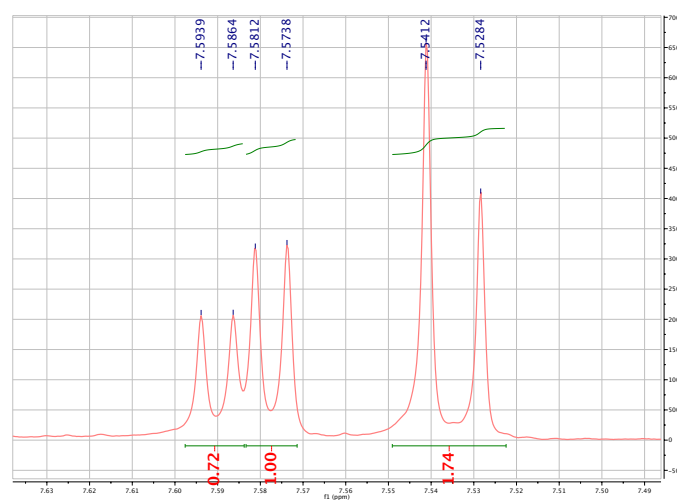


**Figure 4.24.** <sup>1</sup>H NMR of the overlapped proton H-6' and H-7'

Hence, **15** was identified as an stereoisomer of **14** for which the name xanthoradone D<sub>2</sub> is proposed. Even though a mixture was used, we were able to successfully determine the absolute configuration of both compounds with the help of the TDDFT ECD calculations.



Compound isolated from the endophytic fungus *Chaetomium aureum*Xanthoradone E<sub>1</sub> and xanthoradone E<sub>2</sub> (**16/17**, New)

<b>Xanthoradone E<sub>1</sub> / Xanthoradone E<sub>2</sub></b>	
Synonym(s)  Biological source Sample amount Physical Description Molecular Formula Molecular Weight Retention time HPLC Optical rotation $[\alpha]_D^{20}$ UV spectrum $\lambda_{\max}$	1,4-Naphthalenedione, 6-[(3R)-3,4-dihydro-9,10-dihydroxy-7-methoxy-3-methyl-1-oxo-1H-naphtho[2,3-c]pyran-8-yl]-5-hydroxy-2-methoxy <i>Chaetomium aureum</i> 6 mg Orange-brown powder C <sub>26</sub> H <sub>20</sub> O <sub>9</sub> 476 g/mol 32.92 min (standard gradient) +1 (c 1.0, CHCl <sub>3</sub> ) 220.1, 264.8 and 377.7 nm
No ionisation at the Positive mode	

**16** was isolated from *Chaetomium aureum* grown at room temperature for 30 days in Fernbach flasks on solid rice medium. The EtOAc extract was portioned between *n*-hexane and 90% MeOH. The MeOH fraction was chromatographed over a successive Sephadex LH-20 column using CH<sub>2</sub>Cl<sub>2</sub>/MeOH (1:1) as eluent (repeated three times), then purified by semi-preparative HPLC (Merck, Hitachi L-7100) using a Eurosphere 100–10 C18 column (300 x 8mm, L x i.d.) with the following gradient (MeOH/H<sub>2</sub>O): 0 min, 10% MeOH; 5 min, 10% MeOH; 35 min, 100% MeOH; 45 min, 100 % MeOH, Compound **16** was obtained as a mixture with compound **16** forming an orange-brown powder (yield, 6 mg). It showed UV absorbance at  $\lambda_{\text{max}}$  (MeOH) 220.1, 264.8 and 377.7 nm. Negative ESI-MS of **16/17** exhibited a prominent peak at *m/z* 475.3 [M-H]<sup>-</sup> (base peak), indicating a molecular weight of 476 g/mol, which established a molecular formula of C<sub>26</sub>H<sub>20</sub>O<sub>9</sub> with a 16 mass unit decrease compared to **14/15**. The absence of one hydroxyl group was supposed.

In <sup>1</sup>H NMR spectrum (Table 4.18) showed the presence of 20 protons signals, which are almost overlapped with the proportional of (1:1). The proton signals are identical to those of **14/15** (Table 4.15), except the presence of one more aromatic proton at ( $\delta_{\text{H}}$  6.11 ppm) and the absence of one hydroxygroup at ( $\delta_{\text{H}}$  10.89 ppm).

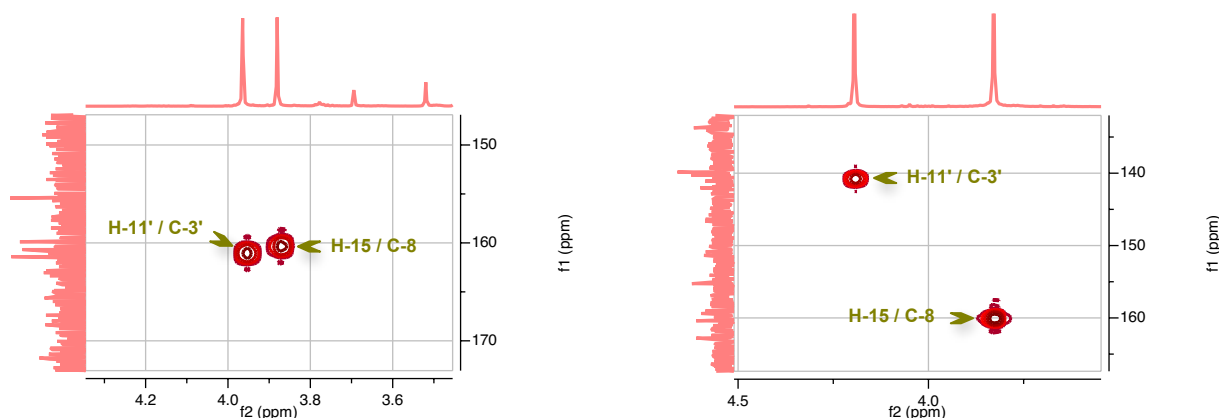


**Figure 4.25.** The comparison of H-C-3' of **14/15** and **16/17** in <sup>13</sup>C-<sup>1</sup>H HMBC NMR

The <sup>13</sup>C NMR spectrum (in CDCl<sub>3</sub>) showed 26 resolved signals, which are almost identical to those of **14/15**, except the chemical shift of 3 carbons, C-1' that in **14/15** was at ( $\delta_{\text{C}}$  186.0 ppm) and in **16/17** C-1' moved to ( $\delta_{\text{C}}$  190.7 ppm), C-2' that was upfield at ( $\delta_{\text{C}}$  159.0 ppm) in **14/15** compared to **16/17** ( $\delta_{\text{C}}$  110.1 ppm) and C-3' that was downfield ( $\delta_{\text{C}}$  141.0 ppm) in

**14/15** compared to **16/17** ( $\delta_C$  161.3 ppm). These data confirm that the hydroxyl group in the position 2' of **14/15** is absent in the mixture of compounds **16/17**.

The  $^1\text{H}$ - $^1\text{H}$  NMR COSY of **16/17** spectra showed the same correlations as **14/15**. Furthermore,  $^{13}\text{C}$ - $^1\text{H}$  long range couplings of  $^2J$  and  $^3J$  observed in  $^{13}\text{C}$ - $^1\text{H}$  heteronuclear multiple bond coherence (HMBC) spectrum of **16/17** gave the same linkages as **14/15** except of the presence of one more cross peaks from H-2' ( $\delta_H$  6.11 ppm) to C-1' ( $\delta_C$  190.7 ppm), C-3' ( $\delta_C$  161.3 ppm), C-4' ( $\delta_C$  179.4 ppm) and C-10' ( $\delta_C$  114.2 ppm) as shown in Figure 3.23.

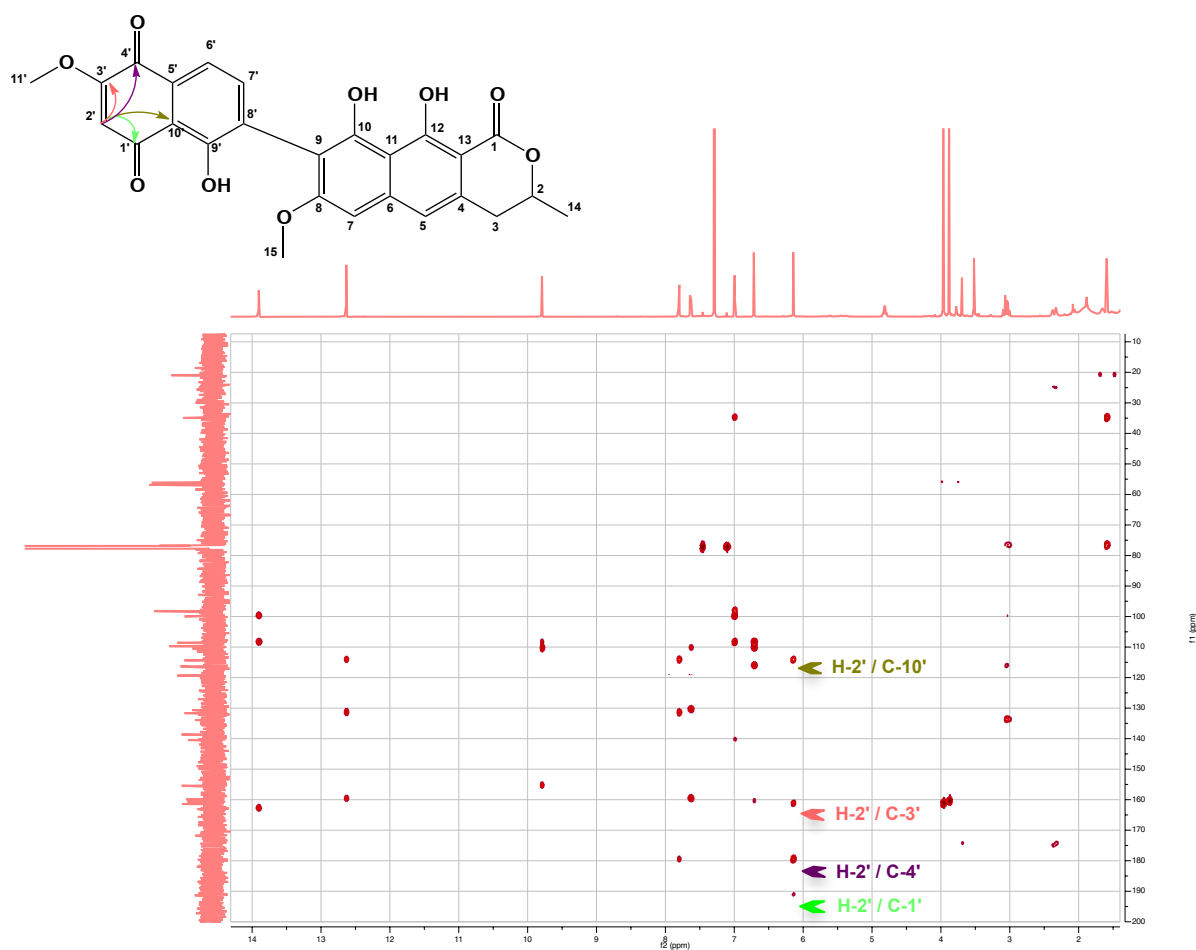


**Figure 4.26.** Selected  $^{13}\text{C}$ - $^1\text{H}$  HMBC NMR correlations of **16/17**

Hence, **16/17** was identified as mixture of two xanthoradones derivative for which the name xanthoradone E<sub>1</sub> and E<sub>2</sub> are proposed.

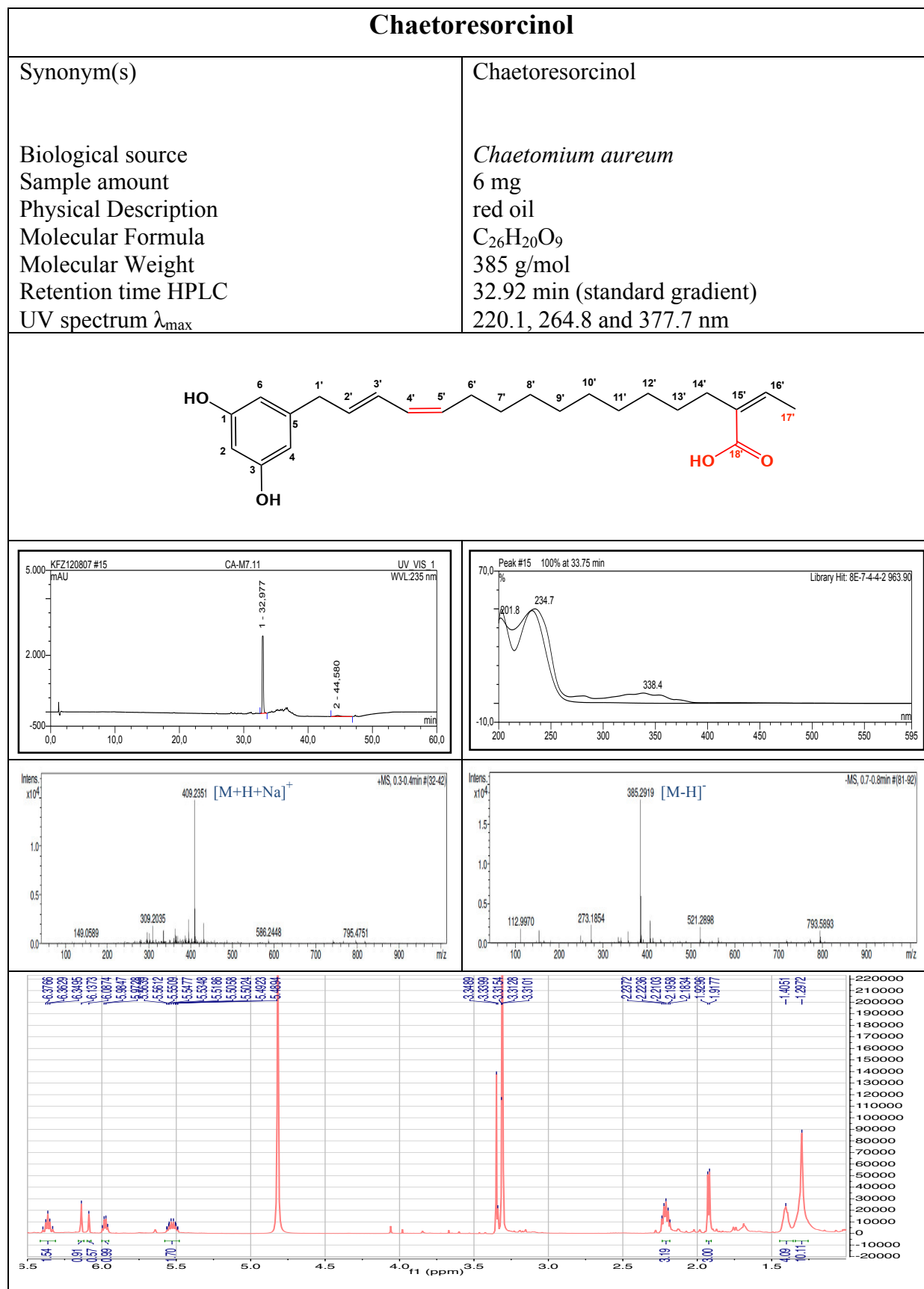
The stereochemistry of xanthoradones E<sub>1</sub> and E<sub>2</sub>, which has one chiral carbon center at C-2, was determined by TDDFT ECD calculations of their solution conformers.

**Table 4.18.**  $^1\text{H}$  and  $^{13}\text{C}$  NMR chemical shifts of xanthoradones A, D and E  
(Yamazaki et al., 2009)

Position	Xanthoradone A (in $\text{CDCl}_3$ )		Xanthoradone E (in $\text{CDCl}_3$ )		Xanthoradone D (in $\text{CDCl}_3$ )	
	$\delta_{\text{C}}$	$\delta_{\text{H}}$	$\delta_{\text{C}}$	$\delta_{\text{H}}$	$\delta_{\text{C}}$	$\delta_{\text{H}}$
1	171.5	-	171.5	-	171.3	-
2	76.8	4.79 m	76.5	4.79 m	76.7	4.77 m
3	34.7	ax: 3.00 dd ( $J=17.0, 10.0$ Hz) eq: 3.06 dd ( $J=17.0, 4.0$ Hz)	34.7	ax: 2.99 dd ( $J=16.2, 10.4$ Hz) eq: 3.05 dd ( $J=16.1, 3.4$ Hz)	34.8	ax: 2.99 dd ( $J=15.8, 10.4$ ) eq: 3.05 dd ( $J=16.1, 3.4$ )
4	133.5	-	133.4	-	133.8	-
5	116.1	6.99 s	116.1	6.96 s	116.0	6.96 s
6	140.0	-	141.7	-	140.2	-
7	98.1	6.71 s	98.1	6.68 s	98.1	6.68 s
8	160.3	-	160.6	-	160.3	-
9	109.0	-	109.6	-	109.6	-
10	154.7	-	155.3	-	155.2	-
10-OH		9.73 s		9.76 s		9.75 s
11	108.4	-	108.1	-	108.0	-
12	162.7	-	162.4	-	162.7	-
12-OH		13.9 s		13.87 s		13.88 s
13	99.7	-	99.8	-	99.4	-
14	20.7	1.57 d ( $J=7.0$ Hz)	20.8	1.57 d ( $J=3.1$ Hz)	20.1	1.56 d ( $J=6.3$ )
15	56.0	3.84 s	56.0	3.85 s	55.4	3.84 s
1'	190.6	-	190.7	-	<b>186.0</b>	-
2'	109.6	6.08 s	110.1	6.11 s	<b>159.0</b>	-
2'-OH		-		-		-
3'	160.9	-	161.3	-	<b>141.0</b>	-
4'	179.8	-	179.4	-	180.2	-
5'	129.8	-	130.4	-	129.9	-
6'	121.3	7.67 s	<b>119.1</b>	<b>7.77 d (<math>J=7.7</math> Hz)</b>	119.4	7.73 d ( $J=7.5$ Hz)
7'	147.2	-	<b>138.3</b>	<b>7.60 d (<math>J=7.6</math> Hz)</b>	139.7	7.6 d ( $J=7.6$ Hz)
8'	130.6	-	131.5	-	130.4	-
9'	159.7	-	159.5	-	159.3	-
9'-OH		12.5 s		12.6 s		11.5 s
10'	112.0	-	114.2	-	111.9	-
11'	56.6	3.92 s	56.7	3.93 s	60.8	4.2 s
12'	20.5	2.21 s	-	-	-	-

**Table 4.19.**  $^1\text{H}$  chemical shifts of the atropisomers of xanthoradone D and E

Position	Xanthoradone E (in $\text{CDCl}_3$ )		Xanthoradone D (in DMSO)	
	$\delta_{\text{H}}$ of D-1	$\delta_{\text{H}}$ of D-2	$\delta_{\text{H}}$ of E-1	$\delta_{\text{H}}$ of E-2
1	-	-	-	-
2	4.78 m	4.79 m	4.86 m	4.86 m
3	ax: 2.99 dd ( $J= 16.2, 10.4$ Hz) eq: 3.04 dd ( $J= 16.0, 3.3$ Hz)	ax: 2.99 dd ( $J= 16.2, 10.4$ Hz) eq: 3.05 dd ( $J= 16.1, 3.4$ Hz)	ax: 3.00 dd ( $J= 15.1, 10.9$ Hz) eq: 3.14 dd ( $J= 15.7, 2.7$ Hz)	ax: 2.99 dd ( $J= 15.8, 11.6$ ) eq: 3.14 dd ( $J= 15.7, 2.7$ )
4	-	-	-	-
5	6.96 s	6.96 s	7.15 s	7.15 s
6	-	-	-	-
7	6.68 s	6.68 s	6.95 s	6.95 s
8	-	-	-	-
9	-	-	-	-
10	-	-	-	-
10-OH	9.76 s	9.76 s	9.63 br	9.63 br
11	-	-	-	-
12	-	-	-	-
12-OH	13.86 s	13.87 s	13.69 br	13.69 br
13	-	-	-	-
14	1.56 d ( $J=3.0$ Hz)	1.57 d ( $J= 3.1$ Hz)	1.45 d ( $J= 6.2$ )	1.45 d ( $J=6.2$ )
15	3.85 s	3.85 s	3.79 s	3.79 s
1'	-	-	-	-
2'	6.11 s	6.11 s	-	-
2'-OH	-	-	10.89 br	10.89 br
3'	-	-	-	-
4'	-	-	-	-
5'	-	-	-	-
6'	7.77 d ( $J= 7.6$ Hz)	7.77 d ( $J= 7.7$ Hz)	7.58 d ( $J= 7.6$ Hz)	7.57 d ( $J= 7.5$ Hz)
7'	7.60 d ( $J= 7.6$ Hz)	7.60 d ( $J= 7.6$ Hz)	7.53 d ( $J= 7.6$ Hz)	7.53 d ( $J= 7.6$ Hz)
8'	-	-	-	-
9'	-	-	-	-
9'-OH	12.60 s	12.60 s	11.85 s	11.85 s
10'	-	-	-	-
11'	3.93 s	3.93 s	3.92 s	3.92 s

Compound isolated from the endophytic fungus *Chaetomium aureum*Chaetoresorcinol (**18**, New)

**18** was isolated from *Chaetomium aureum* grown at room temperature for 30 days in Fernbach flasks on solid rice medium. The EtOAc extract was portioned between *n*-hexane and 90% MeOH. The MeOH fraction was chromatographed over a successive sephadex LH-20 column using CH<sub>2</sub>Cl<sub>2</sub>/MeOH (1:1) as eluent (repeated three times), then purified by semi-preparative HPLC (Merck, Hitachi L-7100) using a Eurosphere 100–10 C18 column (300 x 8mm, L x i.d.) with the following gradient (MeOH/H<sub>2</sub>O): 0 min, 10% MeOH; 5 min, 10% MeOH; 35 min, 100% MeOH; 45 min, 100 % MeOH. Compound **18** was obtained as a red oil and showed three UV maxima at 201, 234 and 338 nm. ESIMS exhibited strong pseudomolecular base peak at *m/z* 385.3 [M-H]<sup>-</sup> in the negative mode, indicating a molecular weight of 386 g/mol. The chemical formula of **18** was deduced as C<sub>24</sub>H<sub>33</sub>O<sub>4</sub> from the prominent peak appearing at *m/z* 409.2351 [M+Na]<sup>+</sup> in the HRESIMS (calcd for C<sub>24</sub>H<sub>34</sub>O<sub>4</sub>Na 409.2355).

<sup>13</sup>C and DEPT experiments (Table 4.20) exhibited 24 carbon atoms attributable to one olefinic methyl group, ten methylenes, eight olefinic methines, four quaternary carbons, and one carbonyl carbon.

Analysis of 2D NMR data indicated that **18** is a resorcinol derivative containing a side chain of 18 carbons.

<sup>1</sup>H-<sup>1</sup>H COSY confirmed the presence of three spin systems assigned for CH<sub>3</sub>(17')H(16'), a continuous spin system CH<sub>2</sub>(1')→CH<sub>2</sub>(14') and the resorcinol ring system H(2)H(4)H(6), whereas the connection of these spin systems was established by inspection of <sup>2</sup>J and <sup>3</sup>J HMBC correlations (Figure 4.27).

CH<sub>2</sub>-14' showed a <sup>2</sup>J correlation to the olefinic quaternary carbon C-15' ( $\delta_C$  135.2 ppm) and <sup>3</sup>J correlations to C-16' and C-18', appearing at  $\delta_C$  136.5 and 172.0 ppm, respectively (Figure 4.28). A strong <sup>3</sup>J correlation was also detected for the olefinic proton H-16' to C-14' ( $\delta_C$  35.9 ppm), the latter correlating also with the methyl group CH<sub>3</sub>-17' via a <sup>4</sup>J correlation. On the other hand, the aliphatic methylene protons CH<sub>2</sub>-1' correlated to two overlapping aromatic carbons, which were attributed to C-4 and C-6 ( $\delta_C$  108.0 ppm), as well as to an isolated aromatic carbon assigned to C-5 ( $\delta_C$  144.1 ppm), thus, establishing the connection between the identified spin systems.

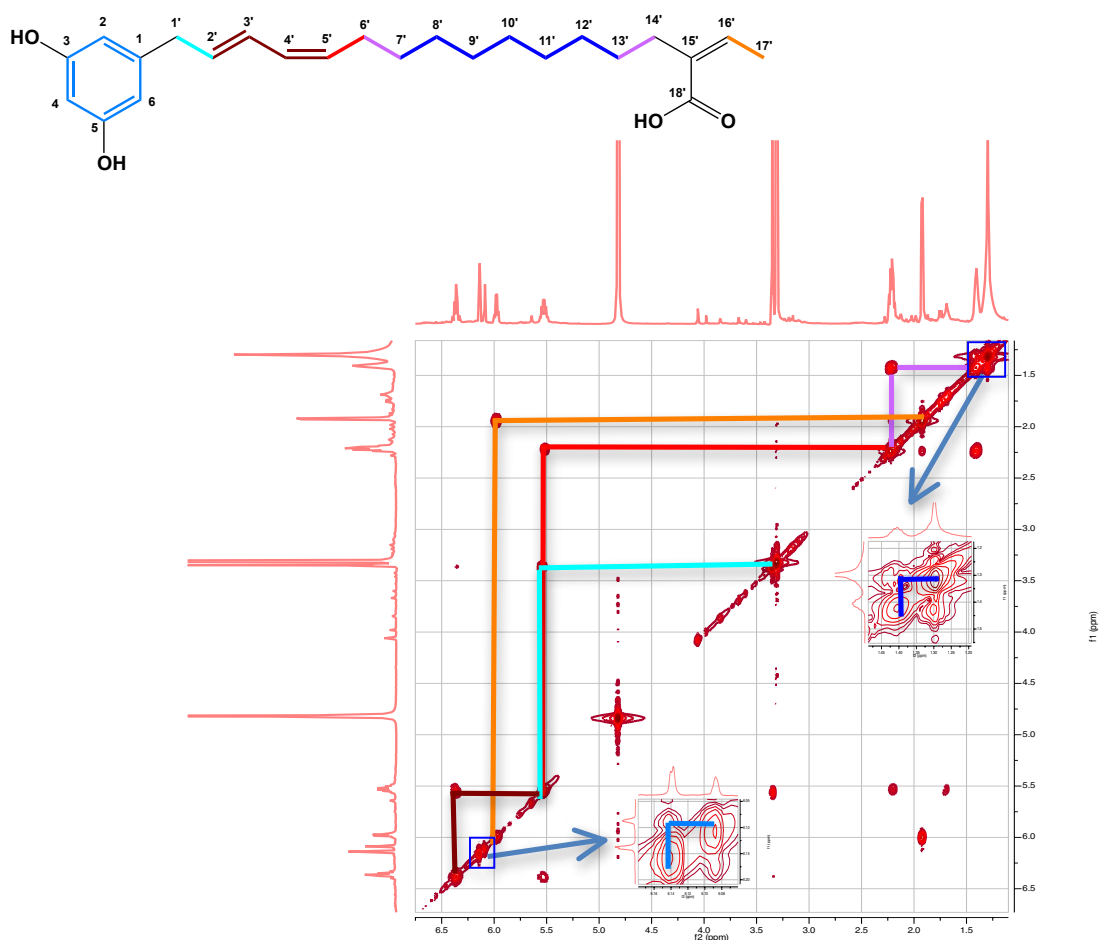


**Figure 4.27.**  $^1\text{H}$  -  $^1\text{H}$  COSY NMR correlations of **18**

The configuration of the double bonds at C-2', C-4' and C-15' of the side chain was obtained by comparison of the observed chemical shifts of the respective carbons with  $^{13}\text{C}$  NMR data of 5-heptadeca-8'Z,11'Z-dienylresorcinol (Barrow *et al.*, 1991; Jin and Zjawiony, 2006), 5-heptadeca-8'Z,11'Z,16-trienylresorcinol and 5-heptadeca-9'E,11'Z,16-trienylresorcinol (Jin and Zjawiony, 2006). For instance,  $\Delta^{2',3'}$  and  $\Delta^{15',16'}$  were assigned to have *E*-configuration since the neighboring carbons C-1' and C-14' resonated at about  $\delta_{\text{C}}$  35 ppm, whereas the allylic carbon of C-5' (C-6') appeared upfield ( $\delta_{\text{C}}$  28.6 ppm) in comparison to C-1' and C-14' and hence indicated a *Z*-configuration for the double bond  $\Delta^{4',5'}$ . This is in agreement with other known congeners (Suzuki *et al.*, 1996) where the allylic carbon of an *E*-configured double bond resonates more downfield than that of a *Z*-configured one. The configuration of the  $\Delta^{15',16'}$  double bond was further confirmed by a ROESY experiment, where the olefinic proton H-16' showed a strong correlation with CH<sub>2</sub>-14' (Figure 4.29). Accordingly, **18** was identified as a new natural product for which the name chaetorcinol is proposed.



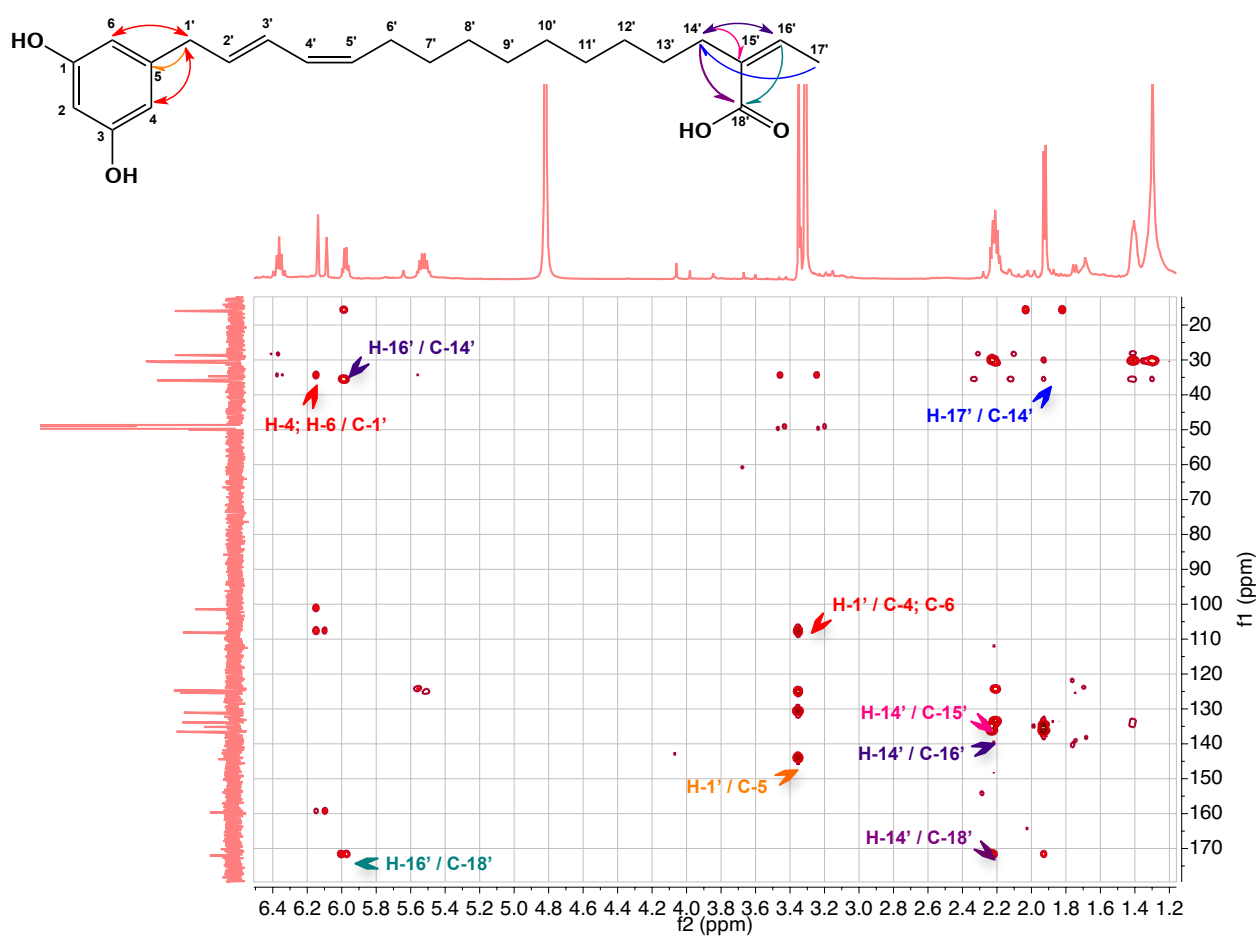


Figure 4.28. Selected  $^{13}\text{C}$ - $^1\text{H}$  HMBC NMR correlations of **18**

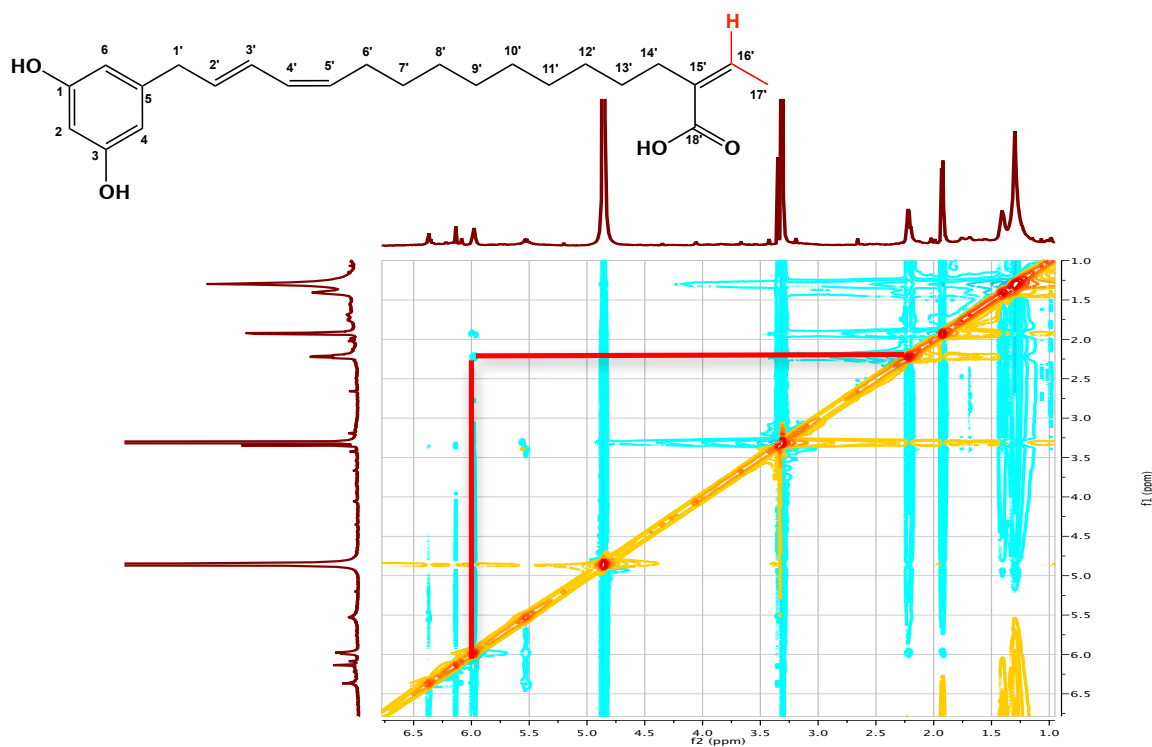


Figure 4.29. Selected  $^1\text{H}$ - $^1\text{H}$  ROESY NMR correlations of **18**

**Table 4.20.**  $^1\text{H}$  and  $^{13}\text{C}$  NMR data of 18 in MeOH at 600 MHz for  $^1\text{H}$  and 150 for  $^{13}\text{C}$ .

Position	18	
	$\delta_{\text{C}}$	$\delta_{\text{H}}$
1	159.7	-
2	101.1	6.08 (1H, s)
3	161.7	-
4	108.0	6.13 <sup>b</sup> (1H, s)
5	144.1	-
6	108.0	6.14 <sup>b</sup> (1H, s)
1'	34.7	3.35 <sup>c</sup> (1H, br)
2'	131.05	5.54 (1H, m)
3'	125.3	6.35 (1H, m)
4'	124.7	6.38 (1H, m)
5'	133.8	5.52 (1H, m)
6'	28.6	2.20 (2H, m)
7'	30.34 <sup>a</sup>	1.44 (2H, m)
8'	30.38 <sup>a</sup>	1.33 (2H, m)
9'	30.44 <sup>a</sup>	1.33 (2H, m)
10'	30.63 <sup>a</sup>	1.33 (2H, m)
11'	30.69 <sup>a</sup>	1.25 (2H, m)
12'	30.76 <sup>a</sup>	1.25 (2H, m)
13'	30.86	1.37 (2H, m)
14'	35.9	2.22 (2H, m)
15'	135.2	-
16'	136.5	5.97 (q, $J=7.1$ Hz)
17'	15.9	1.92 (d, $J=7.1$ Hz)
18'	172.0	-

<sup>a,b</sup> may be exchangeable<sup>c</sup> overlapped with solvent peak

#### 4.5. Bioactivity test results for compounds isolated from the endophytic fungus *Chaetomium aureum*

The isolated compounds were subjected to cytotoxicity (Table 4.21), protein kinase bioassays (Table 4.22) and Hsp 90 chaperone inhibition assays (Figure 4.30). The new compounds were also subjected to antibacterial tests (Table 4.23).

**Table 4.21.** Cytotoxicity test results for the compounds isolated from endophytic fungus *Chaetomium aureum*

Nr.	Compounds tested	L5178Y growth in %* (Conc. 10 µg/mL)
-	Control	0
13	SB 236050	87
14	Xanthoradone D <sub>1</sub>	-3.5
14/15	Xanthoradone D <sub>1</sub> + Xanthoradone D <sub>2</sub>	- 3.5
16/17	Xanthoradone E <sub>1</sub> + Xanthoradone E <sub>2</sub>	1.6

\*Data provided by Prof. W. E. G. Müller, Mainz

Only SB 236050 showed moderate activity against L5178Y cell line, whereas no activity was detected for the other compounds.

**Table 4.22.** Protein kinase assay results for the compounds isolated from endophytic fungus *Chaetomium aueum*

Compound tested (Conc. 1 µg/mL)	Activity on various protein kinases based on IC <sub>50</sub> [g/mL]*															
	AKT1	ALK	ARK 5	Aurora-B	AXL	FAK	IGF 1-R	MEK 1 wt	MET wt	NEK 2	NEK 6	PIM 1	PLK 1	PRK 1	SRC	VEGF-R2
(+)-Sclerotiorin	A	A	M	S	M	A	A	0	S	A	A	A	M	M	A	A
(+)-Isochromophilone IV	0	0	0	M	0	M	M	0	0	0	0	M	0	0	M	0
(+)-Sclerotioramin	0	M	0	M	0	M	A	0	0	0	0	0	0	0	A	A
SB 236050	0	0	0	S	0	M	M	0	0	M	0	M	M	0	0	M
Chaetoresorcinol	0	A	0	A	M	A	S	0	M	A	M	0	0	0	A	A

\* Data provided by ProQinase, Freiburg.

S: strongly active, A: active, M: moderately active, 0: not active

The results of the protein kinase assay showed a different activity profile than the cytotoxicity assay results. (+)-Sclerotiorin was active against most of protein kinases in spite of their low activity in the cytotoxicity assay, whereas its derivatives, isochromophilone VI and sclerotioramin inhibited only few of the tested enzymes. On the other hand, the new compounds, chaetoresorcinol and SB 236050, were also active against the tested protein kinases.

**Table 4.23.** Antibacterial test results for the new compounds isolated from endophytic fungus *Chaetomium aureum*

Nr.	Name	The Minimum Inhibitory Concentration													
		<i>MRSA</i> [ $\mu\text{g/ml}$ ]	<i>Strep. Pneumonia</i>	<i>Entero. Faecalis</i>	<i>Staph. Epidermidis</i>	<i>Entero. cloace</i>	<i>E. Coli</i>	<i>Klep. Pneumonia</i>	<i>Pseudo. aeruginosa</i>	<i>Acin. Baumannii</i>	<i>Entero-bacter</i>	<i>C. albicans</i>	<i>C. krusei</i>	<i>Asp. Faecalis</i>	<i>Asp. Fumigatus</i>
13	SB 236050	n.a	n.a	n.a	n.a	n.a	n.a	n.a	n.a	n.a	n.a	n.a	n.a	n.a	n.a
14	Xanthoradone D <sub>1</sub>	n.a	n.a	n.a	n.a	n.a	n.a	n.a	n.a	n.a	n.a	n.a	n.a	n.a	n.a
14/15	Xanthoradone D <sub>1</sub> + Xanthoradone D <sub>2</sub>	n.a	n.a	n.a	n.a	n.a	n.a	n.a	n.a	n.a	n.a	n.a	n.a	n.a	n.a
16/17	Xanthoradone E <sub>1</sub> + Xanthoradone E <sub>2</sub>	n.a	n.a	n.a	n.a	n.a	n.a	n.a	n.a	n.a	n.a	n.a	n.a	n.a	n.a
18	Chaetoresorcinol	n.a	n.a	n.a	n.a	n.a	n.a	n.a	n.a	n.a	n.a	n.a	n.a	n.a	7.81

\* Data provided by Mr. Pretsch, Vienna.

Chaetoresorcinol was moderately active against only *Asp. Fumigatus*, whereas the other compounds were not active.

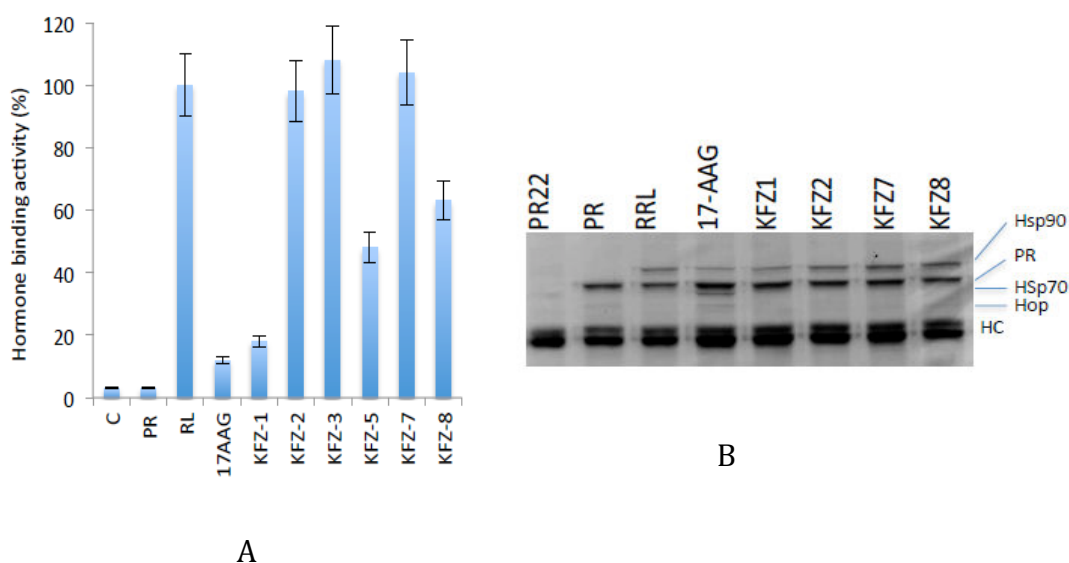
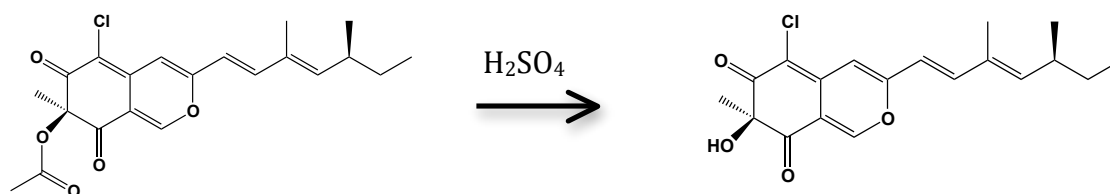


**Figure 4.30.** Effect of 1-6 on the Hsp90 chaperoning machine *in vitro*. A- PR hormone binding activity was reconstituted using rabbit reticulocyte lysate without (RL) or with metabolites KFZ-1: (+)-Sclerotiorin, KFZ-2: (+)-Isochromophilone VI, KFZ-3: SB 236050, KFZ-5: Chaetoresorcinol, KFZ-7: Sclerotioramin and KFZ-8: Isochromophilone VII. 17-AAG is used as a positive control. B- Samples from (A) were used for analysis of protein complexes by SDS-PAGE and Coomassie blue staining. PR22 indicates the PR antibody incubated with RRL. PR indicates the PR alone with no RRL.

As shown in (Figure 4.30), sclerotiorin efficiently inhibits the recovery of PR hormone binding activity using RRL. Sclerotiorin showed similar efficiency to that of 17-AAG, the classical inhibitor of Hsp90, whereas the other compounds showed much less activity than sclerotiorin.

Cytotoxicity test showed that sclerotiorin is not toxic to breast cancer cell line Hs578T, MCF7, MDA-MB-231, MDA-MB-453, Prostate cancer cell line LNCaP and cervical cancer cell line HeLa.

In an attempt to increase the cytotoxicity of sclerotiorin, a deacetylation was carried out.



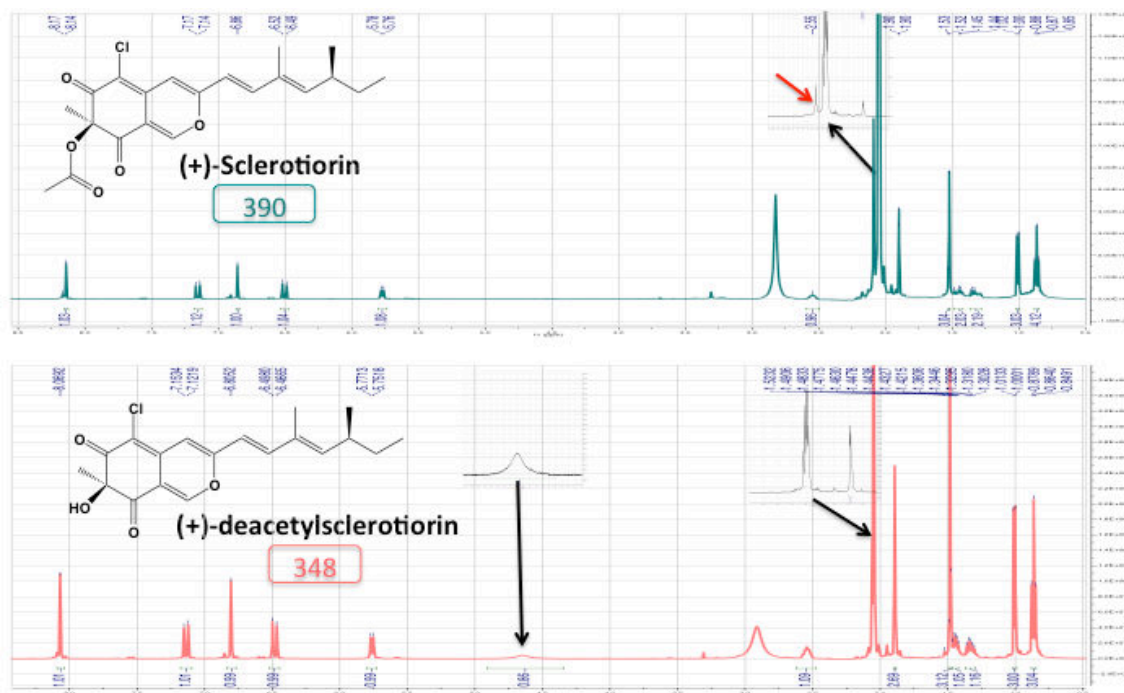


**Figure 4.31.** Comparison of  $^1\text{H}$  NMR and the molecular weight of sclerotiorin and deacetylsclerotiorin

The  $^1\text{H}$  NMR (DMSO) of deacetylsclerotiorin showed the absence of the methyl group at ( $\delta_{\text{H}}$  2.11 ppm) and the presence of a broad proton signal at ( $\delta_{\text{H}}$  4.6 ppm) assigned to the hydroxyl group, which replaced the acetyl group.

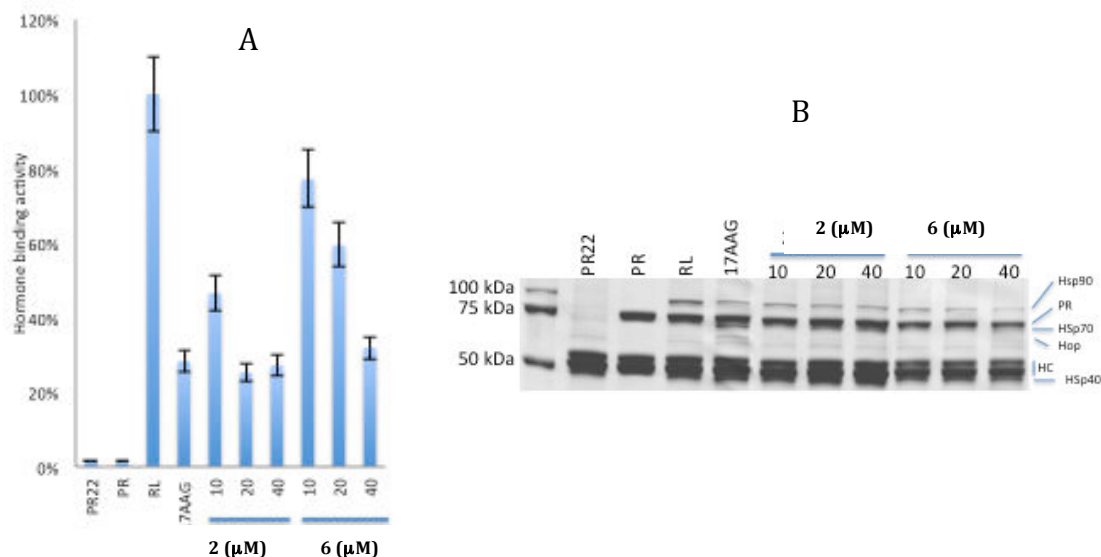


**Figure 4.32.** Comparison of sclerotiorin (2) and deacetylsclerotiorin (6). A- effect increasing concentration of sclerotiorin (2) and deacetylsclerotiorin (6) on PR hormone binding activity. B- Effect of sclerotiorin (2) and deacetylsclerotiorin (6) on PR protein complexes. Molecular chaperones are indicated on the right. HC represents the heavy chains of the PR antibody PR22.

The deacetylated sclerotiorin (**6**) is relatively less efficient in inhibiting the Hsp90 *in vitro*. The mechanism by which sclerotiorin and deacetylsclerotiorin inactivate the Hsp90 machine is not clear but it seems to be different from that of the 17-AAG.

As compared to 17-AAG, protein complexes analysis showed that sclerotiorin and deacetylsclerotiorin lower the level of Hsp90 without increase of Hop (Figure 4.32.B). Furthermore, deacetylsclerotiorin does not increase Hsp70 level in PR complexes (Figure 4.32.B).

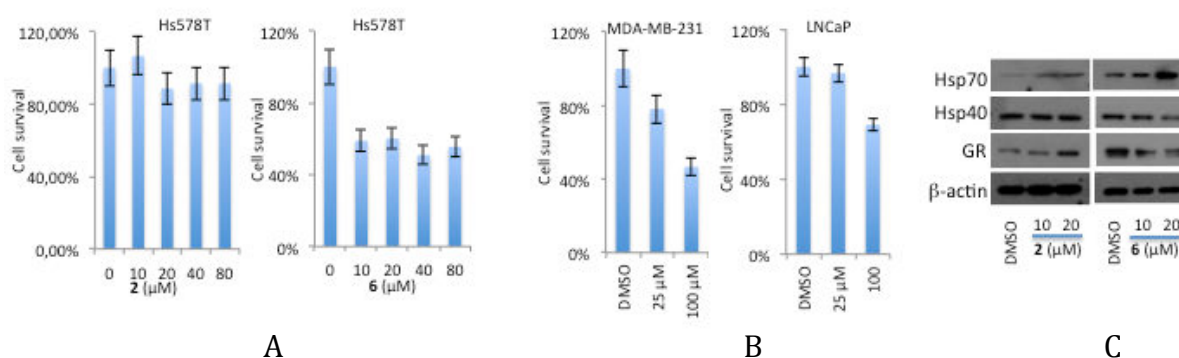


**Figure 4.33.** A- Comparison of the effect of sclerotiorin (**2**) and deacetylsclerotiorin (**6**) on cell survival of the breast cancer cell line Hs578T using MTS assay. B- Deacetylsclerotiorin (**6**) inhibits the growth of breast cancer cell line MDA-MB-231 and prostate cancer cell line LNCaP. C- Western blot analysis comparing the effect of sclerotiorin (**2**) and deacetylsclerotiorin (**6**) on the expression of Hsp70, Hsp40 and GR. b-actin is used as a loading control.

Surprisingly, at inhibitory concentrations, deacetylsclerotiorin becomes cytotoxic to Hs578T, MDA-MB-231 and LNCaP cell lines over a period of 48h (Figure 4.33.A-B). Western blot analysis (Figure 4.33.C) showed that sclerotiorin induces overexpression of Hsp70 and degradation of Hsp90 client proteins such as glucocorticoid receptor in Hs578T cells, indicating that the Hsp90 machine may be inhibited *in vivo*. It is worth noting however, that sclerotiorin also induces degradation of the heat shock protein 40 (Hsp40) (Figure 4.33.C) which may contribute to some of sclerotiorin's cytotoxicity.

## 5. Discussion

### 5.1. The use of medicinal plants in Morocco

The ethnopharmacological approach has been the platform for research programs with the objective to study plants used in traditional medicine in different cultures and to select one of the most used medicinal plant for its anticancer effect. For this, the choice of the National Institute of Oncology was taken based on the heterogeneous origin and the different socio-professional level of the patients, which are coming from different regions of Morocco.

In Morocco, the use of medicinal plants for therapeutic purposes is considered by many people as not being very efficient, but for being at least well tolerated because it is natural and is part of “soft” medicine. In all regions of Morocco, each home has a stock of medicinal plants that are used as home pharmacy for a number of diseases (Weniger, 1991). Moreover, people have free access to medicinal plants “without prescription” (Claisse, 1990).

Furthermore, the majority of patients who use medicinal plants have a low income and live far from the hospital, which explains their resorting to medicinal plants to be cured. The origin and their educational level were also a variable because in traditional medicine, the statements of an illiterate or of an expert are not the same. Many studies have shown that traditional medicine is still used all over Morocco. To approve the biological activity of each plant scientifically, plant extracts must be evaluated for their suspected biological effect.

### 5.2. Selection of interesting medicinal plants based on an ethnopharmacology survey

Fifty-five plants have been cited during this investigation. Among these plants 28 are proven to have anticancer activity. *Aristolochia longa*, *Trigonella foenum-graecum*, *Cassia absus* and *Nigella sativa* are the most used plants. However, there are plants that have been found to be toxic such as *Pinus halepensis*, *Peganum harmala*, *Aristolochia longa* and *Euphorbia resinifera*. Regardless of their toxicity these plants are used by patients in the INO irrespective of the degree of toxicity or side effects.

*Thymelaea lythroides* was used by two patients, which have uterus cancer. The plant was taken as tea three times a day. Side effects by using this plant were not observed, in contrary to the effects of chemotherapy, but the effectiveness was similar.



From the best of our knowledge, *Thymelaea lythroides* has not been yet investigated for their anti-cancer activity, even though many herbalists have recommended the use of this plant for that purpose.

### 5.3. Chemical diversities of the genus *Thymelaea* secondary metabolites

*Thymelaeaceae* is a medium size family of dicotyledons comprising about 1200 species distributed in 67 genera and occurs in all continents in latitudes south of 40°N. It is found in both temperate and tropical regions, but is more diverse in the southern than in northern hemisphere (Ferreira *et al.*, 2009).

*Thymelaea* genera have a lot of uses in folk medicine. Over the years, this species has been used as a laxative, diuretic, antibacterial, antitussive, expectorant, antiparasitic and also as an antitumor agent (Ferreira *et al.*, 2009).

*Thymelaea* Mill. comprises 31 species of xerophyllous shrubs and herbs. *Thymelaea* is a Mediterranean genus belonging to a primarily tropical and subtropical family. The genus *Thymelaea* is poorly investigated. Only 4 species are studied: *T. hirsute*, *T. passerina*, *T. tartonraira* and *T. microphylla*. The Table 5.1 summarizes the bioactive metabolites reported from the genus *Thymelaea*.

**Table 5.1.** Bioactive metabolites from the genus *Thymelaea* (Borris *et al.*, 1988)

Compounds	Species	References
<b>Coumarins</b>		
Daphnetin	<i>Thymelaea hirsuta</i>	Rizk et al., 1975
Daphnetin-8-β-D-glucoside	<i>Thymelaea hirsuta</i>	Rizk et al., 1975
Daphnin	<i>Thymelaea hirsuta</i>	Rizk et al., 1975
Daphnoretin	<i>Thymelaea hirsuta</i>	Rizk et al., 1975; Rizk et al., 1972
	<i>Thymelaea tartonraira</i>	Garcia-Grandos, 1980
Daphnorin	<i>Thymelaea hirsuta</i>	Rizk et al., 1975
Esculetin	<i>Thymelaea hirsuta</i>	Rizk et al., 1975
Scopoletin	<i>Thymelaea hirsuta</i>	Rizk et al., 1975
Sphondin	<i>Thymelaea passerina</i>	George and Rishi, 1982
Umbelliferone	<i>Thymelaea hirsuta</i>	Rizk et al., 1975
	<i>Thymelaea passerina</i>	George and Rishi, 1982
<b>Flavonoids</b>		
Genkwanin	<i>Thymelaea tartonraira</i>	Garcia-Grandos, 1980
Genkwanin-5-O-β-D-	<i>Thymelaea tartonraira</i>	Garcia-Grandos, 1980

primeverosyl		
Kaempferol	<i>Thymelaea tartonraira</i>	Garcia-Grandos, 1980
Orientin	<i>Thymelaea tartonraira</i>	Garcia-Grandos, 1980
Vicenin-2	<i>Thymelaea hirsuta</i>	Nawwar et al., 1977
	<i>Thymelaea tartonraira</i>	Garcia-Grandos, 1980
Vitexin	<i>Thymelaea tartonraira</i>	Garcia-Grandos, 1980
<b>Triterpenes</b>		
β-Amyrin	<i>Thymelaea hirsuta</i>	Garcia-Grandos, 1980
	<i>Thymelaea passerina</i>	George and Rishi, 1982
Betulin	<i>Thymelaea hirsuta</i>	Garcia-Grandos, 1980
Erythrodiol	<i>Thymelaea hirsuta</i>	Garcia-Grandos, 1980
Lanosterol	<i>Thymelaea hirsuta</i>	Garcia-Grandos, 1980
Lupeol	<i>Thymelaea hirsuta</i>	Garcia-Grandos, 1980
<b>Sterols</b>		
Campesterol	<i>Thymelaea hirsuta</i>	Rizk et al., 1974
Cholesterol	<i>Thymelaea hirsuta</i>	Garcia-Grandos, 1980
β-sitosterol	<i>Thymelaea hirsuta</i>	Rizk et al., 1975
	<i>Thymelaea passerina</i>	George and Rishi, 1982
β-sitosterol-β-D-glucoside	<i>Thymelaea hirsuta</i>	Rizk et al., 1972
	<i>Thymelaea passerina</i>	George and Rishi, 1982
Stigmasterol	<i>Thymelaea hirsuta</i>	Gharbo et al., 1970
<b>Lipids</b>		
n-Docosanol	<i>Thymelaea hirsuta</i>	Rizk et al., 1974
n-Heptacosane	<i>Thymelaea hirsuta</i>	Rizk et al., 1974
n-Hexacosanol	<i>Thymelaea hirsuta</i>	Rizk et al., 1974
n-Nonacosane	<i>Thymelaea hirsuta</i>	Rizk et al., 1974
n-Octacosane	<i>Thymelaea hirsuta</i>	Rizk et al., 1974
n-Octacosanol	<i>Thymelaea hirsuta</i>	Rizk et al., 1974
	<i>Thymelaea hirsuta</i>	Rizk et al., 1974
n-Tetracosanol	<i>Thymelaea hirsuta</i>	Rizk et al., 1974
n-Triacontane	<i>Thymelaea hirsuta</i>	Rizk et al., 1974
<b>Fatty acids</b>		
Arachidic acid	<i>Thymelaea hirsuta</i>	Rizk et al., 1974
Dihydromalvalic acid	<i>Thymelaea hirsuta</i>	Rizk et al., 1974
Linoleic acid	<i>Thymelaea hirsuta</i>	Rizk et al., 1974
Linolenic acid	<i>Thymelaea hirsuta</i>	Rizk et al., 1974
Myristic acid	<i>Thymelaea hirsuta</i>	Rizk et al., 1974
Oleic acid	<i>Thymelaea hirsuta</i>	Rizk et al., 1974
Palmitic acid	<i>Thymelaea hirsuta</i>	Rizk et al., 1974
Stearic acid	<i>Thymelaea hirsuta</i>	Rizk et al., 1974

#### **5.4. Methodologies for profiling of the metabolites**

Isolation and structure elucidation processes enrich the chemistry of natural products (Butler, 2004). Hence, interesting fungal strains can be elected to be screened, which together with the use of spectroscopic methods in addition to chemoinformatics can be used as part of an effective dereplication protocol (Larsen *et al.*, 2005). Secondary metabolites profiling is not an easy task to be applied since natural products display very diverse chemical structures. Thus, a single analytical method does not exist, which is capable of profiling all natural products in the investigated extract (Wolfender *et al.*, 2005). However, advanced analytical and spectroscopic techniques, like the hyphenated techniques linked with HPLC, can provide a good idea about the substructures and/or functional groups in the chemical structure.

##### **5.4.1. HPLC/UV**

With the advancement of HPLC as well as much more stable and better columns for high resolution separation, combined with fast UV diode array detectors, it has become easy to acquire the UV spectrum of practically every single component from an extract, provided a suitable chromophore is existing. Consequently the UV spectrum has turned into one of the most readily accessible pieces of information related to structure of natural products that increased the interest in exploiting its usefulness (Cannall, 1998).

In the present study, a lot of chemical compounds that share similar chromophoric functions were examined by the hyphenated HPLC/UV-photodiode array detection (LC/UV-DAD) technique, which showed very often similar UV spectra, even though there were significant differences in additional non-chromophoric functions.

##### **5.4.2. HPLC/ESI-MS**

Electrospray ionization mass spectrometry (ESI-MS) and the associated techniques provided the scientific community with a highly versatile method for studies of secondary metabolites. ESI-MS is a soft and sensitive ionization technique which can be adjusted to produce mainly protonated or sodiated ions (assuming positive ESI) from a wide range of natural products (Smedsgaard and Frisvad, 1996). Moreover, this method is also useful in establishing the related secondary metabolites. In the context of the present study, this proved extremely valuable in detecting azaphilone derivatives (9, 10, 11 and 12) and xanthoradone derivatives (14, 15, 16 and 17).

---

---

### 5.5. Secondary metabolites isolated from the plant *Thymelaea lythroides*

*Thymelaea lythroides* is growing wild in Mâamora forest, called by Moroccan people as “Methnan” and used as a folk remedy for otitis, diabetes, rheumatism and inflammation of the prostate (Gmira *et al.*, 2007).

Eight compounds were isolated from areal parts of *Thymelaea lythroides* including one depsipeptide (**1**), two coumarins (**2**, **3**), one dicoumarin (**4**), two lignans (**5**, **6**), one flavonoid glucoside (**7**) and one dicoumarin glycoside (**8**).

#### 4.5.1. Depsipeptides

Natural or synthetic compounds having sequences of amino and hydroxy carboxylic acid residues (usually  $\alpha$ -amino and  $\alpha$ -hydroxy acids), exhibit commonly but not necessarily regularly alternating units. In cyclodepsipeptides the residues are connected in a ring (IUPAC, 1997).

Romidepsin is an epsipeptide and is a member of the bicyclic peptide class of histone deacetylase inhibitors and was first isolated as a fermentation product from *Chromobacterium violaceum* by the Fujisawa Pharmaceutical Company (Yurek-George *et al.*, 2007). It is being used in the treatment of some cancers where it is thought to reactivate silenced genes.

The depsipeptide etamycin, a newly isolated natural product from a marine actinomycete, shows potent activity in vitro and in mice against MRSA (Haste *et al.*, 2010). It was first observed to have a positive role on gene expression in 1990. A clinical trial was conducted in 1996 for treating T cell lymphoma (Piekarz and Bates, 2004). Another natural depsipeptide HDAC inhibitor is spiruchostatin A (Yusuke *et al.*, 2006).

#### 5.5.2. Coumarins

Coumarin is a fragrant compound in the benzopyrone chemical class and is a colorless crystalline substance in its standard state. It is found naturally in many plants. Coumarins are used in the pharmaceutical industry as precursor molecules in the synthesis of a number of synthetic anticoagulant pharmaceuticals similar to dicoumarol. Coumarins have shown many biological activities, but are approved for only a few medical uses as pharmaceuticals. Reported coumarin activity includes anti-HIV, anti-tumor, anti-hypertension, anti-arrhythmia,

anti-inflammatory, anti-osteoporosis, antiseptic, and analgesic activity. It is also used in the treatment of asthma and lymphedema (Liu *et al.*, 2011).

### **5.5.3. Flavonoids**

Flavonoids are polyphenolic compounds that are ubiquitous in nature. Over 4,000 flavonoids have been identified. The widespread distribution of flavonoids, their variety and their relatively low toxicity compared to other active plant compounds (for instance alkaloids) mean that many animals, including humans, ingest significant quantities in their diet. Preliminary research indicates that flavonoids may modify allergens, viruses, and carcinogens, and so may be biological "response modifiers". *In vitro* studies show that flavonoids also have anti-allergic, anti-inflammatory, anti-microbial, anti-cancer, anti-diarrheal and antiviral activities (Spencer, 2008; Yamamoto *et al.*, 2001; Cushnie *et al.*, 2005; Cushnie and Lamb, 2011; de Sousa *et al.*, 2007; Schuier *et al.*, 2005; González *et al.*, 1990).

### **5.5.4. Lignans**

Lignans are polyphenols found in plants. Their precursors are found in a wide variety of plant-based foods, including seeds, whole grains, legumes, fruits, and vegetables.

Lignan-rich foods are part of a healthful dietary pattern, but the role of lignans in the prevention of hormone-associated cancers, osteoporosis, and cardiovascular diseases is not yet clear.

## **5.6. Biosynthesis of the secondary metabolites**

Secondary metabolites are organic molecules that are not involved in the normal growth and development of an organism, while primary metabolites play a key role in the survival of the species, playing an active function in the photosynthesis and respiration. Most of the secondary metabolites are classified based on their biosynthetic origin. Before looking at individual pathways in detail, it is helpful to consider the overall pathway of carbon from carbon dioxide and the photosynthetic formation of sugars. This is shown in Figure 5.1.

In this context a distinction may be drawn between primary and secondary metabolic pathways. The former are involved in the storage and release of energy and in the synthesis of essential cellular constituents such as the amino acids and the nucleic acids. The latter involve the biosynthesis of the metabolites, which are characteristic of each species. Different classes of these metabolites are often associated to a narrow set of species within a phylogenetic

group and constitute the bioactive compounds in several medicinal, aromatic, colorant, and spice plants and/or functional foods.

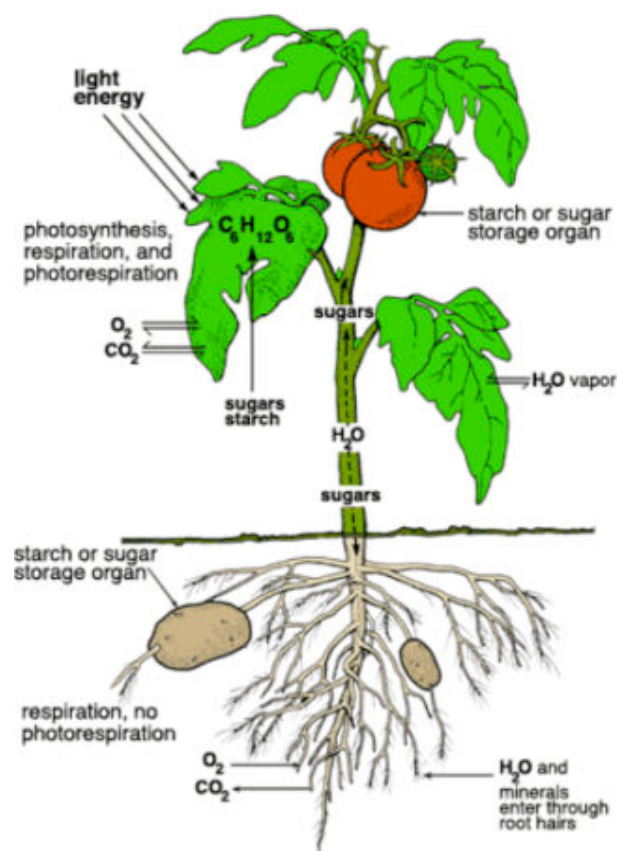
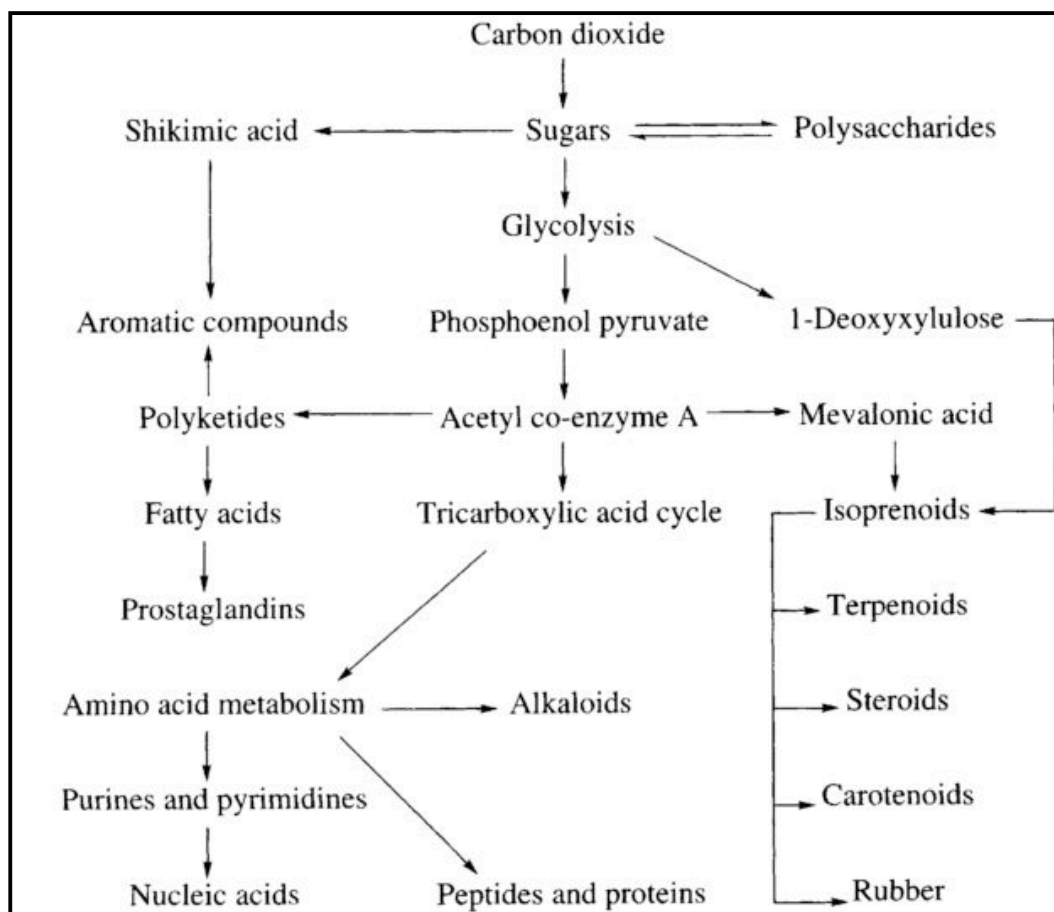


**Figure 5.1.** Photosynthesis, respiration, leaf and water exchange and translocation of sugar in plant (Silverstein *et al.*, 2008)

In this context a distinction may be drawn between primary and secondary metabolic pathways. The former are involved in the storage and release of energy and in the synthesis of essential cellular constituents such as the amino acids and the nucleic acids. The latter involve the biosynthesis of the metabolites, which are characteristic of each species. Different classes of these metabolites are often associated to a narrow set of species within a phylogenetic group and constitute the bioactive compounds in several medicinal, aromatic, colorant, and spice plants and/or functional foods.

In essence, secondary metabolism utilizes a limited number of metabolites available from primary metabolism in novel ways. Four major pathways have emerged and two of them in particular show a considerable degree of structural homogeneity (Scheme 5.1). In the first, the “**isoprene pathway**”, the precursor is mevalonic acid derived from acetyl-CoA. In the

second, the “**polyketide pathway**”, the primary metabolites are the CoA derivatives of lower fatty acids together with their carboxylated derivatives; typical examples are acetyl-CoA and malonyl-CoA, propionyl-CoA and methylmalonyl-CoA, and butyryl-CoA and ethylmalonyl-CoA. Multiple condensations lead to polyketomethylene structures; thus, 1 acetyl-CoA and  $n$  malonyl-CoA yield  $\text{CH}_3\text{-CO-(CH}_2\text{-CO)}_n\text{-CoA}$ , and 1 propionyl-CoA and  $n$  methylmalonyl-CoA give  $\text{CH}_3\text{-CH}_2\text{-CO-(CH[CH}_3\text{]-CO)}_n\text{-CoA}$ .



**Scheme 5.1.** The major biosynthesis pathways of secondary metabolites

The remaining two major pathways are less easily summarized because of the structural diversity of the secondary metabolites. The “**shikimate pathway**” uses shikimic acid itself as the primary metabolite or, alternatively, either an intermediate involved in shikimate formation or a further primary metabolite derived from shikimate (e.g., isochorismate). Many aromatic products originate in this way, as well as some nonaromatic, cyclohexane structures. Finally, the fourth major pathway involves secondary metabolites constructed from “**amino acids**” as precursors; many plant alkaloids are formed in this way. In some cases, secondary metabolite formation requires more than one amino acid. While these four pathways are the

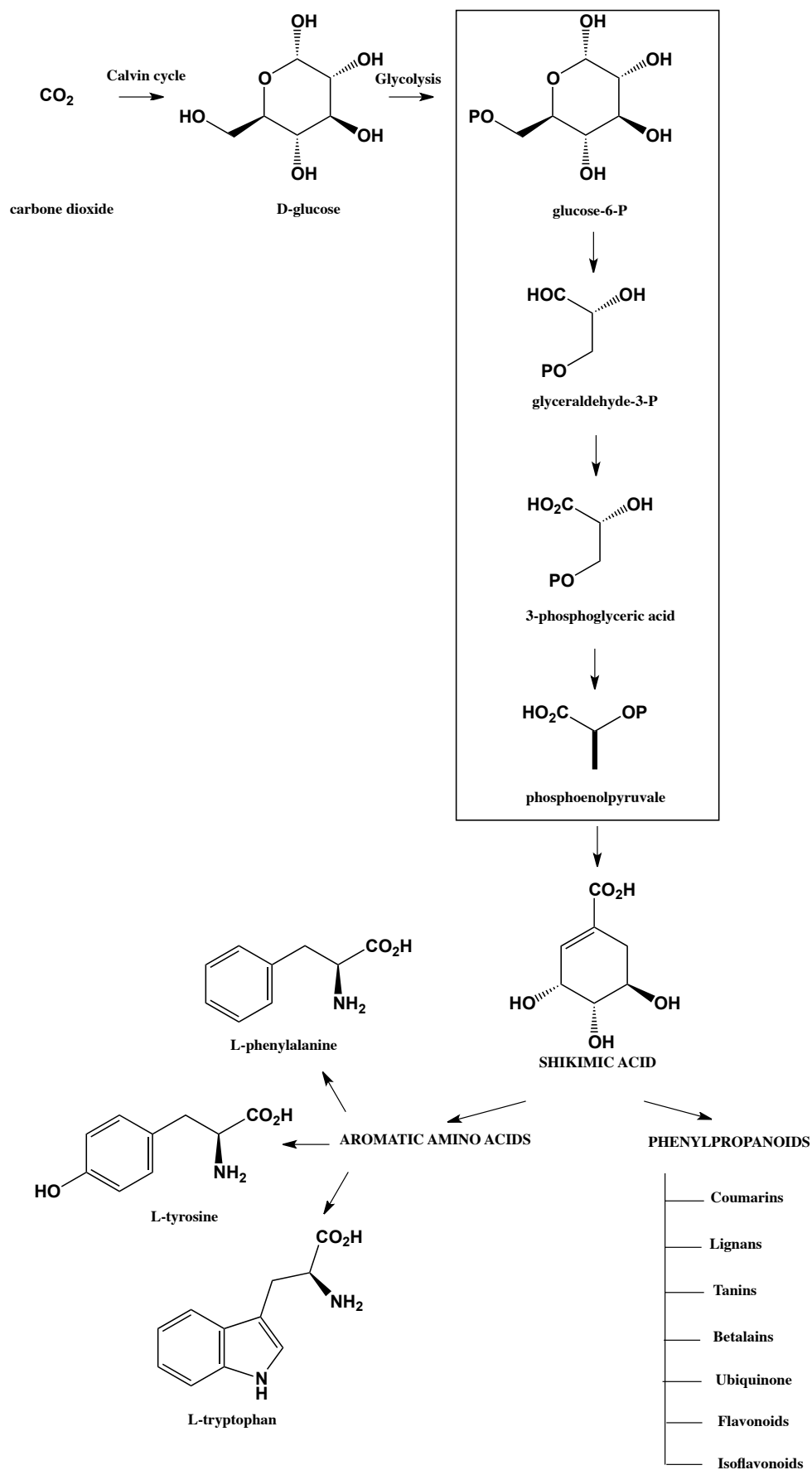
major biosynthetic routes to secondary metabolites, there are still other possibilities such as the compounds that are derived directly from carbohydrates without cleavage of the carbon chain and those derived from intermediates of the tricarboxylic acid cycle. Moreover, many secondary metabolites are biosynthesized by a mixed process involving a combination of two (or more) of these major pathways. A classic example is the ergot alkaloid biosynthesis involving the amino acid, tryptophan, and addition of a single isoprene unit.

#### **5.6.1. Biosynthesis pathway of the isolated compounds from *Thymelaea lythroides***

All isolated compounds were derived from the shikimate biosynthesis pathway. The shikimate pathway provides an alternative route to aromatic compounds, particularly the aromatic amino acids L-phenylalanine, L-tyrosine, and L-tryptophan. This pathway is employed by microorganisms and plants, but not by animals; accordingly, the aromatic amino acids feature among the essential amino acids for man and have to be obtained in the diet. A central intermediate in the pathway is shikimic acid, a compound which had been isolated from plants of *Illicium* species (Japanese 'shikimi') many years before its role in metabolism had been discovered. Phenylalanine and tyrosine form the basis of phenylpropane units found in many natural products, e.g. coumarins, lignans, and flavonoids, and along with tryptophan are precursors of a wide range of alkaloid structures.

Nevertheless, distinct differences in the basic biosynthetic pathways exist. For example, plants and microorganisms can synthesize their amino acids from simple building blocks, whereas most animals lost this ability in the course of their adaptation to heterotrophic life. Thus, many biosynthetic pathways are regarded as specific for certain groups of organisms. The ability to form thousands of structurally diverse natural products due to secondary metabolism is considered a typical feature of plants and microbes.





**Scheme 5.2.** The shikimate pathway: aromatic amino acids and phenylpropanoids

---

---

## 5.7. Bioactivity of the isolated compounds from *Thymelaea lythroides*

### 5.7.1 Bioactivity of coumarins and dicoumarins isolated from *T. lythroides*

Coumarins and dicoumarins derivatives isolated from *T. lythroides* were subjected to cytotoxicity testing toward L5178Y (mouse lymphoma) cell line. (+)-Dapheolone (3) was the most active of the compounds, whereas daphnoretin (6) and rutarensin (7) were found to be inactive. However, dapheolone and daphnoretin were inactive in the protein kinase inhibition assay, nevertheless the dicoumarin glucosides rutarensin (7) was active against Aurora-B, IGF 1-R and VEGF-R2, which suggests that rutarensin can not pass through the cell membrane. Furthermore, all compounds were inactive in the Hsp 90 chaperone machinery inhibition assay.

Despite the activity of rutarensin against the mentioned protein kinases, it was inactive against the Hsp 90 chaperone machinery, indicating that the mechanism of the inhibition of the protein kinases could not have an interaction with protein kinases.

### 5.7.2. Bioactivity of lignans isolated from *T. lythroides*

(-)-Wikstromol (4) and  $\delta$ -sesamin (5) were inactive against cytotoxicity tests toward the L5178Y (mouse lymphoma) cell line, protein kinase inhibition assay and Hsp 90 chaperone machinery inhibition assay, although in the literature, (-)-wikstromol (4) has cytotoxic potential against human cancer cell lines (Singh *et al.*, 2007), and  $\delta$ -sesamin (5) showed mild antiplasmodial activities and cytotoxicity (IC<sub>50</sub> 3.37 and 3.50  $\mu$ g/mL resp.) without noticeable toxicity on mammalian normal cells (Risoleta *et al.*, 2011).

### 5.7.3. Bioactivity of flavonoid glycosides isolated from *T. lythroides*

The flavonoid glycosides *trans*-tilliroside (8) was inactive against cytotoxicity tests toward the L5178Y (mouse lymphoma) cell line, which suggested that *trans*-tilliroside protein kinase activity against Aurora-B, ALK and VEGF-R2 is not occurring *in vivo*, as the compound can not enter in the cell.

### 5.7.3. Bioactivity of depsipetides isolated from *T. lythroides*

Bassiatin (1) was inactive against cytotoxicity test toward the L5178Y (mouse lymphoma) cell line, protein kinase inhibition assay and Hsp 90 chaperone machinery inhibition assay, however, bassiatin was reported to have cytotoxicity activity against breast cancer cells (MCF-7) (Li *et al.*, 2012).

---

---

### 5.8. Selection of the interesting endophytic fungus strains isolated from *Thymelaea lythroides*

Five endophytic fungus strains, *Chaetomium aureum*, *Pleospora sp.*, *Cladosporieum sp.*, *Alternaria sp.* and *Epicoccum nigrum*, were isolated from healthy stem tissues of *Thymelaea lythroides* (*Thymelaeaceae*). The pure fungus strains were cultivated on rice solid medium. Preliminary biological assay (antibacterial and cytotoxicity assay) with the analysis of HPLC chromatogram of the EtOAc extracts of the five pure fungus strains showed that extracts of *Chaetomium aureum* were much more active, displaying a variety of chemical classes based on analysis of UV spectra.

This fungus strain was cultivated more than five times under the same conditions to evaluate its stability. All extracts showed the same HPLC chromatogram, which reinforces the choice of this fungus as a subject of the study by the factor of stability.

### 5.9. Choice of culture media

Medium composition and culture conditions are one of the factors having great impact on growth and production of secondary metabolites from microorganisms (Bills, 1995). The physiology of secondary metabolism has often been ignored and still few of the regulatory features involved in the biosynthesis of natural products have been elucidated. Thus it is important to grow the organism in different media in order to have a broad range of secondary metabolites as possible candidates for a given strain to increase the chance to generate novel drug candidates (Larsen *et al.*, 2005). Furthermore, some natural products are only produced under certain environmental conditions and only when all trace metals, phosphate and other medium factors are present in certain ranges of concentrations (Knight *et al.*, 2003).

Thus, optimal media for good metabolite production can change for different genera being investigated (Larsen *et al.*, 2005).

Different and relatively easy to control conditions to investigate in a discovery program include growing cultures at both solid and liquid conditions, incubation at two or more temperatures, incubation at two or more shaker speeds, incubation for at least two different time periods, media with at least two different pH levels, choosing carbon and nitrogen sources at different concentrations, high- or low phosphate content, adding trace minerals etc. (Knight *et al.*, 2003).

Some authors strongly argue in favor of using solid substrate fermentations in studies of fungal metabolites since fungi, unlike other microorganisms, typically grow in nature on solid substrates such as wood, roots and leaves of plants (Nielsen *et al.*, 2004). On the other hand, some believe and argue that all metabolites can be expressed in liquid culture by varying carbohydrate composition, nitrogen source, oxygen tension, pH, redox potential, water activity, as the right conditions will produce intracellular conditions that will trigger production of a certain metabolite. It was found that metabolites associated to spore or sclerotia formation are often produced under solid conditions, whereas the production of other metabolites is enhanced under liquid conditions (Larsen *et al.*, 2005, Nielsen *et al.*, 2004).

In a screening effort aimed at the discovery of novel natural products, which includes a variety of different strains, one has to focus on a limited set of parameters, since otherwise the sheer number of extracts generated will easily be overwhelming. Thus, in this study selected fungal strain was cultured in liquid (Wickerham) medium as well as on eleven solid media. Bioactivity and chemical profiles of the obtained extracts from all cultures were compared and subjected to further investigation.

HPLC chromatograms of the EtOAc extracts of liquid and solid cultures showed different chemical patterns for the fungal strain investigated in this study. Moreover, when EtOAc extracts of liquid and solid cultures were compared, it was found that the yield of dry extract obtained from rice cultures was higher than that the others media. However, it cannot be excluded that this finding, at least to a certain degree, was due to the fact that more polar material, e.g. sugars or amino acids, were extracted from the culture medium in the case of the solid rice cultures compared to the liquid medium.

#### **4.10. Chemical diversities of the genus *Chaetomium* secondary metabolites**

Fungi have proved to be a rich source of a huge number of secondary metabolites with a large variety of chemical structures and diverse biological activities. Fungal metabolites are of considerable importance as new lead compounds for medicine as well as for plant protection (Zhang *et al.*, 2012).

*Chaetomium* is a large genus of the fungal family Chaetomiaceae (subdivision Ascomycota) which contains over one hundred of both marine- and terrestrial-derived species. Members of this filamentous fungal genus, *Chaetomium atrobrunneum*, *C. funicola*, *C. globosum* and *C.*

---

---

---

*strumarium*, are most commonly found in soil, air, and plant debris, and are encountered as causative agents of infections in humans. In the past decades, fungi of the *Chaetomium* genus have been revealed to be a rich source of fascinating and structurally complex natural products. To date, more than 200 compounds have been reported from this genus. A huge number of new and bioactive secondary metabolites associated with unique and diverse structural types, such as chaetoglobosins, epipolythiodioxopiperazines, azaphilones, depsidones, xanthonones, anthraquinones, chromones, terpenoids, and steroids, have been isolated and identified. Many of the compounds have been reported to possess significant biological activities, such as antitumor, antimalarial, cytotoxic, enzyme inhibitory, antibiotic, phytotoxic, phytotoxic and other activities (Zhang *et al.*, 2012).

### 5.11. Secondary metabolites isolated from the endophytic fungi *Chaetomium aureum*

In this investigation, 18 compounds were isolated from the endophytic fungi *Chaetomium aureum* including four azaphilones derivatives (9-12), one pyranochromone (13), four xanthonones derivatives (14-17) and one alkylresorcinol (resorcinolic lipid) (18).

One azaphilone derivative (19) was semi-synthetic from one of the isolated compounds.

#### 5.11.1. Azaphilones

The azaphilones are a family of structurally diverse fungal polyketides possessing a pyranoquinone ring systems and containing a chiral quaternary center and a highly oxygenated bicyclic core, and sometimes bearing a five membered lactone ring. To date, 29 compounds of this class have been discovered in the genus *Chaetomium*, some of them displayed antifungal, antibacterial, antimalarial and selectively cytotoxic activities (Zhang *et al.*, 2012).

#### 5.11.2. Pyranochromones

From the genus *Chaetomium* only three pyranochromones, SB236050, SB238569, and SB236049, were identified from a strain of *Chaetomium funicola*, which are metallo- $\beta$ -lactamase inhibitors in the *Bacillus cereus* II enzyme assay. Of these compounds SB238569 was the most active. Analysis of the crystal structure of SB236050 complexed in the active site of CfiA indicates that SB236050 exhibits key polar interactions with Lys184, Asn193, and His162 and a stacking interaction with the indole ring of Trp49 in the flap, which is in the closed conformation over the active site groove (Payne *et al.*, 2002).

### 5.11.3. Xanthones

Xanthones are a structurally diverse group of natural products, derived from plants, lichens, and fungi, with a broad range of biological activities. Two xanthones, O-methylsterigmatocystin and sterigmatocystin were first isolated in 1979 from cultures of *Chaetomium thielavioideum*.

### 5.11.4. Alkylresorcinols

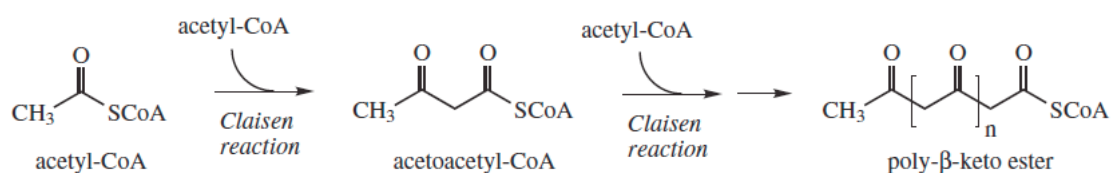
Alkylresorcinols, also known as resorcinolic lipids, are phenolic lipids composed of long aliphatic chains and resorcinol-type phenolic rings. Alkylresorcinols have been found to have multiple biological activities, including antimicrobial, molluscicidal, and antitumor properties.

## 5.12. Biosynthesis of isolated secondary metabolites from the endophytic fungi *Chaetomium aureum*

All isolated compounds are derived from the polyketide biosynthesis pathway. Polyketides constitute a large class of natural products grouped together on purely biosynthetic grounds. In addition to exhibiting a staggering range of functional and structural diversity, they boast a wealth of medically important activities, including antibiotic, anticancer, antifungal, antiparasitic and immunosuppressive properties. Even before the full extent of their utility was known, scientists became interested in how these complicated molecules are assembled. Their diverse structures can be explained as being derived from poly- $\beta$ -keto chains.

The formation of the poly- $\beta$ -keto chain could be envisaged as a series of Claisen reactions, the reverse of which are involved in the  $\beta$ -oxidation sequence for the metabolism of fatty acids. Thus, two molecules of acetyl-CoA could participate in a Claisen condensation giving acetoacetyl-CoA, and this reaction could be repeated to generate a poly- $\beta$ -keto ester of appropriate chain length (Scheme 5.3).

*Claisen reaction: acetyl-CoA*



**Scheme 5.3.** The formation of the poly- $\beta$ -keto chain

### 5.13. Bioactivity of isolated secondary metabolites from the endophytic fungi *Chaetomium aureum*

#### 5.13.1. Bioactivity of azaphilone derivatives isolated from *Chaetomium aureum*

Sclerotiorin (9) inhibits efficiently the Hsp90 machine chaperoning activity. Sclerotiorin showed similar effectiveness to that of 17-AAG (Geldanallycin derivative), the classical inhibitor of Hsp90. However, sclerotiorin has no cytotoxic effect on breast cancer Hs578T, MDA-MB-231 and prostate cancer LNCaP cell lines. Interestingly, deacetylation of sclerotiorin increases its cytotoxicity toward the tested cell lines over a period of 48h. Sclerotiorin showed also strong activity against all of the tested protein kinases except MEK 1 wt. In the best of our Knowledge, the protein kinase MEK 1 wt is not Hsp 90 client protein (Jiao *et al.*, 2011; Citri *et al.*, 2006), which concord with the result of its resistance at (+)-sclerotiorin.

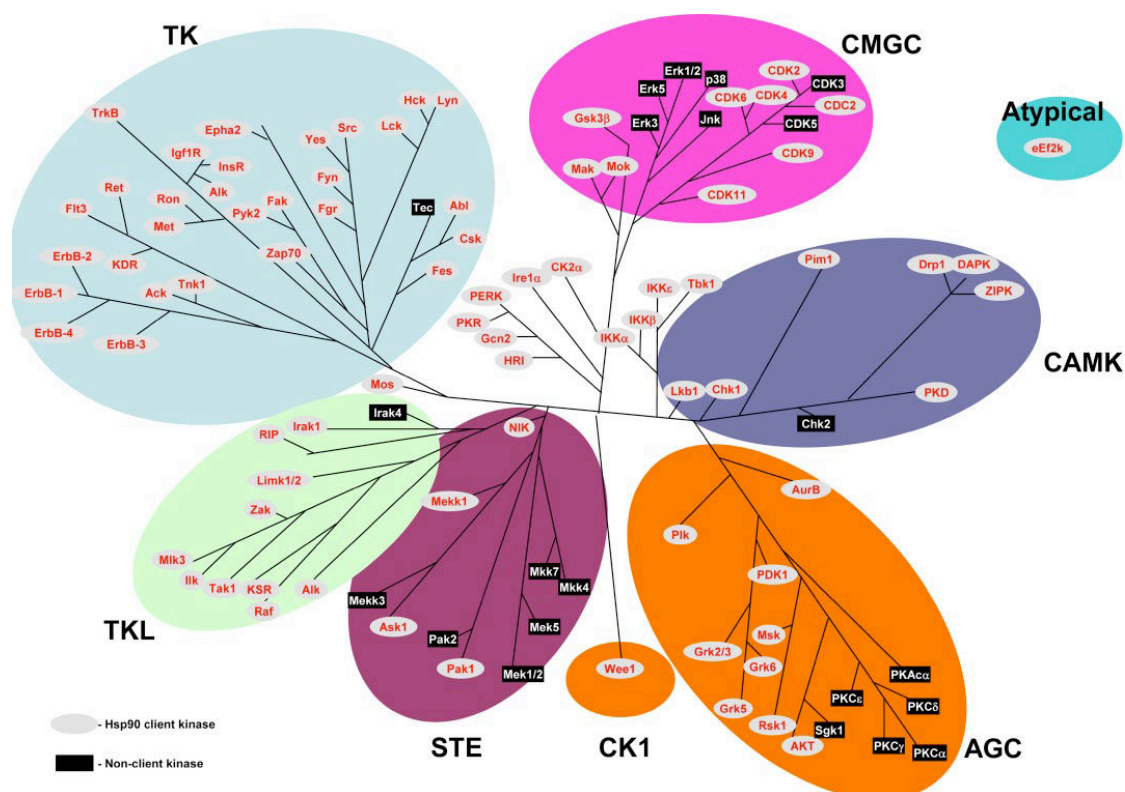


**Figure 5.2.** Diversity of established Hsp90 clients within the human kinome.

Hsp90 client kinases are represented by red letters on an elliptical gray background, whereas non-clients appear in white letters on a rectangular black background. The overall structure of the scheme was based on a previously published analysis of the human kinome.

**Table 5.2.** Distribution of Hsp90 clients within kinase families

Kinase Family	TK	TKL	CAMK	CMGC	AGC	CK1	STE	Other	Atypical	Total
Clients	28	12	7	9	8	1	4	10	1	80
Non-clients	1	2	1	8	6	0	7	0	0	25
Total	29	14	8	17	14	1	11	10	1	105
Total in group	90	43	74	61	63	12	47	83	45	518

The tabulation of the diversity of Hsp90 clientele according to kinase families. The data is based on data available in the literature.

**- Sclerotiorin inhibits the Hsp90 chaperoning of progesterone receptor (PR) *in vitro***

Sclerotiorin efficiently inhibited the recovery of PR hormone binding activity using RRL (Figure 3.5.1). Sclerotiorin showed similar efficiency to that of 17-AAG, the classical inhibitor of Hsp90. Importantly, the oxygen atom of the heterocycle is essential for this inhibitory activity. Indeed, sclerotioramine and isochromophilone VI, where a nitrogen atom replaces the oxygen atom, are inactive. This is in line with previous reports showing that sclerotioramine and isochromophilone VI were unable to inhibit the activity of cholesterol ester transfer protein (CETP) (Tomoda *et al.*, 1999). Isochromophilone VII showed much less activity than sclerotiorin.

**- Sclerotiorin is not cytotoxic to breast cancer Hs578T cells**

The cytotoxicity assay showed that sclerotiorin is not toxic to breast cancer cell line Hs578T and MCF7, MDA-MB-231, MDA-MB-453, prostate cancer cell line LNCaP and cervical cancer cell line HeLa. This is in contrast to a report showing that sclerotiorin induces apoptosis in colon cancer (HCT-116) cells through the activation of BAX, and down-regulation of BCL-2 (Giridharan *et al.*, 2012).

**- Deacetylsclerotiorin is less efficient at inhibiting the Hsp90 chaperoning of progesterone receptor (PR) *in vitro* than sclerotiorin.**

The deacetylated sclerotiorin was relatively less efficient in inhibiting the Hsp90 *in vitro* than sclerotiorin. The mechanism by which sclerotiorin and deacetylsclerotiorin inactivate the Hsp90 machine is not clear but it seems to be different from that of the 17-AAG. As compared to 17-AAG, protein analysis of complex formation by SDS-PAGE showed that sclerotiorin and deacetylsclerotiorin lower the level of Hsp90 without increase of Hop. Furthermore, deacetylsclerotiorin did not increase Hsp70 level in PR complexes.



---

---

### - Deacetylsclerotiorin is cytotoxic to cancer cells

At inhibitory concentrations, deacetylsclerotiorin becomes cytotoxic to Hs578T, MDA-MB-231 and LNCaP cell lines over a period of 48h. For Western blotting, cell lines were harvested at 48 h and cell lysates were made. 10 µg of each protein lysate was analyzed by Western blotting using home made antibodies (HMGR) for GR, for Hsp70 and for Hsp40 and sc-47778 (Santacruz) for β-actin. Western blot analysis showed that sclerotiorin induces overexpression of Hsp70 and degradation of Hsp90 client proteins such as glucocorticoid receptor in Hs578T cells, indicating that the Hsp90 machine may be inhibited in vivo. It is worth noting however, that sclerotiorin also induces degradation of the heat shock protein 40 (HSP40) which may contribute to some of sclerotiorin's cytotoxicity.

### - Mechanism of action of Sclerotiorin

Sclerotiorin and several isochromophilone analogues were also shown to inhibit gp120-CD4 binding (Sun *et al.*, 1996) and the activity of cholesterol ester transfer protein (CETP) (Tomoda *et al.*, 1999). From these studies, it was concluded that the electrophilic sites at the C6 and C8 position are required for the sclerotiorin inhibition but the chlorine atom at the C-5 position and the acetyl residue at the C-7-OH are not. Furthermore, the oxygen atom of the heterocycle is also essential since sclerotioramine and isochromophilone VI where the oxygen atom is replaced by a nitrogen atom are less active. Long ago, sclerotiorin has been reported to react with primary amine (Eade *et al.* 1957) and this was the proposed mechanism for inactivation of CETP implying that sclerotiorin modifies primary amines such as lysine residues or the N-terminal amino acid in the CETP (Tomoda *et al.*, 1999). It is very possible that the inhibitory activity of sclerotiorin toward the Hsp90 machine could be through its reactivity with amine groups of components such as Hsp90, Hsp70, Hsp40, Hop and p23 leading to their inactivation. The loss of Hsp40 upon cell treatment with sclerotiorin could be the consequence of such covalent modifications.

### 5.13.2. Bioactivity of xanthone derivatives isolated from *Chaetomium aureum*

Xanthoradone D<sub>1</sub> and D<sub>2</sub> (14, 15) and xanthoradone E<sub>1</sub> and E<sub>2</sub> (16, 17) were subjected to cytotoxicity testing toward L5178Y (mouse lymphoma) cell line, protein kinases inhibition assays, antibacterial activity and Hsp 90 chaperone inhibition. All compounds were inactive. In contrast to literature, all xanthoradone derivatives were active against methicillin-resistant *Staphylococcus aureus*, produced by *Penicillium radicum* (Yamazaki *et al.*, 2009).

### **5.13.3. Bioactivity of alkylresorcinol derivative isolated from *Chaetomium aureum***

Chaetoresorcinol (18) was active against only *Asp. Fumigatus*, whereas it showed no antibacterial activities, which makes it selectively only against *Asp. Fumigatus*. Chaetoresorcinol was active against most of protein kinases, despite its inactivation against Hsp 90.

## 6. Conclusion

Medicinal plants and endophytic fungi produce natural products with a large diversity of chemical structures, which might prove to be suitable for specific medicinal applications. Most of these secondary metabolites show biological activities in pharmaceutically relevant bioassay systems and thus represent potential lead structures, which could be optimized to yield effective therapeutic and bioactive agents.

The Heat shock protein 90 plays a crucial role in maintaining oncogenic protein homeostasis. Hsp90 inhibition offers great promise in the treatment of a wide variety of solid and haematological malignancies. Numerous natural Hsp90 inhibitors have been developed in recent years, some of which exhibit excellent antitumor activities and have entered clinical trials.

The aim of this work was the isolation of secondary metabolites from the selected plant *Thymelaea lythroides* and its endophytic fungus *Chaetomium aureum*, followed by structure elucidation and examination of the antitumor activity of isolated compounds by screening their inhibitory activity on the Hsp90 machinery.

The medicinal plant *Thymelaea lythroides* was selected from fifty five medicinal plants used as traditional medicine by the patients of the National Institute of Oncology in Morocco. Five endophytic fungal strains (*Alternaria sp.*, *Chaetomium sp.*, *Cladosporium sp.* and *Pleospora sp.*), were isolated from *Thymelaea lythroides*. The fungal strain *Chaetomium aureum* was chosen for further investigation. It was grown in liquid Wickerham medium as well as on eleven solid media for a period of three to four weeks. The extracts obtained were then subjected to different chromatographic separation techniques in order to isolate the secondary metabolites. Structure elucidation of the isolated secondary metabolites was performed using state of the art techniques, including mass spectrometry (MS) and nuclear magnetic resonance (NMR) spectroscopy experiments.

Finally, the isolated compounds were subjected to various bioassays to examine their antitumor activity by testing their ability to inhibit the chaperone Hsp90 machinery. Besides, the isolated compounds were also tested for their antimicrobial, antifungal and cytotoxic activities as well as inhibitory profiles towards selected protein kinases.

---

---

### 6.1. Compounds isolated from the plant *Thymelaea lythroides*

Eight secondary metabolites were isolated from the medicinal plant *Thymelaea lythroides* including one depsipeptide (**1**; bassiatin), two coumarins (**2**; daphneone and **3**; daphneolone), one dicoumarin (**4**; daphnoretin), two lignans (**5**; wikstromol and **6**;  $\delta$ -sesamin), one flavonoid glucoside (**8**; trans tiliroside), and one dicoumarin glucoside (**7**; rutarensine).

Bassiatin (**1**) is an unusual plant secondary metabolite, which was previously reported exclusively from endophytic fungi. Thus, this is the first report of this compound from *Thymelaea lythroides*.

Daphneone (**2**) showed strong cytotoxic activity when tested against L5178Y mouse lymphoma cell line. Only trans tiliroside (**8**) and rutarensine (**7**) inhibited several of the tested protein kinases. All the compounds isolated from *Thymelaea lythroides* were inactive against the Hsp90 chaperone machinery.

### 6.2. Compounds isolated from the endophytic fungi *Chaetomium aureum*

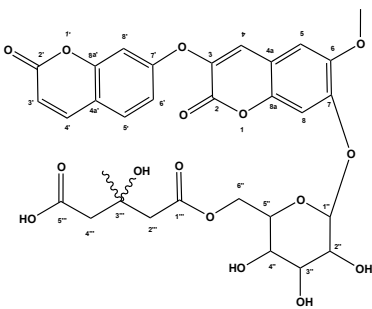
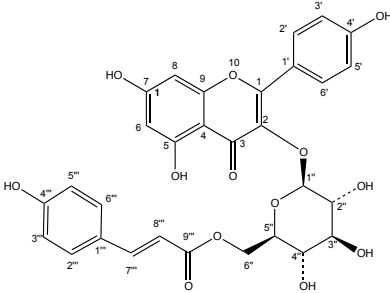
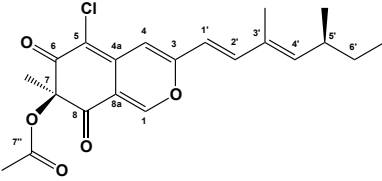
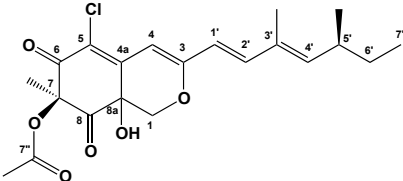
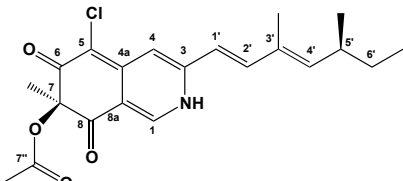
Six new compounds were obtained from this fungal strain, including a new alkylresorcinol derivative (**18**; chaetoresorcinol), four new xanthoradone derivatives (**14**; xanthoradone D1, **15**; xanthoradone D2, **16**; xanthoradone E1 and **17**; xanthoradone E2), and one pyrochromone derivative (**13**; SB 236050), together with four known azaphilone derivatives (**9**; sclerotiorin, **10**; isochromophilone VII, **11**; sclerotioramin and **12**; isochromophilone VI).

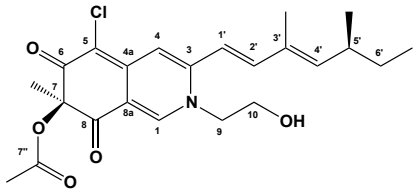
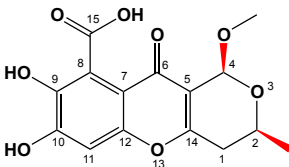
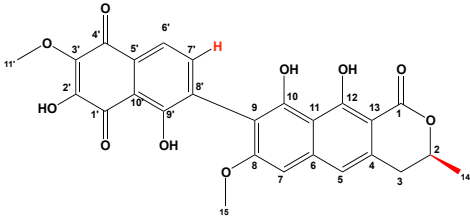
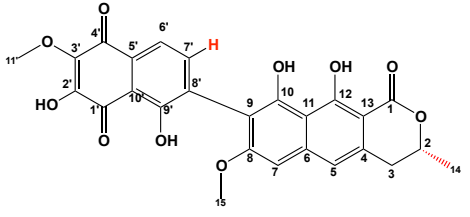
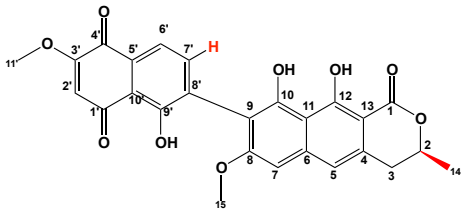
(+)-Sclerotiorin (**9**), (+)-isochromophilone VII (**10**), (+)-sclerotioramin (**11**) and isochromophilone VI (**12**) were not active upon testing their cytotoxic potential toward the L5178Y mouse lymphoma cell line. However, (+)-sclerotiorin (**9**) was active against all the tested protein kinases except MEK 1 wt, whereas its derivatives, isochromophilone VI (**12**) and sclerotioramin (**11**), inhibited only few of the tested enzymes. Furthermore, all compounds were tested in the Hsp 90 chaperone machinery inhibition assay. Only (+)-sclerotiorin exhibited prominent activity with similar efficiency as the famous Hsp-90 inhibitor 17-AAG (geldanamycin derivative).

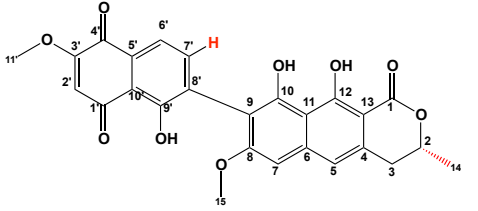
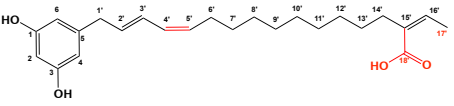
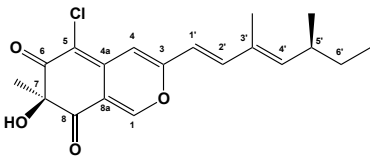
Chaetoresorcinol (**18**) showed selective moderated antifungal activity against *Aspergillus fumigatus*.

Table 6.1. Summary of the isolated compounds

Compound name	Structure	Source	Comment
<b>Bassiatin</b>		<i>Thymelaea lythroides</i>	Known
<b>Daphneone</b>		<i>Thymelaea lythroides</i>	Known
<b>Daphneolone</b>		<i>Thymelaea lythroides</i>	Known
<b>Wikstromol</b>		<i>Thymelaea lythroides</i>	Known
<b>δ-Sesamin</b>		<i>Thymelaea lythroides</i>	Known
<b>Daphnoretin</b>		<i>Thymelaea lythroides</i>	Known

Retarensin		<i>Thymelaea lythroides</i>	Known
<i>trans</i> -Tiliroside		<i>Thymelaea lythroides</i>	Known
(+)Sclerotiorin		<i>Chaetomium aureum</i>	Known
(+)Isochromphilone VII		<i>Chaetomium aureum</i>	Known
(+)Sclerotioramin		<i>Chaetomium aureum</i>	Known

<b>(+)-Isochromophilone</b>		<i>Chaetomium aureum</i>	Known
<b>SB 236050</b>		<i>Chaetomium aureum</i>	New
<b>Xanthoradone D<sub>1</sub></b>		<i>Chaetomium aureum</i>	New
<b>Xanthoradone D<sub>2</sub></b>		<i>Chaetomium aureum</i>	New
<b>Xanthoradone E<sub>1</sub></b>		<i>Chaetomium aureum</i>	New

<b>Xanthoradone E<sub>2</sub></b>		<i>Chaetomium aureum</i>	New
<b>Chaetoresorcinol</b>		<i>Chaetomium aureum</i>	New
<b>(+)-Deacetylsclerotiorin</b>		Semi-synthetic	Known



---

---

## 7. References

- Adegawa, S.; Miyase, T. and Fukushima, S. Sesquiterpene glycosides from *Youngia denticulate* (Houtt.) kitam. **1986**. *Chem. Pharm. Bull.*, *34*, 3769-3773
- Aly A.H. Novel Natural Products from Endophytic Fungi of Egyptian Medicinal Plants - Chemical and Biological Characterization. **2007**. Dissertation
- Aly, A.H., Debbab, A. and Proksch, P. Fungal endophytes: unique plant inhabitants with great promises. **2011**. *Appl. Microbiol. Biotechnol.*, *90*, 1829-45
- Amna, T.; Puri, S.C.; Verma, V.; Sharma, J.P.; Khajuria, R.K.; Musarrat, J.; Spitteller, M. and Qazi, G.N. Bioreactor studies on the endophytic fungus *Entrophospora infrequens* for the production of an anticancer alkaloid camptothecin. **2006**. *Can. J. Microbiol.*, *52*, 189-196
- Arai, N.; Shiomi, K.; Tomoda, H.; Tabata, N.; Yang, D.J.; Masuma, R.; Kawakuboand, T.; Omura, S. Isochromophilones III ~ VI, inhibitors of Acyl-CoA: Cholesterol acyltransferase produced by *Penicillium multicolor* FO-3216. **1995**. *J. Antibio.*, *48*, 696-702
- Arnold, A.E. Diversity and ecology of fungal endophytes in tropical forests. **2005**. In Current Trends in Mycological Research, D. Deshmukh, ed. (New Delhi, India: Oxford & IBH Publishing Co. Pvt. Ltd.), pp. 49-68
- Arnold, A.E. Endophytic fungi: hidden components of tropical community ecology. **2008**. In Tropical Forest Community Ecology, W.P. Carson and S.A. Schnitzer, eds. (West Sussex, UK: Wiley-Blackwell), pp. 254-271
- Arnold, A.E. Understanding the diversity of foliar endophytic fungi: progress, challenges, and frontiers. **2007**. *Fungal Biol. Rev.*, *21*, 51-66
- Arnold, A.E.; Mejía, L.C.; Kylo, D.; Rojas, E.I.; Maynard, Z.; Robbins, N. and Herre, E.A. Fungal endophytes limit pathogen damage in a tropical tree. **2003**. *Proc. Natl. Acad. Sci. USA*, *100*, 15649-15654
- Arvigo, R.; and Balick, M. Rainforest Remedies : One hundred healing herbs of Belize. **1993**. *Lotus Press, Twin Lakes*, *15*, 221-232

- 
- Bacon, C. W. and White, J. F. Microbial Endophytes. **2000**. Marcel Dekker inc. New York, pp. 341-388
- Balunas, M.J. and Kinghorn, A.D. Drug discovery from medicinal plants. **2005**. *Life Sci.*, *78*, 431-41
- Banerji, J.; Dhara, K. P. Lignan and amides from *Piper sylvaticum*. **1974**. *Phytochemistry*, *13*, 2327-2328
- Bannerman, R.H.O.; Burton, J.; Chen, W.C. Traditional Medicine and Health Care Coverage: A Reader for Health Administrators and Practitioners. **1983**. WHO
- Bao, L.; Xu, Z.; Niu, S.B.; Namikoshi, M.; Kobayashi, H.; Liu, H.W. (-)-Sclerotiorin from an unidentified marine fungus as an anti-meiotic and anti-fungal agent. **2010**. *Nat. Prod. Commun.*, *5*, 1789-1792
- Barrow, R.A.; Capon, R.J. Alkyl and alkenyl resorcinols from an Australian marine sponge, *Haliclona* sp. (Haplosclerida: Haliclونidae). **1991**. *Aust. J. Chem.*, *44*, 1393-1405
- Bellakhdar, J.; Claisse, R.; Fleurentin, J.; Younos, C. Repertory of standard herbal drugs in the Moroccan pharmacopoeia. **1991**. *J. Ethnopharm.*, *35*, 123-143
- Bellakhdar, J.; Honda, G., Miki, W. Herb drugs and herbalists in the Maghreb. **1982**. *ILCAA (Tokyo)*, *1982*, 339-344
- Bellakhdar, J. Médecine traditionnelle et toxicologie ouest-sahariennes. Contribution à l'étude de la pharmacopée marocaine. **1978**. Editions techniques nord-africaines, Rabat, pp. 358.
- Benjelloun W. Phytotherapy of hypertension and diabetes in oriental Morocco. **1997**. *J. Ethnopharm.*, *58*, 45-54
- Bentley, R. Secondary metabolite biosynthesis: the first century. **1999**. *Crit. Rev. biotech.*, *19*, 1-40
- Bounejmate, M. Conservation et utilisation des espèces fourragères et pastorales autochtones du Maroc: acquis et perspectives. **1995**. Programme Fourages, I. N.R. A. - Rabat
- Budzianowski, J.; Skrzypczak, L. Phenylpropanoid esters from *Lamium album* flowers. **1995**. *Phytochemistry*, *18*, 997-1001
-

- 
- Butler, M. S. Natural products to drugs: natural product-derived compounds in clinical trials. **2008**. *Nat. Prod. Rep.*, *25*, 475-516
- Butler, M.S. The role of natural product chemistry in drug discovery. **2004**. *J. Nat. Prod.*, *67*, 2141-2153
- Calvo, A.M.; Wilson, R.A.; Bok, J.W.; Keller, N.P. Relationship between secondary metabolism and fungal development. **2002**. *Microbiol. Mol. Biol. Rev.*, *66*, 447-459
- Cao, S.; Radwan, M.M.; Norris, A.; Miller, J.S.; Ratovoson, F.; Mamisoa, A.; Andriantsiferana, R.; Rasamison, V.E.; Rakotonandrasana, S.; Kingston, D.G.I. Cytotoxic and Other Compounds from the *Didymochlaena truncatula* from the Madagascar Rainforest. **2006**. *J. Nat. Prod.*, *69*, 284-289
- Carroll, G.C. Beyond pest deterrence - alternative strategies and hidden costs of endophytic mutualisms in vascular plants. **1991**. In *Microbial Ecology of Leaves*, J.A. Andrews and S.S. Hirano, eds. (New York: Springer-Verlag), pp. 358-375
- Chadli, A.; Felts, S. J. and Toft, D.O. GCUNC45 is the first Hsp90 co-chaperone to show alpha/beta isoform specificity. **2008**. *J. Biol. Chem.*, *283*, 9509-9512
- Chen, H.; Zhang, W.; Su, J.; Chen, Y.; Shen, Y. Phenols constituents in stem and leaf of *Daphne bholua*. **2009**. *Zhongcaoyao*, *40*, 1033-1035
- Chen, Y.Y.; Duan, J.A.; Tang, Y.P.; Guo, S. Chemical constituents from flower buds of *Daphne genkwa*. **2013**. *Hongcaoyao*, *44*, 397-402
- Chidananda, C.; Rao, L. Jagan M.; Sattur, A.P. Sclerotiorin, from *Penicillium frequentans*, a potent inhibitor of aldose reductase. **2006**. *Biotechnol. Lett.*, *28*, 1633-1636
- Clay, K. Fungal endophytes of grasses. **1990**. *Annu. Rev. Ecol. Syst.*, *21*, 255-297
- Cragg, G.M.; Newman, D.J. A tale of two tumor targets: topoisomerase I and tubulin. The Wall and Wani contribution to cancer chemotherapy. **2004**. *J. Nat. Prod.*, *67*, 232-244
- Cushnie, T.P.T.; Lamb, A.J. Antimicrobial activity of flavonoids. **2005**. *Int. J. Antimicrob. Agents*, *26*, 343-356
-

- 
- Cushnie, T.P.T.; Lamb, A.J. Recent advances in understanding the antibacterial properties of flavonoids. **2011**. *Int. J. Antimicrob. Agents*, *38*, 99-107
- de Bary, A. Morphologie und Physiologie der Pilze, Flechten, und Myxomyceten. **1866**. Hofmeister's Handbook of Physiological Botany, Volume II (Germany)
- de Sousa, R.R.; Queiroz, K.C.; Souza, A.C.; Gurgueira, S.A.; Augusto, A.C.; Miranda, M.A.; Peppelenbosch, M.P.; Ferreira, C.V.; Aoyama, H. Phosphoprotein levels, MAPK activities and NFkappaB expression are affected by fisetin. **2007**. *J. Enzyme Inhib. Med. Chem.*, *22*, 439-444
- Desantis, C.; Naishadham, D. and Jemal, A. Cancer Statistics for African Americans, **2013**. *CA Cancer J. Clin.*, *63*, 151-166
- Dewick, P.M. Medicinal natural products: A biosynthetic approach. **2002**. John Wiley & Sons Ltd., Chichester, England
- Eade, R. A.; Page, H.; Alexander, A.; Turner, K. and Whalley, W. B. The chemistry of fungi. Part XXVIII. Sclerotiorin and its hydrogenation products. **1957**. *J. Chem. Soc.*, *1957*, 4913-4924
- El-Emary, N.A.; Attia, A.A. Lignans and sesquiterpene lactones from the root bark of *Artemisia argentea*. **1988**. *Bull. Pharm. Sci.*, *11*, 154-61
- Fabricant, D. S. and Farnsworth, N. R. The value of plants used in traditional medicine for drug discovery. **2001**. *Environ. Health Perspect.*, *109*, 69-75
- Farinola, N.; Piller, N. Pharmacogenomics: Its role in re-establishing coumarin as treatment for lymphedema. **2005**. *Lymphat. Res. Biol.*, *3*, 81-86
- Farnsworth, N. R.; Akerele, O.; Bingel, A. S.; Soejarto, D. D. and Guo, Z. Medicinal plants in therapy. **1985**. *Bull. WHO*, *63*, 965-981
- Farnsworth, N.R. and Bingel, A.S. Problems and prospects of discovering new drugs from higher plants by pharmacological screening. **1977**. In: *New Natural Products and Plant Drugs with Pharmacological, Biological or Therapeutical Activity* (Wagner H, Wolff P, eds). Berlin:Springer, pp, 1-22
-

- 
- Farnsworth, N.R. Biological and phytochemical screening of plants. **1966.** *J. Pharm. Sci.*, *55*, 225-276
- Farnsworth, N.R. Screening plants for new medicines. **1988.** In: Biodiversity (Wilson EO, ed). Washington DC:National Academy Press, pp, 83-97
- Ferreira, A.M.V.D.; Carvalho, M.J.M.; Carvalho, L.H.M. Studies on the biological activity of the plants of the family Thymelaeaceae (1990-2007). **2009.** *Nat. Prod.*, *12*, 293-303
- Fischer, H.; Römer, A.; Ulbricht, B. and Arens, H. A new biscoumarin glucoside ester from *Ruta chalepensis* cell cultures. **1988.** *Planta Med.*, *54*, 398-400
- Fox, E.M. and Howlett, B.J. Secondary metabolism: regulation and role in fungal biology. **2008.** *Curr. Opin. Microbiol.*, *11*, 1-7
- Garcia-Grandos, A. and Saenz de Buruaga, J.M. Thymelaeaceae Phytochemistry I. Diterpenes, triterpenes and sterols of *Thymelaea hirsuta* L. leaves. **1980.** *Anales de Quimico, Series C*, *76*, 94-95
- Garcia-Grandos, A. and Saenz de Buruaga, J.M. Thymelaeaceae Phytochemistry II. Flavone and coumarin components of *Thymelaea tartonraira* L. **1980.** *Anales de Quimica, Series C*, *76*, 96-97
- George, V. and Rishi, A.K. Constituents of *Thymelaea passerina*. **1982.** *Fitoterapio*, *53*, 191-192.
- Gharbo. S.A.; Khafagy, S.M. and Sarg, T.M. Phytochemical investigation of *Thymelaea hirsuta*. **1970.** *J. Pharma. Sc.*, *11*, 101-106
- Giridharan, P.; Verekar, S.A.; Khanna, A.; Mishra, P.D.; Deshmukh, S.K. Anticancer activity of sclerotiorin, isolated from an endophytic fungus *Cephalotheca faveolata* Yaguchi, Nishim. & Udagawa. **2012.** *Indian J. Exp. Biol.*, *50*, 464-468
- Gmira, N.; Doumi, L.; Bsaibis, F. and Hmamouch, S. *Thymelaea lythroides* (Barr. et Murb): Approche ethnobotanique et Activité Biologique. **2007.** *Rev. Microbiol. Ind. San. et Environn.*, *1*, 31-43
-

- 
- Goldfrank, L. Lewin N.; Flomenbaum N.; Howland M.A. The Pernicious Panacea: Herbal Medicine. **1982**. *Hosp. Physician*, *10*, 64-86
- González, M.E.; Martínez-Abarca, F.; Carrasco, L. Flavonoids: Potent inhibitors of poliovirus RNA synthesis. **1990**. *Antivir. Chem. Chemother.*, *1*, 203-209
- Gregory, E.M.; Turner, W.B. 7-Episclerotiorin. **1963**. *Chem. Ind.*, *40*, 1625-1631
- Guerin, P. Sur la presence d'un champignon dans l'ivraie. **1989**. *J. Botanique.*, *12*, 230-238
- Gunatilaka A.A.L. Natural products from plant-associated microorganisms: distribution, structural diversity, bioactivity, and implication of their occurrence. **2006**. *J. Nat. Prod.*, *69*, 509-526
- Hamburger, M., Hostettmann, K. Bioactivity in plants: the link between phytochemistry and medicine. **1991**. *Phytochemistry*, *30*, 3864-3874
- Harvey, A. Strategies for discovering drugs from previously unexplored natural products. **2000**. *Drug Discov. Today*, *5*, 294-300
- Haste, N.M.; Perera, V.R.; Maloney, K.N.; Tran, D.N.; Jensen, P.; Fenical, W.; Nizet, V.; Hensler, M.E. Activity of the streptogramin antibiotic etamycin against methicillin-resistant *Staphylococcus aureus*. **2010**. *J. Antibiotics*, *63*, 219-223
- Ho, W.S., Xue, J.Y.; Samuel, S.M. Sun, Ooi, V.E.C. and Li Y.L. Antiviral activity of Daphnoretin isolated from *Wikstoemia indica*. **2010**. *Phytotherapy research.*, *24*, 657-661
- Hu, X.; Jin, H.; Yan, L.; Zhang, W. Chemical constituents of *Daphne retusa*. **2011**. *Tianran Chanwu Yanjiu Yu Kaifa*, *23*, 20-24
- Huang, S.Z.; Zhang, X.J.; Li, X.Y.; Jiang, H.Z.; Ma, Q.Y.; Wang, P.C.; Liu, Y.Q.; Hu, J.M.; Zheng, Y.T.; Zhou, J.; Zhao, Y.X. Phenols with anti-HIV activity from *Daphne acutiloba*. **2012**. *Planta Medica.*, *78*, 182-185
- IUPAC, Compendium of Chemical Terminology, 2nd ed. **1997**. (the "Gold Book")
- Jemal, A.; Murray, T.; Ward, E.; Samuels, A.; Tiwari, R.C.; Ghafoor, A.; Feuer, E.J.; Thun, M.J. Cancer statistics, 2005. **2005**. *Cancer Journal for Clinicians*, *55*, 10-30
-

- 
- Ji, H.F.; Li, X.J. and Zhang, H.Y. Natural products and drug discovery. Can thousands of years of ancient medical knowledge lead us to new and powerful drug combinations in the fight against cancer and dementia? **2009**. *EMBO Rep.* *10*, 194-200
- Jin, W.; Zjawiony, J.K. 5-alkylresorcinols from *Merulius incarnates*. **2006**. *J. Nat. Prod.*, *69*, 704-706
- Kabbaj, F.Z.; Marmann, A.; El Amrani, M.; Proksch, P. and Debbab, A. *Chaetomium aureum* genomic DNA containing 18S rRNA gene, ITS1, 5.8S rRNA gene, ITS2 and 28S rRNA gene, isolate MM10S2-1. **2012**. *GenBank*. HF546136.1
- Kagamizono, T.; Nishino, E.; Matsumoto, K.; Kawashima, A.; Kishimoto, M.; Sakai, N.; He B.M.; Chen, Z.X.; Adachi, T.; Morimoto, S.; Hanada, K. Bassiatin, a new platelet aggregation inhibitor produced by *Beauveria bassiana* K-717. **1995**. *J. Antibiotics*, *48*, 1407-1412
- Kashiwada, Y.; Nonaka, G. I. and Nishioka, I. Isolation and characterization of new phydroxyphenylbutanones, stilbenes and gallic acid glucosides. **1986**. *Chem. Pharm. Bull.*, *34*, 3237-3243
- Kempken, F. and Rohlfs, M. Fungal secondary metabolite biosynthesis – a chemical defence strategy against antagonistic animals? **2010**. *Fungal Ecol.*, *3*, 107-114
- Kinghorn, A.D. The discovery of drugs from higher plants. **1994**. *Biotechnology*, *26*, 81-108
- Kjier J. New Natural Products from Endophytic Fungi from Mangrove Plants – Structure Elucidation and Biological Screening. **2009**. Dissertation
- Kogel, K.H.; Franken, P., Hückelhoven, R. Endophyte or parasite - what decides? **2006**. *Curr. Opin. Plant Biol.*, *9*, 358-363
- Kogiso, S.; Hosozawa, S.; Wada, K.; Munakata, K. Daphneolone in roots of *Daphne odora*. **1974**. *Phytochemistry*, *13*, 2332-2334
- Kreher, B.; Neszmélyi, A. and Wagner, H. Triumbellin, a tricoumarin rhamnopyranoside from *Daphne mezereum*. **1990**. *Phytochemistry*, *29*, 3633-3637
-

- 
- Kuo, Y.C.; Lin, L.C.; Don, M.J.; Liao, H.F.; Tsai, Y.P.; Lee, G.H. and Chou, C.J. Cyclodesipeptide and dioxomorpholine derivatives isolated from the insectbody portion of the fungus *Cordyceps cicadae*. **2002**. *J. Chin. Med.*, *13*, 209-219
- Kusari, S. and Spiteller, M. Metabolomics of endophytic fungi producing associated plant secondary metabolites: progress, challenges and opportunities. **2012**. In *Metabolomics*, U. Roessner, ed. pp. 241-266
- Kusari, S.; Hertweck, C. and Spiteller, M. Chemical ecology of endophytic fungi: origins of secondary metabolites. **2012**. *Chem. Biol.*, *19*, 792-798
- Larsen, T.O.; Smedsgaard, J.; Nielsen, K.F.; Hansen, M.E. and Frisvad, J.C. Phenotypic taxonomy and metabolite profiling in microbial drug discovery. **2005**. *Nat. Prod. Rep.*, *22*, 672-695
- Lin, R.W.; Tsai, L.L.; Duh, C.Y.; Lee, K.H. and Chen, I.S. New Lignans and cytotoxic constituents from *Wikstroemia lanceolata*. **2004**. *Planta Med.*, *70*, 234-238
- Lingen, Z.; Seligmann, O.; Jurcic, K. and Wagner, H. Constituents of *Daphne tangutica*. **1982**. *Planta Medica.*, *45*, 172-176
- Liu, H. Extraction and Isolation of Compounds from Herbal Medicines. **2011**. In: Willow, J. and H. Liu (Eds.) *Traditional Herbal Medicine Research Methods*. John Wiley and Sons, Inc.
- Livingston, A.L.; Bickoff, E.M.; Jurd, Leonard. Isolation of daphnoretin from *Ladino clover*. **1964**. *J. Agric. Food Chem.*, *12*, 535-536
- Lozoya, X. Two decades of Mexican ethnobotany and research in plant drugs. **1994**. *Ciba Found. Symp.*, *185*, 130-140
- Meng, L.; Tao, H.; Dong, G.; Yang, T.; Zhang, W.; Zhu, W.; Huang, C. ERK1/2 and Akt pathway activated during (3R,6R)-bassiatin(1)-induced apoptosis in MCF-7 cells. **2012**. *Cell Biol. Int. Rep.*, *36*, 345-348
- Mentz, L.A. and Schenkel, E.P. A coerência e a confiabilidade das indicações terapêuticas. **1989**. *Cad. Farm.*, *5*, 93-119
-



- 
- Natsume, M.; Takahashi, Y. and Marumo, S. Chlamyospore-like Cell-inducing Substances of Fungi: Close Correlation between Chemical Reactivity. **1988**. *Agric. Biol. Chem.*, *52*, 307-312
- Nawwar, M.A.M.; Ishak, M.S.; ElSherbieny, A. and Meshaal, S.A. Flavonoids of *Reaumeria mucronata* and *Thymelaea hirsuta*. **1977**. *Phytochemistry*, *16*, 1319-1326
- Neckers, L. and Workman, P. Hsp90 molecular chaperone inhibitors: are we there yet? **2012**. *Clin. cancer res.*, *18*, 64-76
- Newman, D. J. and Cragg, G.M. Natural products as sources of new drugs over the last 25 years. **2007**. *J. Nat. Prod.*, *70*, 461-477
- Newman, D. J. Natural products as lead to potential drugs: an old process or the new hope for drug discovery. **2008**. *J. Med. Chem.*, *51*, 2589-2599
- Newman, D. J.; Cragg, G. M. and Snader, K. M. The influence of natural products upon drug discovery. **2000**. *Nat. Prod. Rep.*, *17*, 215-234.
- Newman, D.J.; Cragg, G.M.; Snader, K.M. Natural products as sources of new drugs over the period 1981-2002. **2003**. *J. Nat. Prod.*, *66*, 102-1037
- Oberlies, N.H.; Kroll, D.J.; Camptothecin and taxol: historic achievements in natural products research. **2004**. *J. Nat. Prod.* *67*, 129-135
- Parkin, D.M.; Bray, F.; Ferlay, J.; Pisani, P. Estimating the world cancer burden: Globocan 2000. **2001**. *Inter. J. Cancer*, *94*, 153-156
- Parkin, D.M. Global cancer statistics in the year 2000. **2001**. *Lancet Oncol.*, *2*, 533-543
- Payne, D.J.; Hueso-Rodríguez, J.A.; Boyd, H.; Concha, N.O.; Janson, C.A.; Gilpin, M.; Bateson, J.H.; Cheever, C.; Niconovich, N.L.; Pearson, S.; Rittenhouse, S.; Tew, D.; Díez, E.; Pérez, P.; Fuente, J.; Rees M.; Rivera-Sagredo, A. Identification of a Series of Tricyclic Natural Products as Potent Broad-Spectrum Inhibitors of Metallo- $\beta$ -Lactamases. **2002**. *Antimicrob. Agents Chemother.*, *6*, 1880-1886
-

- 
- Payne, G.; Bringi, V.; Prince, C.; Shuller, M. The quest for commercial production of chemicals from plant cell culture. **1991**. In: *Plant Cell and Tissue Culture in Liquid Systems*, Oxford University Press, Oxford
- Phillipson, J.D.; Anderson, L.A. Ethnopharmacology and Western medicine. **1989**. *J Ethnopharmacol.*, *25*, 61-72
- Piekarz, R.; Bates, S. A review of depsipeptide and other histone deacetylase inhibitors in clinical trials. **2004**. *Curr. Pharm. Des.*, *10*, 2289-98
- Rao, J.M.; Tiwari, A.K.; Srinivas, P.V.; Yadav, J.S.; Raghavan, K.V. Use of two plant phenols in the treatment of arteriosclerosis. **2002**. U.S. Pat. Appl. Publ. US 20020094351 A1 20020718
- Rastogi, R.P.; Dhawan BN. Research on medicinal plants at the Central Drug Research Institute, Lucknow (India). **1982**. *Indian J. Med. Res.*, *76*, 27-45
- Rates, S.M.K. Plants as source of drugs. **2001**. *Toxicon*, *39*, 603-613
- Raza, M.A. Role for physicians in ethnopharmacology and drug discovery. **2006**. *J. Ethnopharmacol.*, *104*, 297-301
- Redman, R.S.; Dunigan, D.D.; Rodriguez R.J. Fungal symbiosis: from mutualism to parasitism, who controls the outcome, host or invader? **2001**. *New Phytol.*, *151*, 705-716
- Risk, A.M. and Rimpler, H. Isolation of daphnoretin and  $\beta$ -sitosterol- $\beta$ -p-glucoside from *Thymelaea hirsuta*. **1972**. *Phytochemistry*, *11*, 473-475
- Risk, A.M.; Hammouda, F.M. and Ismail, S.I. Phytochemical investigation of *Thymelaea hirsuta* III. Coumarins. **1975**. *Acta Chimica Academicum Hungaricae*, *85*, 107-115
- Rizk, A.M.; Hammouda, F.M. and Ismail, S.I. Phytochemical investigation of *Thymelaea hirsuta* II. Lipid fraction. **1974**. *Planta Medico.*, *26*, 346-358
- Rohlf, M. and Churchill, A.C.L. Fungal secondary metabolites as modulators of interactions with insects and other arthropods. **2011**. *Fungal Genet. Biol.*, *48*, 23-34
- Saikkonen, K. Forest structure and fungal endophytes. **2007**. *Fungal Biol. Rev.*, *21*, 67-74
-

- 
- Saikkonen, K.; Faeth, S.H.; Helander, M.; Sullivan, T.J. Fungal endophytes: a continuum of interactions with host plants. **1998**. *Annu. Rev. Ecol. Syst.* *29*, 319-343
- Saikkonen, K.; Wäli, P.; Helander, M.; Faeth, S.H. Evolution of endophyte-plant symbioses. **2004**. *Trends Plant Sci.*, *9*, 275-280
- Schardl, C.L.; Liu, J.S.; White, J.F.; Finkel, R.A.; An, Z.; Siegel, M.R. Molecular phylogenetic relationships of nonpathogenic grass mycosymbionts and clavicipitaceous plant pathogens. **1991**. *Plant Syst. Evol.*, *178*, 27-41
- Schurier, M.; Sies, H.; Illek, B.; Fischer, H. Cocoa-related flavonoids inhibit CFTR-mediated chloride transport across T84 human colon epithelia. **2005**. *J. Nutr.*, *135*, 2320-2325
- Schulz, B. and Boyle, C. The endophytic continuum. **2005**. *Mycol. Res.*, *109*, 661-686
- Schulz, B.; Römmert, A.K.; Dammann, U.; Aust, H.J. and Strack, D. The endophyte-host interaction: a balanced antagonism. **1999**. *Mycol. Res.*, *103*, 1275-1283
- Schulz, B.J.E. and Boyle, C.J.C. What are endophytes? **2006**. In : Microbial Root Endophytes. eds. (Berlin: Springer-Verlag), pp. 1-13
- Sefkow, M. Enantioselective Synthesis of (-)-Wikstromol Using a New Approach via Malic Acid. **2001**. *J. Org. Chem.*, *66*, 2343-2349
- Singh, S.K.; Shanmugavel, M.; Kampasi, H.; Singh, R.; Mondhe, D.M.; Rao, J.M.; Adwankar, M.K.; Saxena, A.K.; Qazi, G.N. Chemically standardized isolates from *Cedrus deodara* stem wood having anticancer activity. **2007**. *Planta Medica.*, *73*, 519-526
- Sneider, W. Drug Prototypes and Their Exploitation. **1996**. Wiley, UK
- Song, L.; Lu, J.; Yan, P.; Tan, L.; Li, X.; Jin, Y. RP-HPLC determination of tiliroside in *Daphne genkwa*. **2009**. *Zhongguo Zhong Yao Za Zhi.*, *34*, 301-303
- Spencer, J.P.E. Flavonoids: modulators of brain function? **2008**. *British Journal of Nutrition* *99*, ES60-77
- Stierle, A.; Strobel, G.; Stierle, D. Taxol and taxane production by *Taxomyces andreanae*, an endophytic fungus of Pacific yew. **2003**. *Science*, *260*, 214-6
-

- 
- Strobel, G. A.; Stierle, A.; Stierle, D. and Hess, W. M. *Taxomyces andreanae* a proposed new taxon for a bulbiferous hypomycete associated with Pacific yew. **1993**. *Mycotaxon*, *47*, 71-78
- Strobel, G.; Daisy, B.; Castillo, U.; Harper, J. Natural products from endophytic microorganisms. **2004**. *J. Nat. Prod.*, *67*, 257-268
- Strobel, G.; Daisy, B. Bioprospecting for microbial endophytes and their natural products. **2003**. *Microbiol. Mol. Biol. Rev.* *67*, 491-502
- Sun, W.X.; Zhang, Q.; Jiang, J.Q. Chemical constituents of *Daphne giraldii* Nitsche. **2006**. *JIPB*, *48*, 1498-1501
- Sun, X.L.; Takayanagi, H.; Matsuzaki, K.; Tanaka, H.; Furuhashi, K.; Omura, S. Synthesis and inhibitory activities of isochromophilone analogues against gp120-CD4 binding. **1996**. *J. Antibio.*, *49*, 689-692
- Suzuki, Y.; Esumi, Y.; Hyakutake, H.; Kono, Y.; Sakurai, A. Isolation of 5-(8'-Z-heptadecenyl)-resorcinol from etiolated rice seedlings as an antifungal agent. **1996**. *Phytochem.*, *41*, 1485-1489
- Takenaka, Y.; Tanahashi, T.; Nagakura, N.; Hamada, N. (-)-Sclerotiorin, a major metabolite of *Penicillium hirayamae*. **1963**. *Chem. Pharm. Bull.*, *11*, 366-367.
- Takenaka, Y.; Tanahashi, T.; Nagakura, N.; Hamada, N. Production of xanthenes with free radical scavenging properties, emodin and sclerotiorin by the cultured lichen mycobionts of *Pyrenula japonica*. **2000**. *J. Biosci.*, *55*, 910-914
- Tan, R.X. and Zou, W.X. Endophytes: A rich source of functional metabolites. **2001**. *Nat. Prod. Rep.*, *18*, 448-459
- Tandon S. and R.P. Rasiig. Wikstromol, a new lignan from *Wikstroemia viridiflora*. **1976**. *Phytochemistry*, *15*, 1789-1791
- Targeted Therapies for Multiple Myeloma Tutorial- @cancer.gov.com
- Tazi, M.A.; Er-Raki, A. and Benjaafar, N. Cancer incidence in Rabat, Morocco: 2006 - 2008. **2013**. *Ecancermedicalscience*, *7*, 338
-

- 
- Tejesvi, M. V.; Nalini, M. S.; Mahesh, B.; Prakssh, H. S.; Kini, K. R.; Shetty, H. S. and Subbiah, V. New hopes from endophytic fungal secondary metabolites. **2007**. *Bol. Soc. Quim. Mes.*, *1*, 19-26
- Tomoda, H.; Matsushima, C.; Tabata, N.; Namatame, I.; Tanaka, H.; Bamberger, M.J.; Arai, H.; Fukazawa, M.; Inoue, K.; Omura, S. Structure-specific inhibition of cholesteryl ester transfer protein by azaphilones. **1999**. *J. Antibio.*, *52*, 160-170
- Tschesche, R.; Schacht, U.; Legler, O. Über Daphnorin, ein neues Cumaringlucosid aus *Daphne mezereum*. **1963**. *Naturwissenschaften*, *50*, 521-522
- Unterseher, M.; Schnittler, M. Species richness analysis and ITS rDNA phylogeny revealed the majority of cultivable foliar endophytes from beech (*Fagus sylvatica*). **2010**. *Fungal Ecol.*, *3*, 366-378
- Vlietinck, A.J. and Vanden, B.D.A. Can ethnopharmacology contribute to the development of antiviral drugs? **1991**. *J. Ethnopharmacol.*, *32*, 141-153
- Vulto, A.G. and Smet, P.A.G.M.; Meyler's Side Effects of Drugs, **1988**. 11th Ed. Elsevier, Amsterdam, pp. 999-1005.
- Wall, M.E.; Wani, M.C. Camptothecin and taxol: from discovery to clinic. **1996**. *J. Ethnopharmacol.*, *51*, 239-253
- Wang, X.; Filho, J.G.S.; Hoover, A.R.; King, J.B.; Ellis, T.K.; Powell, D.R. and Cichewicz, R.H. Chemical Epigenetics Alters the Secondary Metabolite Composition of Guttate Excreted by an Atlantic-Forest-Soil-Derived *Penicillium citreonigrum*. **2010**. *J. Nat. Prod.* *73*, 942-948
- Weber, D.; Sterner, O.; Anke, T.; Gorzalczancy, S.; Martino, V.; Acevedo, C. Phomol. A new antiinflammatory metabolite from an endophyte of the medicinal plant *Erythrina cristagalli*. **2004**. *J. Antibiot.*, *57*, 559-563
- Wei Y.; Liang G.Y.; Wang Y.; Jiang X.H.; Wang D.P.; Masao H. Chemical constituents from rhizome of *Daphne papyracea* var. *crassiuscula*. **2012**. *China Journal of Chinese Materia Medica*, *37*, 3434-7
-

- 
- Williamson, E.; Okpako, D.T.; Evans, F.J. Selection, Preparation and Pharmacological Evaluation of Plant Material. **1996**. Wiley, Chichester.
- Workman, P. and Powers, M.V. Chaperoning cell death: a critical dual role for Hsp90 in small-cell lung cancer. **2007**. *Nat. Chem. Biol.*, *3*, 455-7
- Workman, P. Combinatorial attack on multistep oncogenesis by inhibiting the Hsp90 molecular chaperone. **2004**. *Cancer Lett.*, *206*, 149-157
- Wu, Z.H.; Wang, L.B.; Gao, H.Y.; Huang, J.; Sun, B.H.; Li, S.H.; Wu, L.J. The chemical constituents of the tissue culture cells of *Daphne giraldii* callus. **2009**. *Chinese Chemical Letters*, *20*, 1335-1338
- Xu, P.; Xia, Z.; Lin, Y. Chemical constituents from *Edgeworthia gardneri* (Thymelaeaceae). **2012**. *Biochem. Sys. Ecol.*, *45*, 148-155
- Xu, W.Z.; Jin, H.Z.; Fu, J.J.; Hu, X.J.; Yan, S.K.; Shen, Y.H.; Zhang, W.; Zhang, W.D. Chemical constituents of *Daphne pedunculata*. **2008**. *Zhongguo Tianran Yaowu*, *6*, 30-32
- Yamamoto, Y.; Gaynor, R.B. Therapeutic potential of inhibition of the NF- $\kappa$ B pathway in the treatment of inflammation and cancer. **2001**. *J. Clin. Invest.*, *107*, 135-42
- Yamamoto, Y.; Nishikawa, N. Metabolic product of *Penicillium implicatum*. II. Structure of sclerotiorin. **1959**. *Yakugaku Zasshi*, *79*, 297-302
- Yamazaki, H.; Omura, S. and Tomoda, H. Xanthoradones, new potentiators of imipenem activity against methicillin-resistant *Staphylococcus aureus*, produced by *Penicillium radicum* FKI-3765-2 II. Structure elucidation. **2009**. *J. Antibio.*, *62*, 435-437
- Yang, D.J.; Hiroshi T.; Noriko T.; Rokuro M. and Satoshi O. New Isochromophilones VII and VIII Produced by *Penicillium sp.* FO-4164. **1995**. *J. Antibio.*, *49*, 223-229
- Yurek-George, A.; Cecil, A.R.L.; Mo, A.H.K.; Wen, S.; Rogers, H.; Habens, F.; Maeda, S.; Yoshida, M. The First Biologically Active Synthetic Analogues of FK228, the Depsipeptide Histone Deacetylase Inhibitor. **2007**. *J. Med. Chem.*, *50*, 5720-5726
- Yusuke, I.; Takayuki, D.; Ganesan, A.; Kazuo, S.; Takashi, T. Total Synthesis of Spiruchostatin A. **2006**. *Nippon Kagakkai Koen Yokoshu*, *86*, 1657-1664
-

Zang, L.Y.; Wei, W.; Wang, T.; Guo, Y.; Tan, R.X. and Ge, H.M. Isochromophilones from an endophytic fungus *Diaporthe sp.* **2012**. *Nat. Prod. Bioprospect.*, *2*, 117-120

Zhang H.W.; Song YC.; Tan RX. Biology and chemistry of endophytes. **2006**. *Nat. Prod. Rep.*, *23*, 753-771

Zhang, Q.; Li, H.Q.; Zong, S.C.; Gao, J.M. and Zhang, A.L. Chemical and bioactive diversities of the genus *Chaetomium* secondary metabolites. **2012**. *Mini reviews in medicinal chemistry*, *12*, 127-48

Zhang, W.; Zhang, W. D.; Liu, R. H.; Shen, Y. H.; Zhang, C.; Cheng, H. S.; Fu, P.; Shan, L. Two new chemical constituents from *Daphne odora* Thunb. var. *marginata*. **2006**. *Nat. Prod. Res.*, *20*, 1290-1294

---

---

## 8. List of Abbreviations

$[\alpha]_D$	specific rotation at the sodium D-line
br	broad signal
$CDCl_3$	deuterated chloroform
$CHCl_3$	chloroform
CI	chemical ionization
COSY	correlation spectroscopy
d	doublet
DCM	dichloromethane
dd	doublet of doublet
DEPT	distortionless enhancement by polarization transfer
DMSO	dimethyl sulfoxide
DNA	Deoxyribonucleic acid
ED	effective dose
EI	electron impact ionization
ESI	electrospray ionization
et al.	<i>et altera</i> (and others)
EtOAc	ethyl acetate
eV	electronvolt
FAB	fast atom bombardment
g	gram
HMBC	heteronuclear multiple bond connectivity
HMQC	heteronuclear multiple quantum coherence
$H_2O$	water
HPLC	high performance liquid chromatography
$H_3PO_4$	phosphoric acid
hr	hour
HR-MS	high resolution mass spectrometry
Hsp	Heat Shoc Protein
Hz	Herz
IZ	inhibition zone
L	liter



LC	liquid chromatography
LC/MS	liquid chromatography-mass spectrometry
m	multiplet
M	molar
MeOD	deuterated methanol
MeOH	methanol
mg	milligram
MHz	mega Herz
min	minute
mL	milliliter
mm	millimeter
MS	mass spectrometry
MTT	microculture tetrazolium assay
m/z	mass per charge
µg	microgram
µL	microliter
µM	micromol
NaCl	sodium chloride
ng	nanogram
NMR	nuclear magnetic resonance
NOE	nuclear Overhauser effect
NOESY	nuclear Overhauser and exchange spectroscopy
PCR	polymerase chain reaction
ppm	parts per million
PR	progesterone receptor
q	quartet
ROESY	rotating frame overhauser enhancement spectroscopy
RP 18	reversed phase C 18
RRL	rabbit reticulocyte lysate
s	singlet
t	triplet
TFA	trifluoroacetic acid
THF	tetrahydrofuran
TLC	thin layer chromatography

UV	ultra-violet
VLC	vacuum liquid chromatography

---

## 9. List of Figures

**Figure 1.1.** Steps of drug discovery process

**Figure 2.1.** Natural products of medicinal importance

**Figure 2.2.** Bioactive fungal metabolites used in medicine

**Figure 2.3.** Chemical-Ecological Schematic Interpretation of Plant-Fungus Cost-Benefit Interactions with Emphasis on Endophytic Fungi

**Figure 2.4.** Flow chart of sequence for the study of plants used in traditional medicine. Adapted from Farnsworth et al.

**Figure 2.5.** Leading Sites of New Cancer Cases and Deaths Among African Americans, 2013 Estimates

**Figure 2.6.** Age-Adjusted Cancer Incidence and Mortality Rates Among African Americans by Sex, 1975 to 2009

**Figure 2.7.** The expression of Hsp90 in normal and multiple myeloma cell

**Figure 2.8.** Chemical structures of selected Hsp90 inhibitors

**Figure 2.9.** Inhibition of Hsp90 leads to apoptosis in small-cell lung cancer (SCLC)

**Figure 3.1.** *Thymelaea lythroides*. (1: Aerial part of *T. lythroides*. 2: Leaf. 3: Flower. 4: Flower male. 5: Flower female. 6: Seed)

**Figure 3.2** Collection area of *Thymelaea lythroides*.

**Figure 3.3.** Pure fungal strain from *Thymelaea lythroides*

**Figure 3.4.** *Chaetomium aureum* (A: *Thymelaea lythroides*; B: pure strain in plate agar; C: Culture on solid rice medium)

**Figure 3.5.** Extraction and fractionation of solid rice culture

**Figure 4.1.** Use of Traditional Medicine according to the origin

**Figure 4.2.** HPLC chromatogram of methanol fraction of *Thymelaea lythroides*

**Figure 4.3.**  $^1\text{H}$ - $^1\text{H}$  NMR COSY

**Figure 4.4.** Selected  $^{13}\text{C}$ - $^1\text{H}$  NMR HMBC correlations

**Figure 4.5 A)**  $^1\text{H}$ - $^1\text{H}$  COSY correlations **B)** selected  $^{13}\text{C}$ - $^1\text{H}$  NMR correlations of **2**

**Figure 4.6.**  $^1\text{H}$ - $^1\text{H}$  COSY correlations of **3**

**Figure 4.7. A)**  $^1\text{H}$ - $^1\text{H}$  COSY correlations **B)** Selected  $^{13}\text{C}$ - $^1\text{H}$  NMR correlations of **4**

**Figure 4.8.** The partial structure 1 and 2

**Figure 4.9. A)**  $^1\text{H}$ - $^1\text{H}$  COSY correlations **B)** selected  $^{13}\text{C}$ - $^1\text{H}$  NMR correlations of **5**

**Figure 4.10. A)**  $^1\text{H}$ - $^1\text{H}$  COSY correlations **B)** selected  $^{13}\text{C}$ - $^1\text{H}$  NMR correlations of **6**

**Figure 4.11.** Structure of Daphnorin (R= H)

- 
- Figure 4.12.** Selected correlations of partial structure A
- Figure 4.13.** A)  $^1\text{H}$ - $^1\text{H}$  COSY correlations. B) Selected  $^1\text{H}$ - $^{13}\text{C}$  HMBC correlation of **8**
- Figure 4.14.** Photos of *Chaetomium aureum*
- Figure 4.15.** Comparison of the 11 media cultures of *Chaetomium aureum*. A- Solid rice media. B- liquid Wickerham medium. C- Ten solid media cultures
- Figure 4.16.** A)  $^1\text{H}$ - $^1\text{H}$  COSY correlations of **1** B) selected  $^{13}\text{C}$ - $^1\text{H}$  HMBC correlations
- Figure 4.17.**  $^1\text{H}$ - $^1\text{H}$  COSY correlations of **10**
- Figure 4.19.** A)  $^1\text{H}$ - $^1\text{H}$  COSY correlations B) selected  $^1\text{H}$ - $^{13}\text{C}$  HMBC correlations of **13**
- Figure 4.18.** A)  $^1\text{H}$ - $^1\text{H}$  COSY correlations B) selected  $^{13}\text{C}$ - $^1\text{H}$  HMBC correlations of **12**
- Figure 4.20.**  $^1\text{H}$ - $^1\text{H}$  ROESY correlations
- Figure 4.21.**  $^1\text{H}$ - $^1\text{H}$  NMR COSY
- Figure 4.22.** Selected  $^{13}\text{C}$ - $^1\text{H}$  HMBC correlations
- Figure 4.23.** The structure of xanthorathode D<sub>1</sub>
- Figure 4.24.**  $^1\text{H}$  NMR of the overlapped proton H-6' and H-7'
- Figure 4.25.** The comparison of H-C-3' of 14/15 and 16/17 in  $^{13}\text{C}$ - $^1\text{H}$  HMBC NMR
- Figure 4.26.** Selected  $^{13}\text{C}$ - $^1\text{H}$  HMBC NMR correlations of **16/17**
- Figure 4.27.**  $^1\text{H}$  - $^1\text{H}$  COSY NMR correlations of **18**
- Figure 4.28.** Selected  $^{13}\text{C}$ - $^1\text{H}$  HMBC NMR correlations of **18**
- Figure 4.29.** Selected  $^1\text{H}$  - $^1\text{H}$  ROESY NMR correlations of **18**
- Figure 4.30.** Effect of **1-6** on the Hsp90 chaperoning machine *in vitro*.
- Figure 4.31.** Comparison of  $^1\text{H}$  NMR and the molecular weight of sclerotiorin and deacetylsclerotiorin
- Figure 4.32.** Comparison of sclerotiorin (**2**) and deacetylsclerotiorin (**6**).
- Figure 4.33.** A- Comparison of the effect of sclerotiorin (**2**) and deacetylsclerotiorin (**6**)
- Figure 5.1.** Photosynthesis, respiration, leaf and water exchange and translocation of sugar in plant (Silverstein et al., 2008)
- Figure 5.2.** Diversity of established Hsp90 clients within the human kinome.
- Scheme 3.1.** Isolation and purification of plant extract *Thymelaea lythroides*
- Scheme 3.2.** Isolation and purification of plant extract *Chaetomium aureum*
- Scheme 5.1.** The major biosynthesis pathways of secondary metabolites
- Scheme 5.2.** The shikimate pathway: aromatic amino acids and phenylpropanoids
- Scheme 5.3.** The formation of the poly- $\beta$ -keto chain
-

---

---

## 10. List of Tables

**Table 2.1.** Selected physicians and their contributions in ethnopharmacological investigations

**Table 2.2.** Drugs derived from plants, with their ethnomedical correlations and sources.

**Table 3.1.** Taxonomy of isolated fungi.

**Table 3.2:** List of Protein kinases and their substrates

**Table 4.1.** The incidence of cancer according to its localization

**Table 4.2.** The incidence of cancer according to age

**Table 4.3.** Medicinal plants used in traditional medicine by the patients of the National Institute of Oncology in Rabat

**Table 4.4.** List of plants reported to have anticancer activity

**Table 4.5.** Preliminary biological screening assays of the different fractions of *Thymelaea lythroides*

**Table 4.6.** Comparison of  $^1\text{H}$  and  $^{13}\text{C}$  NMR chemical shifts of **1** with Bassiatin

**Table 4.7.** The  $^1\text{H}$  and  $^{13}\text{C}$  chemical shifts of **2** and **3**

**Table 4.8.**  $^1\text{H}$  and  $^{13}\text{C}$  NMR chemical shifts of (-)-wikstromol (**4**)

**Table 4.9.** Comparison of  $^1\text{H}$  and  $^{13}\text{C}$  NMR chemical shifts of (+)-sesamin (**5**)

**Table 4.10.** Comparison of  $^1\text{H}$  and  $^{13}\text{C}$  NMR chemical shifts of **5** with Daphnoretin

**Table 4.11.** Comparison of  $^1\text{H}$  and  $^{13}\text{C}$  NMR chemical shifts of **7** with Rutarensin

**Table 4.12.** Comparison of  $^1\text{H}$  and  $^{13}\text{C}$  NMR chemical shifts of **8** with *trans*-Tiliroside

**Table 4.13.** Cytotoxicity test results for the compounds isolated from *Thymelaea lythroides*

**Table 4.14.** Protein kinase assay results for the compounds isolated from *Thymelaea lythroides*

**Table 4.15.** Preliminary biological screening assays of the five pure strains

**Table 4.16.**  $^1\text{H}$  and  $^{13}\text{C}$  NMR chemical shifts of sclerotin and its derivatives

**Table 4.17.** Comparison of  $^1\text{H}$  and  $^{13}\text{C}$  NMR chemical shifts of **13** with SB 236050

**Table 4.18.**  $^1\text{H}$  and  $^{13}\text{C}$  NMR chemical shifts of xanthoradones A, D and E

**Table 4.19.**  $^1\text{H}$  chemical shifts of the atropisomers of xanthoradone D and E

**Table 4.20.**  $^1\text{H}$  and  $^{13}\text{C}$  NMR data of **18** in MeOH at 600 MHz for  $^1\text{H}$  and 150 for  $^{13}\text{C}$ .

**Table 4.21.** Cytotoxicity test results for the compounds isolated from endophytic fungus *Chaetomium aureum*

**Table 4.22.** Protein kinase assay results for the compounds isolated from endophytic fungus *Chaetomium aueum*

**Table 4.23.** Antibacterial test results for the new compounds isolated from endophytic fungus *Chaetomium aureum*

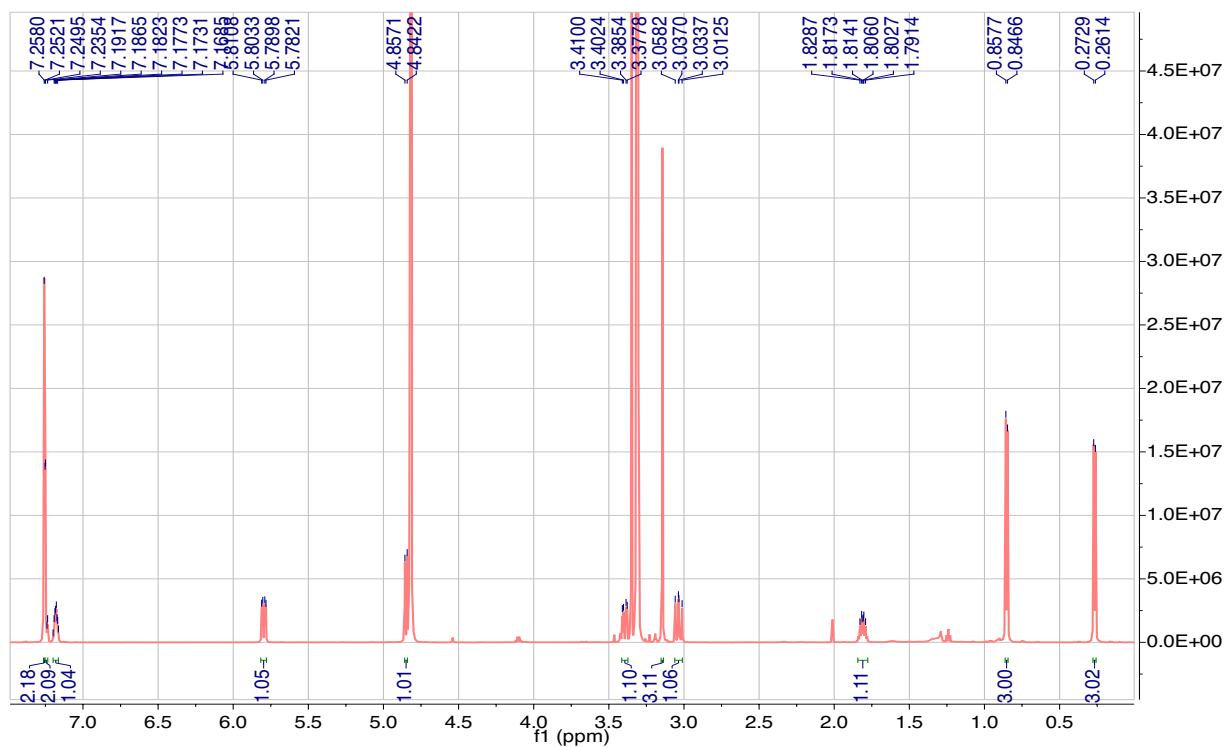
**Table 5.1.** Bioactive metabolites from the genus *Thymelaea*

**Table 5.2.** Distribution of Hsp90 clients within kinase families

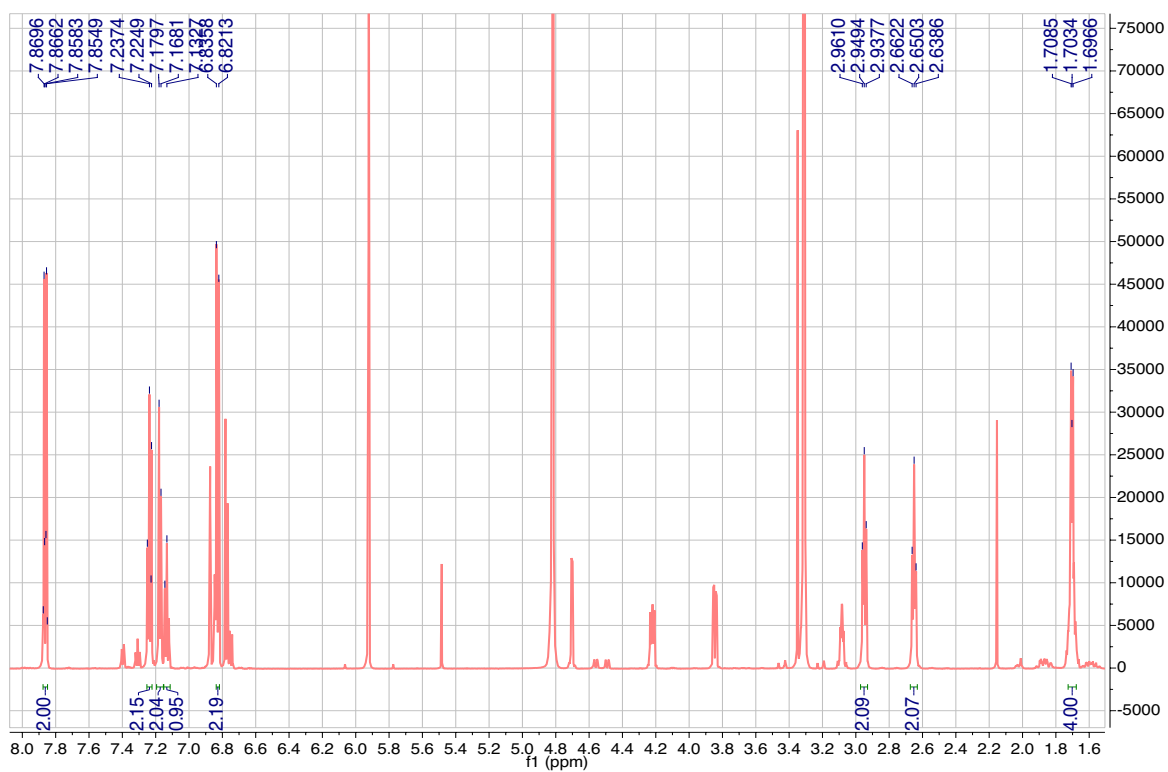
**Table 6.1.** Summary of the isolated compounds

## 11. Attachments

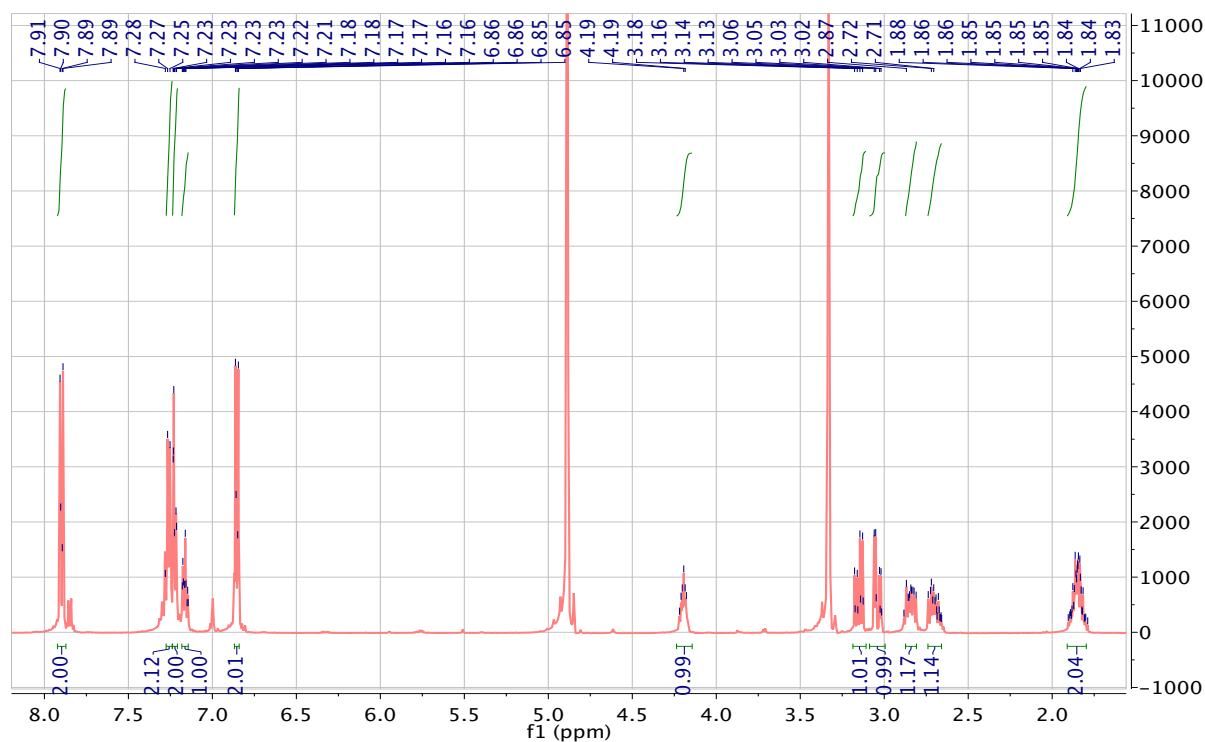
Attachment 1. The  $^1\text{H}$  NMR spectrum of bassiatin (1)



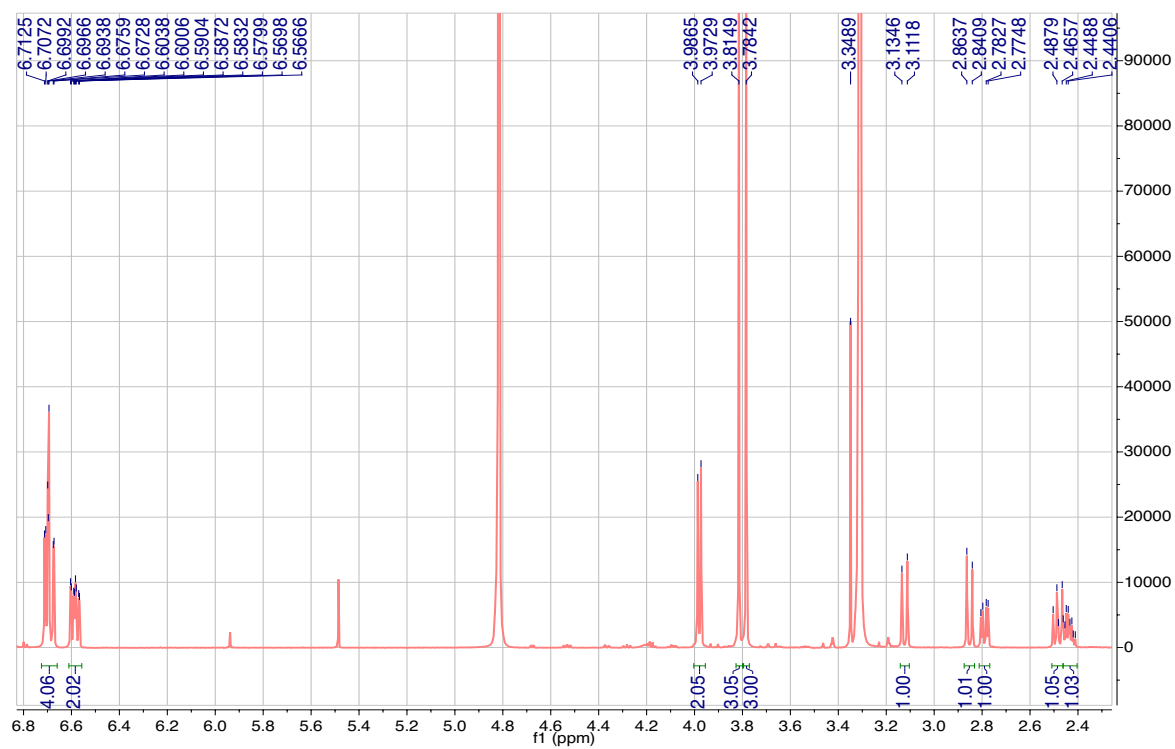
Attachment 2. The  $^1\text{H}$  NMR spectrum of daphneone (2)



Attachment 3. The  $^1\text{H}$  NMR spectrum of daphneolone (3)

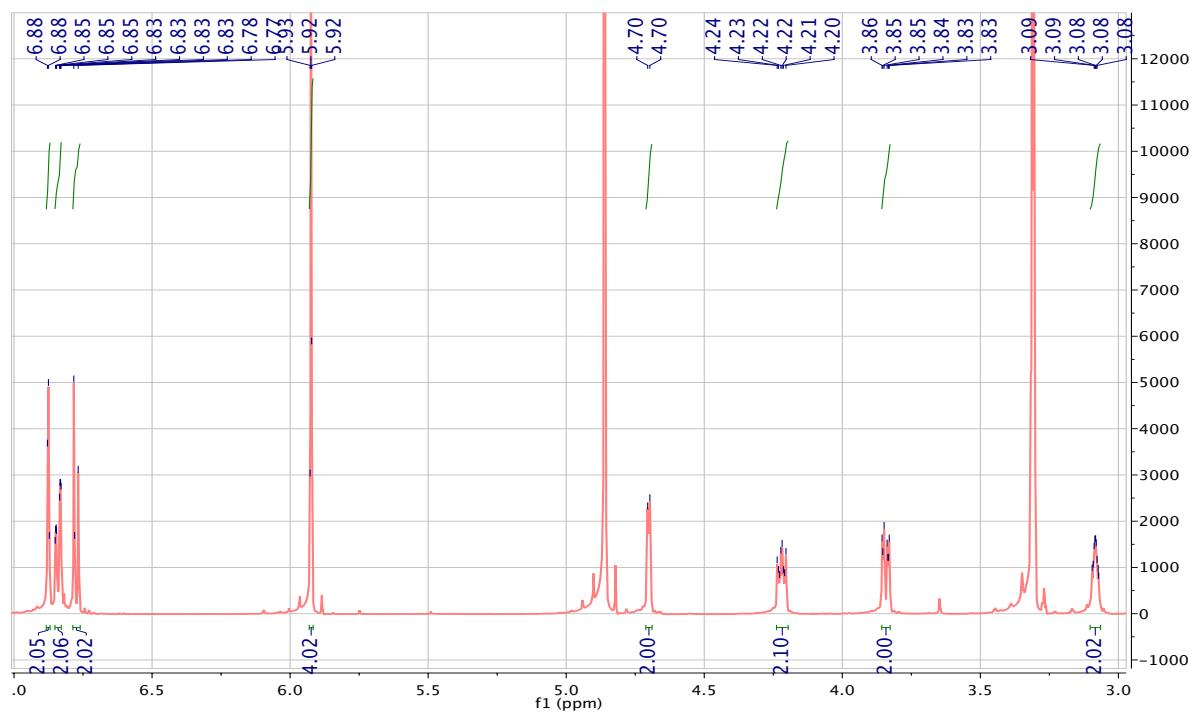


Attachment 4. The  $^1\text{H}$  NMR spectrum of (-)-wikstromol (4)

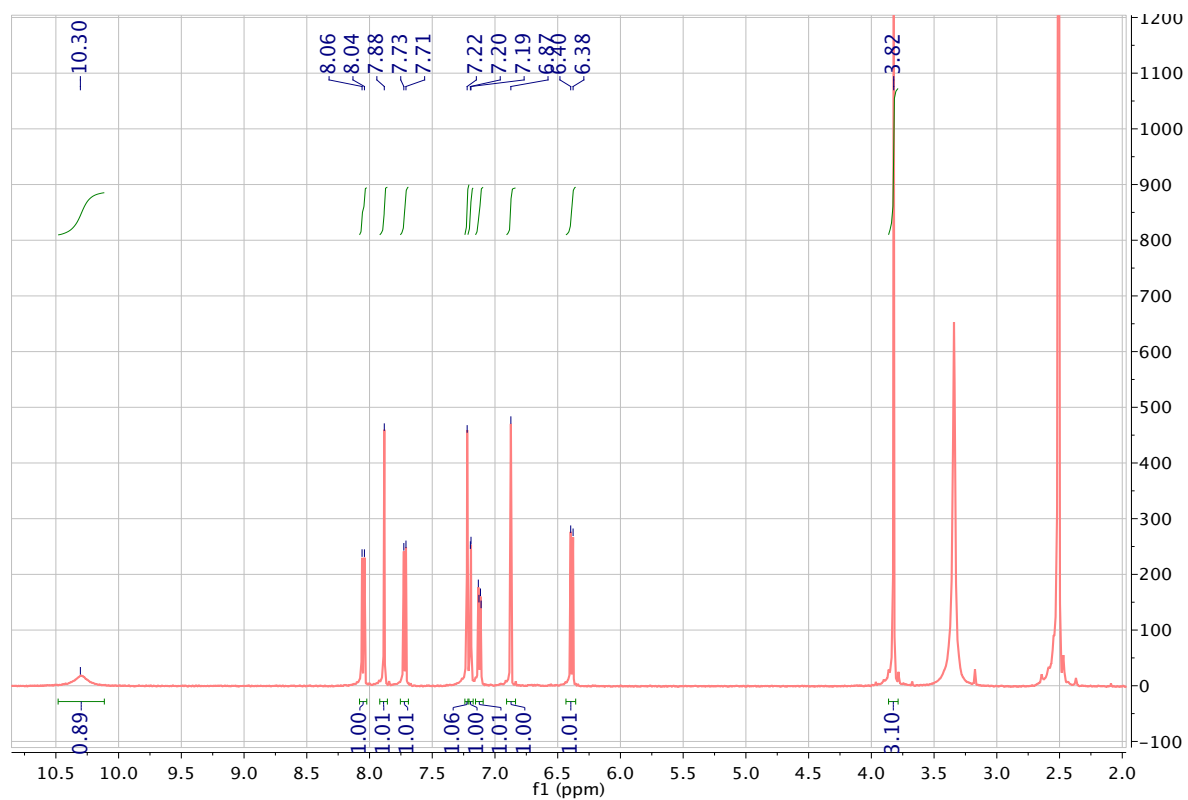




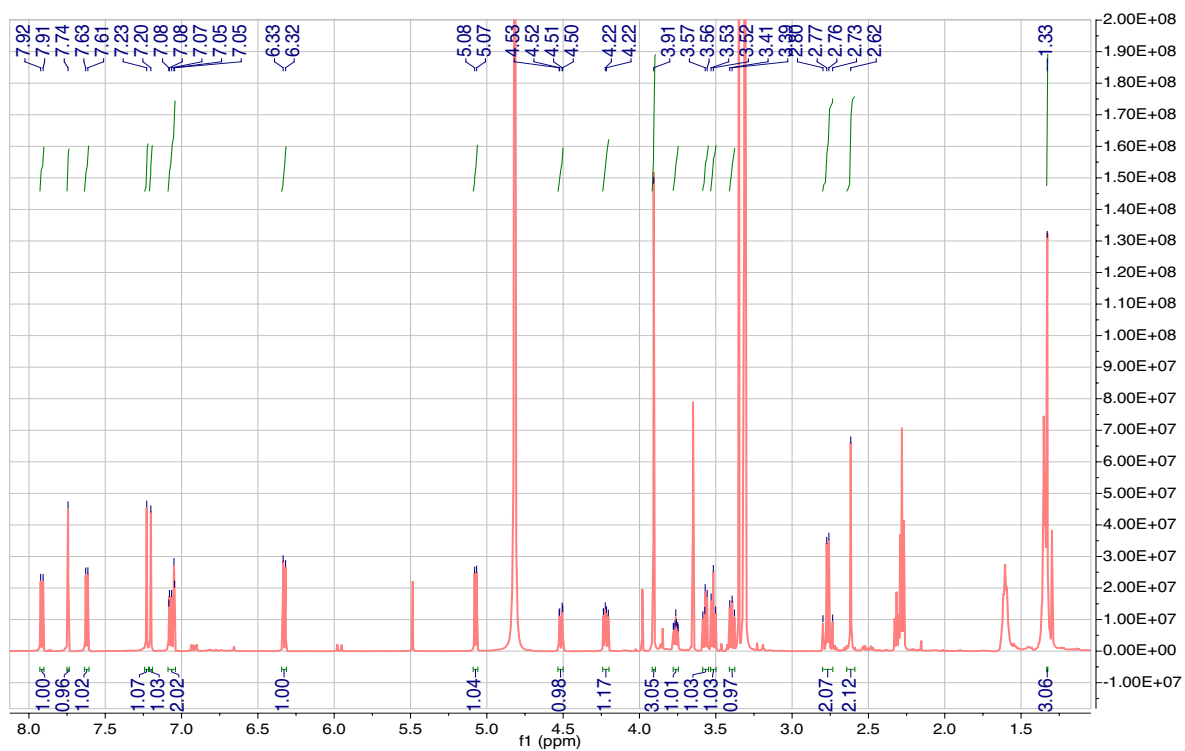
Attachment 5. The  $^1\text{H}$  NMR spectrum of  $\delta$ -sesamin (5)



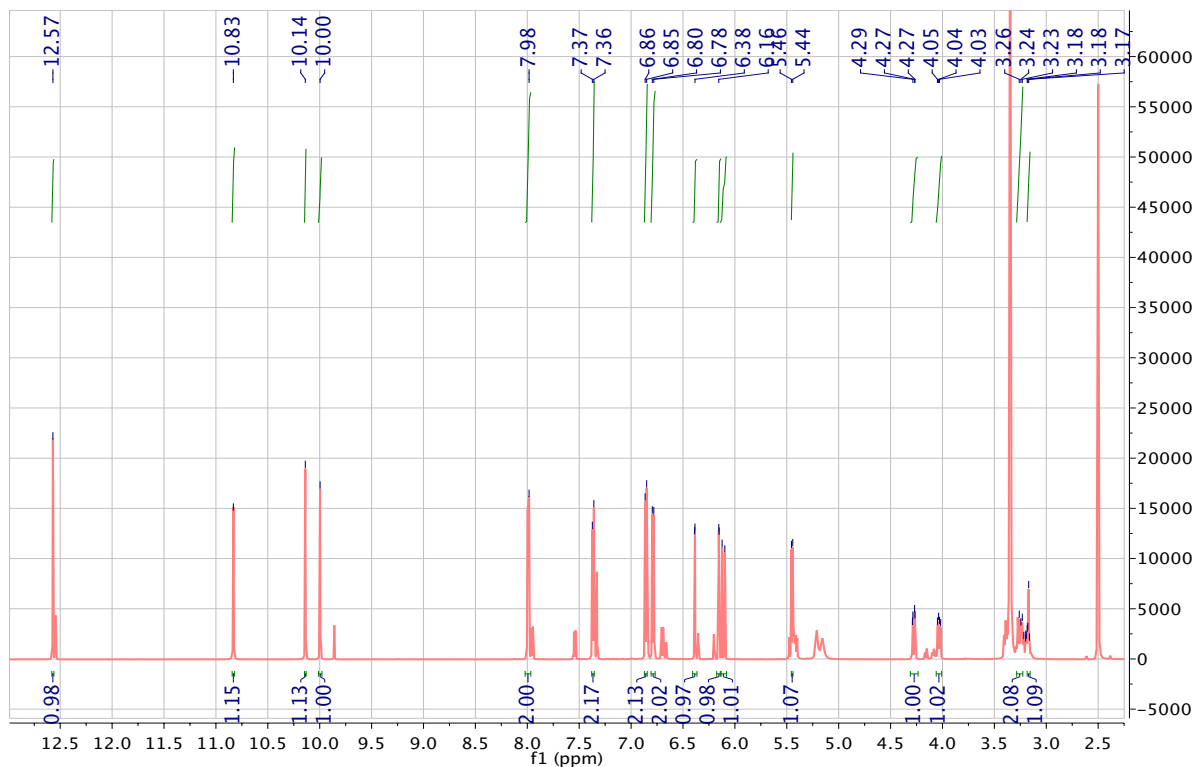
Attachment 6. The  $^1\text{H}$  NMR spectrum of daphnoretin (7)



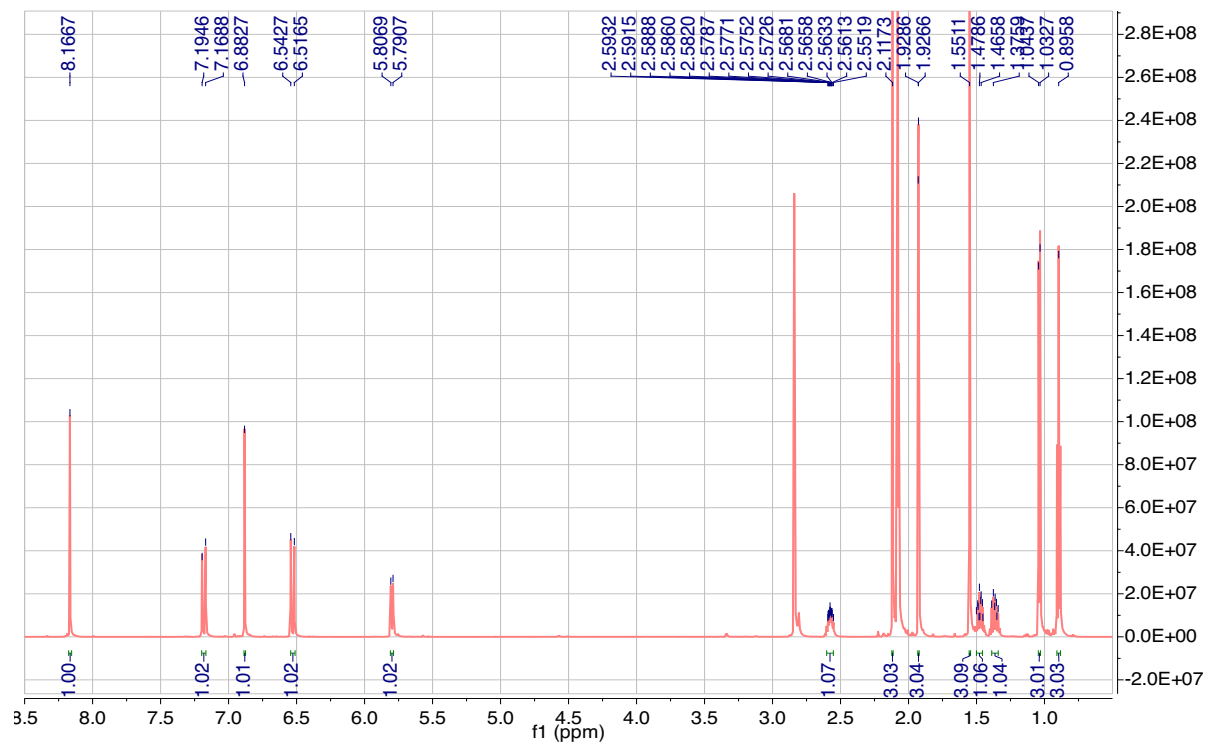
Attachment 7. The  $^1\text{H}$  NMR spectrum of rutarensin (7)



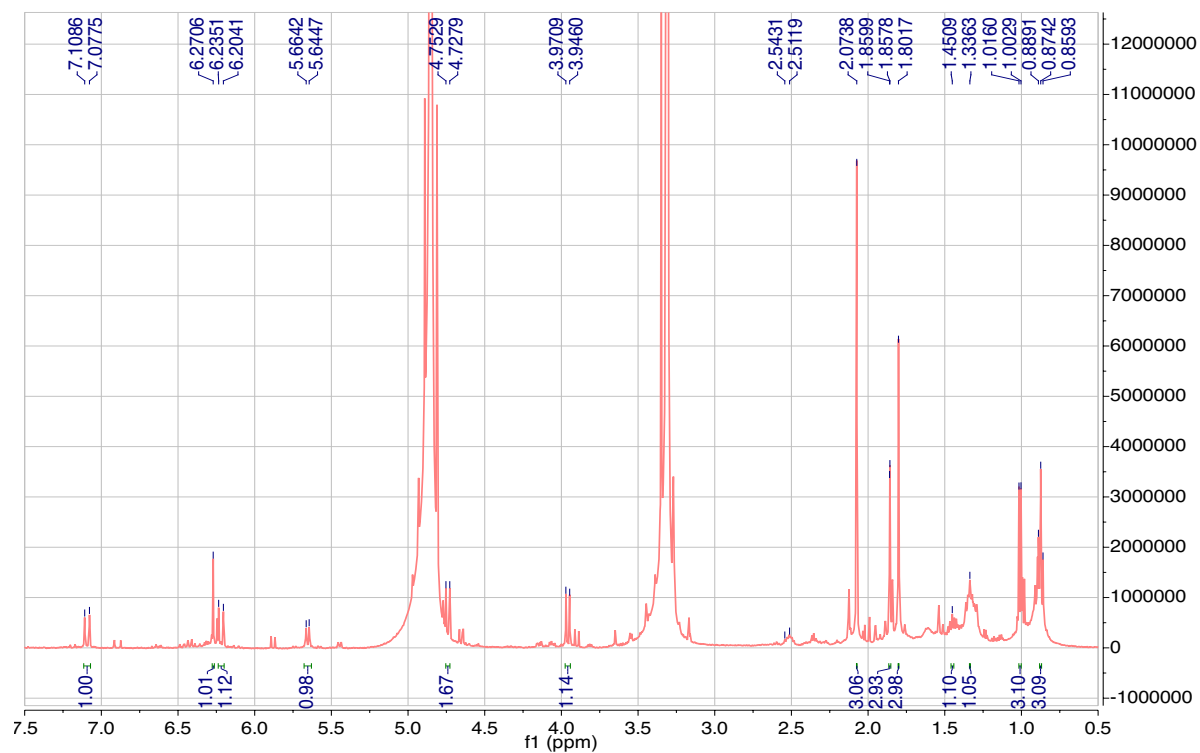
Attachment 8. The  $^1\text{H}$  NMR spectrum of *trans*-tiliroside (8)



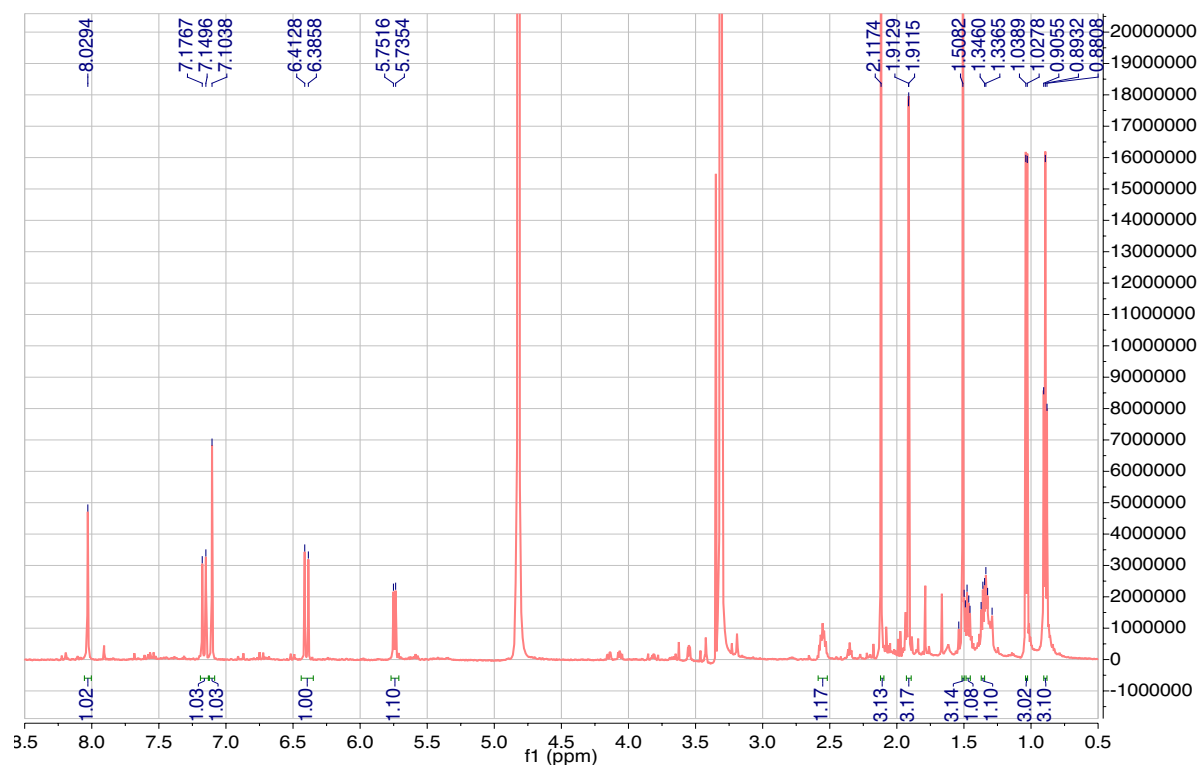
Attachment 9. The  $^1\text{H}$  NMR spectrum of (+)-sclerotiorin (9)



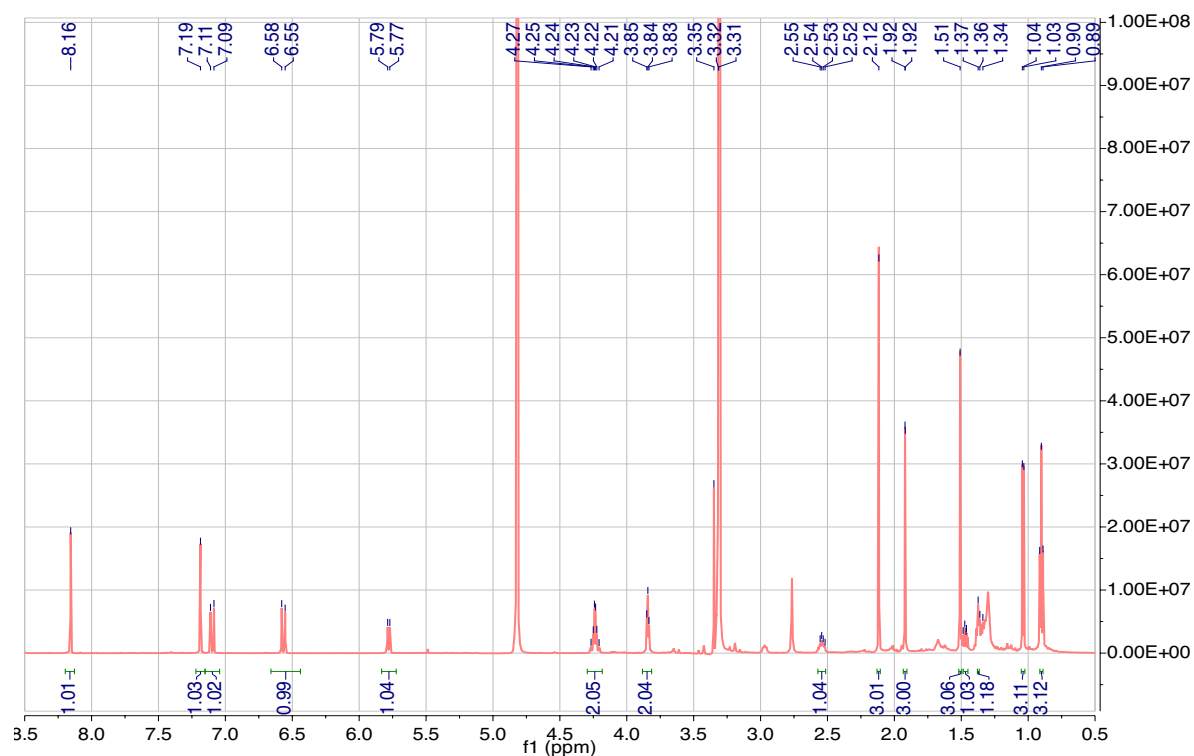
Attachment 10. The  $^1\text{H}$  NMR spectrum of (+)-isochromophilone VII (10)



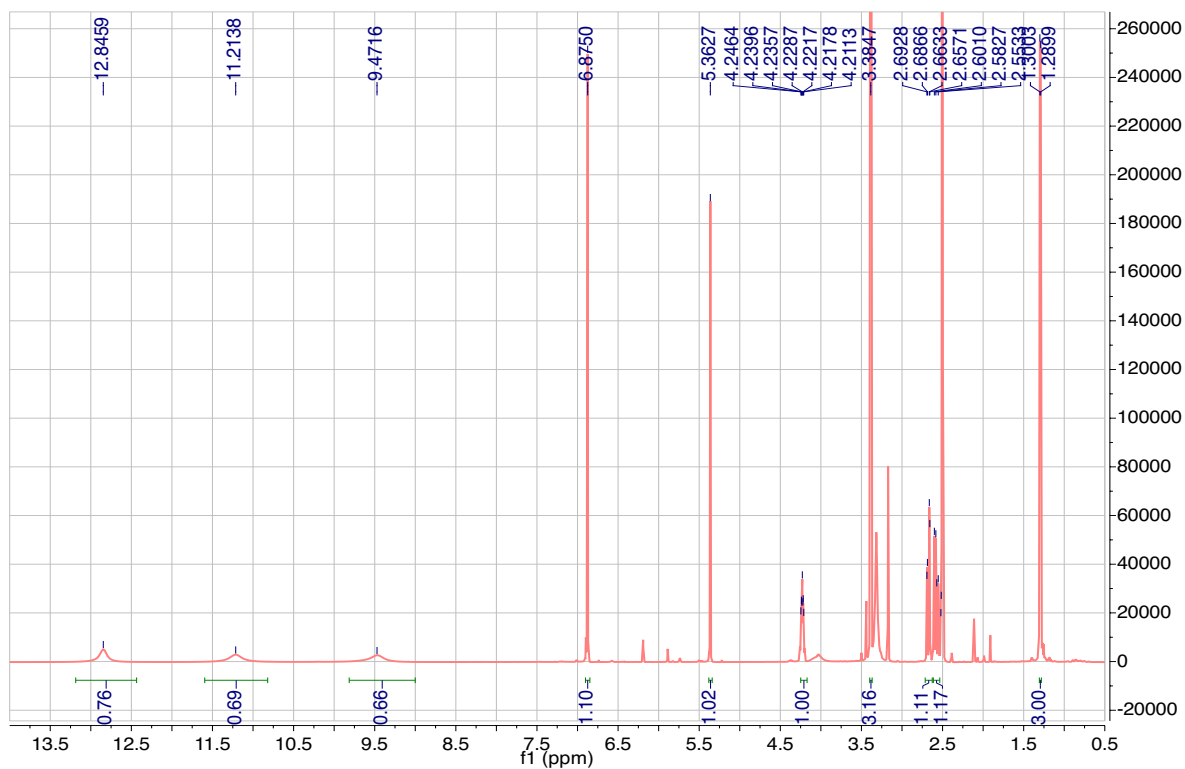
Attachment 11. The  $^1\text{H}$  NMR spectrum of (+)-sclerotioramin (11)



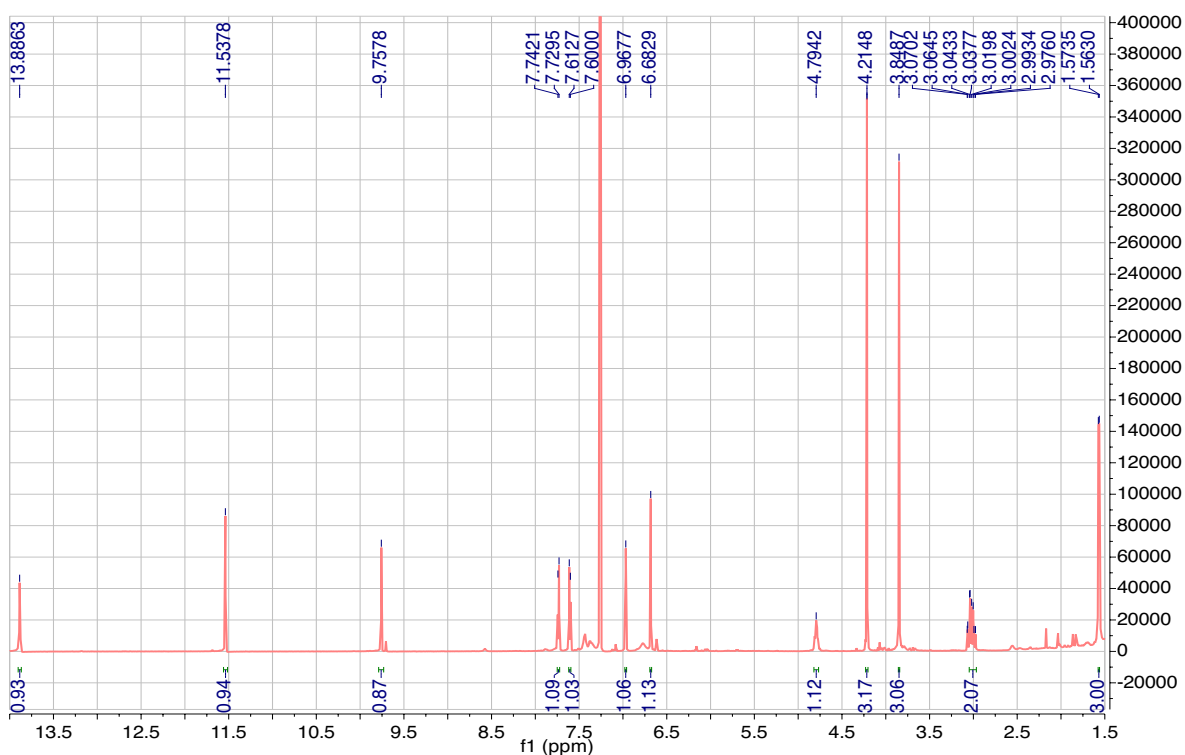
Attachment 12. The  $^1\text{H}$  NMR spectrum of (+)-isochromophilone VI (12)



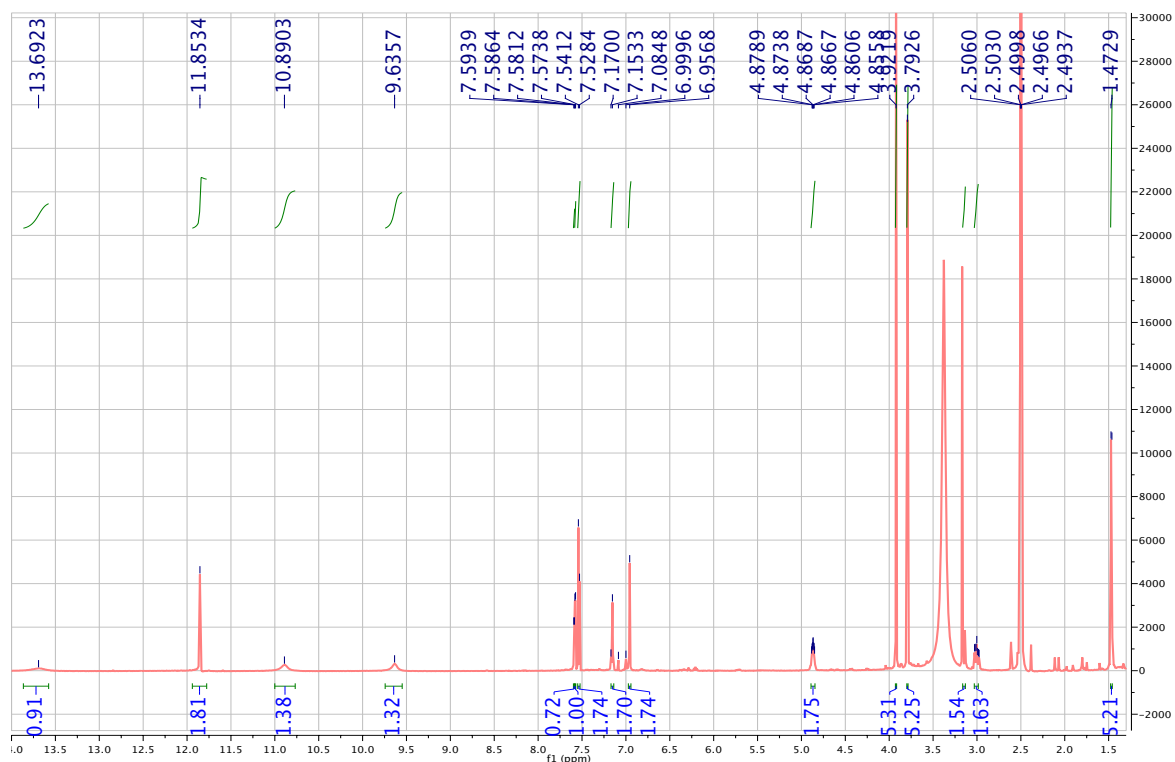
Attachment 13. The  $^1\text{H}$  NMR spectrum of SB 236050 (13)



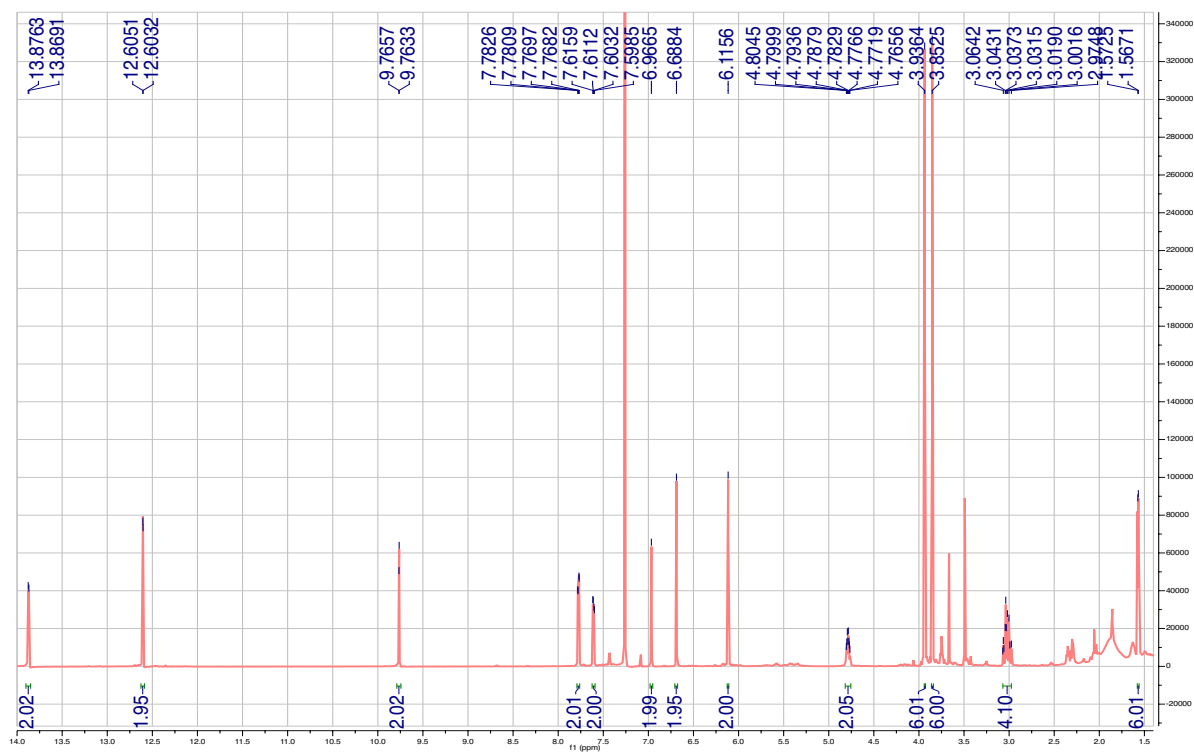
Attachment 14. The  $^1\text{H}$  NMR spectrum of xanthoradone D<sub>1</sub> (14)



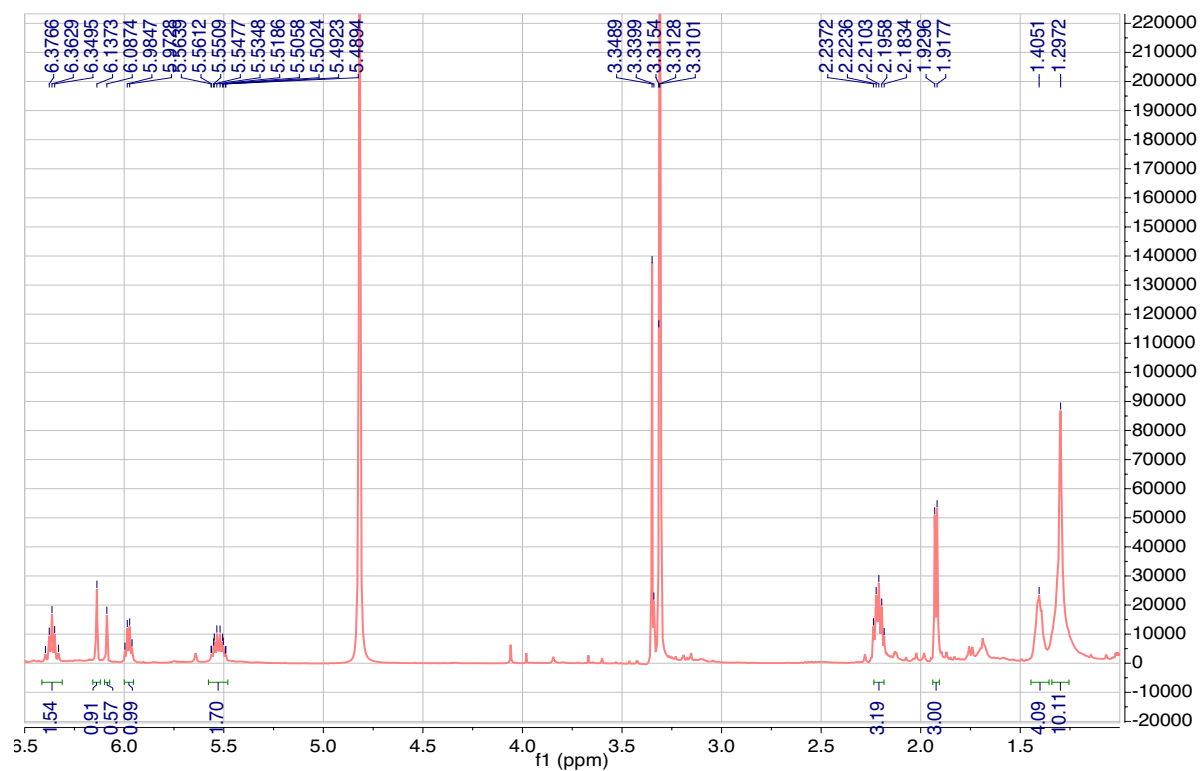
Attachment 14/15. The  $^1\text{H}$  NMR spectrum of xanthoradone D<sub>1</sub> and D<sub>2</sub> (14/15)



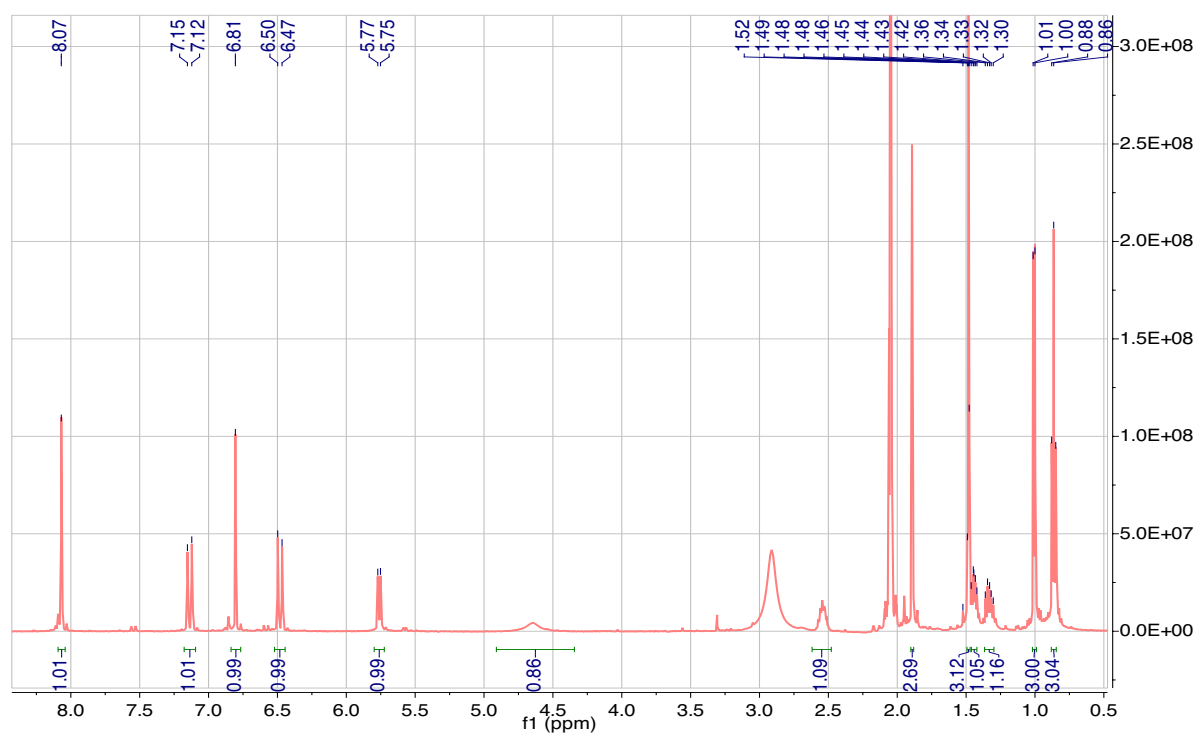
Attachment 16/17. The  $^1\text{H}$  NMR spectrum of xanthoradone E<sub>1</sub> and E<sub>2</sub> (16/17)



Attachment 18. The  $^1\text{H}$  NMR spectrum of chaetoresorcinol (**18**)



Attachment 19. The  $^1\text{H}$  NMR spectrum of (+)-deacetylsclerotiorin (**19**)



# Dr. rer. nat. Fatima Zahra Kabbaj

## Curriculum vitae

### Personal Data

---

Name	Fatima Zahra Kabbaj
Birth date and place	22.09.1983, Rabat, Morocco
Marital Status	Married
E-Mail	kabbaj.fatimazahra@gmail.com

### Study

---

12 April 2010 / 25 November 2013	Ph D studies in "Chemistry of Natural Products" at the University 'Bergische Universität Wuppertal' in Germany, Laboratory of Organic Chemistry under the supervision of Prof. Hans-Josef Altenbach,
January 2009 / 25 November 2013	Ph D studies in "Science of Medicine" at University Mohammed V-Souissi, Faculty of Medicine and Pharmacy, Rabat, Morocco. Laboratory Pharmacology and Toxicology under the supervision of Prof. Moulay El Abbes Faouzi,
2008	Master Degree in Immunological and Biochemical Genius (IBG) at the university Mohammed V, Faculty of Science, Rabat. Mention: very well.
04/2008	Distance Learning General Course on Intellectual Property issued by the Worldwide Academy of the World Intellectual Property
2006	License in animal biology option Immunology at the university Mohammed V, Faculty of Science, Rabat
2004	University certification in Biology Geology at the university Mohammed V, Faculty of Science, Rabat. Mention: good.
2001	High school diploma experimental sciences, Lalla Nezha secondary school, Rabat



## Professional experiences (training)

---

November 2011	Cooperation with the Institute of Pharmaceutical Biology and Biotechnology (Prof. Peter Proksch) at the University 'Heinrich Heine Düsseldorf' in Germany
April 2010	Ph D research at the University 'Bergische Universität Wuppertal' in Germany, Laboratory of Organic Chemistry under the supervision of Prof. Hans-Josef Altenbach.
09/2009-03/2010	Ethnopharmacological survey on cancer patients using traditional plants as herbal therapeutics in National Institute of Oncology in Rabat-Morocco
01/2008-07/2008	6-month training period end of study at the Faculty of Medicine and Pharmacy, Laboratory of Pharmacology and Toxicology under the supervision of Prof. A. Faouzi. Title of the topic "Quality control of antibiogram discs by high-performance liquid chromatography and research for new antibacterial herbal medicines."
03/2008-06/2008	3 months of Training in the laboratory of microbiology at the hospital IBN SINA in Rabat (realization and reading of antibiogramme, identification of the CMI of the resistant stumps).
02/2008	1 month training in the national laboratory of medicines control (Service of quality insurance, service physico-chimimie, service of the biological tries).
10/2007-11/2007	2 months of training at "Pharmaceutical Institute" in Ain Aouda (quality assurance Unit laboratory of quality control, production unit, stores raw materials and finished products, maintenance unit).
07/2005	1 month of training in the Laboratory of Biochemistry at the National Institute of Hygiene. (Analysis of: glycemia, Urea, creatinine, urates, Cholesterol, HDL cholesterol, LDL cholesterol, Triglycerides, direct and total ALAT, ASAT, PALE, GGT, Bilirubine, Sodium, Potassium, Calcium, Phosphates, magnesium).

## Scientific Production

---

2013	<b>Kabbaj, F.Z.;</b> Lai, D.; Meddah, B.; Altenbach H.J.; Cherrah, Y.; Proksch, P.; Faouzi MA.; Debbab, A. Chemical constituents from aerial parts of <i>Thymelaea lythroides</i> . <b>2013</b> . <i>Biochem. Syst. Ecol.</i> <b>51</b> , 153–155
2013	<b>Kabbaj, F.Z.;</b> Lu, Su; Faouzi, My El Abbés; Meddah, Bouchra; Proksch, Peter; Cherrah, Yahya; Altenbach, Hans-Josef; Aly, Amal; Chadli, Ahmed; Debbab, Abdessamad. .Bioactive Metabolites from <i>Chaetomium aureum</i> : Structure elucidation and inhibition of the Hsp90 machine chaperoning activity. <b>2013</b> . <i>J. Med. Chem.</i> ( <i>submitted</i> ) Manuscript ID: jm-2014-00495q.
2013	<b>Kabbaj, F.Z.;</b> Aly, A.H.; Marmann, A.; Faouzi M.A.; Meddah, B.; Cherrah, Y.; Altenbach H.J.; Proksch, P.; Debbab, A. New Xanthoradone Derivatives from <i>Chaetomium aureum</i> – Structures Elucidation and Biological Activity. <b>2013</b> ( <i>In</i>

*progress)*

2013 Marmouzi, I.; **Kabbaj, F.Z.**; Marmann, A.; Meddah, B.; Saidi, N.; Cherrah, Y.; Debbab A.; Faouzi, M.A.; Proksch, P. New secondary metabolites of *Chaetomium globosum*. 2013. GenBank. HG423571

2012 **Kabbaj, F.Z.**; Marmann, A.; El Amrani, M.; Proksch, P. and Debbab, A. *Chaetomium aureum* genomic DNA containing 18S rRNA gene, ITS1, 5.8S rRNA gene, ITS2 and 28S rRNA gene, isolate MM10S2-1. 2012. GenBank. HF546136.1

## Languages

---

German

DSH 3

English

Upper intermediate (B2)

French

Mother tongue 2

Arabic

Mother tongue 1